Technical Report

TR-05-20

The colloid investigations conducted at the Äspö Hard Rock Laboratory during 2000–2004

Marcus Laaksoharju, Geopoint

Susanna Wold, School of Chemical Science and Engineering, Nuclear Chemistry, KTH

December 2005

Svensk Kärnbränslehantering AB
Swedish Nuclear Fuel
and Waste Management Co
Box 5864
SE-102 40 Stockholm Sweden
Tel 08-459 84 00
+46 8 459 84 00
Fax 08-661 57 19
+46 8 661 57 19

The colloid investigations conducted at the Äspö Hard Rock Laboratory during 2000–2004

Marcus Laaksoharju, Geopoint

Susanna Wold, School of Chemical Science and Engineering, Nuclear Chemistry, KTH

December 2005

Keywords: Bentonite colloids, Colloid stability, Colloid concentration, Saline groundwater, Microbes.

Foreword

In 2000, SKB initiated an international colloid project at the Äspö Hard Rock Laboratory (HRL) in Sweden to study the stability, generation and mobility of especially bentonite colloids. The participating organisations in the project were: INE/Forshungszentrum Karlsruhe, Germany; Posiva, Finland and SKB, Sweden. Project contributors, SKB and INE managers (Fred Karlsson, Bernhard Kienzler, Ignasi Puigdomenech and Peter Wikberg) are acknowledged for their excellent work and support of the project during 2000–2004. Claude Degueldre reviewed the document and is acknowledged for the helpful comments.

Main project contributors (Appendices 1–15):

Appendix 1 Ola Karnland, Clay Technology AB

Appendix 2 Susanna Wold and Trygve Eriksen, KTH

Appendix 3 Wolfgang Hauser, Robert Götz, Horst Geckeis and Bernhard Kienzler, INE

Appendix 4 Gunnar Buckau, INE

Appendix 5 Ulla Vuorinen, VTT Processes

Appendix 6 Minna Rantanen, Consulting Engineers and Paavo Ristola, Industry and Power Plant Chemistry

Appendix 7 Christina Mattsén, SKB

Appendix 8 Susanna Wold and Trygve Eriksen, KTH

Appendix 9 Karsten Pedersen, Gothenburg University

Appendix 10 Iona Gurban, 3D Terra

Appendix 11 Claude Degueldre, PSI

Appendix 12 Marcus Laaksoharju, Geopoint

Appendix 13 Krister Wedholm and Magnus Holmqvist, Geosigma

Appendix 14 Gert Nilsson and Pia Wacker, Geosigma

Appendix 15 Ulla Vuorinen and Hannele Hirvonen, VTT Processes

Abstract

In 2000, SKB decided to initiate an international colloid project at the Äspö Hard Rock Laboratory in Sweden. The objectives of the colloid project are to: (i) study the role of bentonite as a colloid source, (ii) verify the background colloid concentration at Äspö HRL and, (iii) investigate the potential for colloid formation/transport in natural groundwater concentrations. The experimental concepts for the colloid project are: laboratory experiments with bentonite, background field measurements of natural colloids, borehole specific bentonite colloid stability experiments and a fracture specific transport experiment. The activities concerning the laboratory experiments and background field measurements are described in this work; the other activities are ongoing or planned. The following conclusions were made:

- The bentonite colloid stability is strongly dependent on the groundwater ionic strength.
- Natural colloids are organic degradation products such as humic and fulvic acids, inorganic colloids (clay, calcite, iron hydroxide) and microbes.
- Microbes form few but large particles and their concentration increase with increasing organic carbon concentrations. The small organic colloids are present in very low concentrations in deep granitic groundwater. The concentrations can be rather high in shallow waters.
- The colloid concentration decreases with depth and salinity, since colloids are less stable in saline waters.
- The colloid content at Äspö is less than 300 ppb.
- The colloid content at repository level is less than 50 ppb.
- The groundwater variability obtained in the boreholes reflects well the natural groundwater variability along the whole HRL tunnel.

Sammanfattning

År 2000 initierade SKB ett internationellt kolloidprojekt i berglaboratoriet på Äspö. Syftet med projektet är: (i) studera bentonitbarriärens roll som kolloidkälla, (ii) verifiera den naturliga kolloidhalten i grundvattnen på Äspö och, (iii) studera kolloidformations och transport potentialen i naturliga grundvatten. De experimentella koncepten för kolloidprojektet är: laboratorieförsök med bentonit lera, bakgrundsmätningar av den naturliga kolloidhalten i grundvatten, borrhåls specifika kolloidgenereringsförsök och sprickspecifika kolloidtransportförsök. I detta arbete beskrivs laboratorieförsöken med bentonit och bakgrundsmätningar av den naturliga kolloidhalten, eftersom de övriga aktiviteterna är pågående eller planeras. Av det utförda arbetet kan man dra följande slutsatser:

- Bentonitkolloiders stabilitet styrs främst av jonstyrkan i grundvattnet.
- Naturliga kolloider i grundvatten består av organiska nedbrytningsprodukter såsom humus och fulvosyra, oorganiska (lera, kalcit, järnhydroxider) kolloider samt mikrober.
- Mikrober förekommer som få men stora kolloider. Mikrobkoncentrationen ökar med ökad halt organisk kol. De organiska kolloiderna är små och återfinns i mycket låga halter i djupa grundvatten. I ytligare grundvatten kan däremot halterna vara betydligt högre.
- Kolloidhalten på Äspö minskar med ökat djup och salthalt eftersom kolloider inte är stabila i salta vatten.
- Kolloidhalten på Äspö är mindre än 300 ppb.
- Kolloidhalten på förvarsdjup på Äspö är mindre än 50 ppb.
- Variationerna i salthalten i de mätta borrhålen täcker in den naturliga salthaltsvariationen som påträffas längs med hela Äspö tunneln.

Contents

1 Background and objectives

Colloids are small particles in sizes ranging from 10^{-3} to 10^{-6} mm. Due to their small sizes, they can stay in solution for long times. The colloids are of interest for the safety of a repository for spent nuclear fuel because of their potential to transport radionuclides from a defective waste canister to the biosphere.

SKB has conducted field measurements of colloids for more than 10 years. The outcome of those studies performed nationally and internationally concluded that the colloids in the Swedish granitic bedrock consist mainly of clay, silica and iron hydroxide particles and that the mean concentration is around 20–45 ppb which is considered to be a low value /Laaksoharju et al. 1995/. The low colloid concentration is controlled by the attachment onto the rock, which reduces the stability of the colloids and their mobility in aquifers, as well due to the high salinity and near neutral pH of the deep granitic groundwaters.

It has been argued that e.g. plutonium is immobile owing to its low solubility in groundwater and strong sorption onto rocks. Field experiments at the Nevada Test Site, where hundreds of underground nuclear tests were conducted, indicate however that plutonium is associated with the colloidal fraction of the groundwater or travel as eigencolloids. The $^{240}Pu/^{239}Pu$ isotope ratio of the samples established that an underground nuclear test 1.3 km north of the sample site is the origin of the plutonium /Kersting et al. 1999/.

The findings of potential transport of solutes by colloids and access to more sensitive instruments for colloid measurements motivated a colloid project at Äspö HRL (Hard Rock Laboratory). The project was initiated by SKB in 2000 and is planned to continue with the Colloid Dipole project until the end of the 2007.

The participating organisations in the project are:

- INE/Forschungszentrum Karlsruhe, Germany.
- Posiva, Finland.
- SKB, Sweden.

The objectives of the Colloid project are to study:

- The stability and mobility of colloids.
- Measure background colloid concentration in the groundwater at Äspö.
- Bentonite as a colloid source.
- The potential of colloids to enhance radionuclide transport.

The results from the project will be used mainly in future development of safety assessment modelling of radionuclide migration. The project was conducted in 2000–2004.

The aim of this report is to present the results obtained in 2000–2004. The persons contributing with scientific project results are referred to in the text below and the contributions not printed elsewhere are presented as Appendix 1–11 in this report.

2 Experimental concept

The experimental concepts for the colloid project are: laboratory experiments, background measurements, borehole specific experiments and fracture specific experiments. The aim of the laboratory experiments is to study the behaviour of bentonite under prevailing groundwater conditions at Äspö HRL. Background measurements of colloids aim to establish the natural colloid content in the Äspö groundwaters. The borehole and fracture specific experiments aim at describing the colloid stability and transport potential of the bentonite but since these experiments are ongoing or in a planning phase they are not described further here. The laboratory and background measurements are described in the next sections.

2.1 Laboratory experiments

Initial laboratory tests

The mobility of radionuclides associated within a bentonite barrier of a repository for spent nuclear fuel may change if the radionuclides strongly bind to bentonite colloids. The risk for clay and humic/fulvic colloids to enter the bentonite with the saturating groundwater is considered to be rather low, bentonite colloids, however, can be released from the bentonite barrier, and, if they are stable, travel to the biosphere. The stability of bentonite colloids in contact with different solutions has been studied in laboratory experiments /Wold and Eriksen 2001, Karnland 2002/.

Bentonite was dispersed in solutions with different salinity and the degree of sedimentation was studied, see Figure 2-1. The results from the laboratory tests show that the bentonite colloid stability is strongly correlated to the solutions' ionic strength, where they are stable in dilute waters. A very low concentration of colloids stayed stable in solutions during a week of ionic strengths 0.1 and 1 M. At 0 and 0.01 M on the other hand sedimentation is slower and colloids are stable in solution.

Detailed laboratory tests

The laboratory experiment on bentonite was extended to investigate in more detail the influence of background electrolytes $NaClO_4$ and $CaCl_2$ at 0, 0.001, 0.01, 0.1 and 1 M , type and amount of bentonite (MX-80, Na- and Ca-bentonite), temperature (20 and 60°C), and pH /Karnland 2002, Wold and Eriksen 2002/. Colloid concentration as well as colloidal size distributions were measured in the solutions after 7 to 21 days with PCS–dynamic light scattering. ICP-MS and ICP-AES analyses were performed with particular attention on monitoring Si, Al, Fe, Mg and Ca in the solutions. Al in the solutions is assumed to be a marker for bentonite colloids.

Increasing Ca^{2+} concentration decreases the distance between the montmorillonite sheets in the bentonite resulting in lower stability for the colloids. Colloidal stability in the solutions is mainly controlled ionic strength. Aggregation and flocculation increases with increasing ionic strength and colloids sediment with time, see Figure 2-2 /Karnland 2002, Wold and Eriksen 2002/.

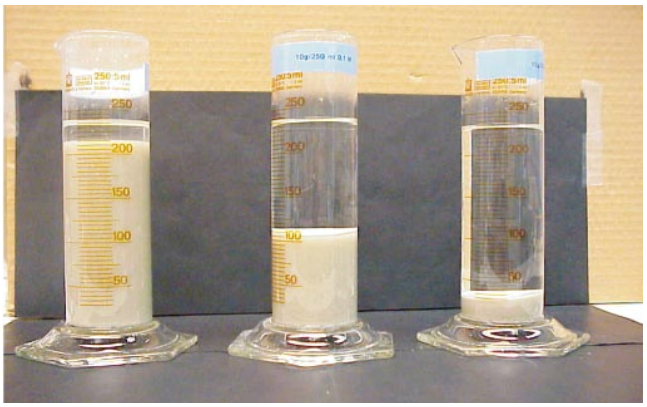

Figure 2-1. *The salinity of the water influences colloid stability. The experiments show different degrees of sedimentation of bentonite depending on the ionic strengths (NaCl) in the water. At low ionic strength colloids are stabile and the sedimentation is slow. The experimental conditions: Dry bentonite, 10 g/250 ml in contact with 0.01, 0.1 and 1 M solution at 20°C after 1.5 weeks /Wold and Eriksen 2001, 2002).*

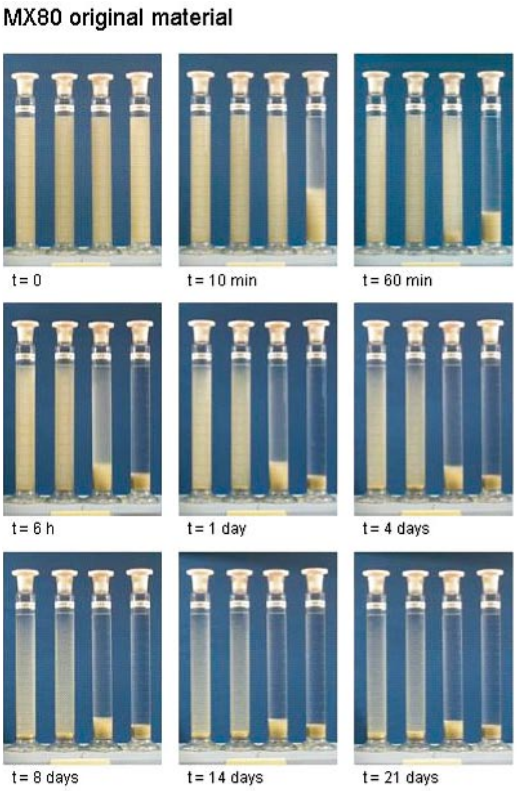

Figure 2-2. *Photographs of the MX-80 material in 250 ml water solutions after different sedimentation periods in time. From left to right in each picture, NaCl was added in order to yield a concentration of: 0 M, 0.001 M, 0.01 M and 0.1 M solutions /Karnland 2002/.*

2.2 Background colloid measurements along Äspö HRL

The aim of this activity was to measure the natural background colloid concentrations from 8 different boreholes along the Äspö HRL tunnel (Figure 2-3) by applying different techniques. The boreholes represent different water types with a TDS (Total Dissolved Solids) of 286–21,760 mg/L. It is well known that the colloid stability can change with the ion content of the groundwater. Some of the techniques were applied on all boreholes but others only on some specific boreholes. Also, additional samplings outside the selected boreholes were used. The techniques used and some of the major findings are presented below; more detailed descriptions are found in the referred appendices.

LIBD measurements

The colloid content was measured on-line from the boreholes using a new high pressure detection cell connected to modified laser based equipment LIBD (Laser-Induced Breakdown-Detection) developed by INE in Germany (Figure 2-4). The advantage is that the resolution of this equipment is higher compared with standard light scattering equipment. It is therefore possible to detect the colloid content at much lower concentrations than previously /Hauser et al. 2002/. The results from the measurements show increased colloid stability and concentration in low salinity groundwaters (Figure 2-5) and in waters with high humic like organics. From EQ3/6 thermodynamic calculations, super saturation of mainly carbonates was used as an indicator that these phases may form many of the colloids. The method was also used to indicate the sensitivity of the measurements to contamination from atmospheric gases /Hauser et al. 2002/.

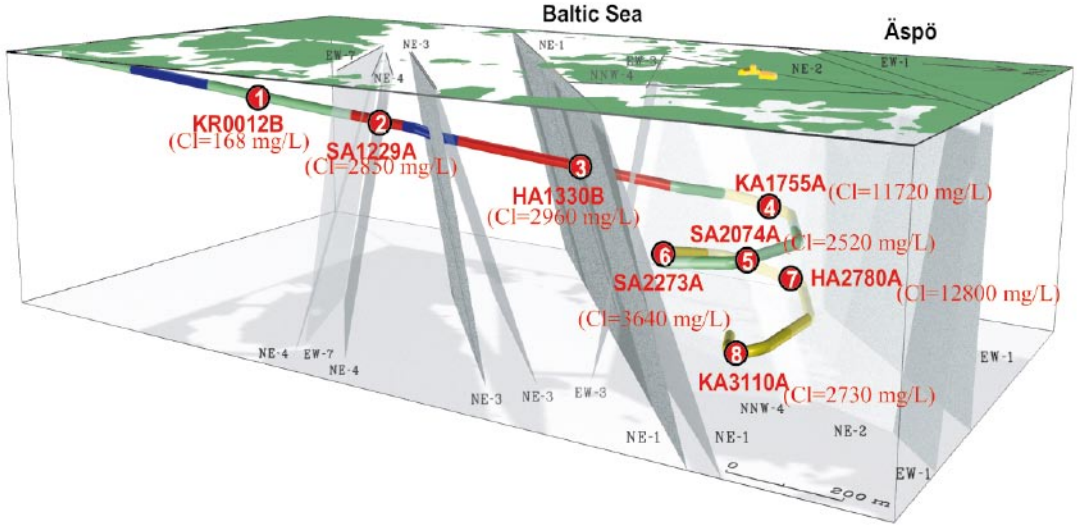

Figure 2-3. *The 8 boreholes sampled for colloids along the Äspö HRL tunnel. The Cl content of the groundwater is given in brackets. The reason for the large differences in the salinity along the tunnel is that the boreholes intersect different fracture zones with different orientations containing groundwater with different origins and ages.*

Figure 2-4. *The equipment for Laser-Induced Breakdown-Detection (LIBD) of colloids is installed in a van in order to allow mobility and on-line measurements at boreholes /Hauser et al. 2002/.*

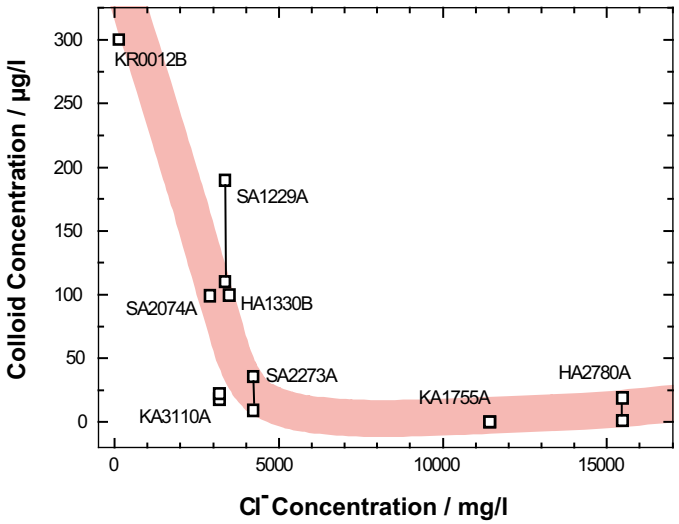

Figure 2-5. *The natural colloid concentration decreases with groundwater salinity but also with depth /Hauser et al. 2002/.*

Humic measurements

A feasibility study was conducted for the isolation of sufficient amounts of fulvic acid from Äspö groundwaters. Dissolved organic carbon (DOC) and UV/VIS Spectroscopy of original water samples as well as fulvic acid concentrates was used to quantify the fulvic acid. The study shows that sufficient fulvic acid is available in all waters. It is also shown that sorption of fulvic acid on precipitates generated during shipping and handling of groundwater samples is not a problem.

For chemical, spectroscopic and isotopic (especially ^{14}C) characterization around 200 mg fulvic acid is required (around 100 mg C). In groundwaters where the concentration of fulvic acid is around 1 mgC/L or higher, 100 L of groundwater can be sampled and sent

to the laboratory for direct treatment. In two of the twelve investigated water samples the fulvic acid concentrations are so low that on-site pre-concentration by reverse osmosis appears to be the method of choice /Buckau and Wolf 2002/.

Ultrafiltration

Two boreholes were sampled (sampling point 6 and 7, see Figure 2-3) and the sampled groundwater was ultra-filtrated in an inert atmosphere. An example of the results from the SEM micrographs and EDS spectra analysis are presented in Figure 2-6. The SEM/EDS results indicate that the dominating particle phases may be calcite, silica, iron hydroxide and clay particles. The obtained results did not allow calculation of the actual concentration of the elements associated with the different phases nor of the amount of particles /Vuorinen 2002/.

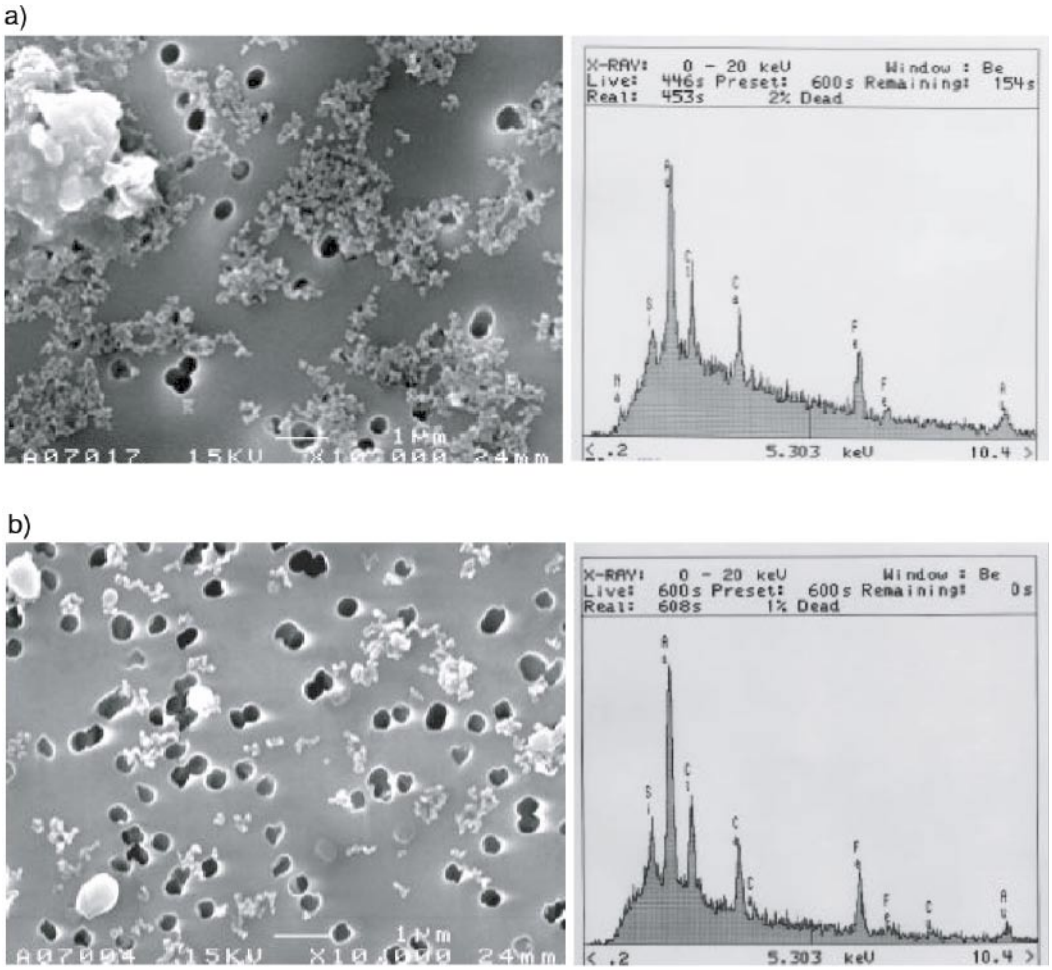

Figure 2-6. *SEM micrographs (to the left) of the 0.4 µm membrane (magnification = ×10,000) and the EDS spectrum (to the right). a) The sample from borehole SA2273A contains some large particles but also some small aggregates, the EDS spectra indicate the presence of Fe, Ca, Si (Au is a method artefact; Cl is a due to saline groundwater precipitation). b) The sample from borehole HA2780A shows a more homogeneous size distribution but similar elemental peaks /Vuorinen 2002/.*

Comparison of groundwater analytical results

Groundwater sampling and analysis can be challenging when dealing with deep groundwaters. To ensure quality, the Posiva group wanted to sample the boreholes used for colloid sampling located in the deeper part of the tunnel (sampling locations HA2780A, SA2273A and KA1755A, see Figure 2-3). The results show good agreement with the SKB analytical results (Appendix 7) despite some different sampling occasions and considering the ±5% uncertainty in the measurements /Rantanen and Mäntynen 2002/.

Groundwater analytical results

The complete groundwater analytical results of the boreholes sampled for the colloid project was performed by SKB, following routines for class 4 (complete chemical characterisation) and class 5 (complete chemical characterisation including special isotope analysis). The results are presented in Appendix 7 /Mattsén 2002/, the salinity (Cl) distribution along the tunnel is depicted in Figure 2-3.

Colloid filtration and PCS measurements

Two different techniques for colloid concentration measurements were applied: on-line filtration and PCS-Dynamic light scattering measurement applied on pressurised groundwater samples. A filter system, with 3,000, 450, 220 and 50 nm, was connected in series to the borehole. The filters were flushed with argon to prevent artefact colloid formation from groundwater coming in contact with atmospheric gases. Groundwater volumes of 50–1,000 ml were flushed through the filter system. The filters were acidified and the solutions analysed using ICP-MS and ICP-AES. The inorganic colloids in Äspö waters are presumably composed of iron hydroxides, silica and clay mineral. The analysed Fe, Si and Al were therefore assumed to represent the inorganic colloid phases in the Äspö groundwaters. The colloid concentrations in the Äspö groundwaters are in the range of 1–149 ppb. Colloids in the size range of $> 50 < 220$ nm dominate in all the Äspö water samples except for the water sampled in borehole SA2273 A. The colloid concentrations are low and it is therefore doubtful if the size distributions can be defined. All the samples contained lower colloid concentrations than the PCS detection limit of 0.6 mg/L /Wold and Eriksen 2002/.

Microorganisms in the groundwater

Microorganisms generally range between 2×10^{-4} to 10^{-2} mm, thereby overlapping colloids in size. Their organic character, with many different functional groups directed outwards from the cell surface, e.g. phosphates, amines, hydroxyl- and carboxyl-groups, makes them potent as radionuclide sorbents. The sampled boreholes along the Äspö HRL represented different water types since it is well known that the colloid stability and the micro-organisms can change with the ion content of the groundwater. A test rack with 50 ml sterile plastic tubes with screw lids filled with 3 ml 30% formaldehyde was used for sampling. The water was filtered and the filters were examined using microscopy under fluorescent light in order to count the microbes. The numbers ranged up to more than two orders of magnitude, with the highest numbers in the shallowest and the deepest borehole investigated, KR0012B and KA3110A. A comparison of the obtained data with earlier data on the total number of microorganisms in Fennoscandian Shield groundwater is shown in Figure 2-7. The

obtained data lies within the range of all available data. There was an obvious difference in size and appearance between the boreholes, from 0.2 µm up to several µm. Borehole HA1330B showed the largest cells, most other boreholes had small or very small cells, see Figure 2-8 /Pedersen 2002/. The microbial content increases with the organic content in the groundwater (see Figure 2-9). Generally shallow water contains more organic material than deep groundwater.

Measurements of electrical conductivity along the Äspö HRL tunnel

The aim of the sampling was to measure the electrical conductivity of all the major water venues at the Äspö tunnel and to compare it with borehole data to ensure that the borehole data reflects the natural groundwater and colloid variability at the site. A total of 195 groundwater samples were collected along the tunnel. The results are shown in Figure 2-10.

The results indicate that both data sets give the same basic information concerning groundwater composition (salinity) but greater detail variability is seen in the data collected along the tunnel. This indicates that data collected along the tunnel reflects local variability better than data from boreholes, but when sampling the tunnel wall close to the boreholes the groundwater salinity is the same in the borehole as in the water dripping from the wall. These results support the colloid project, by showing that the groundwater composition obtained from the boreholes reflect well the major groundwater variability obtained in the whole tunnel /Gurban 2002/.

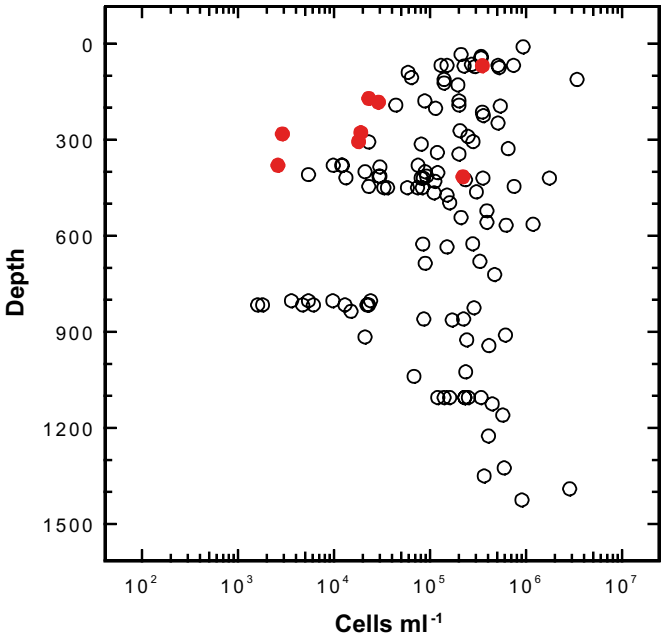

Figure 2-7. *The means of the number of microorganisms along the depth of the Äspö HRL. The results are compared with data from the Stripa research mine, Laxemar boreholes KLX and investigation sites in Finland (Olkiluoto, Hästholmen, Kivetty, Romuvaara) and the natural uranium analogue in Palmottu, Finland /Pedersen 2002/.*

a)

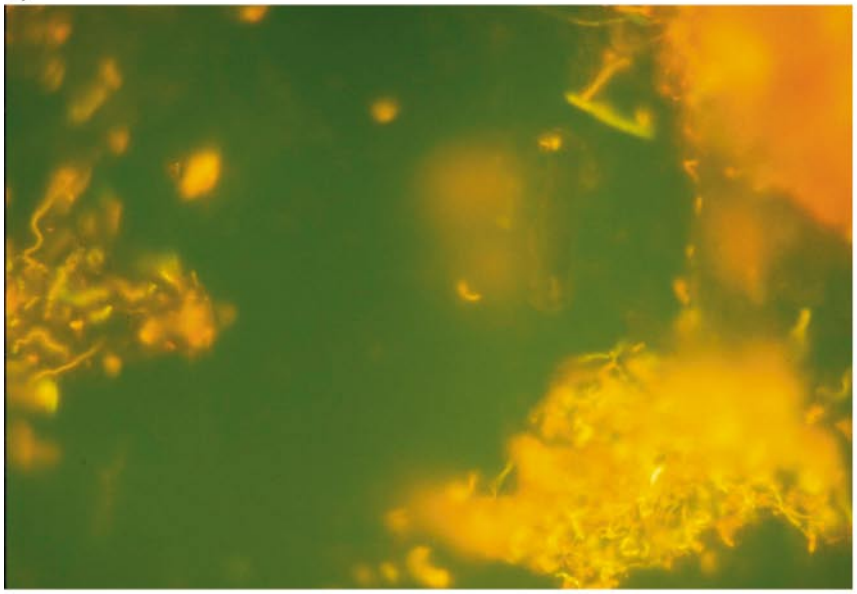

b)

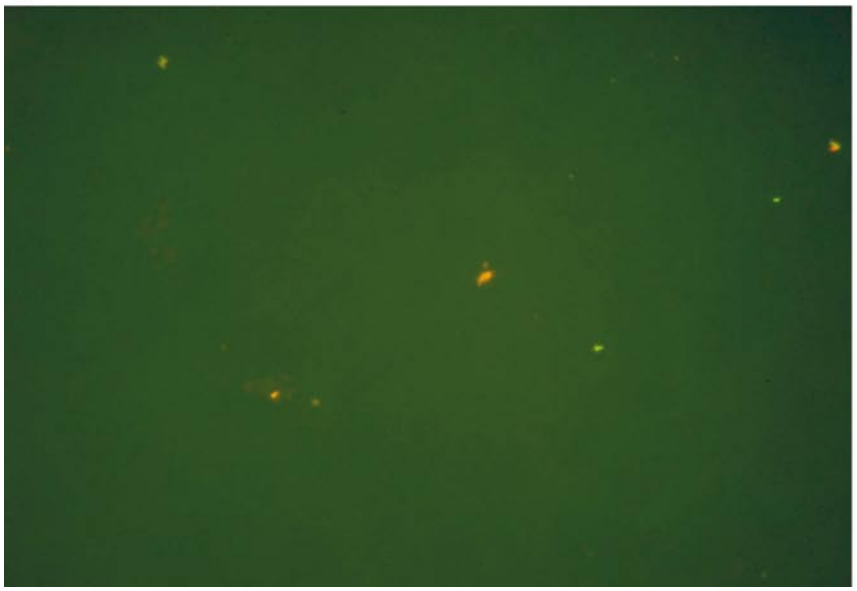

Figure 2-8. *a) A borehole with large cells (HA1330B) and b) a borehole with small cells (HA2780). The figures represent the 2B filters with a frame size of 130×85 µm /Pedersen 2002/.*

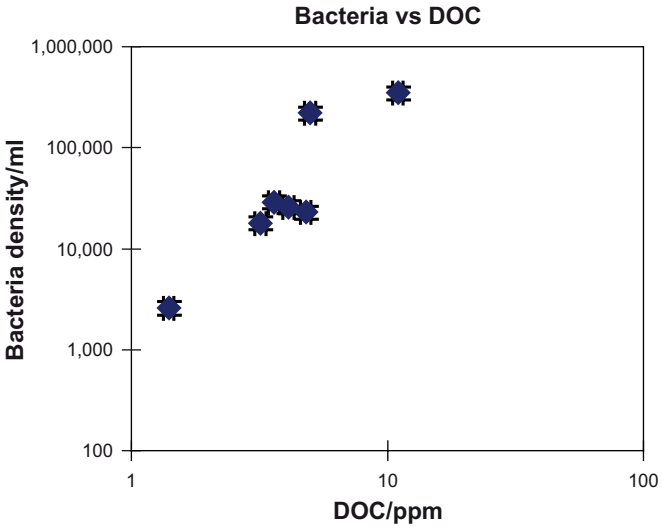

Figure 2-9. *The microbial content increases with the organic content in the groundwater /Degueldre 2002/.*

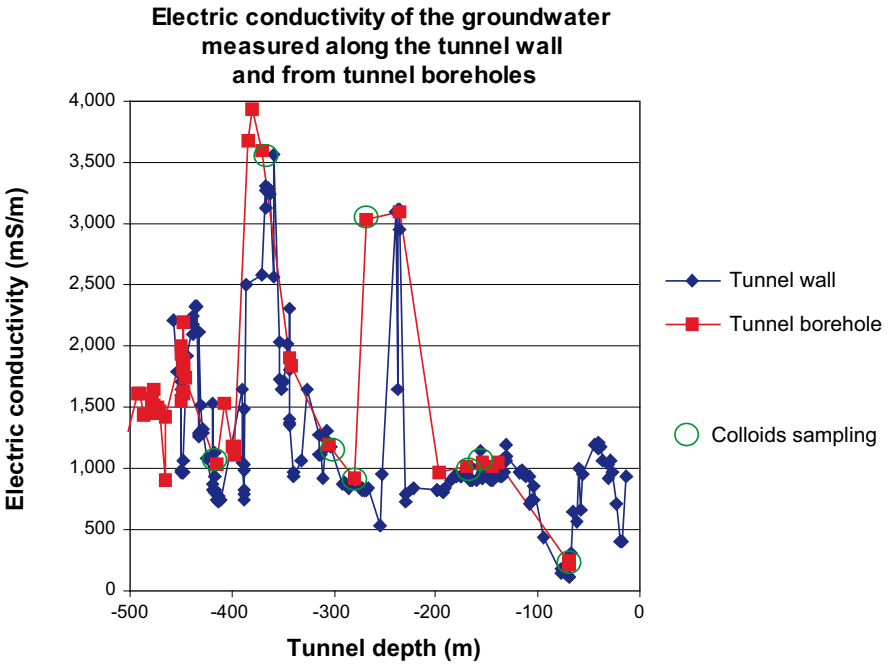

Figure 2-10. *Electrical conductivity measured along the tunnel walls (blue) and electrical conductivity data measured in the tunnel boreholes (red) versus the tunnel depth. The green circles indicate the 8 boreholes used for colloid sampling /Gurban 2002/.*

Review comments

The project contributions (Appendices 1–14) have been reviewed /Degueldre 2002/. Many of the important findings were summarised during this review process e.g. that the natural colloidal particles at Äspö consist of organics, inorganic colloids (clay, calcite, iron hydroxide) and of microbes. Microbes form few but large particles, organic particles are small but can have a high concentration especially in shallow waters (Figure 2-7). The colloid concentration decreases with depth and salinity.

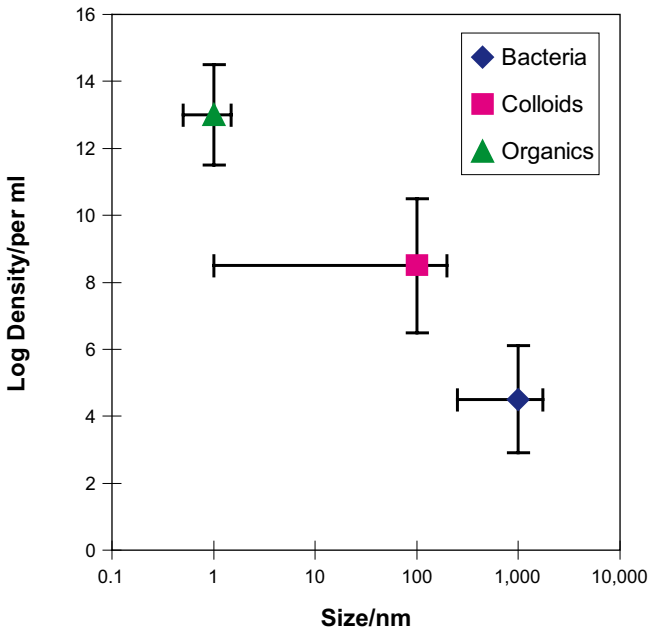

Figure 2-11. *Schematic presentation of concentration and size distribution of the dominating colloidal particles at Äspö HRL /Degueldre 2002/.*

2.3 Colloid generation tests along Äspö HRL and in Olkiluoto using colloid reactors

2.3.1 Background and aim

If a water bearing fracture is in contact with the bentonite barrier, bentonite colloids can, if stable, enhance radionuclide transport to the biosphere. In laboratory experiments conducted by /Karnland 2002, Wold and Eriksen 2003/ bentonite colloids have been shown to be stable in groundwaters containing less than 0.01–0.1 Na^+ and/or 0.0001–0.001 M Ca^{2+} for periods up to three weeks. In deep Swedish granitic groundwaters the concentrations of both Na^+ and Ca^{2+} are expected to exceed these concentrations. However, the exact concentration limits were not obtained in these experiments, and laboratory conditions are quite different from in situ ones. To state what happens if groundwater is in contact with the bentonite barrier an in situ experiment was conducted. Crushed and sieved bentonite was capsulated in textile reactors which were placed in boreholes at Äspö HRL and Olkiluoto. The Äspö and Olkiluoto groundwaters are different as regards ion and dissolved organic carbon content. Water flowed through the bentonite reactors with different flow rates, and the colloid content in the groundwater was measured before contact with the bentonite reactor and with time.

2.3.2 Laboratory reactor optimisation tests

To test if the reactors were suitable for in situ experiments, pre-tests were performed at the laboratory. The material in the reactors was polypropylene filter textile which was sewn together. The seams of the tubes were covered by a strip of the same material glued to the inside with textile paste. MX-80 was crushed and sieved through a 2 mm sieve, to ensure that the material was in the smallest size-range possible. The bentonite was tightly packed into the filter reactors, and the ends were sealed with plastic plugs, which were fastened

with steel casings under high pressure. The 40 cm-long reactors were filled with about 600 grams of bentonite. The experiments were performed with drinking water. The reactor was placed in a bucket filled with 1.8 L water. The reactor was in contact with the water for 1 to 7 days. Water was filtered for 5 minutes using a constant under pressure of 0.3 bars. The analytical procedure consisted of comparing the filtered volume of water from the test setups with the blank sample consisting of drinking water. It was assumed that the larger the difference of the filtered volumes between the samples from test setups and the blank, the larger the content of colloids and particles from the colloid reactor. The results show that bentonite colloid passed the textile filter and did not clog the reactors. Two other tests were performed in higher salinities, at 0.03 and 0.37 M ionic strengths. During 10 days, water saturated the bentonite; sampling was started thereafter. Sampling of water before and after contact with the reactor was analyzed with ICP-MS for Al, Si and Fe, which are markers for bentonite colloids. No bentonite colloids were detected which means that bentonite colloids are not stable at 0.03 and 0.37 M ionic strengths.

2.3.3 Field tests in Äspö and Olkiluoto HRLs

Bentonite reactors were installed in boreholes KA1755A, SA2273A, SA2780A and KA3385A at Äspö and PVA1 and PVA at Olkiluoto. After installation, groundwater was equilibrated with the bentonite for a minimum of three weeks. The flow was then stabilized to the desired flow rate of 10 ml/min (the first flow to be sampled). The sampling at 10 ml/min was followed by sampling of 5 ml/min about one month later and finally of 1 ml/min one month after that. Water was sampled before and after contact with the reactors. Fixed volumes of water were was pumped through the colloid catching filters of 450, 220 and 50 nm pore size. The filters were acidified and the solutions sent to a commercial laboratory for ICP-AES and ICP-SMS analysis of Al, Si and Fe. The solutions were also analyzed for alkalinity and pH. After the experiment, the reactors were taken out from the boreholes and they were photographed – Figure 2-8. It was clear that the bentonite was saturated and had been swelling. Spots on the textile show where colloids have migrated through the reactor textile. Samples from the experiments performed at a flow of 10 ml/minute generally have higher concentrations of Al, Fe and Si compared to the samples from the experiments with flow rates of 5 and 1 ml/min. When larger volumes pass the filter series the cation concentration decreases. This means that this is an artefact originating from filling material which is more easily suspended at higher flow rates.

From the comparison of groundwater before and after contact with the bentonite no colloids were detected. The concentration of Al, Fe and Si seems to be the same in the “before” and “after” samples. The Al content in the solutions from the various-sized filters is largest from the 450 nm filters from Äspö; otherwise no trend can be seen in the filter analysis.

The bentonite reactor experiments conclude that the chances for colloids to migrate from the bentonite barrier out towards the biosphere in groundwaters with compositions as studied here are minor.

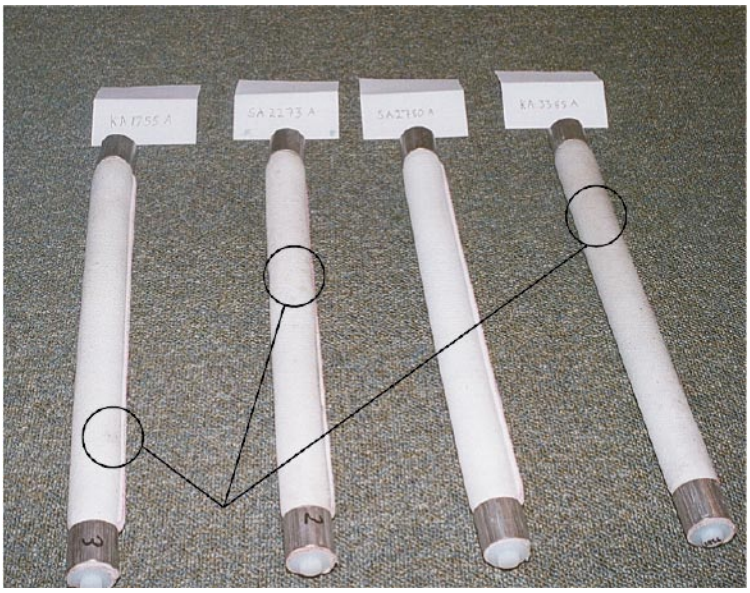

Figure 2-12. *The reactors after being taken out from the boreholes. The bentonite was saturated and had been swelling. The spots on the textile indicate that the colloids migrated through the reactor textile.*

3 Conclusions

The major result from the laboratory experiments is that bentonite colloid stability is strongly correlated to the background electrolyte and its concentration. The stability limit for bentonite colloids in Na^+ solutions is in the range of 0.01–0.1 M and in Ca^{2+} solutions 0.0001–0.001 M.

The major finding from the background colloid measurements at Äspö HRL is that despite different techniques the colloid content at repository level is at ppb level /Degueldre 2002, Hauser et al. 2002, Wold and Eriksen 2002, Vuorinen 2002, Gurban 2002, Wold and Eriksen 2002, Mattsén 2002, Rantanen and Mäntynen 2002, Pedersen 2002/. These results support the earlier measurements and modelling of colloids which indicated low colloid concentrations in deep groundwaters at Äspö /Laaksoharju et al. 1995/.

The conclusions are as follows:

- Bentonite colloid stability is strongly dependent on the ionic strength of the solution at the bentonite buffered pH around 8.
- Natural colloidal particles consist of organics, inorganic colloids (clay, calcite, ironoxohydroxide) and microbes.
- Microbes form few but large particles; organic particles are small but can be numerous in shallow waters.
- The microbe content increases with the content of organic carbon.
- The colloid concentration decreases with depth and salinity.
- The colloid content at Äspö is less than 300 ppb.
- The colloid content at repository level is less than 50 ppb.
- Bentonite colloids are not stable in the deep bedrock groundwaters of Äspö and Olkiluoto.
- Groundwater variability obtained in the sampled boreholes reflects well the natural groundwater variability along the whole HRL tunnel.

4 References

Buckau G, Wolf M, 2002. Origin, stability and mobility of humic colloids in Äspö groundwater: Feasibility study. See Appendix 4.

Degueldre C, 2002. Review comments to the Äspö Colloid Workshop 5th of March 2002. See Appendix 11.

Gurban I, 2002. Electric conductivity measurements along the Äspö tunnel. See Appendix 10.

Hauser W, Götz R, Geckeis H, Kienzler B, 2002. In-situ Colloid Detection in Granite Groundwater along the Äspö Hard Rock Laboratory Access Tunnel. See, Appendix 3.

Karnland O, 2002. Colloid stability in Wyoming bentonite. See Appendix 1.

Kersting A, Efurd D, Finnegan D, Rokop D, Smith D, Thompson J, 1999. Migration of plutonium in the ground water at the Nevada Test Site. Nature, Vol 397, January 1999, pp 56–59.

Laaksoharju M, Degueldre C, Skårman C, 1995. Studies of colloids and their importance for repository performance assessment. SKB Technical Report TR 95-24, Stockholm, Sweden.

Mattsén C, 2002. Compilation of groundwater chemistry data October 2001. See Appendix 7.

Pedersen K, 2002. Total number of microorganisms in groundwater sampled during background colloid measurements along the Äspö HRL tunnel. See Appendix 9.

Rantanen M, Mäntynen M, 2002. Groundwater sampling in Äspö tunnel. See Appendix 6.

Vuorinen U, 2002. Bentonite as a Colloid Source in Groundwaters at Olkiluoto. See Appendix 5.

Wold S, Eriksen T, 2001. Formation of inorganic colloids in solutions of different ionic strength in contact with bentonite. SKB ITD-01-02.

Wold S, Eriksen T, 2002. Bentonite colloid stability. Effects of bentonite type, pH and ionic composition in solution. See Appendix 2.

Wold S, Eriksen T, 2003. Background inorganic colloid measurements in different Äspö waters. See Appendix 8.

Appendix 1

Stability of bentonite colloid suspensions

– A laboratory study

Ola Karnland

Clay Technology AB

Contents

1 Background

Highly compacted bentonite clay is planned to be used as a buffer material in the KBS-3 type repository for spent nuclear fuel. The main component in bentonite is montmorillonite, which consists of mineral flakes with a thickness of approximately 1 nanometer. Consequently, there is a potential risk that these flakes will act as colloids if the highly compacted buffer material is exposed to water and free to expand. Such dispersion may jeopardize the buffer function by loss of material to fractures and possible continuous transport by groundwater. Further, radioactive material may be adsorbed on the clay particles and thereby transported to the biosphere. It is not likely that the bentonite will disperse into the groundwater, but it can not be excluded that some process such as rock displacement or gas evolution from canister corrosion will lead to partial dispersion of the montmorillonite. The main question is then, under which conditions does such a dispersion lead to a stable colloidal system.

2 Objectives

The main objectives in this laboratory test series are to:

- estimate bentonite colloid stability at different salt concentrations,
- estimate the difference between mono- and divalent cations with respect to colloid stability,
- examine the role of original salt content in the bentonite,
- test if chemical analyses are a possible tool to detect clay colloids in groundwater.

The test solution concentrations were chosen in order to identify limits and were not aimed to be representative for repository groundwater. However, the highest examined concentrations are in the same range as the concentrations in Äspö groundwater.

3 Test program

The main test series included 15 tests in which a water solution of 250 ml and 1 g of bentonite material were placed in a mixing cylinder (Table A1-1). The original clay was used in 4 tests, and Na- and Ca-converted clay was used in 4 tests, respectively. Two tests were made with the final supernatant in the Na-conversion stage, described below, which included some colloids observed by the naked eye (CoA13, CoA14). Three additional tests including Na converted clay exposed to $CaCl_2$ solutions were made (CoA16–CoA18). Two reference analyses with water only were made, one with starting de-ionized water (CoA15) and one with the same starting water but treated as the clay samples and placed in the test cylinders for the maximum testing time (CoA19).

The clay was actively dispersed in the solutions by daily shaking for a few minutes during a period of 1 week. The cylinders were thereafter left to rest in order to permit natural sedimentation by gravitation only.

Table A1-1. Test program.

Project colloids											
Series CoA											
	Solution				Solution analyses					Mineral	
Test no	V	C	Salt	Bentonite	ICP/AES	IC	Colloids	κ	pH	XRD	ICP/AES
	ml	mM						S/cm			
CoA01	250		none	MX-80	1	1	1	138	8.2	1	1
CoA02	250	1	NaCl	MX-80	1	1	1	264	7.4		
CoA03	250	10	NaCl	MX-80	1	1	1	1,400	6.8		
CoA04	250	100	NaCl	MX-80	1	1	1	11,400	6.6		
CoA05	250		none	MX-80 Na	1	1	1	64	8.4	1	1
CoA06	250	1	NaCl	MX-80 Na	1	1	1	215	7.3		
CoA07	250	10	NaCl	MX-80 Na	1	1	1	1,300	7		
CoA08	250	100	NaCl	MX-80 Na	1	1	1	11,800	6.7		
CoA09	250		none	MX-80 Ca	1	1	1	33	8.5	1	1
CoA10	250	1	$CaCl_2$	MX-80 Ca	1	1	1	258	6.3		
CoA11	250	10	$CaCl_2$	MX-80 Ca	1	1	1	2,400	6.1		
CoA12	250	100	$CaCl_2$	MX-80 Ca	1	1	1	20,000	5.8		
CoA13	250		prevalent	MX-80 Na f	1	1	1	181	7.8		
CoA14	250		prevalent	MX-80 Na f	1	1	1	207	7.8		
CoA15	250		none	none	1	1	1	1.2	8.4		
CoA16	250	1	$CaCl_2$	MX-80 Na	1	1	1	286	7.1		
CoA17	250	10	$CaCl_2$	MX-80 Na	1	1	1	2,300	6.2		
CoA18	250	100	$CaCl_2$	MX-80 Na	1	1	1	19,000	5.9		
CoA19	250	0	none	none	1	1	1	1.7	8.4		

4 Test material

Wyoming bentonite sold under the commercial name MX-80 was the source material for the three types of test materials which were used. It was delivered in a 25 kg sack by Askania AB and produced by Volclay LTD, Merseyside, UK.

According to an old characterisation /Müller-Vonmoos 1983/ the material is dominated by natural sodium montmorillonite clay (~ 75% by weight). The rest consists of quartz (~ 15%), feldspars (~ 7%), carbonates (~ 1.4%) sulphides (~ 0.3%), organic carbon (~ 0.4%). Dispersed in distilled water the clay fraction (d < 2 µm), makes up around 80%. The mean mineralogical composition of the montmorillonite part is given by:

$(Al_{3.10}\ Fe^{3+}_{0.4}\ Fe^{2+}_{0.02}\ Mg_{0.48})$	$(Si_{7.92}\ Al_{0.08})$	$O_{20}\ (OH)_4$	$Na_{0.48}\ Ca_{0.04}\ Mg_{0.02}$
octahedral cations	tetrahedral cations	structural O/OH	exchangeable cations

The cation exchange capacity is around 0.8 eq/kg bulk material and around 1.0 eq/kg clay in the minus 2 µm fraction. The natural exchangeable cations are sodium (~ 85%), calcium (~ 10%), magnesium (~ 4%) and small amounts of potassium (~ 0.3%). The specific surface area is around 550 m^2/gram material and the grain density is around 2.75 g/cm^3.

In this study the bentonite material was used in its original state, and in cleaned and Na- and Ca-converted states, respectively. The latter two materials were produced in the following way. Ten grams of the original MX-80 material was dispersed in 1 L of de-ionized water

and the fraction coarser than 2×10^{-6} m was settled as calculated by Stoke's law and removed by decantation. NaCl or $CaCl_2$ was added to give a concentration of 3 M in the decanted dispersion, respectively. The dispersion was left to settle and the supernatant was removed and new de-ionized water was added. This procedure was repeated, and as the salt concentration was lowered the settlement was enhanced by centrifugation. The electrical conductivity of the supernatants were measured after each washing in order to ensure that only insignificant amounts of salt finally was left in the material. The material was thereafter dried at 105°C and the material was analyzed by ICP/AES (Table A1-2) and by XRD (Figure A1-1).

Table A1-2. Results from ICP/AES analyses of the bentonite materials. Figures in the first section indicate % and in the second section ppm.

Element	MX-80	MX-Na	MX-Ca
Al2O3	20.6	21.1	20.2
CaO	1.39	0.118	2.67
Fe2O3	3.93	3.88	3.79
K2O	0.572	0.216	0.306
S	0.301	0.0921	0.149
MgO	2.5	2.43	2.24
MnO2	0.0131	0.0041	0.0067
Na2O	2.32	2.76	0.217
P2O5	0.0589	0.0739	0.0468
SiO2	62.1	63.1	60.1
TiO2	0.172	0.164	0.157
LOI	6.1	6	6.5
Total	100.1	99.9	96.4
Ba	326	72.2	144
Be	1.44	1.54	1.55
Co	< 6	6.54	< 5
Cr	274	< 10	< 10
Cu	< 6	< 5	11.3
La	57.9	65.2	61.3
Mo	< 6	< 5	< 5
Nb	34.7	32.9	32.2
Ni	< 10	< 10	< 10
S	3,010	921	1,490
Sc	5.8	6.54	6
Sn	< 20	< 20	< 20
Sr	271	27.7	35.8
V	4.75	< 2	< 2
W	< 60	< 50	< 50
Y	42.6	49.3	40.8
Zn	101	54.4	63.7
Zr	212	200	199

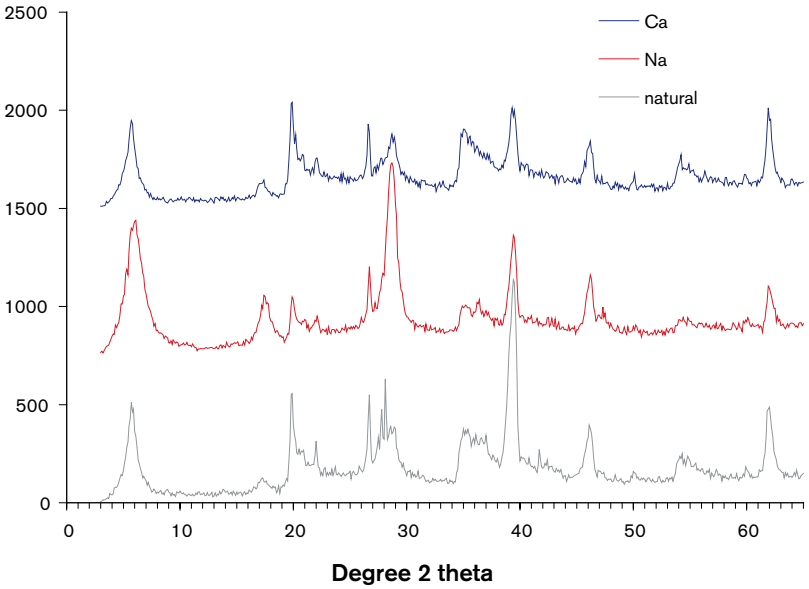

Figure A1-1. *XRD analyses of the bentonite material used in the test series. Upper curve shows result from Ca converted material, middle curve from Na converted material and lower curve from the original MX-80 material. The main difference is the loss of accessory minerals (mainly feldspars) in the treated material.*

The chemical formula of the converted montmorillonite material was roughly calculated based on the ICP/AES analyses of the Na and Ca converted material, respectively. The Si, Al, Mg and Fe results were used to give a best fit to the ideal montmorillonite formula Si_8 $Al_{(4-y)}$ Mg_y O_{20} $(OH)_4$ + $Na_{(x+y)}$. Since silica obviously still is present in the form of quartz, according to the XRD analyses, the silica content was reduced in order to meet the expected cation exchange capacity of 1.0 eq/kg. In both cases the reduction was 6% units in ICP/AES analyses.

The calculated formula for the Ca material was $Si_{7.72}$ $Al_{0.28}$ $Al_{3.12}$ $Mg_{0.48}$ $Fe_{0.41}$ O_{20} $(OH)_4$ $Ca_{0.38}$ and the formula for the Na material was $Si_{7.74}$ $Al_{0.26}$ $Al_{3.11}$ $Mg_{0.49}$ $Fe_{0.40}$ O_{20} $(OH)_4$ $Na_{0.75}$.

5 Analyses

The cylinders were photographed after defined time intervals during the sedimentation and the results are shown in Figures A1-13 to A1-16.

After 21 days of sedimentation the upper 30 ml of solution was removed and analyzed with respect to (Table A1-3 to A1-7):

- Electrical conductivity (Figure A1-2),
- pH (Figure A1-3),
- major cations and some trace elements by ICP/AES (Figure A1-5 to A1-12),
- SO_4^{2-}, by ICP
- Colloid concentration (Figure A1-4).

In addition, pure test water was analyzed before and after 21 days of exposure to a test cylinder. Further, 2 water solutions from the production of Na-converted bentonite material were analyzed. These samples represent the finest part of the Na converted material since it was not removed from the dispersion despite the intensive centrifugation (4,000 rpm for 30 minutes).

Table A5-1. Analyze results from the MX-80 test suspensions.

Sample			CoA01	CoA02	CoA03	CoA04
planned	clay	cation	Na/Ca	Na/Ca	Na/Ca	Na/Ca
		mass, g	1	1	1	1
	solution	cation		Na	Na	Na
		anion		Cl	Cl	Cl
		C, M	low	0.001	0.010	0.100
		volume, ml	250	250	250	250
measured	ICP/AES, mg/L	Al	92.7	47.0	2.245	0.028
		B	0.423	0.536	0.175	0.067
		Ba	0.054	0.053	0.025	0.178
		Ca	4.97	4.65	2.18	15.85
		Cd	0.002	0.002	0.000	0.000
		Co	0.000	0.000	0.001	0.001
		Cr	0.002	0.002	0.000	0.000
		Cu	0.000	0.001	0.001	0.001
		Fe	19.20	21.60	0.487	0.011
		K	1.340	1.470	1.957	3.426
		Li	0.027	0.030	0.014	0.016
		Mg	11.000	12.100	0.692	3.560
		Mn	0.030	0.028	0.001	0.009
		Mo	0.009	0.010	0.012	0.006
		Na	31.00	50.50	230.37	1,715
		Ni	0.000	0.000	0.001	0.000
		P	0.125	0.127	0.169	0.017
		Pb	0.005	0.010	0.002	0.001
		S	7.680	4.530	5.31	5.99
		Si	243.0	128.0	9.772	1.921
		Sr	0.160	0.160	0.0711	0.5410
		Ti	0.52	0.56	0.014	0.000
		V	0.009	0.009	0.001	0.000
		Zn	0.467	0.039	0.002	0.006
	IC, mg/L	Cl^-	1.1	27.7	386.3	3,609.6
		SO_4^{2-}	6.1	4.2		
		NO_3^-	0.1	< 0.01		
		PO_4^{3-}	< 0.02	< 0.02		
	titration, (mM)	(HCO_3^-)	0.8	0.8	0.5	0.5
	TOC, mg/L	C-inorg.	7.8	7.6	7.0	6.0
		C-org	4.6	2.1	1.4	2.6
Sample	mass/250 ml	mg tot	231	167	352	2,943
Sample	mass/250 ml	mg MM Si	202	107	8	2

Table A1-4. Analyze results from the MX-Na test suspensions.

Sample			CoA05	CoA06	CoA07	CoA08
planned	clay	cation	Na	Na	Na	Na
		mass, g	1	1	1	1
	solution	cation		Na	Na	Na
		anion		Cl	Cl	Cl
		C, M	low	0.001	0.010	0.100
		volume, ml	250	250	250	250
measured	ICP/AES	Al	292.0	233.0	188.0	0.041
		B	1.230	1.140	1.040	0.077
		Ba	0.018	0.017	0.018	0.016
		Ca	0.85	0.90	0.61	0.86
		Cd	0.006	0.005	0.004	0.000
		Co	0.001	0.000	0.000	0.001
		Cr	0.004	0.003	0.002	0.000
		Cu	0.011	0.009	0.008	0.001
		Fe	57.50	55.40	45.50	0.000
		K	0.535	0.664	0.576	1.500
		Li	0.066	0.064	0.063	0.006
		Mg	30.500	29.300	24.000	1.996
		Mn	0.059	0.055	0.047	0.001
		Mo	0.000	0.000	0.000	0.000
		Na	48.60	70.60	302.00	2,120
		Ni	0.000	0.000	0.000	0.000
		P	0.115	0.083	0.093	0.069
		Pb	0.001	0.000	0.004	0.007
		S	0.960	1.330	0.628	0.91
		Si	760.0	610.0	500.0	4.348
		Sr	0.024	0.022	0.020	0.0210
		Ti	1.58	1.49	1.36	0.001
		V	0.019	0.018	0.015	0.000
		Zn	0.151	0.474	0.061	0.000
	IC	Cl^-	0.4	33.4	333.5	3,710.9
		SO_4^{2-}	1.2	1.1	0.4	
		NO_3^-	0.0	< 0.01	< 0.01	
		PO_4^{3-}	0.1	< 0.02	< 0.02	
	titration, (mM)	(HCO_3^-)	0.3	0.3	0.2	0.2
	TOC	C-inorg.	4.1	3.8	2.4	2.0
	TOC	C-org	2.5	3.4	2.2	0.7
Sample	mass/250 ml	mg tot	657	571	768	3,209
Sample	mass/250 ml	mg MM Si	633	508	416	4

Table A1-5. Analyze results from the MX-Ca test suspensions.

Sample			CoA09	CoA10	CoA11	CoA12
planned	clay	cation	Ca	Ca	Ca	Ca
		mass, g	1	1	1	1
	solution	cation		Ca	Ca	Ca
		anion		Cl	Cl	Cl
		C, M	low	0.001	0.010	0.100
		volume, ml				
measured	ICP/AES	Al	20.2	0.210	0.047	0.073
		B	0.481	0.223	0.172	0.197
		Ba	0.019	0.034	0.095	0.125
		Ca	8.17	35.17	361.35	5,200
		Cd	0.001	0.000	0.000	0.000
		Co	0.001	0.000	0.001	0.003
		Cr	0.001	0.000	0.000	0.002
		Cu	0.001	0.001	0.001	0.000
		Fe	4.88	0.048	0.001	0.001
		K	0.464	0.439	0.468	0.708
		Li	0.008	0.004	0.007	0.011
		Mg	2.730	0.271	0.924	1.219
		Mn	0.009	0.000	0.000	0.001
		Mo	0.001	0.000	0.000	0.000
		Na	0.82	0.80	0.74	1.43
		Ni	0.000	0.000	0.000	0.009
		P	0.014	0.008	0.000	0.000
		Pb	0.008	0.000	0.000	0.000
		S	0.560	0.90	6.10	48.17
		Si	11.2	10.100	9.986	9.777
		Sr	0.007	0.0160	0.1016	0.7778
		Ti	0.15	0.001	0.000	0.000
		V	0.002	0.000	0.000	0.000
		Zn	0.018	0.007	0.015	0.022
	IC	Cl^-	0.2	75.0	687.6	6,820.6
		SO_4^{2-}	0.4			
		NO_3^-	0.0			
		PO_4^{3-}	< 0.02			
	titration, (mM)	(HCO_3^-)	0.4	0.2	0.1	0.1
	TOC	C-inorg.	3.1	2.0	2.0	1.0
	TOC	C-org	1.3	0.9	0.7	1.4
Sample	mass/250 ml	mg tot	28	68	587	6,639
Sample	mass/250 ml	mg MM Si	9	8	8	8

Table A1-6. Analyze results from the MX-Na/Ca test suspensions.

Sample			CoA05	CoA16	CoA17	CoA18
planned	clay	cation	Na	Na	Na	Na
		mass,g	1	1	1	1
	solution	cation		Ca	Ca	Ca
		anion		Cl	Cl	Cl
		C, M	low	0.001	0.01	0.1
		volume, ml				
measured	ICP/AES	Al	292.0	198.0	0.1	0.0
		B	1.230	1.151	0.091	0.000
		Ba	0.018	0.041	0.025	0.038
		Ca	0.85	20.13	429.00	3,525
		Cd	0.006	0.002	0.000	0.000
		Co	0.001	0.000	0.000	0.000
		Cr	0.004	0.000	0.000	0.000
		Cu	0.011	0.012	0.000	0.000
		Fe	57.50	48.15	0.00	0.00
		K	0.535	1.97	0.46	0.83
		Li	0.066	0.060	0.014	0.016
		Mg	30.500	27.51	2.61	2.91
		Mn	0.059	0.029	0.000	0.000
		Mo	0.000	0.000	0.000	0.000
		Na	48.60	56.03	84.54	90.50
		Ni	0.000	0.071	0.000	0.004
		P	0.115	0.241	0.043	0.032
		Pb	0.001	0.049	0.000	0.000
		S	0.960	1.04	5.84	78.50
		Si	760.0	425.9	5.9	6.0
		Sr	0.024	0.027	0.087	0.623
		Ti	1.58	1.337	0.000	0.000
		V	0.019	0.002	0.000	0.000
		Zn	0.151	0.060	0.001	0.008
	IC	Cl^-	0.4	68.42	610.09	4,568
		SO_4^{2-}	1.2	0.85	0.84	0.74
		NO_3^-	0.0	0.00	0.07	0.05
		PO_4^{3-}	0.1	0.15	0.00	0.00
	titration, (mM)	(HCO_3^-)	0.3	0.30	0.30	0.00
	TOC	C-inorg.	4.1	2.7	1.7	1.7
	TOC	C-org	2.5	1.8	1.2	1.0
Sample	mass/250 ml	mg tot	657	468	626	4,546
Sample	mass/250 ml	mg MM Si	633	355	5	5

Table A1-7. Analyze results from the final suspensions ions from the preparation of the MX-Na material, and from test water before and after exposure to a test cylinder.

Sample			CoA13	CoA14	CoA15	CoA19
planned	clay	cation	Na	Na		
		mass, g				
	solution		undefined	undefined	test water	test water
					start	final
		C, M	low	low	low	low
		volume, ml				
measured	ICP/AES	Al	117.0	216.0	0.0	0.0
		B	0.560	0.943	0.017	0.010
		Ba	0.005	0.008	0.001	0.001
		Ca	0.23	0.41	0.00	0.11
		Cd	0.002	0.004	0.000	0.000
		Co	0.001	0.001	0.000	0.000
		Cr	0.001	0.003	0.000	0.000
		Cu	0.002	0.003	0.000	0.000
		Fe	23.80	42.20	0.04	0.00
		K	0.350	0.305	0.022	0.00
		Li	0.025	0.046	0.000	0.008
		Mg	13.000	23.200	0.075	0.01
		Mn	0.029	0.050	0.000	0.000
		Mo	0.002	0.000	0.000	0.000
		Na	48.80	61.00	0.01	0.06
		Ni	0.000	0.000	0.000	0.000
		P	0.106	0.131	0.000	0.000
		Pb	0.001	0.004	0.000	0.000
		S	0.756	0.648	0.008	0.00
		Si	289.0	500.0	0.6	1.1
		Sr	0.007	0.014	0.000	0.000
		Ti	0.57	1.04	0.00	0.000
		V	0.009	0.015	0.000	0.000
		Zn	0.034	0.060	0.000	0.000
	IC	Cl^-	29.6	28.3	< 0.02	2.00
		SO_4^{2-}	0.8	0.9	< 0.02	0.00
		NO_3^-	< 0.01	< 0.01	< 0.01	0.06
		PO_4^{3-}	< 0.02	< 0.02	< 0.02	0.00
	titration, (mM)	(HCO_3^-)	0.6	0.7	0.0	0.00
	TOC	C-inorg.	6.2	6.9	0.4	0.0
	TOC	C-org	1.8	3.8	1.6	2.5
Sample	mass/250 ml	mg tot	288	481	0	
Sample	mass/250 ml	mg MM Si	241	416	0	1

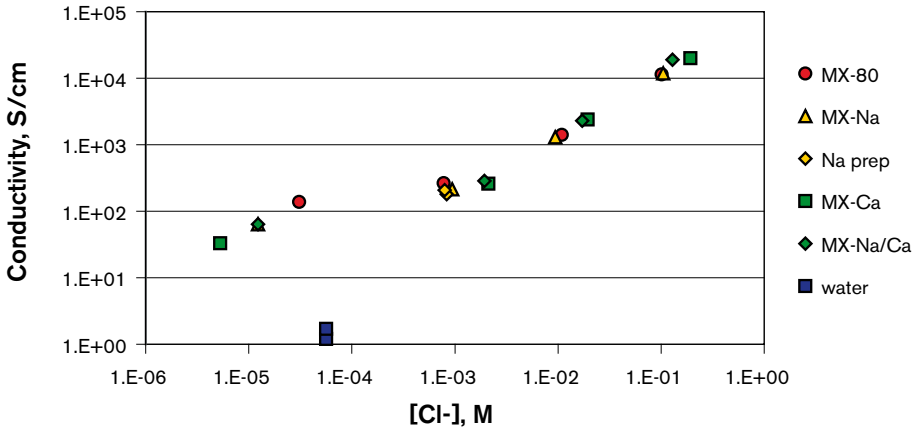

Figure A1-2. *Electric conductivity of the analyses solutions/dispersions versus measured chloride concentration.*

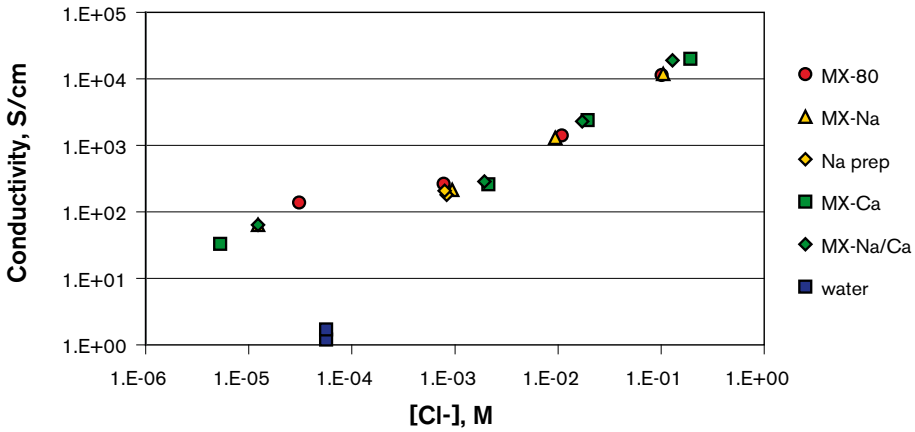

Figure A1-3. *pH of the analyzed solutions/dispersions versus measured chloride concentration.*

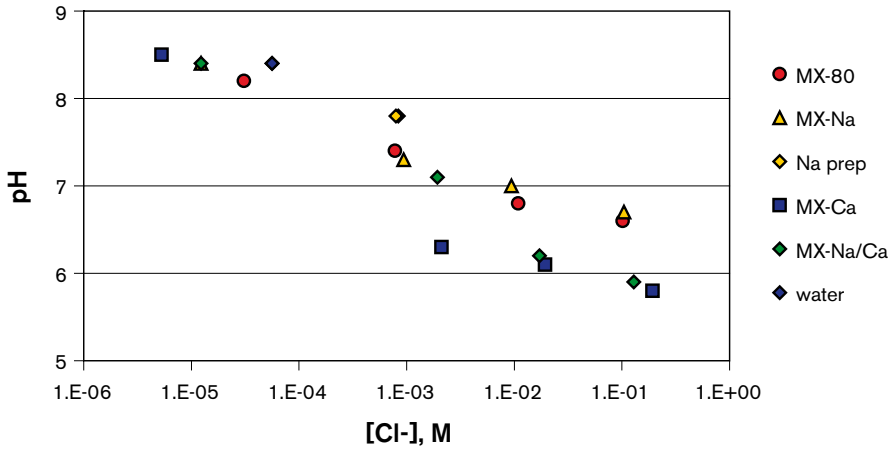

Figure A1-4. *Signal size (intensity) of PCS measurements of the analyzed solution/dispersion versus chloride concentration.*

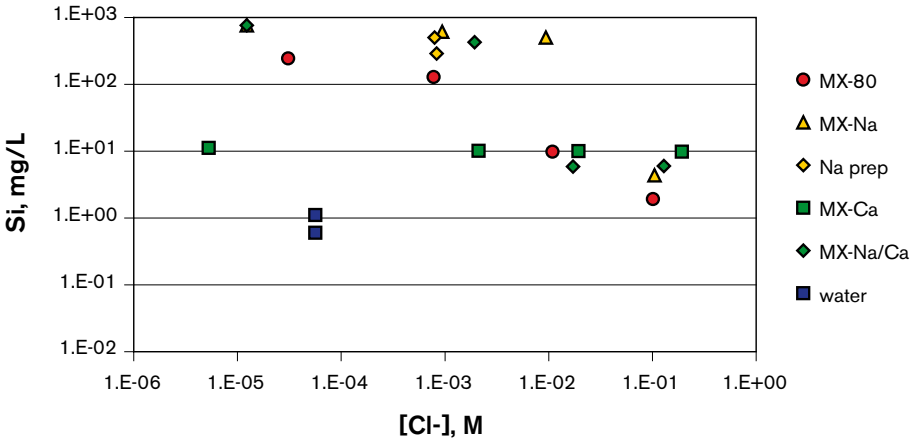

Figure A1-5. *Si content in the analyzed solution/dispersion versus chloride concentration.*

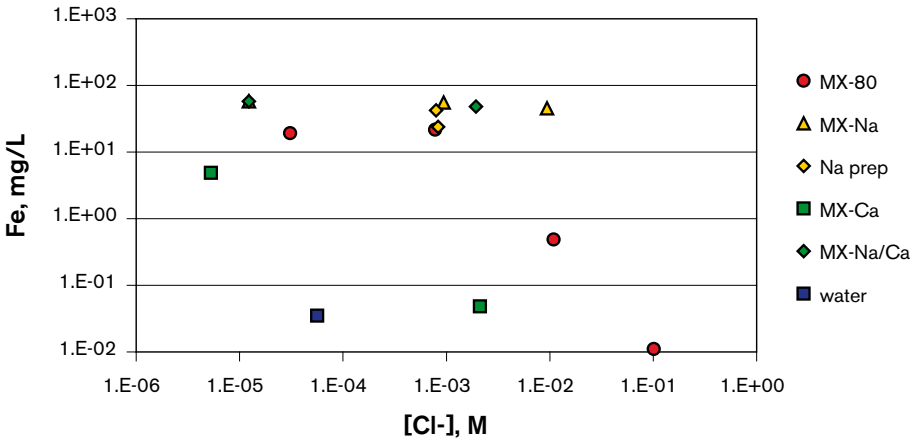

Figure A1-6. *Fe content in the analyzed solution/dispersion versus chloride concentration.*

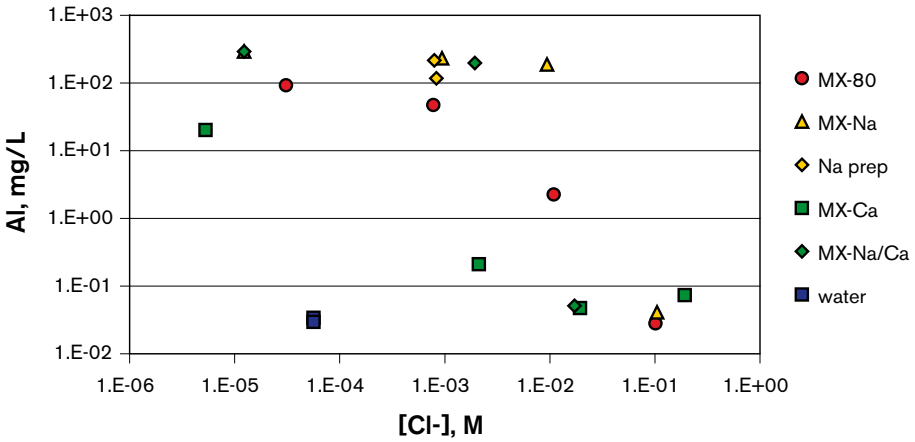

Figure A1-7. *Al content in the analyzed solution/dispersion versus chloride concentration.*

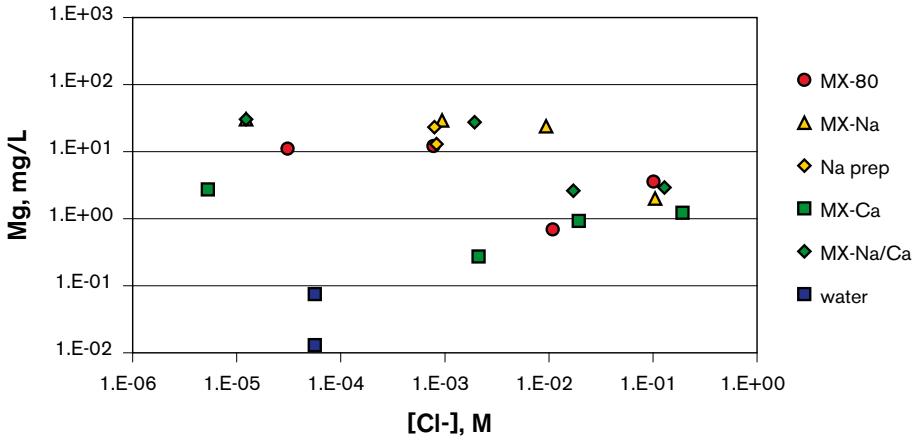

Figure A1-8. *Mg content in the analyzed solution/dispersion versus chloride concentration.*

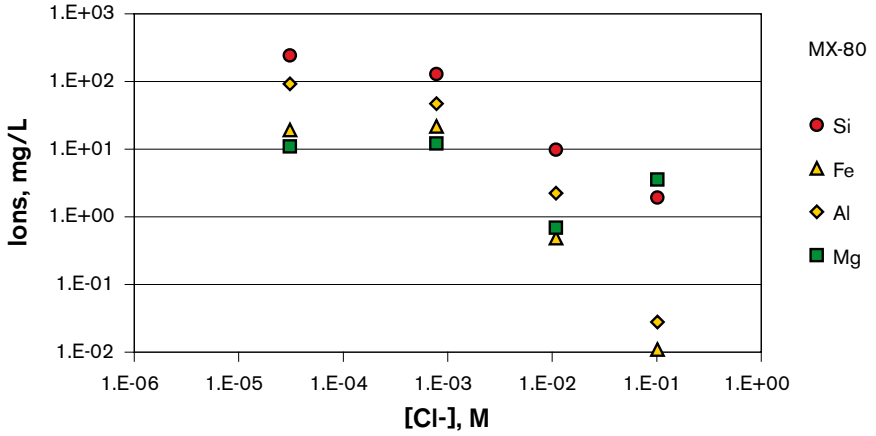

Figure A1-9. *Si, Fe, Al and Mg content in the MX-80 sample/NaCl solutions versus chloride concentration.*

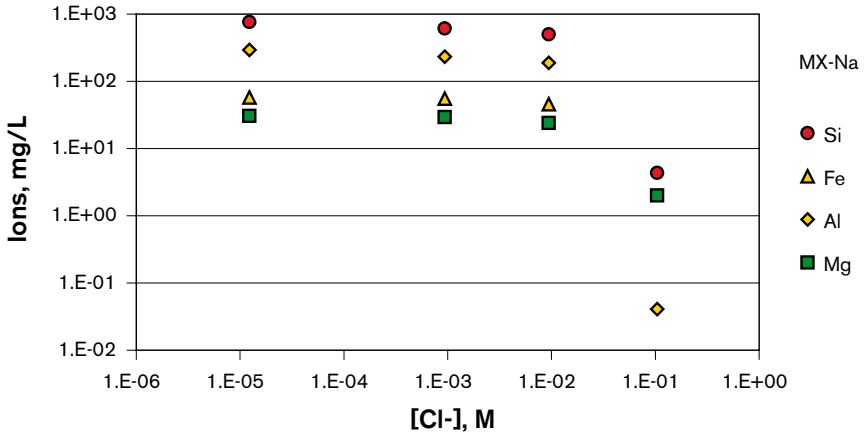

Figure A1-10. *Si, Fe, Al and Mg content in the MX-Na sample/NaCl solutions versus chloride concentration.*

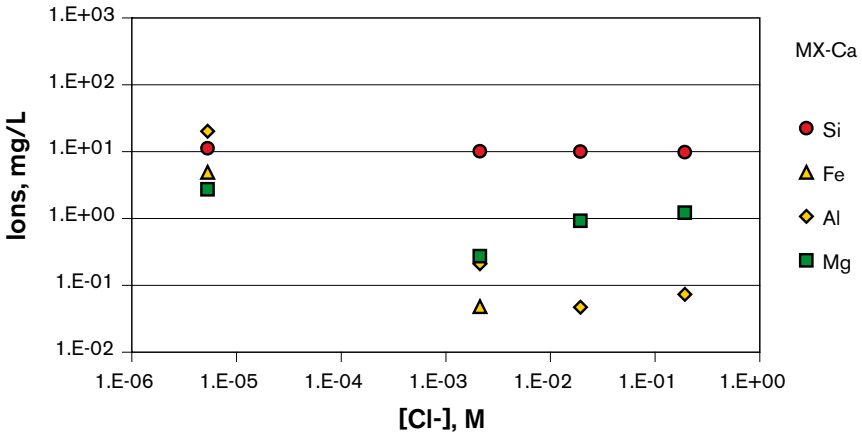

Figure A1-11. *Si, Fe, Al and Mg content in the MX-Ca sample/$CaCl_2$ solutions versus chloride concentration.*

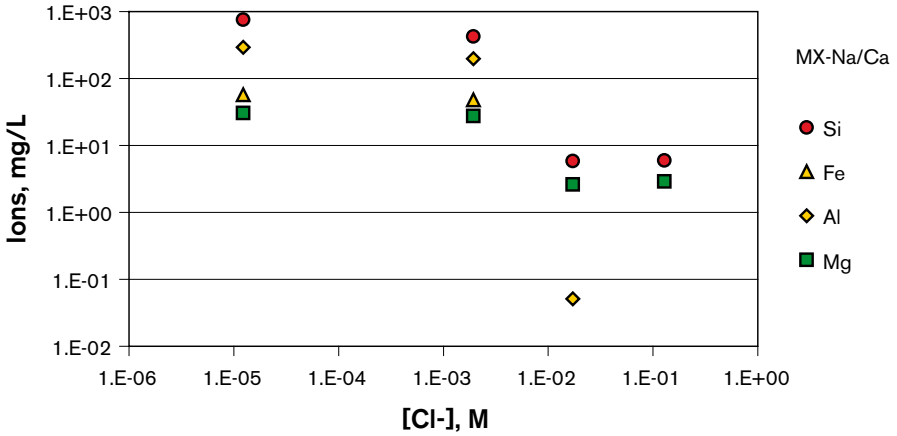

Figure A1-12. *Ion concentrations in the MX-Na sample/$CaCl_2$ solutions versus chloride concentration.*

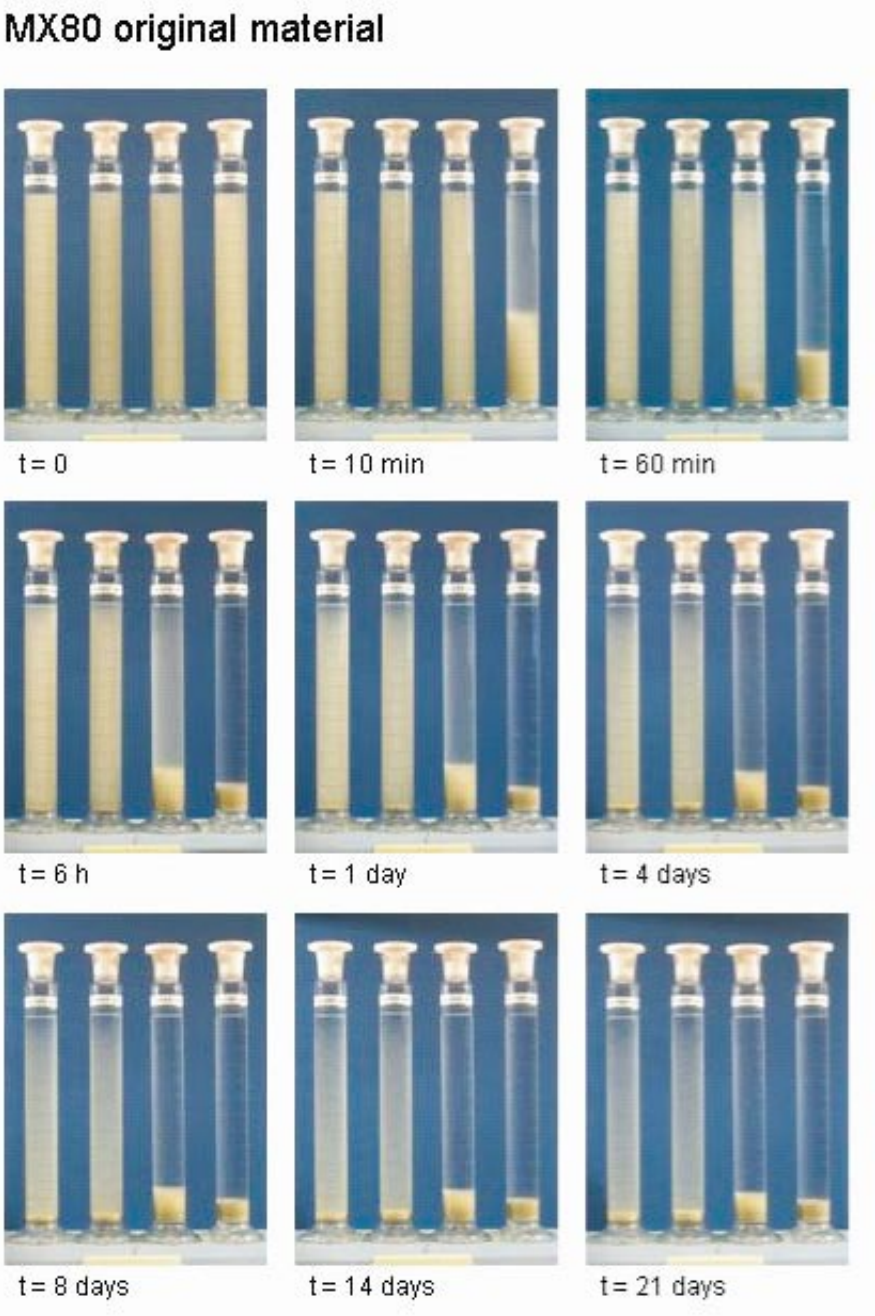

Figure A1-13. *Photographs of the MX-80 material in 250 ml water solutions after different sedimentation periods. From left to right in each picture, NaCl was added in order to give a concentration of: 0.000 M, 0.001 M, 0.01 M and 0.1 M.*

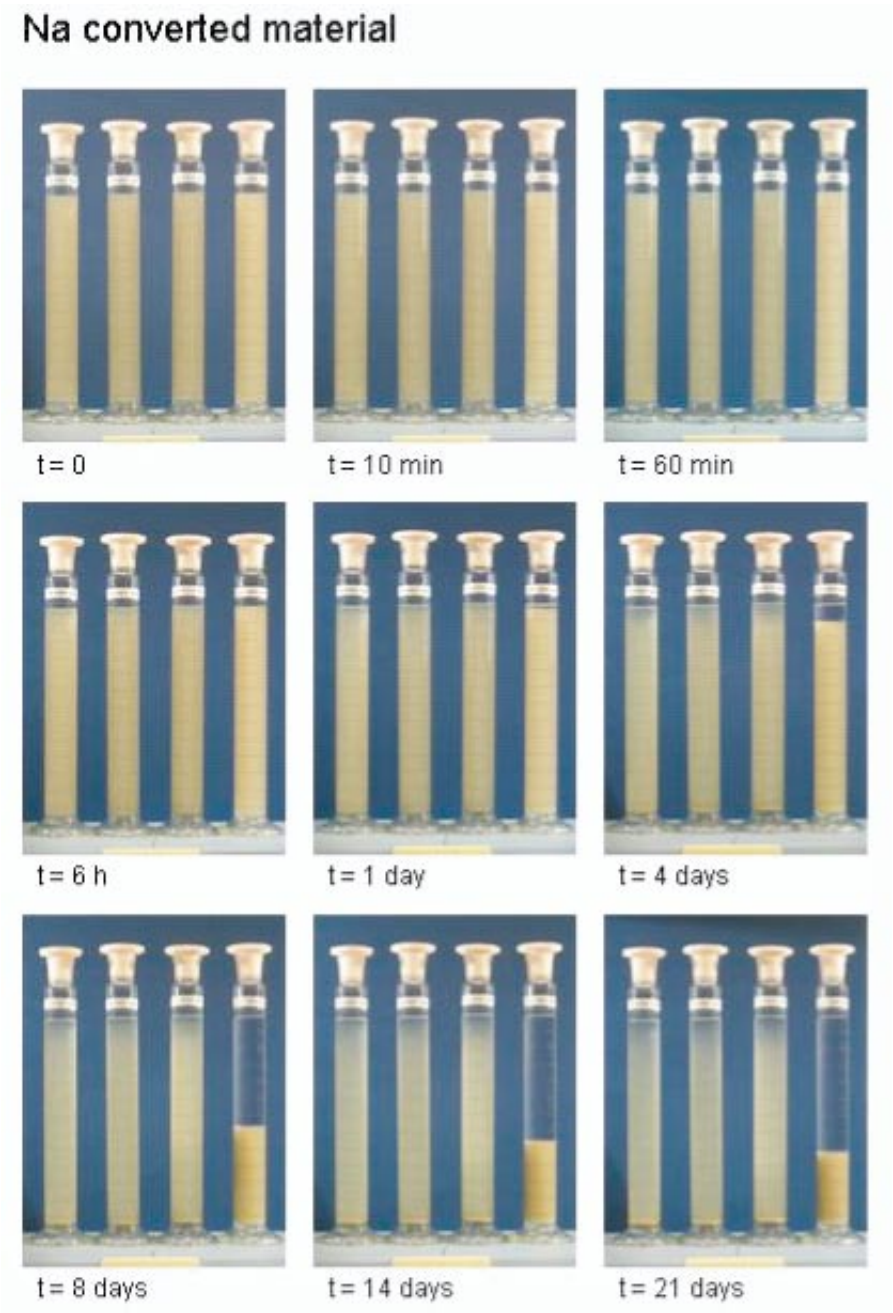

Figure A1-14. *Photographs of the MX-Na material in 250 ml water solutions after different sedimentation periods. From left to right in each picture, NaCl was added in order to give a concentration of: 0.000 M, 0.001 M, 0.01 M and 0.1 M.*

Figure A1-15. *Photographs of the MX-Ca material in 250 ml water solutions after different sedimentation periods. From left to right in each picture, NaCl was added in order to give a concentration of: 0.000 M, 0.001 M, 0.01 M and 0.1 M.*

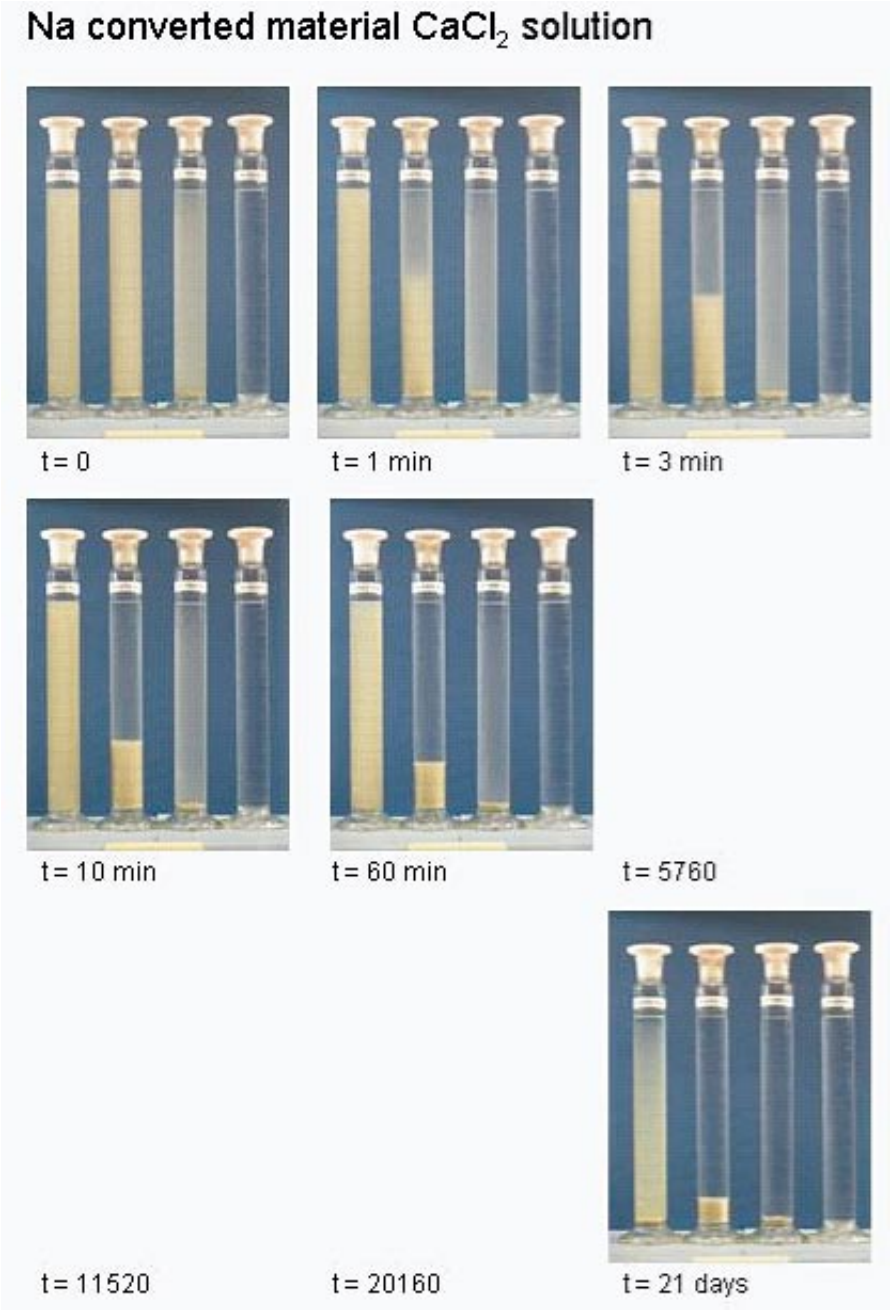

Figure A1-16. *Photographs of the MX-Na material in 250 ml water solutions after different sedimentation periods. From left to right in each picture, $CaCl_2$ was added in order to give a concentration of: 0.001 M, 0.01 M, 0.1 M. The rightmost cylinder only contains water and no bentonite material.*

6 Discussion

According to double layer theory it is possible to roughly estimate the separation between the montmorillonite flakes at different salt concentrations and type of ions by use of:

$$\kappa = \sqrt{\frac{2Z^2F^2C_0}{\varepsilon_0\varepsilon_r RT}} \qquad (1)$$

where κ generally is called the Debye-Hückel parameter and

Z = charge of the cations

F = Faradays constant

C_0 = electrolyte concentration

ε_0 = permittivity of vacuum

ε_r = relative permittivity of the solvent

R = gas constant

T = temperature

The thickness of the diffuse layer is 1/κ and for the actual montmorillonite in sodium state the calculated basal spacings are shown in Figure A1-17.

Figure A1-18 shows experimental results from /Norrish 1954/, which is in fair agreement with the results calculated by use of the Debye-Hückel parameter.

E.g. The distance between the montmorillonite flakes is calculated to be around 200 Å in the lowest examined NaCl concentration (0.001 M). The sample containing 1 g of clay is then expected to have a volume of approximately 7 cm^3. From the photographs in Figure A1-14 it is obvious that the volume of the expanded clay also has a larger volume in the test with the highest salt concentration (0.1 M). However, in all samples there is a clear tendency of clay volume decrease with time, and the calculated values likely represent a final equilibrium stage.

The dramatic effect of Ca-ions compared with Na-ions is in agreement with the Schultze-Hardy rule for lyophobic sols which are stabilized only by double-layer interaction. The critical coagulation concentration is largely dependent on the valence of the clay counter-ions but practically independent of the specific character of the various ions and of the charge and type of the co-ions. Typical critical coagulation concentrations for monovalent ions are 100 mM, for divalent ions 1 mM, and for trivalent 0.1 mM.

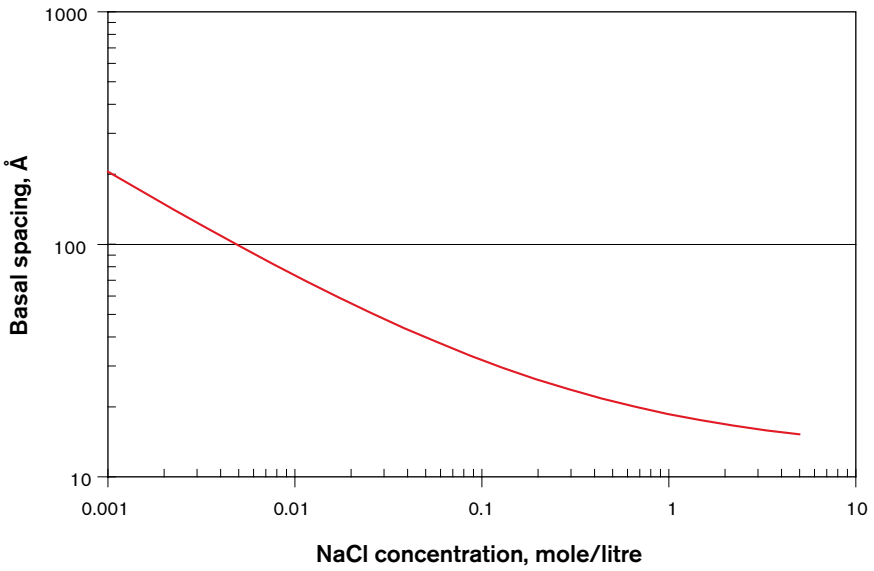

Figure A1-17. *Basal spacing in bentonite calculated from the Debey-Hückel parameter according to Equation 1.*

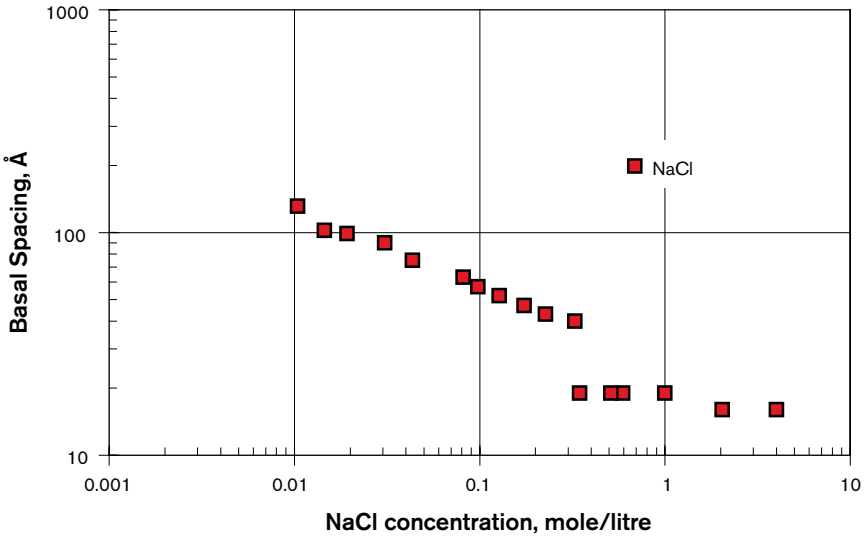

Figure A1-18. *Norrish experimental data /Norrish 1954/.*

It is not possible to perform ion chromatography (IC) analysis of test solutions without pre-filtration, due to practical reasons, and the results are thereby only representative for dissolved substances. However, the ICP-AES technique admits analyses of untreated solutions including colloids. The present analyses show typical montmorillonite ratios between Si, Al, Fe and Mg in the tests where colloids are present according to laser measurement (Figure A1-9 to A1-12). The analyses give typical montmorillonite "fingerprints" which may be used for qualitative information of the colloids, and to some extent also for quantification (Figure A1-9 and A1-10), at least at a relatively high content of colloids.

7 Conclusions

The results from the settlement tests may be summarized as follows:

- Colloid stability, achieved from the sedimentation rate tests, is strongly affected by the salt concentration in the test solutions; the critical concentration for a fast coagulation (sedimentation in three weeks) in the sodium case is between 10 and 100 mM.
- Divalent ions have a much more pronounced effect on stability compared to monovalent ions; the critical concentration for a relatively fast coagulation in the calcium case is around 1 mM.
- Concentration below critical coagulation concentration does not stop sedimentation but makes it much slower.
- The bentonite material seems in principle to follow the Schultze-Hardy rule.

In principle, the results do confirm previous laboratory tests /Le Bell 1978/.

Further, the ICP/AES analyses of test solutions show that the results are typical for the clay mineral and can be used for identification and to some extent also for quantification of colloids in the water.

8 References

Müller-Vonmoos M, Kahr G, 1983. Mineralogiche Untersuchungen von Wyoming Bentonit MX-80 und Montigel. NTB 83-12, Baden.

Le Bell J C, 1978. Colloid chemical aspects of the “confined bentonite concept”. KBS Teknisk Rapport 97, Stockholm 1978.

Norrish K, 1954. The swelling of montmorillonite. Trans. Faraday Soc. 18, 120–134.

Appendix 2

Bentonite colloid stability

– Effects of bentonite type, temperature, pH and ionic composition in solution

Susanna Wold, Trygve Eriksen
KTH

June 2003

Edited by: Susanna Wold, KTH, September 2005.

Contents

1 Background

Colloids are small particles with diameters between 1 and 1,000 nm and, due to the Brownian motion can stay in solution for long time periods. Possible radionuclide carrying colloids in groundwater are clay and humic/fulvic colloids, as well as mineral oxides and silicates. The bentonite barrier itself can, when in contact with a water bearing fracture, release bentonite colloids. If the colloids released are stable they can transport radionuclides to the geosphere. Therefore the colloid stability in solutions in contact with bentonite and the influence of background electrolyte concentration, type and amount of bentonite and temperature has been studied.

2 Experimental

Two types of bentonite were used in the experiments.

1. MX-80. Clay content 85% and montmorillonite 80–90 wt % of this fraction. Remaining silt fraction contains quartz, feldspar and some micas, sulfides and oxides.
2. Na-bentonite. Prepared from MX-80 with the accessory minerals removed /Wieland et al. 1994/.

Sodium perchlorate solutions 0.01, 0.1 and 1 M were used in the experiments. All solutions were prepared from analytical grade chemicals and Millipore deionized, triple distilled water.

3 Experimental setup

Graduated 250 ml glass cylinders, 5 cm in diameter, and with glass lids were used throughout the experiments. Different amounts of bentonite were poured into solutions of varying ionic strength using two techniques.

1. Dry bentonite was poured into the solutions so that particles could settle separately. The suspensions were left standing for one day, after which the suspensions were shaken. This bentonite is referred to as dry bentonite.
2. Dry bentonite was poured into graduated cylinders. The solutions were then poured in to the bentonite and it was left to absorb the solutions for 5 minutes; the solutions were then poured into the cylinders. This bentonite is referred to as wet bentonite.

The cylinders were placed in a thermostat box for one week with the temperature set at 20°C and 60° ± 0.2°C. pH and conductivity in the solutions were measured daily. A u-formed syringe was used for sampling to avoid disturbance of the bentonite.

3.1 PCS – Photon Correlation Spectrocopy

The signal in the PCS is roughly proportional to the concentration of colloids. To enable measurements of particle concentration as well as particle size distributions, the PCS equipment was calibrated with solutions containing latex colloids with defined average sizes.

The colloidal size distribution and colloidal concentration was measured at a wavelength of 488 nm with a dynamic light scattering instrument (90 Plus Particle Size Analyzer) equipped with a 2 W Lexus Laser Model 95 Ion Laser. The data were evaluated with Brookhaven size particle software.

3.2 ICP-MS and ICP-AES analysis

To follow the chemistry in the water in contact with the bentonite, 20 ml water samples were acidified with 0.5 ml 65% suprapure HNO_3 in acid washed vessels and sent to SGAB commercial laboratory for ICP-MS, ICP-AES analysis. The ICP analysis provides the concentration of a wide range of metals. Montmorillonite is assumed to be the potential provider of colloids even if the assessory minerals can also contribute. Al, Si are markers for the bentonite colloids in solution. There is, however a relation between Al concentration and colloid concentration, which is not valid for Si, since SiO_2 is more soluble /Degueldre et al. 1996/.

4 Results and discussion

Very low concentrations, ≤ 0.5 mg/L colloids are found in 0.1 and 1 M $NaClO_4$ solutions regardless of the way the bentonite is initially introduced to the solutions or the amount of bentonite added. The mean sizes of the colloids are in the range of 50 to 500 nm. At 60°C the colloid concentration is slightly higher than at 20°C, but the tendency is otherwise the same.

The Al- and colloid concentrations follow each other, which is why it seems reasonable to use Al as a marker for colloids. Filtration of the samples to separate the colloids from the solution is optimal, but the volumes in these experiments are too low to enable collection of detectable concentrations of colloids. It can be seen that the bentonite expands at low but not at high background electrolyte concentrations. The osmotic pressure is high when Na^+ concentration is low in the water and colloids are released.

At temperatures of 20° and 60°C the colloid concentrations are lowest at pH 7.8 to 8.4 with increasing concentration at both lower and higher pH. At low Na^+ ionic strength, the osmotic pressure is high, the gel structure in the clay is very loose and colloids can form and migrate into the bulk water. The behaviour depends strongly on the cation, in this case Na^+ or Ca^{2+}.

Colloid stability depends on ionic strength of solution. High ionic strength favors aggregation and flocculation /Luckham and Rossi 1999/, therefore colloids will settle with time.

The Na bentonite expanded significantly in the experiments with background electrolyte concentrations of 0.01 and 0.1 M. Almost no clear water zone was observed. The water contained high Al concentrations compared to the parallel experiments with MX-80. The colloid concentrations were also higher than in the experiments with MX-80. In the Na bentonite experiments the osmotic pressure was high and there were no ions with a higher charge like Ca^{2+} and Mg^{2+} which could compress the montmorillonite sheets. The texture was very loose, and ions and colloids could migrate into the bulk water.

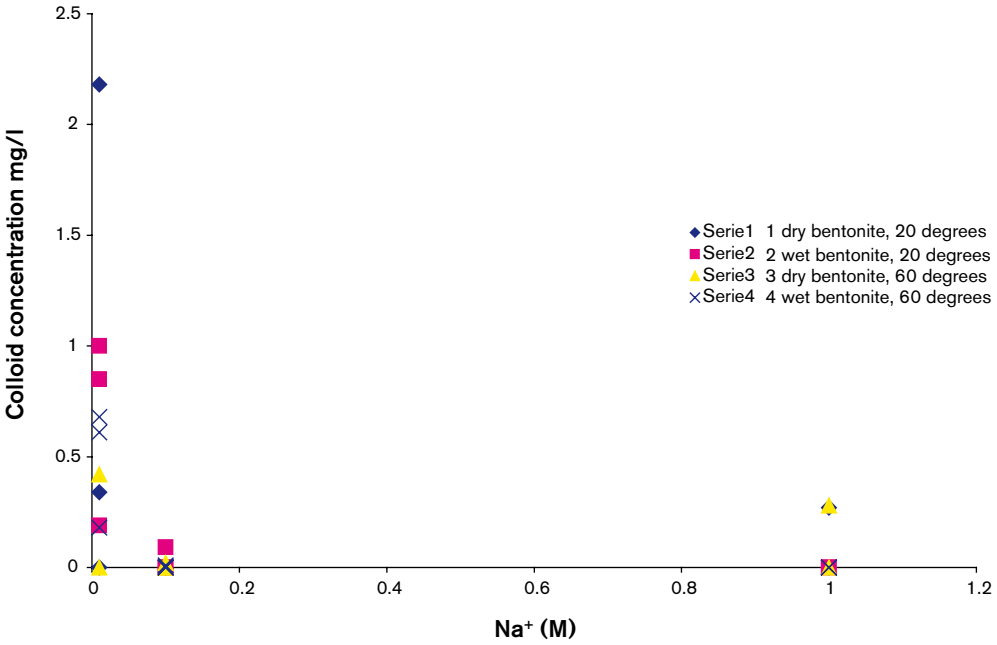

Figure A2-1. *Colloid concentration as a function of Na^+ concentration in supporting electrolyte. The data set includes both experiments with MX-80 and Na-bentonite. The highest value is from a Na-bentonite experiment.*

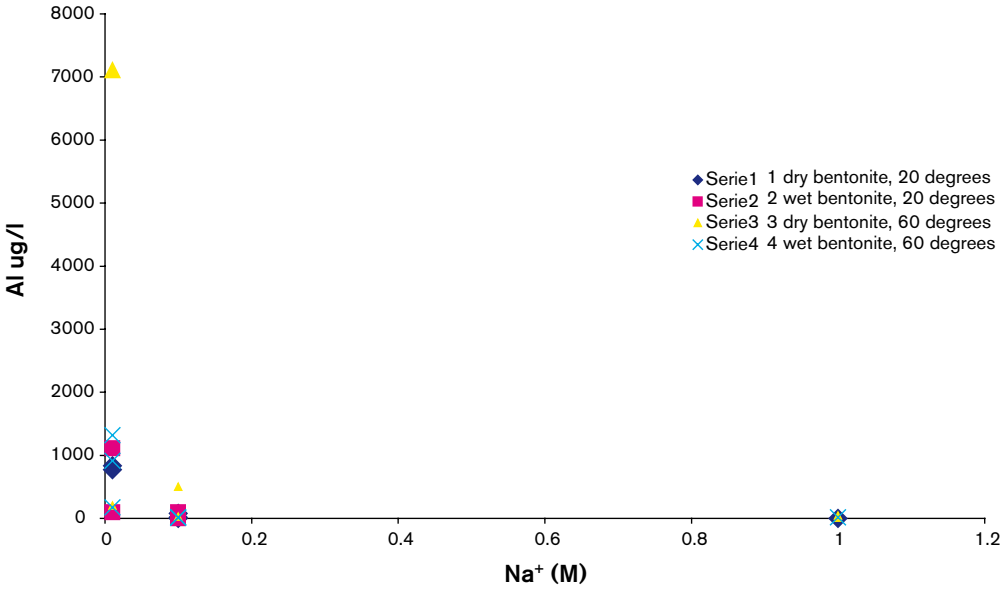

Figure A2-2. *Aluminium concentration as a function of Na^+ concentration in supporting electrolyte. The data set includes both experiments with MX-80 and Na-bentonite. The highest value is from a Na-bentonite experiment.*

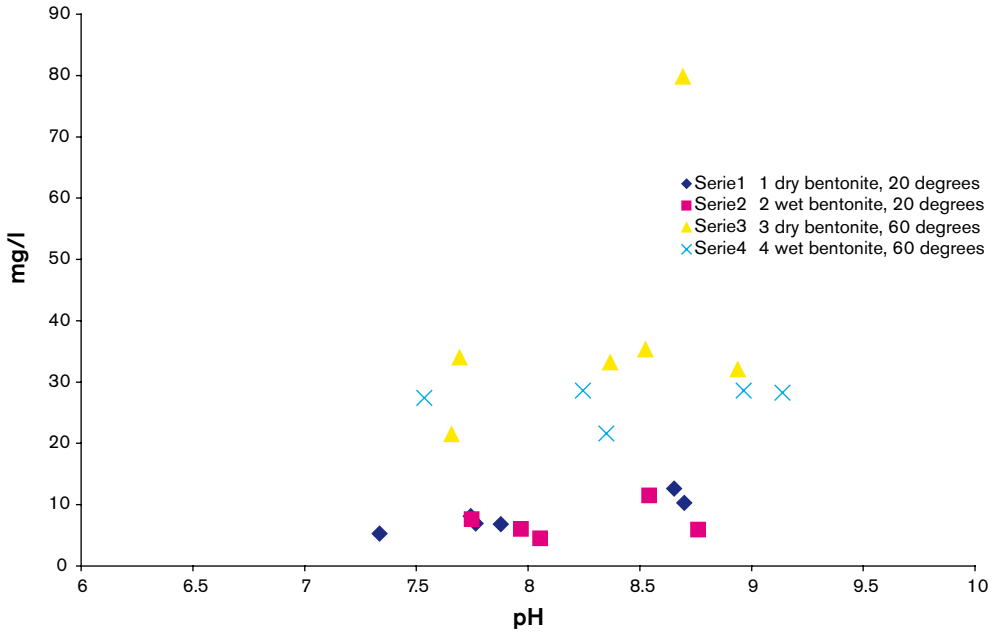

Figure A2-3. *Colloid concentration as a function of pH. The data set includes both experiments with MX-80 and Na-bentonite. The highest value origins is a Na-bentonite experiment.*

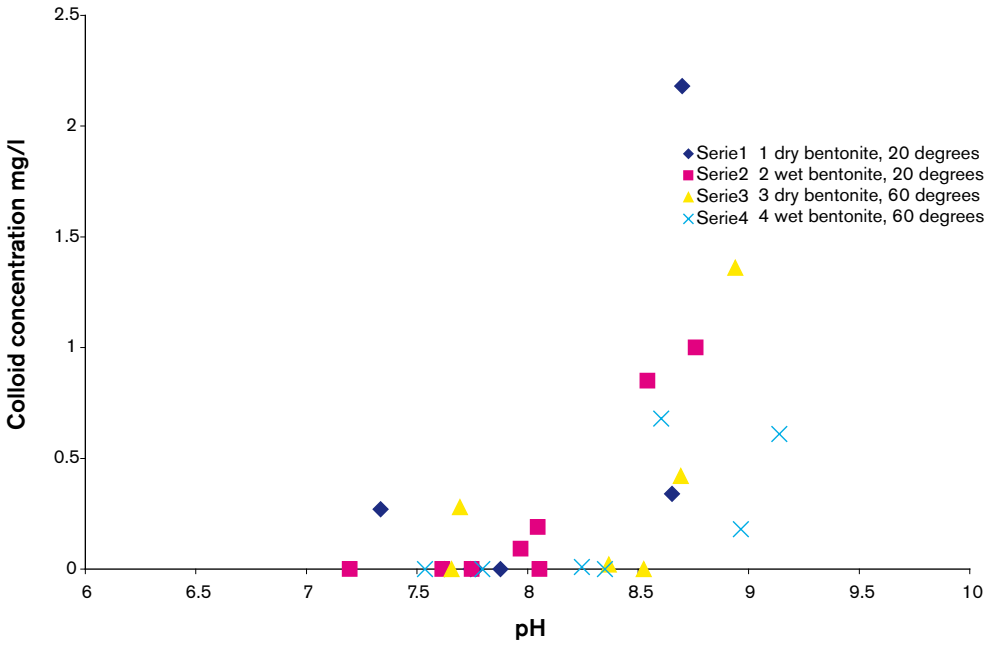

Figure A2-4. *Colloid concentrations as a function of pH. The data set includes both experiments with MX-80 and Na-bentonite. The highest value is from a Na-bentonite experiment.*

Table A2-1. Overview of analytical data.

Volume (ml)	Clay	Type wet/dry	Amount (g)	Ionic strength (M)	pH	conc-PCS mg/l	Ca mg/l	Mg mg/l	Al µg/l	Si mg/l
250	MX-80	d	5	0.01	8.7	2.2	2.96	0.57	771	9.5
250	MX-80	d	10	0.01	8.7	0.3	3.68	0.73	833	11.8
250	MX-80	d	5	0.1	7.9	0	37.1	5.15	1.54	6.8
250	MX-80	d	10	0.1	7.8	0	42.9	5.44	14.2	6.9
250	MX-80	d	10	1	7.3	0.3	153	21.5	–	5.3
250	Na	d	2	0.01		–	–	–	–	–
250	MX-80	d	5	1	7.6	0	–	–	–	–
250	Na	d	2	0.1	7.7	0	2.12	3.30	77.7	8.0
250	MX-80	w	5	0.01	8.8	1.0	2.34	0.35	95	5.8
250	MX-80	w	5	0.1	8.1	0	27.1	3.88	7.25	4.5
250	MX-80	w	5	1	7.6	0	–	–	–	–
250	MX-80	w	10	0.01	8.0	0.2	–	–	–	–
250	MX-80	w	10	1	7.2	0	–	–	–	–
250	MX-80	w	10	0.1	8.0	0.1	30.2	4.6	2	6.0
250	Na	w	2	0.01	8.5	0.9	0.16	0.44	1,110	10.4
250	Na	w	2	0.1	7.7	0	1.96	3.09	97.5	7.5
250	MX-80	d	5	0.01	8.9	1.4	3.03	0.48	205	31.9
250	MX-80	d	10	0.01	8.7	0.4	40.5	12.6	7,110	72.7
250	MX-80	d	5	0.1	8.4	0	44.7	4.37	29	33.2
250	MX-80	d	10	0.1	8.5	0	47	4.79	501	34.8
250	MX-80	d	5	1	7.7	0.3	115	11.1	43.6	34
250	Na	d	2	0.1		–	–	–	–	–
250	Na	d	2	0.01		–	–	–	–	–
250	MX-80	d	10	1	7.7	0	191	26.8	8.72	21.5
250	Na	w	2	0.1		–	–	–	–	–
250	MX-80	w	5	0.01	9.0	0.2	3.34	0.57	915	27.7
250	MX-80	w	5	0.01	9.1	0.6	4.21	0.63	172	28.1
250	MX-80	w	5	0.1	8.4	0	23.3	3.38	17.9	21.6
250	MX-80	w	5	0.1	8.2	0.01	42	4.86	10.5	28.6
250	MX-80	w	5	1	7.5	0	105	10.9	14.5	27.4
250	Na	w	2	0.01	8.6	0.7	0.454	0.64	1,320	13.8
250	MX-80	w	5	1	7.8	0	–	–	–	–

5 References

Degueldre C, Pfeiffer H-R, Alexander B, Wernli B, Bruetsch R, 1996. Colloid properties in granitic groundwater in granitic groundwater systems. I: Sampling and characterisation. Applied Geochemistry, 11 (677–695).

Luckham P, Rossi S, 1999. The colloidal and rheological properties of bentonite suspensions. Advances in Colloid and Interface Science, 82 (43–92).

Wieland E, Wanner H, Albinsson Y, Wersin P, Karnland O, 1994. A surface chemical of the bentonite/water interface and its implication for modelling the near field chemistry for spent fuel. SKB TR 94-26. Svensk Kärnbränslehantering AB.

Appendix 3

In-situ colloid detection in granite groundwater along the Äspö HRL access tunnel

Wolfgang Hauser, Robert Götz, Horst Geckeis, Bernhard Kienzler
Institut für Nukleare Entsorgung (INE)
Forschungszentrum Karlsruhe GmbH

The present work was performed in the framework of the Project Agreement between the Bundesministerium für Wirtschaft und Technologie (BMWi) and Svensk Kärnbränslehantering AB (SKB) in cooperation in the Äspö Hard Rock Laboratory (HRL).

Contents

1 Motivation

In safety assessment for a repository of radioactive waste, aquatic colloids existing in natural water play a role as carrier for the migration of radionuclides, mainly actinide ions from the waste to the biosphere /1, 2, 3, 4, 5/. Apart from actinide oxide/hydroxide colloids, colloids released from backfill bentonite and background colloids present in natural groundwater are of particular importance. In this study the amount of background colloids in natural groundwater in the Swedish Hard Rock Laboratory (HRL) granite formation is determined. The aim is to investigate the colloid occurrence in different groundwater types without any interference by sampling.

The average size of colloids in natural water ranges from less than 50 nm up to a few hundred nm with particle concentrations from ppt (ng/L) to a few hundred ppb (µg/L). With conventional light scattering techniques, aquatic colloids of dilute concentrations are often not detectable /6, 7, 8/. The Laser-Induced Breakdown Detection (LIBD) has been developed for the ultra-trace detection of colloids. The advantage of this method is a several orders of magnitude higher sensitivity particularly for colloids with a size < 100 nm /9, 10, 11, 12/.

A mobile LIBD setup built for in-situ measurements /13/, equipped with a new high-pressure detection cell is used for the background colloid detection in natural groundwater along the access tunnel of the granite Hard Rock Laboratory Äspö, situated at Oskarshamn/ Sweden. The investigations are performed within the scope of an international collaboration between the German 'Institut für Nukleare Entsorgung (INE)' of the 'Forschungszentrum Karlsruhe' and the Swedish 'Svensk Kärnbränslehantering AB (SKB)' as part of the SKB project COLLOID /14/.

2 Experimental

2.1 LIBD instrumentation

The principle of LIBD is based on the generation of a dielectric breakdown in the focus region of a pulsed laser beam /8, 9, 10, 11, 12, 15, 16/. As the threshold energy (irradiance) to incite breakdown for solids is lower than for liquids or gas, the breakdown can be generated selectively on particles dispersed in solution at suitable pulse energy. A schematic diagram of the mobile LIBD set-up used in the present work is shown Figure A3-1. A pulsed laser beam with a frequency of 15 Hz at 532 nm wavelength from a small Nd: YAG-laser (Continuum Minilite I) is focused (15 mm focal length) into the center of a flow-through detection cell, after passing through a variable attenuator and a beam splitter. The plasma generated at a breakdown event is monitored by a microscope equipped with a CCD monochrome camera triggered by the incident laser pulse and recorded by a PC controlled image processing system. A breakdown shock wave propagated in the sample solution is detected simultaneously by an acoustic sensor (piezoelectric transducer) /17/ that is connected to the surface of the cell. Both, the energy and the acoustic signal are recorded by an analog-digital converter interface in a PC. The mobile instrumentation of LIBD is combined with a Millipore ultra-pure water processing unit for on-line cleaning of the flow-through detection cell of LIBD. The whole system, which is set up to a compact mobile unit is transported by a van for the field experiment.

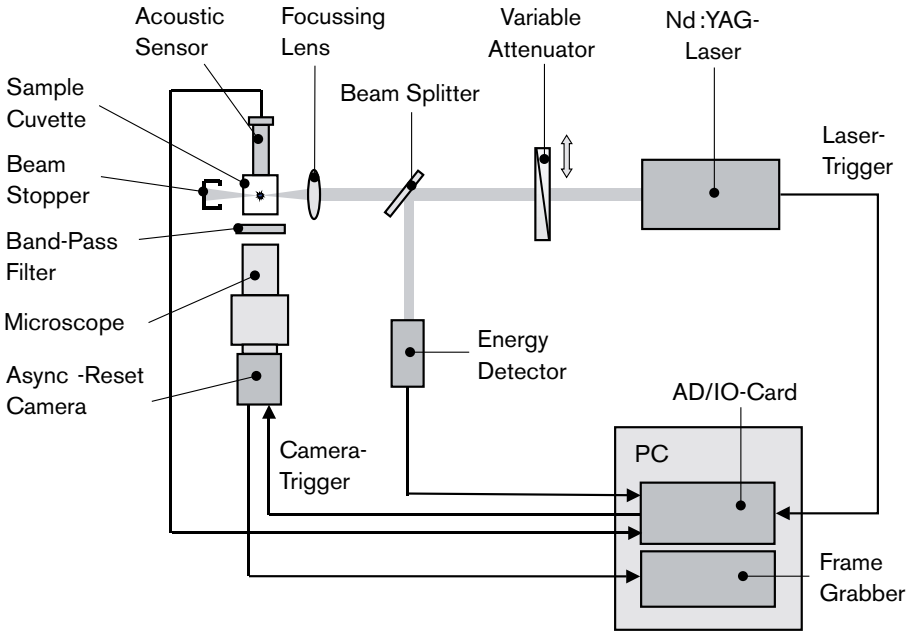

Figure A3-1. *Schematic diagram of the mobile laser-induced breakdown detection system.*

2.2 High-pressure flow-through detection cell

The LIBD has been operated up to now under low pressure conditions with commercially available quartz detection cells (fluorescence cells) for batch or flow-through sampling. These cells have a sample volume of 3 ml at 10 mm absorption length. A new flow-through detection cell had to be developed constraining a water pressure of 32 bars for the investigations in the Äspö tunnel, down to a depth of about –420 m. Figure A3-2 shows the new high-pressure detection cell developed by INE. Without changing the optical path of the laser light, the detection cell fits into the same mount used for the silica cell. The new cell, fabricated from PEEK (polyether etherketone) is lined outside with a stainless steel housing (black parts in Figure A3-2). Four optical windows, one at each side are used for the passing laser light (absorption length 12 mm), the microscope and for inspection. They consist of sapphire 2 mm thick. The groundwater flow enters the inner cell volume of 0.8 ml from the base via a PEEK tubing. The outlet is at the top of the cell. The high-pressure detection cell is successfully tested for water pressure of up to 60 bars.

2.3 LIBD calibration with the high-pressure flow-through detection cell

The quantitative measurement of colloids in the field experiment requires the stable alignment of all optical components of the LIBD system. The exact adjustment of the beam alignment is performed by optical inspection with a laser beam profiler. According to the method described in /14/ the laser pulse energy is adjusted to a constant value, at which the highest signal-to-background ratio is attained for the colloid detection. Such operational energy is selected by comparing the breakdown probability of ‘ultra-pure water’ with that of colloid dispersion as a function of the laser pulse energy. The breakdown probability is appraised by the ratio of the observed breakdown events to the total number of laser trigger pulses[10]. The LIBD sensitivity, as determined with the pure water dispersion of polystyrene reference particles for the smallest size available (19 nm diameter), is attained down to a few ppt at the threshold energy of 1.4 mJ.

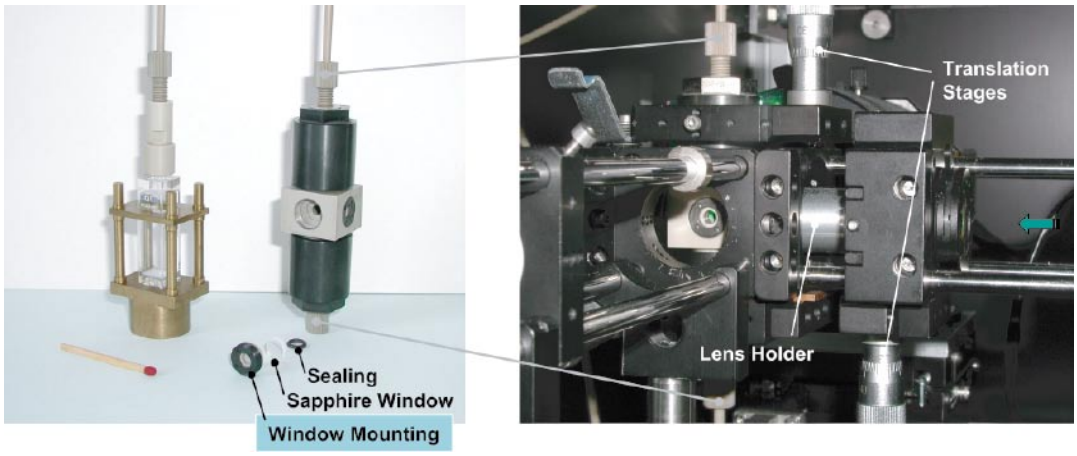

Figure A3-2. *LIBD high-pressure flow-through detection cell (left: flow-through silica detection cell).*

The calibration of the system with a silica detection cell (Hellma cuvette) to derive a colloid mass concentration, or number density, and an average colloid size by measuring the breakdown probability and the spatial extension of the breakdown event distribution in the laser pulse focus area have been described in detail /12, 13/. For the in-situ measurements the quartz detection cell is replaced by the high-pressure cell. Because of its different optical and geometrical properties, the LIBD system has to be re-calibrated completely.

2.4 Concentration calibration (constant energy detection)

The result of the concentration calibration with polystyrene reference particles of different sizes – from 19 nm up to 993 nm – is plotted in Figure A3-3.

Following the calibration, an effective focus volume V_{eff} (m^3) as a function of the particle diameter d(nm) is derived as

$$V_{eff} = 167.7\times10^{-18}\, d^{1.29} \qquad (1)$$

With this effective focus volume, the mass concentration C_p (ppb) of colloids in a given sample solution can be evaluated from the breakdown probability according to [13] with the known parameters for the present experiment:

$$C_p = 10^9(\rho_P / \rho_D)(1-(1-P_{bd})^{Vp\,/\,Veff}) \qquad (2)$$

Where ρ_P is the density of the particles (polystyrene particles $\rho_P = 1.05$ g/cm^3, for natural inorganic colloids $\rho_P = 2.7$ g/cm^3 is taken), ρ_D is the density of the dispersion medium (0.998 g/cm^3) and V_p is the particle volume calculated by $(4/3)\pi(d/2))^3$ with a hard sphere particle diameter d in nm.

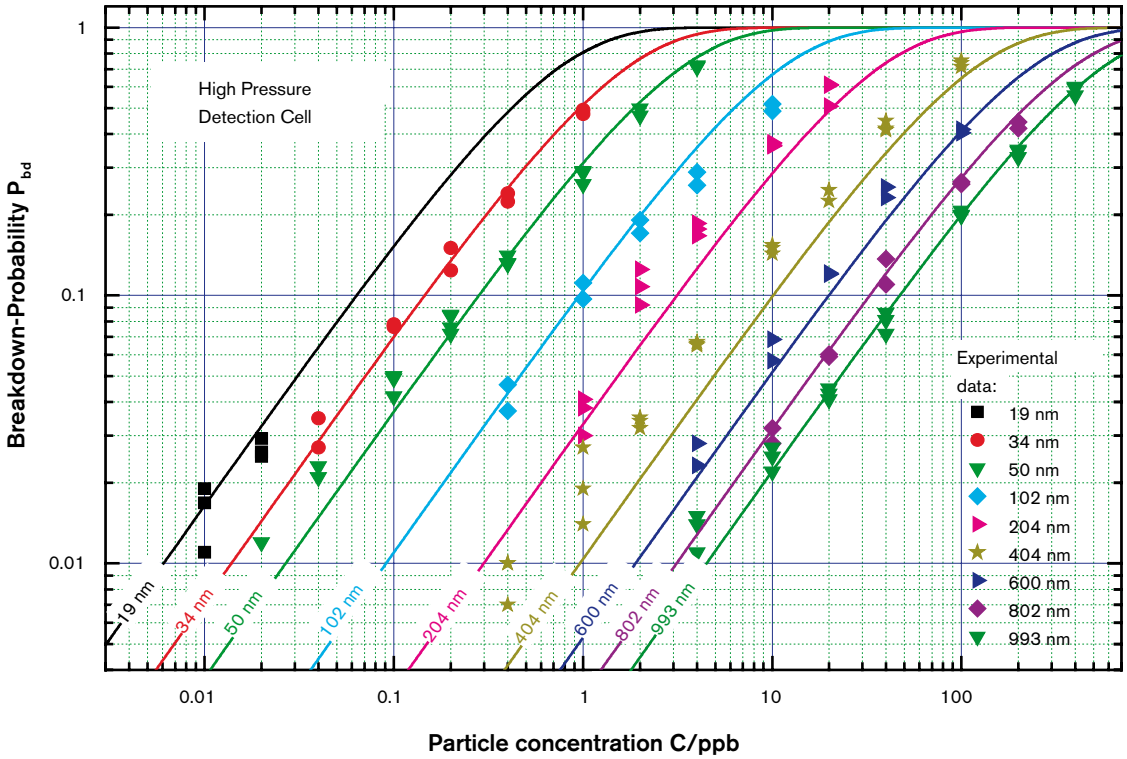

Figure A3-3. *LIBD concentration calibration with constant laser pulse energy (1.4 mJ) for the high pressure detection cell.*

2.4.1 Size calibration (constant energy detection)

The spatial extension of the breakdown event distribution in the laser pulse focus area is found to be a direct function of the particle. Such a distribution is determined in the direction of the laser beam axis (x-coordinate) by monitoring the number of breakdown events in the 2-D spatial area along the x-axis. The number of events N(x) can be well fitted to a Gaussian function by

$$N(x) = (A(x) / (w(x))(\pi / 2)^{1/2} \exp(-2 (x / w(x))^2. \quad (3)$$

A(x) corresponds to the area below the Gaussian curve. The full width at half maximum (FWHM) w(x) is related directly to the effective focus volume V_{eff} as given by Equation (1), thus increasing with a particle size increase. It has been demonstrated that w(x) is correlated linearly with the particle size (d). For the setup with the high-pressure detection cell, the average size of the predominant colloid population can be estimated according to the empirical relation:

$$d = (w(x)-(179.4 \pm 3)) / (0.647 \pm 0.011). \quad (4)$$

with w(x) in µm and d in nm.

For the practical application of this detection and evaluation method the limiting boundaries for the colloid detection must be taken into account. From Figure A3-3 it can be concluded that this method gives precise results for breakdown probabilities below about 0.8. For breakdown probabilities close to 1 the upper detection limit is reached, as there is no definite relation between breakdown probability and particle concentration. According Figure A3-3 it is, for example, not possible to determine colloid concentrations above 4 ppb for 50 nm particles. Therefore, an alternative method must be applied, particularly for highly concentrated colloid dispersions.

2.5 "S-curve" interpretation

As the effective focus volume V_{eff} of the breakdown event distribution in the laser focus region is related linearly with the particle size /11/, each effective volume has its own laser threshold energy. This means that the laser threshold energy can also be correlated to the particle size. Therefore, an average size of colloids can also be determined by a calibration of the laser threshold energy alone.

This threshold energy can be derived by detecting the breakdown-probability as a function of the laser pulse energy (s-curve detection). In Figure A3-4 the breakdown probability is plotted as a function of the laser pulse energy for 993 nm and 19 nm polystyrene reference particle dispersions with different particle concentrations and ultra-pure water. For 993 nm particle dispersions the breakdown probability significantly deviates from 0 (P_{bd} = 0.005) at the same threshold energy of 0.15 mJ for all particle concentrations. Above this size specific threshold energy the breakdown probability increases with the pulse energy. This threshold energy increases with decreasing particle diameter. For 19 nm dispersions the threshold energy is 1.15 mJ (P_{bd} = 0.005).

Furthermore Figure A3-4 demonstrates that the slope of the s-curves increases with the particle concentration without any variation in the threshold energy. For 19 nm and 993 nm particles significant changes in the shape of the s-curves are detected at low as well as at high concentrations. Therefore this method, called the s-curve interpretation method, can alternatively be applied to estimate an average particle diameter and concentration. Compared to the prescribed constant energy method (see Figure A3-3), the s-curve interpretation method (Figure A3-4) enlarges the detection range especially at higher particle concentrations. This is demonstrated in Figure A3-4, where the s-curves for 993 nm particle concentrations > 1 ppm are clearly separated.

However, in low colloid concentrated dispersion (optically transparent) the constant energy method provides the same precise result but in a much shorter detection time.

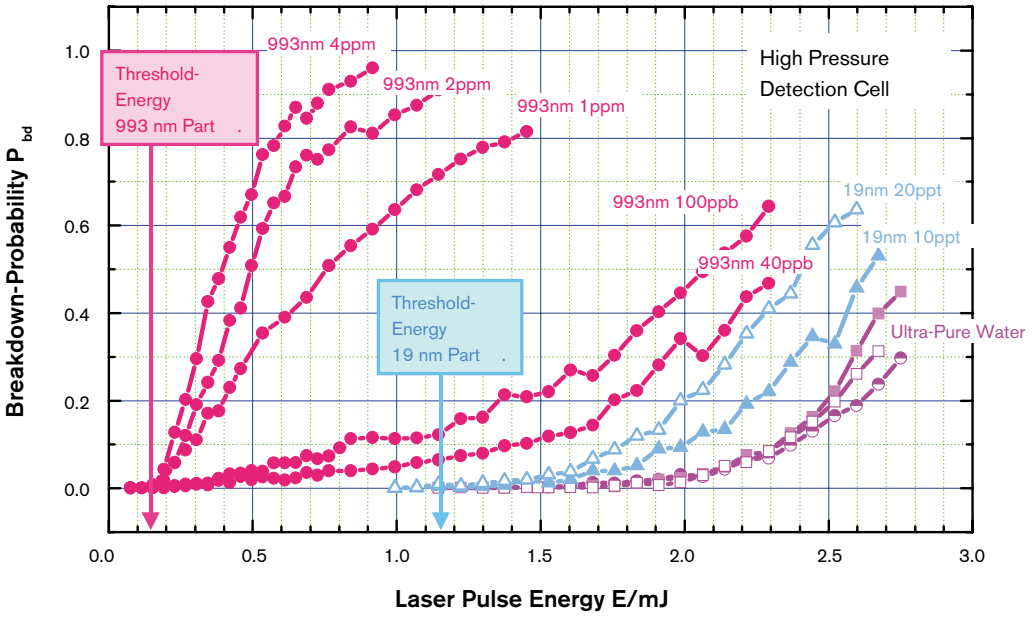

Figure A3-4. *Breakdown-probability as a function of laser pulse energy for different polystyrene reference particle dispersions and ultra-pure water (S-curve interpretation).*

2.6 Configuration of the detection system in the Äspö HRL tunnel

Along the 3.6 km long access tunnel of the Äspö Hard Rock Laboratory at depths from –70 m down to –416 m eight sampling locations with lined boreholes were selected by SKB. Each borehole, designated in Figure A3-5 contains one representative type of groundwater which can be characterized as a mixture of water of different origins, e.g. meteoric, Baltic sea, brine, glacial /18, 19/.

The complete LIBD detection system including the ultra-pure water processing unit was transported to Äspö, where all experiments were performed in the closed, heated transportation van. The instrumented van was installed close to the sampling boreholes, mostly on a ramp to guarantee a horizontal orientation of the setup (see Figure A3-6). For continuous operation, the water processing unit was supplied with fresh drinking water from an external reservoir, separately provided at each location.

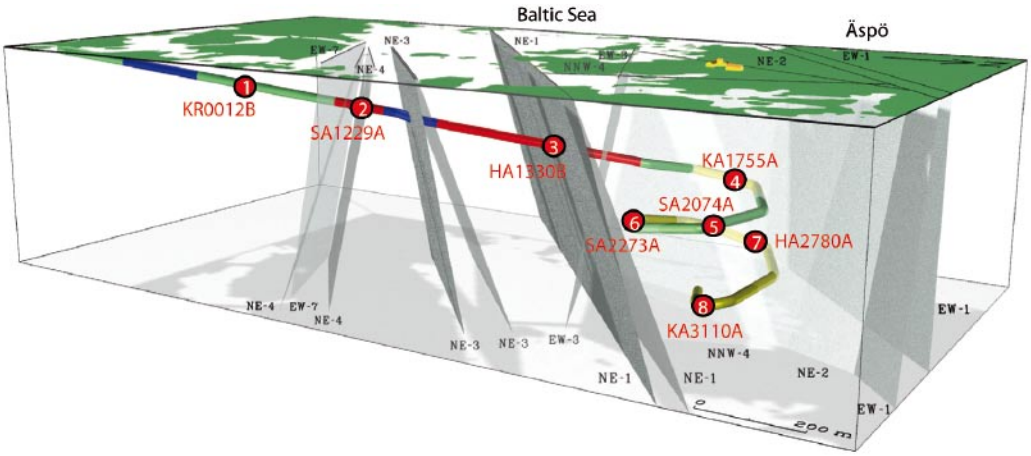

Figure A3-5. *LIBD sampling.*

Figure A3-6. *LIBD instrumentation in the Äspö Hard Rock Laboratory access tunnel.*

The boreholes were equipped with packers and internal tubing for collecting the groundwater in a preset sampling section of the granite rock fracture, several metres from the tunnel wall. The preset sections were between 9 m to 72 m long, as summarized in the sampling data of Table A3-1. From the sampling section the groundwater was conducted by an internal max 6 m long stainless steel or plastic tubing to the borehole valve, installed at the tunnel wall.

In order not to block the tunnel with the van, the LIBD setup had to be placed mostly in niches, several metres apart from the sampling boreholes. A plastic tube (inner diameter 4 mm) with a total length up to 100 m connected the borehole with a bypass valve as described in Table A3-1. This bypass valve was situated close to the instrument van. It was installed to reduce the natural groundwater flow rate of the borehole (max flow rate, see Table A3-1) to the selected flow rate in the LIBD detection cell. Figure A3-7 shows the configuration of the bypass valve between a borehole and the LIBD. The length of the PEEK tubing (inner diameter 2 mm) between the bypass valve and LIBD detection cell is 6–8 m. A constant flow rate through the detection cell of 4 ml/min was established by volume determination with time. The highest groundwater pressure of 33 bars was detected at the position of the lowest borehole – KA3110A. All other maximum borehole pressures are summarized in Table A3-1.

Table A3-1. Summary of borehole sampling configuration and bypass valve data.

	Borehole data			Bypass valve data		
Borehole ID	**Elevation m**	**Sampling section m**	**Internal tubing length m**	**External tubing length m**	**Max flow rate ml/min**	**Max pressure bar**
1 KR0012B	–69	1.2–10.6	1.2 (s)	0	325	5.9
2 SA1229A	–168	6.0–20.5	6.0 (s)	40 (p)	1,150	12.9
3 HA1330B	–82	5.6–32.5	5.6 (s)	55 (p)	290	≥ 8.0
4 KA1755A	–235	88.0–160.0	5.0 (p)	100 (p)	1,140	13.3
				0	2,400	14.4
5 SA2074A	–282	6.0–38.7	6.0 (s)	0	210	21.3
6 SA2273A	–306	5.8–20.0	5.8 (s)	75 (p)	1,050	16.2
7 HA2780A	–370	3.7–43.3	3.7 (s)	70 (p)	2,000	14.3
8 KA3110A	–416	20.1–28.6	5.5 (p)	0.5 (p)	2,400	32.8

(p) Plastic tubing.
(s) Stainless steel tubing.

Figure A3-7. *Bypass valve configuration.*

2.7 Groundwater sampling for chemical analysis

The various boreholes were sampled by SKB some days before the in-situ colloid detection campaign. Directly at each borehole valve, a 3 L glass bottle had been completely filled with the groundwater. Immediately after sampling the bottles were closed with a screwed-on plastic cap. No preparation of samples was performed. The samples were transported to Karlsruhe after the in-situ campaign for chemical analysis with IC, ICP-AES and DOC detection.

3 Results

3.1 LIBD detected colloid size and mass concentration

At the upper boreholes KR0012B, SA1229A, HA1330B, above –200 m depth, respectively, breakdown-probabilities close to 100% were detected with 1.4 mJ constant laser pulse energy for low, as well as for high groundwater flow rate. Therefore, the above described LIBD s-curve interpretation was applied.

This is shown in Figure A3-8 for groundwater KR0012B as an example. For a flow rate of 222 ml/min, the threshold energy corresponds to the threshold energy of a ~ 600 nm reference particle dispersion. From the slope, a colloid mass concentration of ~ 600 ppb is derived. The s-curve for a flow rate of 4 ml/min, with significantly higher threshold energy, characterizes dispersion with colloids of ~ 404 nm average diameter and ~ 300 ppb mass concentration.

For breakdown probabilities which were significantly below 100%, average colloid diameter and colloid concentration were generally detected with constant laser pulse energy by applying image processing as described above. The lowest breakdown probability of 0.2% was detected in groundwater KA1755A. For this breakdown probability, which is in the order of the breakdown probability of ultra-pure water an average colloid diameter of 57 nm with a colloid concentration of 14 ppt was evaluated. Additionally, the s-curve

interpretation method was applied to verify the data. According to Figure A3-9, a colloid diameter of < 19 nm and < 10 ppt colloid concentration must be derived for this groundwater, which is in the same order of magnitude as the data obtained with constant laser pulse energy.

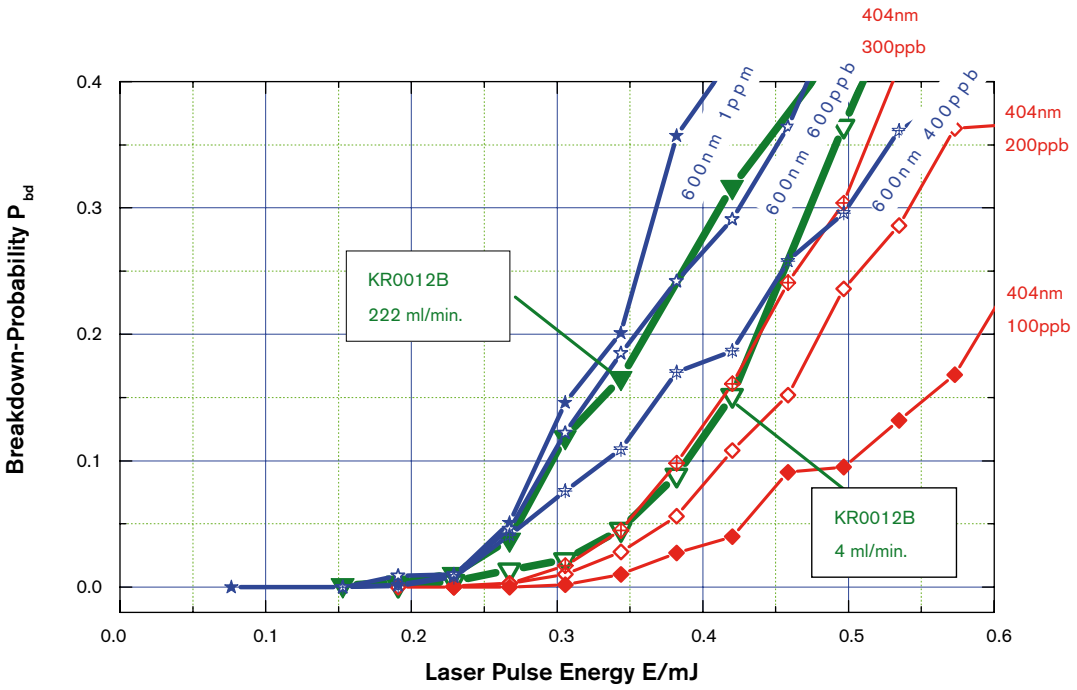

Figure A3-8. *S-curve interpretation for groundwater KR0012B (data compared with polystyrene reference particles in ultra pure water).*

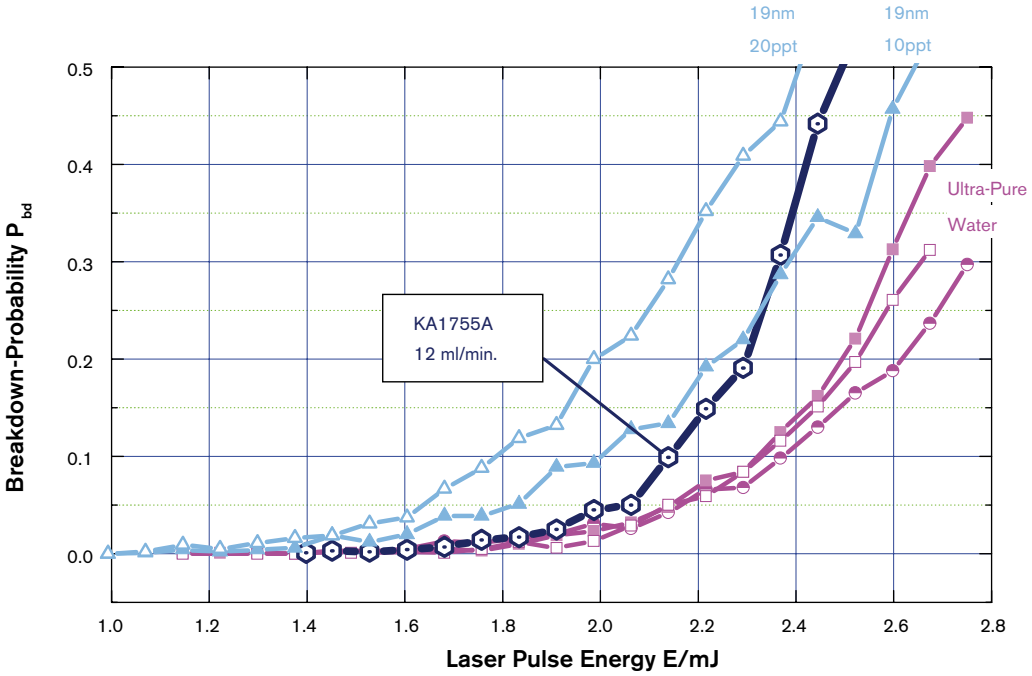

Figure A3-9. *S-curve interpretation of groundwater KA1755A (data compared with polystyrene reference particles in ultra pure water).*

The LIBD data for the different groundwaters are summarized in Table A3-2. At each borehole position the groundwater flow rate adjusted at the bypass valve varies between 4 ml/min and the max flow rate given in Table A3-1. Groundwater properties arising from visual inspection on site, such as "gas generation" (gas bubbles in the dispersion) and "colored dispersion" give some casual information about pressure fluctuations and the amount of colloids. Colloids in KA1755A were detected using 100 m external tubing and no external tubing between bypass valve and borehole in order to investigate the influence of the plastic tubing.

The different groundwaters were sampled and analyzed in September 2000 by SKB (Table A3-3) and one week before the LIBD detection in October 2001 (Table A3-4) by INE. Apart from the total amount of Fe both analyses give comparable results. It is evident, that the lower by several orders of magnitude Fe-content in the October 2001 samples is caused by contact with oxygen. Initially dissolved Fe(II) is oxidized to form FeOOH which is mostly found as precipitated red brown flocks at the bottom of the glass bottles.

Table A3-2. Summary of LIBD results.

				Visual inspection		LIBD data evaluation		
Borehole ID	**Elevation m**	**Tubing length**	**Flow rate ml/min[1]**	**Gas-gen**	**Colrd disp**	**Bd prob %**	**Colloid diameter nm**	**Colloid conc ppb**
1 KR0012B	-69	0	4	no	yes	100	~ 404[2]	~ 300[2]
			222			100	~ 600[2]	~ 600[2]
2 SA1229A	-168	40	4	no	yes	92	~ 600[2]	~ 190[2]
			930			100	~ 300[2]	~ 110[2]
3 HA1330B	-182	55	4	no	yes	100	~ 993[2]	~ 1,000[2]
			125			100	~ 404[2]	~ 100[2]
4 KA1755A	-235	100	4	yes	no	69.5	631[3]	630[3]
			550			3.0	281[3]	4.1[3]
		0	12			0.2	< 19[2], 57[3]	< 0.01[2], 0.014[3]
			1,400			0.4	129[3]	0.15[3]
5 SA2074A	-282	0	4	no	yes	100	~ 600[2]	~ 600[2]
			190			38.8	354[3]	99[3]
6 SA2273A	-306	75	4	no	yes	14.5–26.0	175[3]–263[3]	9.2[3]–35.5[3]
			900			46.0	218[3]	53[3]
7 HA2780A	-370	70	4	yes	no	2.3–18.0	165[3]–296[3]	1.2[3]–19[3]
			11			28.5	456[3]	102[3]
			20			63.1	627[3]	525[3]
			920			14.5	244[3]	16.5[3]
			1,100			17.2	245[3]	19.6[3]
8 KA3110A	-416	0.5	4	no	yes	9.9	365[3]	22[3]
			2,400			9.4	333[3]	18[3]

[1] Flow rate adjusted at bypass valve.
[2] Data s-curve evaluated.
[3] Data evaluated with constant laser pulse energy.

Table A3-3. Groundwater composition (SKB data, sampling date: Sept 2000).

Borehole ID	Na mg/l	K mg/l	Ca mg/l	Mg mg/l	Cl mg/l	SO_4 mg/l	HCO_3 mg/l	Br mg/l	F mg/l	Si mg/l	Fe_{tot} mg/l	Mn mg/l	Li mg/l	Sr mg/l	DOC mg/l	pH pH unit
Measurement uncertainty ⇒	5%	5%	5%	5%	5%	5%	5%	10%	10%	5%	10%	5%	5%	5%	0.1 mg/l	0.1 unit
1 KR0012B	217	3.7	54	11.6	250	47.0	311	1.5	1.4	6.8	0.253	0.18	0.040	0.89	16.0	7.5
2 SA1229A	1,520	25.7	315	131.0	3,120	252.0	264	11.9	1.3	6.7	1.833	0.71	0.093	4.87	7.0	7.2
3 HA1330B[1]	1,610		648	128.0	3,920		252									7.4
4 KA1755A	2,960	10.5	4,130	35.5	11,430	613.0	9	87.5	1.5	4.3	0.190	0.28	2.510	70.00	< 1.0	7.8
5 SA2074A	1,230	9.3	448	85.1	2,770	251.0	169	9.6	1.2	6.1	0.160	0.49	0.150	6.40	5.0	7.7
6 SA2273A	1,570	14.3	684	105.0	3,770	264.0	159	19.0	1.3	5.7	0.803	0.80	0.317	10.20	5.0	7.4
7 SA2783A[2]	3,370	13.5	4,980	36.5	13,920	655.0	13	109.5	1.7	4.3	0.106	0.30	3.080	84.30	1.0	7.8
8 KA3110A	1,470	30.4	372	128.0	3,080	277.0	185	11.7	1.6	5.3	1.234	0.76	0.138	5.40	7.0	7.5

[1] Sampling date: Oct 1992.
[2] Similarities with HA2780A.

Table A3-4. Groundwater composition (INE chemical analysis, sampling by SKB, date: Oct 2001).

Borehole ID	Na mg/l	K mg/l	Ca mg/l	Mg mg/l	Cl mg/l	SO_4 mg/l	NO_3 mg/l	PO_4 mg/l	F mg/l	Si mg/l	Fe_{tot} mg/l	Mn mg/l	Li mg/l	Sr mg/l	DOC mg/l	Pre[1]
Measurement uncertainty ⇒	5%	5%	5%	5%	5%	5%	5%	5%	5%	5%	50%	5%	5%	5%	0.1 mg/l	
1 KR0012B	167	2.1	44	9.4	136	30.7	< 0.1	< 0.1	0.5	6.75	0.11600	0.141	0.031	0.76	15.7	no
2 SA1229A	1,560	32.9	295	128.0	3,381	234.2	< 0.1	< 0.1	5.4	6.15	0.00296	0.714	0.115	4.60	7.0	yes
3 HA1330B	1,590	20.8	348	120.0	3,496	305.2	< 0.1	< 0.1	5.7	4.89	0.00283	0.766	0.117	4.86	6.2	yes
4 KA1755A[2]	2,940	8.6	3,900	32.2	11,044	565.7	31.3	28.7	19.3	4.06	0.11300	0.250	2.240	4.06	1.9	no
5 SA2074A	1,400	11.2	414	84.6	2,913	234.3	< 0.1	< 0.1	4.7	5.70	0.00249	0.464	0.172	5.80	5.4	no
6 SA2273A	1,620	18.6	719	105.0	4,234	260.9	< 0.1	< 0.1	7.1	5.22	0.00344	0.774	0.421	10.60	4.3	yes
7 HA2780A	3,400	21.2	4,510	48.3	15,470	620.4	< 0.1	3.7	22.3	4.11	< det. limit	0.250	4.730	66.20	1.5	no
8 KA3110A	1,490	45.1	277	133.0	3,193	257.9	< 0.1	< 0.1	4.5	5.09	0.00208	0.737	0.100	3.81	6.3	yes

[1] Precipitation in 3 L sampling bottle (red brown flocs).
[2] Sampling date: Jan 2002.

3.2 Interpretation

Colloid concentrations determined by LIBD vary from less than 0.1 ppb to 1,000 ppb. They do not only vary in samples taken at different locations; they also depend on flow rates and the lengths of the tubing from the borehole to the LIBD flow through cells at each sampling site. In the case of borehole KA1755A a clear decrease of colloid concentration appeared when the tubing length was considerably shortened from 100 m to direct coupling. A decrease in the measured colloid population is also achieved by increasing the flow rate in the long tubing. Both facts indicate colloid generation by the in-diffusion of O_2 through the polyamide tube walls. Dissolved Fe(II) is successively oxidized to form colloidal FeOOH. Both shortening the tubing length and increasing the sample flow rate diminishes the O_2 input and thus the colloid formation. Increasing the flow rate to very high rates of 1,400 ml/min and direct connection of the LIBD to the borehole, entails slightly increased colloid concentration. The reason for this finding is most likely a wash out of colloidal material in the water conducting fractures as a consequence of the sheer force of the high flow rates (mechanical erosion). In conclusion, it is assumed that the lowest value for the

colloid concentration analysed at this sampling location is considered to be the one least affected by artefacts. Similar relationships regarding the colloid concentration for different water flow rates can also be found in other sampling boreholes. The groundwater sampled at HA2780A contains the lowest Fe concentration of 0.104 mg/L and thus appears to be less sensitive to colloid formation through O_2 contact. As a consequence, the lowest colloid concentrations are determined at the lowest flow rates. Higher sample flow rates yield increasing colloid concentrations due to colloid release from the fracture infill. The LIBD signals determined for this water fluctuate significantly with time. They are correlated with pressure changes observed at the borehole outlet. The variation of colloid concentrations therefore can be interpreted as a consequence of colloid release due to pressure changes in the environment of the borehole.

For the following considerations, it is assumed that the lowest colloid concentrations measured at each individual borehole are those "closest to the truth" i.e. artefacts are minimized as much as possible. In general, the amount of colloids present in a given groundwater are always found to correlate with ionic strength, presence of stabilizing organic matter (fulvic/humic acid) and chemical or mechanical disturbances /see e.g. 19, 20/. In the present study, chemical disturbance due to O_2 access to the samples is minimized by either increasing the water flow rate or by shortening the tubing length. The lacking correlation of measured colloid concentrations with the total Fe concentrations (Figure A3-10) indicates the successful suppression of oxidative FeOOH colloid generation. Keeping the original water pressure during analysis by the use of the above described pressure flow through cells avoids release of gases and changes of the chemical milieu due to degassing of e.g. CO_2, H_2S.

The influence of mechanical colloid release has also been attempted to be kept at a minimum by variation of the flow rate as well as collecting samples for a long time period at a constant flow rate. Colloid concentrations are determined under steady state conditions and measurements of erroneously high values for colloid populations due to pressure pulses are thus avoided.

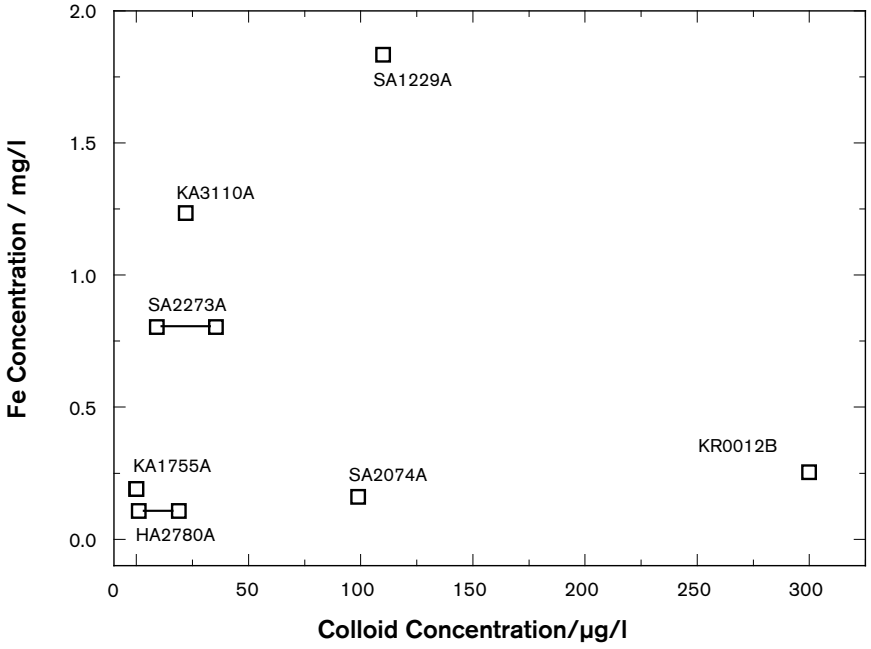

Figure A3-10. *Groundwater Fe concentration versus colloid concentration in the analyzed groundwater samples.*

If we suppose that chemical and mechanical disturbances are successfully suppressed during the sampling campaign, the variation in colloid concentrations and size has to be explained by the different geochemical groundwater conditions influencing colloid stability.

The dependency of colloid concentration on groundwater salinity is shown in Figure A3-11. A clear decrease of the colloid concentration with increasing salinity (indicated by the respective Cl^- concentration) is shown. This observation is in agreement with findings established in other investigations /20, 21, 22, 23/. The ionic strength dependency of the colloid concentration proves the presence of charge stabilized particles at low ionic strength conditions. At high ionic strength conditions, colloids appear to be destabilized and, therefore, only low concentrations are found. At low ionic strength the stability of even larger particles is increased. This is indicated by the increasing mean colloid diameter with increasing colloid concentrations (Figure A3-12).

Figure A3-13 shows the similar relationship for dissolved organic carbon (DOC) with salinity as found for the colloids measured by LIBD. One might argue that in view of the strong correlation of colloid concentration and DOC it is primarily fulvic/humic colloids that are present in the groundwater. A recent study on humic colloid characterization by LIBD /23/ showed that fulvic/humic acid is more or less invisible for LIBD possibly due to its low density. Inorganic or lignite nanoparticles aggregated with fulvic/humic acid, however, can be detected by LIBD. Whether it is purely inorganic colloids or inorganic/organic composites which are determined in the present study cannot be resolved on the basis of the available data. It is however well known that in the presence of organic macromolecules, inorganic colloids are stabilized as organic/inorganic aggregates.

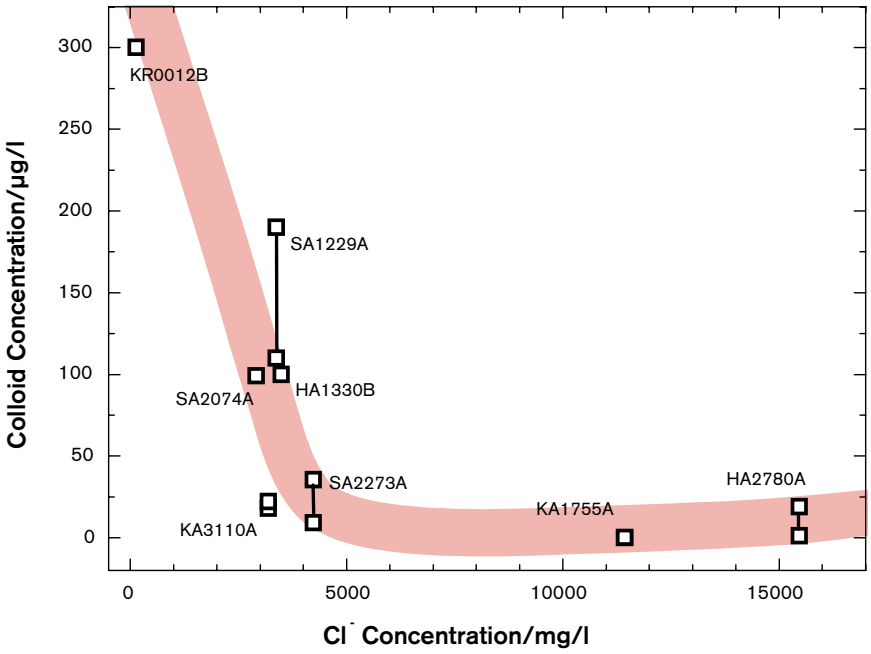

Figure A3-11. *LIBD analyzed colloid concentration as a function of the Cl^- concentration (data from Table A3-4) as an indicator for salinity (data points connected by bars indicate varying colloid concentrations due to pressure fluctuations).*

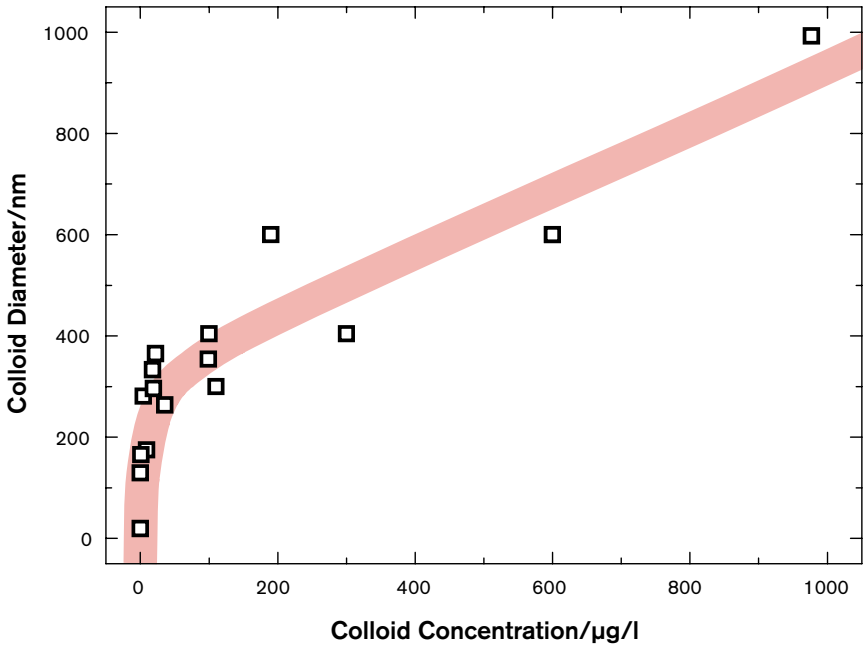

Figure A3-12. *Correlation of colloid concentration with the mean colloid diameter determined by LIBD (data from Table A3-2).*

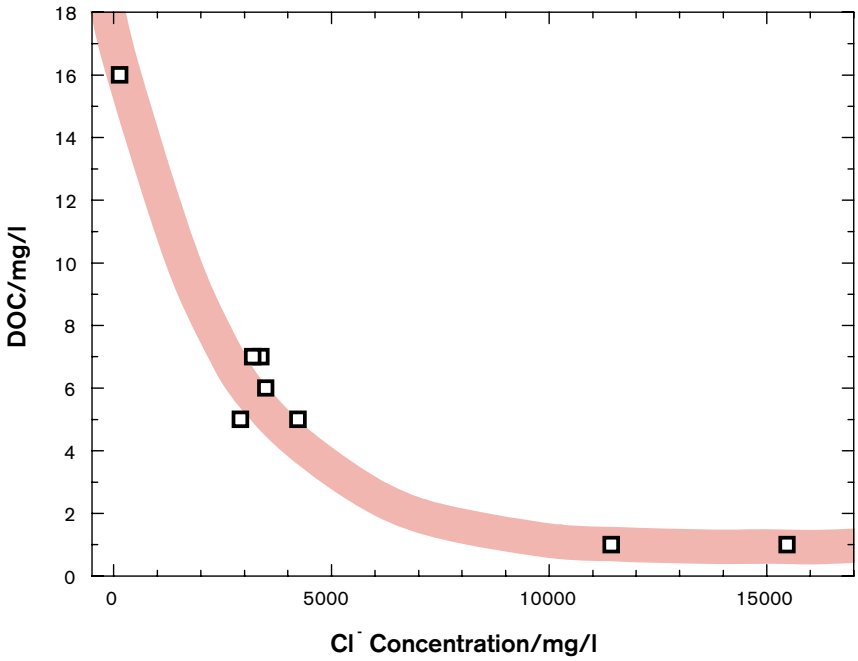

Figure A3-13. *Dissolved organic carbon DOC versus Cl^- concentration as an indicator for salinity (data from Table A3-4).*

3.3 EQ3/6 calculations

Calculations using EQ3/6 /23/ are performed in order to identify possible precipitating solids. EQ3/6, release 7.2 together with the database data0.com.R23 has been applied. For speciation and computation of the groundwater's super saturation, the input for EQ3 is defined using the groundwater compositions in Table A3-3. The Davis activity model is

applied. Redox potentials have not been measured during the present sampling campaign. Due to the presence of pyrite in the granite, a redox potential of ~ –220 mV for the pH given in Table A3-3 is selected. For calculating the equilibrium of the groundwater with EQ6, precipitation of pure minerals and solid solutions are taken into account. Precipitation of Si and Fe sulphide bearing phases is computed to less than 1% of the amount of carbonates. Silicate phases are treated hypothetically because Al was not determined in the analyses (Table A3-3).

The concentration of the precipitates calculated from thermodynamic data and the respective solids are given in Table A3-5. It is assumed that the Redox potentials of the groundwater are reducing and, therefore, Fe(III) phases are not supersaturated. Based on the analytical data available for the respective water samples, mainly carbonates appear to be close to saturation or even supersaturated. Even though these scoping calculations cannot be interpreted in a straightforward manner, they show some correlation of the degree of super saturation with the colloid concentration. From the data shown in Table A3-5 and Figure A3-14 it might be concluded that colloidal species consist mainly of carbonates. This has to be proved in future studies. The outlying high colloid concentration in the groundwater KR0012B in this correlation (Figure A3-14) might be explained by the very low salinity and high DOC in this sample representing very favourable conditions for colloid stabilization.

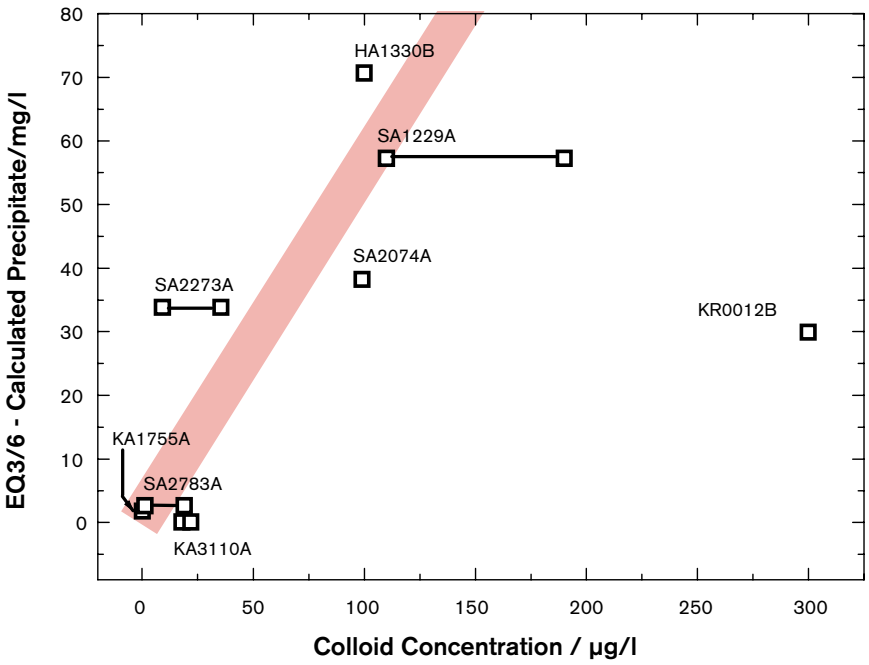

Figure A3-14. *EQ3/6 calculated total precipitate as a function of the LIBD detected colloid concentration.*

Table A3-5. EQ3/6 calculated solid phases.

Borehole ID	Total precipitate mg/l	Solid phases
1 KR0012B	29.94	Dolomite, Carbonate-SolidSolution
2 SA1229A	57.27	Dolomite
3 HA1330B	70.65	Dolomite, Fluorite
4 KA1755A	1.80	Carbonate-SolidSolution
5 SA2074A	38.19	Dolomite
6 SA2273A	33.85	Dolomite, Carbonate-SolidSolution
7 SA2783A	2.65	Strontianite
8 KA3110A	0.05	Hematite

4 Conclusions

The present study proves the appropriateness of mobile LIBD for sensitive in-situ colloid analysis in groundwater. The necessity for an in-situ colloid analysis taking as much care as possible to prevent artefacts is also demonstrated. O_2 access to the groundwater and degassing has to be excluded and moderate constant flow rates have to be applied, in order to ensure that only genuine groundwater colloids are analyzed and possible artefacts are minimized. The data so far show the influence of low salinity and humic like organics on colloid stability in groundwater. Scoping thermodynamic calculations suggest super saturation with regard to mainly carbonates as a possible source for colloid formation.

4.1 Acknowledgements

The support of the investigations and cooperation by SKB and INE/FZK is greatly appreciated. We acknowledge P. Hagman for his technical assistance during the field experiment and C. Mattsén for the groundwater sampling.

5 References

/1/ **Kim J I, 1991.** Actinide colloid generation in groundwater, Radiochim. Acta 52/53 71.

/2/ **Kim J I, 1994.** Actinide colloids in natural aquifer systems, MRS Bull. Vol. XIX(12) 47–53.

/3/ **Kim J I, Zeh P, Delakowitz B, 1992.** Chemical interactions of actinide ions with groundwater colloids in Gorleben aquifer systems, Radiochim. Acta 58/59 (1992) 147–154.

/4/ **Artinger R, Kienzler B, Schüßler W, Kim J I, 1998.** Effects of humic substances on the 241-Am migration in a sandy aquifer: Column experiments with Gorleben groundwater/sediment systems, J.Contam.Hydrol. 35, 261–275.

/5/ **Kersting A B, Efurd D W, Finnegan D L, Rokop D J, Smith D K, Thompson J L, 1999.** Migration of plutonium in groundwater at the Nevada Test Site, Nature 397 56–59.

/6/ **Fillela M, Zhang J, Newman M E, Buffle J, 1997.** Analytical applications of photon correlation spectroscopy for size distribution measurements of natural colloidal suspensions: capabilities and limitations, Coll.&Surf. A, 120, 27–46.

/7/ **Wimmer H, Kim J I, 1992.** Laser-Induzierte optische Spektroskopie zur Speziation von f-Elementen in natürlichen aquatischen Systemen, RCM 00992, Institut für Radiochemie, München.

/8/ **Bundschuh T, Knopp R, Kim J I, 2001.** Laser-induced Breakdown Detection (LIBD) of aquatic colloids with different laser systems, Colloids and Surfaces, Colloids Surf. A, 177 47–55.

/9/ **Kitamori T, Yokose K, Sakagami M, Sawada T, 1989.** Detection and counting of ultrafine particles in ultrapure water using laser breakdown acoustic method, Jpn. J. Appl. Phys. 28 1,195.

/10/ **Scherbaum F J, Knopp R, Kim J I, 1996.** Counting of particles in aqueous solutions by laser-induced photoacoustic breakdown detection, Appl. Phys. B63 299–306.

/11/ **Bundschuh T, Hauser W, Kim J I, Knopp R, Scherbaum F J, 2001.** Determination of colloid size by 2-D optical detection of laser induced plasma, Colloids Surf. A, 180 285.

/12/ **Hauser W, Bundschuh T, 2000.** Verfahren zur Bestimmung der Größe von Partikeln in einer Lösung, Patent: DE 198 33 339.

/13/ **Hauser W, Geckeis H, Kim J I, Fierz T, 2002.** A mobile laser-induced breakdown detection system and its application for the in situ-monitoring of colloid migration, Colloids Surf. A, 203 37–45.

/14/ **Laaksoharju M, 2001.** Äspö Hard Rock Laboratory, Project description of the Äspö project Colloid with the aim to investigate the stability and mobility of colloids, SKB International Progress Report IPR-01-08.

/15/ **Radziemski L J, Cremers D A, 1989.** Laser-induced Plasmas and Applications, Marcel Dekker, New York.

/16/ **Fujimori H, Matsui T, Ajiro T, Yokose K, Hseuh Y M, Izumi S, 1992.** Detection of fine particles in liquids by laser breakdown method, Jpn. J. Appl. Phys. 31 1,514.

/17/ **Hauser W, Götz R, 1999.** Druckwellensensor, Patent: DE 196 02 048.

/18/ **Laaksoharju M, Wallin B (ed), 1997.** Evolution of the groundwater chemistry at the Äspö Hard Rock Laboratory, Proc. of the second Äspö International Geochemistry Workshop, June 6–7, 1995, SKB International Cooperation Report 97-04.

/19/ **Degueldre C, Triay I, Kim J I, Vilks P, Laaksoharju M, Miekeley N, 2000.** Groundwater colloid properties: a global approach, Appl. Geochem. 15 1,043–1,051.

/20/ **Degueldre C, Grauer R, Laube A, Oess A, Silby H, 1996.** Colloid properties in granitic systems (II): stability and transport study, Appl. Geochem. 11, 697–710.

/21/ **Geckeis H, Grambow B, Loida A, Luckscheiter B, Smailos E, Quinones J, 1998.** Formation and Stability of colloids under simulated near field conditions, Radiochim. Acta 82 123–128

/22/ **Bouby M, Ngo Manh T, Geckeis H, Scherbaum F, Kim J I.** Characterization of aquatic colloids by a combination of LIBD and ICP-MS following the size fractionation, accepted by Radiochim. Acta.

/23/ **EQ3/6, 1990–1993.** A Software Package for Geochemical Modeling Version 7.2a, University of California, Lawrence Livermore National Laboratory. Software produced under the Designated Unclassified Subject Area (DUSA) “Yucca”.

Appendix 4

Origin, stability and mobility of humic colloids in Äspö groundwater

Feasibility study

G Buckau
Institut für Nukleare Entsorgung
Forschungszentrum Karlsruhe GmbH

M Wolf
GSF-National Research Center for Environment and Health
Institute of Hydrology

The present study was performed within the context of a project agreement related to radioactive waste disposal studies on the Äspö Hard Rock Laboratory (HRL) between Bundesministerium für Wirtschaft (BMWi) and Swedish Nuclear Fuel and Waste Management Co (SKB).

Contents

Summary

The origin, stability and mobility of colloids in natural aquifer systems surrounding a nuclear waste repository is a key element in developing the basis for long-term safety assessment of nuclear waste disposal. Humic colloids are present in all natural groundwater. They allow analogue studies on humic mobility under natural conditions. In deep granite groundwater, humic colloids are dominated by fulvic acid. Therefore, chemical, spectroscopic and isotopic characterization of fulvic acid from Äspö groundwater has the potential to become a key contributor to the evaluation of colloid mobility in granite groundwater. A further potential benefit is the possible contribution to hydrological modeling through quantification and dating of groundwater contributors.

A feasibility study is thus conducted for the isolation of sufficient amounts of fulvic acid from Äspö groundwaters. Eleven groundwaters are investigated for their fulvic acid content. In addition, Baltic water is studied because it is a possible contributor to some of the groundwaters. Dissolved organic carbon (DOC) and UV/Vis spectroscopy of original water samples as well as fulvic acid concentrates are used to quantify the fulvic acid. The study shows that sufficient fulvic acid is available in all waters. It is also shown that sorption of fulvic acid on precipitates generated during shipping and handling of groundwater samples is not a problem.

The approach for isolation of required amounts of fulvic acid will depend on practical and cost considerations. For chemical, spectroscopic and isotopic (especially ^{14}C) characterization around 200 mg fulvic acid is required (around 100 mg C). In groundwaters where the fulvic acid C-concentration is around 1 mg/L or higher, 100 L of groundwater can be sampled and sent to the laboratory for direct treatment. In two of the twelve investigated water samples the fulvic acid concentrations are so low that on-site pre-concentration by reverse osmosis appears to be the method of choice.

1 Objectives

Determine the feasibility for isolation of sufficient amounts of fulvic acid from Äspö groundwaters for chemical, spectroscopic and isotopic characterization.

2 Introduction

Groundwater humic colloids are aquatic humic and fulvic acids in their natural aquatic state, including associated inorganic components. Fulvic acid dominates the organic component of humic colloids in deep granite groundwater. Humic colloids are a fraction of dissolved organic carbon (DOC). This fraction can vary from close to 100% in groundwaters rich in humic substances, down to 10% in groundwaters with very low humic substance concentrations (DOC in the order of 0.1 mg/L). A previous study on groundwater with fulvic acid C-concentrations of around 0.02 mg/L showed that fulvic acid was introduced into the groundwater after the development of a vegetation layer at the end of the last cold maximum of the past ice age. This fulvic acid is still present and shows no significant retardation or decomposition despite the residence time of around 15,000 years /1/. In an aquifer rich in humic substances there was also no indication of significant decomposition of aquatic humic and fulvic acids /2/. This leads into the question to what extent does fulvic acid introduced into Äspö groundwater from different sources also show an ideal tracer behavior. For this purpose, fulvic acid needs to be isolated in sufficient quantities and characterized with respect to chemical composition, spectroscopic properties and isotopic

composition. With respect to the latter, especially ^{14}C dating of fulvic acid and comparison with groundwater age from hydrological modeling is important. For this reason the present feasibility study is performed in order to determine if the concentrations of fulvic acid in different Äspö groundwaters are sufficiently high for the required isolation and characterization.

3 Samples

Twelve samples were collected in 2 L glass bottles and shipped to FZK/INE. These are:

SA1327B[1] (skb: 003465)	SA1229B (skb: 003471)	KAS09
SA2780A[2] (skb: 003467)	SA2074A (skb: 003468)	Baltic water
KA3110A (skb: 003464)	SA2273A (skb: 003470)	GV1 (011030)
KR0012B (skb: 003466)	KAS03	GV9 (011130)

[1] identical with HA 1330B; [2] identical with HA2780A.

The origin, physical-chemical properties and chemical composition of the waters are shown in Table A4-1. Chemical composition determined by INE and SKB on samples of the present sampling campaign show acceptable agreement with each other. One exception is Fe reflecting oxidation of the samples shipped to INE.

4 Quantification of fulvic acid in selected samples

Fulvic acid in natural water is isolated by XAD-8 chromatography (cf below (4.1)). If the fulvic acid concentration is low, on-site pre-concentration by reverse osmosis is used /3/. For the characterization of fulvic acid about 100 mg carbon is required. Based on the practicability of transporting 100 L water sample to the laboratory for isolation of fulvic acid, on-site pre-concentration is necessary where the fulvic acid C-concentration is in the order of 1 mg/L or lower. In order to determine the need for on-site pre-concentration, fulvic acid is quantified in the samples with the two lowest DOC concentrations (SA2780A and KAS 03). For comparison, fulvic acid is also quantified in the groundwater GV9 with a DOC concentration of 18.8 mg/L. Finally, the sorption of fulvic acid on precipitate generated during shipping and handling is quantified in the groundwater sample SA2273A.

4.1 Experimental

The water samples were filtered with 0.45 micrometer (Roth, Cellulose acetate, E 259.1) syringe-tip filters. UV/Vis spectra were recorded from 200 to 900 nm. Three samples were selected for concentration of fulvic acid by XAD-8 chromatography. Humic and fulvic acids show strong sorption on XAD-8 resin at low pH. At high pH they desorb. Acidified water (pH 2 through addition of HCl) is pumped through a XAD-8 column (dead volume around 10 ml). Fulvic acid is desorbed with 0.1 M NaOH and collected as a concentrate. Concentrates (concentration factor around ten) are characterized by UV/Vis spectroscopy and measurement of DOC. For the sample SA2780A a sample was also concentrated by a factor of 272. Precipitate in the groundwater SA2273A was collected by a large pipette, acidified, and fulvic acid was isolated by XAD-8 chromatography.

Table A4-1. Overview of groundwaters with analytical data by SKB and INE. The samples in the present report refer to the lower two parts (SKB and INE October 2001).

Sample	Depth	Seclow/ secup	pH	Cond	DOC	Na	K	Ca	Mg	HCO_3	Cl	SO_4	Br	F	Si	Fe_{tot}	Mn	Li	Sr	H_2S	NH_4	NO_3	PO_4
	(m)	(m)		(mS/m)	(mgC/L)									(mmol/L)									
SKB September 2000																							
HA1330B[1]	182	0/32.5				9	0.09	1.4	0.48	5.10	7.05	0.49	0.02	0.07	0.21	0.005	0.003	0.006	0.01				
HA2783A[2]	370	0/43.3	7.8		1.0	66	0.66	7.9	5.46	4.33	88.0	2.63	0.15	0.07	0.21	0.033	0.013	0.013	0.06				
KA3110A	416	20.1/26.8	7.5		7.0	129	0.27	103	1.48	0.15	322	6.39	1.09	0.08	0.13	0.003	0.005	0.362	0.80				
KR0012B	69	1.2/10.6	7.5		16.0	53	0.24	11.2	3.55	2.77	78.1	2.61	0.12	0.06	0.19	0.003	0.009	0.022	0.07				
SA1229B	168	6.0/20.5	7.2		7.0	68	0.37	17.1	4.38	2.61	106	2.75	0.24	0.07	0.18	0.014	0.015	0.046	0.12				
SA2074A	282	6.0/38.7	7.7		5.0	147	0.35	124	1.52	0.21	393	6.82	1.37	0.09	0.13	0.002	0.005	0.444	0.96				
SA2273A	306	6.0/20.0	7.4		5.0	64	0.78	9.3	5.33	3.03	86.9	2.89	0.15	0.08	0.17	0.022	0.014	0.020	0.06				
[1] Sampling date: October 1992; [2] Similarities with HA2780A.																							
SKB October 2001																							
HA1330B			7.4	970	3.6	68	0.44	8.4	4.92	3.28	83.5	3.25	0.14	0.11	0.18	0.027	0.014	0.014	0.06	0.0003	0.05		
HA2780A			7.6	3,250	1.4	144	0.39	111	1.48	0.31	361	6.81	1.26	0.14	0.15	0.002	0.005	0.484	0.86	–	0.01		
KA3110A			7.7	910	5.0	62	0.90	6.4	5.33	3.21	77.0	2.80	0.13	0.05	0.18	0.019	0.013	0.012	0.04	0.0028	0.06		
KR0012B			7.5	116	11.0	7	0.07	1.0	0.33	5.38	4.7	0.39	0.01	0.14	0.24	0.004	0.003	0.005	0.01	0.0013	0.01		
SA1229B			7.3	950	4.8	66	0.67	6.9	5.17	4.33	80.4	2.33	0.15	0.11	0.23	0.033	0.012	0.013	0.05	0.0003	0.11		
SA2074A			7.7	850	4.1	54	0.25	9.9	3.35	2.85	71.1	2.47	0.16	0.14	0.21	0.003	0.009	0.022	0.07	0.0016	0.01		
SA2273A			7.5	1,150	3.2	68	0.38	16.9	4.17	2.59	103	2.64	0.20	0.09	0.19	0.014	0.014	0.050	0.12	0.0006	0.03		
INE October 2001																							
SA1327B/ HA1330B				6.2	69	0.53	8.7	5.00		98.6	3.18		0.30	0.15	5×10^{-5}	0.014	0.017	0.06			< 0.002	< 0.001	
SA2780A/ HA2780A				1.5	148	0.54	113	2.01		436	6.46		1.17	0.13	n.d.	0.005	0.682	0.76			< 0.002	0.039	
KA3110A					6.3	65	1.16	6.9	5.54		90.1	2.69		0.24	0.16	4×10^{-5}	0.013	0.014	0.04			< 0.002	< 0.001
KR0012B					15.7	7	0.05	1.1	0.39		3.8	0.32		0.03	0.21	0.0021	0.003	0.004	0.01			< 0.002	< 0.001
SA1229B					7.0	68	0.84	7.4	5.33		95.4	2.44		0.28	0.19	5×10^{-5}	0.013	0.017	0.05			< 0.002	< 0.001
SA2074A					5.4	61	0.29	10.4	3.53		82.2	2.44		0.25	0.18	4×10^{-5}	0.008	0.025	0.07			< 0.002	< 0.001
SA2273A					4.3	70	0.48	18.0	4.38		119	2.72		0.38	0.16	6×10^{-5}	0.014	0.061	0.12			< 0.002	< 0.001
KAS03	1,003	107/252	7.7	850	1.1	56	0.21	11.4	2.78		94.3	0.21		0.03	0.12	3×10^{-6}	0.007	0.051	0.11			< 0.002	0.004
KAS09	451	116/150	7.4	870	6.1	69	1.44	4.1	6.33		92.3	3.06		0.24	0.15	7×10^{-5}	0.013	0.008	0.03			< 0.002	< 0.001
Baltic water	(surface)				10.8	54	1.38	1.7	6.21		70.7	2.90		0.13	0.09	0.003	5×10^{-5}	0.003	0.01			< 0.002	< 0.001
GV1	?				56.8	0.019	0.022	0.36	0.22		0.69	0.19		0.01	0.48	0.089	0.003	0.001	2×10^{-3}			0.002	< 0.001
GV9	?				18.8	0.43	0.042	0.54	0.63		0.37	0.32		0.02	0.28	0.009	0.001	5×10^{-4}	1×10^{-3}			0.006	< 0.001

n.d.: not detected

4.2 DOC and UV/Vis spectroscopy of original and acidified water samples

DOC concentrations vary from 1.1 to 56.8 mgC/L (Table A4-2). In samples with low DOC concentrations, absorption is disturbed by other absorbing components than humic substances (Figure A4-1 and Table A4-2). Estimation of metal ion complexation of fulvic acid shows, that a considerable part of fulvic acid functional groups is complexed. Furthermore, over-saturated phases may associate with fulvic acid and stabilize in solution. This will have an impact on the UV/Vis spectra. For this reason UV/Vis spectra are recorded on both original and acidified water samples (20 µL 10 M HCl to 20 ml water followed by storage for about three weeks). The two samples with the lowest DOC concentrations show considerable deviation from each other, with and without acidification. This is in contradiction with the other samples where deviation in absorption at 300 nm is around ±10%. With decreasing DOC concentration (and thus decreasing absorption from humic and fulvic acids) the spectra also of acidified samples become progressively disturbed (Figure A4-1 and Table A4-2). This shows that absorbing groundwater components disturb the spectra in addition to the impact of fulvic acid complexation.

The relationship between absorption at 300 nm (average between original and acidified) and the DOC concentration is:

$$A_{300} = 0.021\ (\pm 0.001) \times DOC - 0.037\ (\pm 0.013) \quad (1)$$

The specific absorption of humic acid is considerably higher than for fulvic acid. The sample GV1 contains considerable amounts of humic acid. For this reason this sample has been excluded in calculating the above relationship between absorption and DOC.

Table A4-2. DOC concentration, absorption at 300 nm wavelength of original water and acidified water samples stored for three weeks, and DOC after concentration by different factors by XAD-8 chromatography.

No	Sample	DOC (mg/L)	Spectrum[1]	Abs 300 nm (original)	Abs 300 nm (acidified)	DOC (conc ≈ ×10)[2]	DOC (conc ×272)
1	SA1327B	6.2	Background	0.0571	0.0552		
2	SA2780A	1.5	Disturbed[3]	0.0102	0.0079	1.1	0.35
3	KA3110A	6.3		0.101	0.099		
4	KR0012B	15.7		0.309	0.329		
5	SA1229 B	7.0	Shoulder	0.103	0.100		
6	SA2074A	5.4	Background	0.0571	0.0513		
7	SA2273A	4.3	Background	0.0533	0.0468		
8	KAS03	1.1	Disturbed[3]	0.0103	0.0073	1.1	
9	KAS09	6.1		0.0976	0.0940		
10	Baltic water	10.8		0.232	0.220		
11	GV1	56.8		1.751	1.654		
12	GV9	18.8		0.322	0.331	11.8	

Reproducibility of UV/Vis spectroscopy: Eight measurements of the same sample gave deviations of 0.03% and 0.04% for absorption at 300 nm and 400 nm. This should not be confused with correctness.
[1] Negative appearance of UV/Vis spectra of acidified samples (cf Figure A4-1).
[2] Concentration factors are 7.06, 11.7 and 15.6 for SA2780A, KAS03 and GV9, respectively.
[3] Mainly background due to low humic substance concentration.

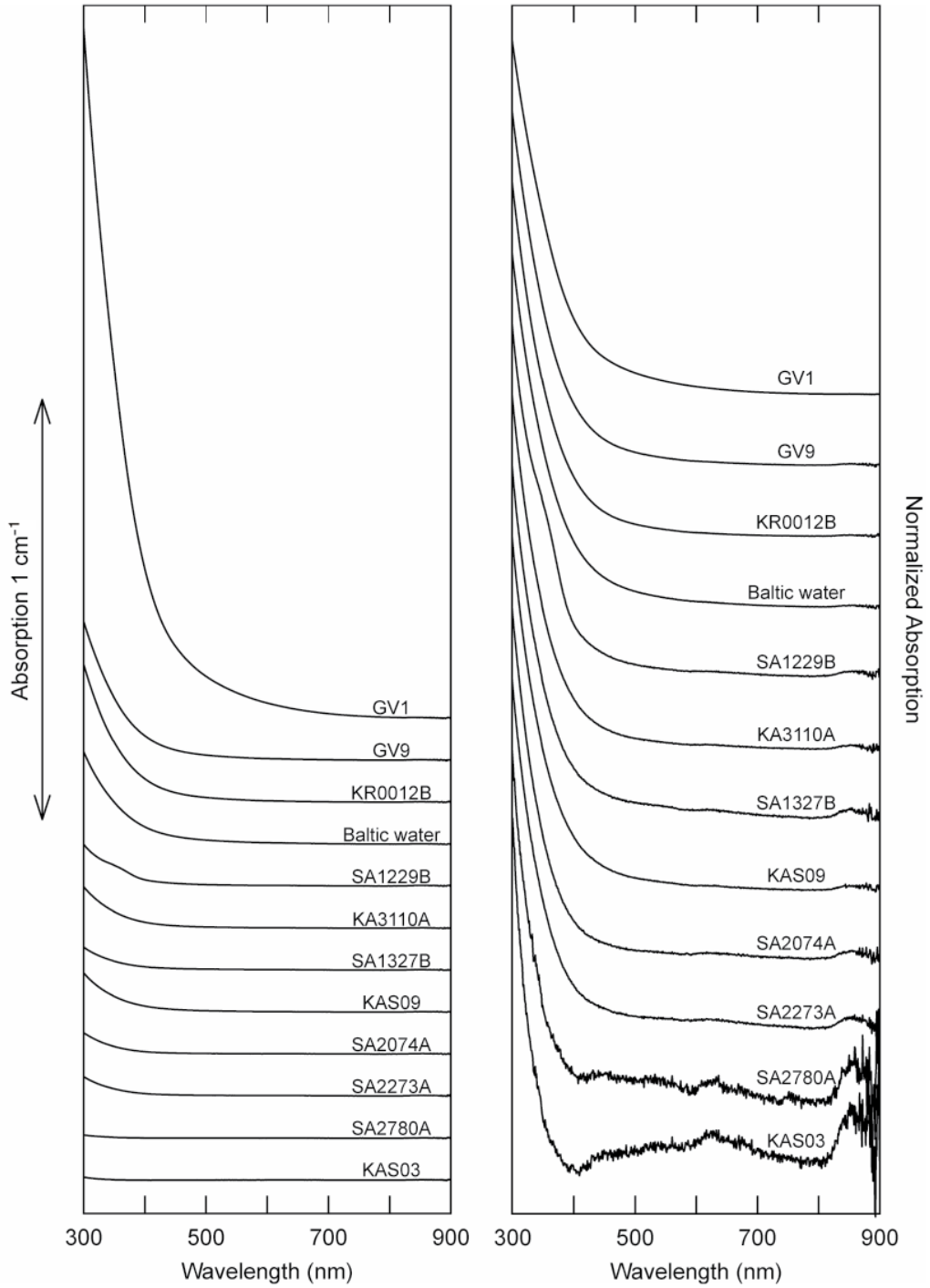

Figure A4-1. *UV/Vis spectra of acidified water samples. Original scale in the left part of the figure, and normalized to the same height (at 300 nm) in the right part.*

Extrapolation to zero absorption at 300 nm results in a DOC value of 1.8 mgC/L. This verifies that DOC consists not only of UV/Vis absorbing humic and fulvic acids but also of non-absorbing organic components. This non-absorbing fraction of DOC is not enriched by XAD-8 chromatography, i.e. does not show hydrophobic character through protonation of functional groups at low pH, and is thus frequently called “hydrophilic organic carbon”.

4.3 Determination of fulvic acid in selected waters

The results of fulvic acid concentration by XAD-8 chromatography are shown in Table A4-2. At a concentration factor of around 10 (cf footnote of Table A4-2 for exact numbers), 63%, 100% and 67% of DOC is evaluated to be fulvic acid for GV9, KAS03 and SA2780A, respectively. These numbers may be elevated through impact of organic contaminants, especially in the two latter samples with low DOC concentrations. Concentration of SA2780A by a factor of 272, 23% of DOC is recovered as fulvic acid. At this concentration factor and with a corresponding large volume of water over the small column, losses of fulvic acid are possible. On the other hand, impact of contaminants is negligible. This number therefore, may be considered as a minimum value.

4.4 Fulvic acid in precipitate of SA2273 A

In this sample, as well as in most of the other groundwaters, the Fe concentration shows a drastic decrease in samples after shipping and handling in the laboratory. Precipitate in 2 L of this water was almost quantitatively sampled, acidified (HCl, ≈ pH 2) and left for dissolution of solid phase. The original solid phase was brown. A residual gray solid phase did not dissolve. Residual brown color was left in the column resisting elution with 0.1 M NaOH. This residual color was washed out with 0.1 M HCl. The concentration of fulvic acid, calculated for the total amount of water from which the precipitate originates, is calculated to be 0.25 mg/L (by application of Equation (1)). This should be compared with 4.3 mgC/L in the prefiltered groundwater sample. The absorption ratio at 300 to 400 nm is found to be 4.05. This is the lowest value found in this study and resembles humic acid rather than fulvic acid. This indicates that a relatively small amount of less hydrophilic humic substance is sorbed/co-precipitated. Humic acid has a higher specific absorption than fulvic acid. Furthermore, applying Equation 1, all dissolved carbon is set to be fulvic acid. For these reasons the calculation of sorbed humic substance by Equation (1) results in an over-estimation. Consequently, the amount of sorbed humic substance will be considerably less than the about 6% calculated from Equation (1). In summary, sorption of fulvic acid on precipitates from water shipped to the laboratory will not significantly affect the isolation of fulvic acid.

5 Conclusions

Fulvic acid concentrations in all investigated water samples allow isolation of sufficient amounts of fulvic acid for the purpose of chemical, spectroscopic and isotopic characterization. In two of the investigated waters, on-situ pre-concentration by reverse osmosis could be considered. As an alternative 300 L or more could be shipped to the laboratory. Inorganic precipitates generated during shipping and handling under normal laboratory conditions will not sorb fulvic acid in amounts that have a significant negative impact.

5.1 Acknowledgements

The technical and administrative support from M. Laaksoharju, Geopoint AB, and water sampling, transport and supply with analytical data from C Mattsén, SKB, is greatly appreciated. For UV/Vis spectroscopy and concentration of fulvic acids by XAD-8 chromatography we thank G. Teichmann and D. Jurrat.

6 References

/1/ **Buckau G, Artinger R, Kim J I, Geyer S, Fritz P, Wolf M, Frenzel B, 2000.** Development of Climatic and Vegetation Conditions and the Geochemical and Isotopic Composition in the Franconian Albvorland Aquifer System, Applied Geochemistry, 15/8, 2000, 1,191–1,201.

/2/ **Buckau G, Artinger R, Fritz P, Geyer S, Kim J I, Wolf M, 2000.** Origin and Mobility of Humic Colloids in the Gorleben Aquifer System, Applied Geochemistry, 15/2, 2000, 171–179.

/3/ **Artinger R, Buckau G, Geyer S, Wolf M, Kim J I, Fritz P, 2000.** Characterization of Groundwater Humic Substances: Influence of Sedimentary Organic Carbon, Applied Geochemistry, 15/1, 2000, 97–116.

Appendix 5

Characteristics of natural colloids in two groundwater samples from the Äspö HRL tunnel

Ulla Vuorinen, VTT Processes

Contents

1 Introduction

Colloidal particles are of interest for the safety in final disposal of spent nuclear fuel because of their potential for transporting radionuclides from a faulty fuel canister in the repository to the biosphere. In general colloids are defined as small particles in the size range of 10^{-6} to 10^{-3} mm. However, in this context the size of colloids, which usually is of interest, is < 0.45 µm, because only colloids which do not sediment in a very slow groundwater flow are potential carriers.

The natural background colloid concentrations and some of their characteristics from various bore holes along the Äspö HRL tunnel were studied by several groups. In this study two bore holes HA2780A (on the 23.10.2001) and SA2273A (on the 24–25.10.2001) were sampled, which are in the following text referred to as GW I and GW II, correspondingly.

2 Sampling

Groundwater from the two boreholes mainly differed in salinity. The groundwater samples were treated on site in a nitrogen (grade 6.0) flushed movable glove-box at ambient temperature and stored in the glove-box about one week until taken to Finland, where the samples were kept in a refrigerator until analysis. The continuous flushing of the glovebox with nitrogen allowed maintaining a slight over pressure throughout the activity. Oxygen content inside the box was measured (Orbisphere) continuously using a probe for dissolved oxygen, which also allowed measurement of the oxygen concentration in GW II sample giving a value of 23 ppb.

Centrifugal ultrafiltration tubes (Gelman) and filter membranes (Nuclepore) were used to treat the groundwater samples. In order to avoid particle contamination from air the filters and centrifugal tubes were assembled under laminar flow. In order to diminish oxygen contamination all equipment, membranes, tubes, sample bottles etc, were taken inside a laboratory glove-box (O_2 < 0.1 ppm) via a vacuum chamber. The assembled filters and ultracentrifugation tubes were closed inside plastic jars and all sample bottles were tightly closed before placing them inside tightly closing steel vessels for transportation. The steel vessels were taken out from the glove box and packed for transportation to Äspö HRL. The movable glove-box was flushed with N_2 already in Finland before transporting it to Äspö HRL where N_2 flushing was continued (O_2 down to 868 ppb) for several hours before taking the closed filter jars etc from the steel vessels into it. N_2 flushing continued throughout the sampling. The actual sampling procedure was not started until the next day. Unfortunately the oxygen meter stopped working in the evening of the first day (last O_2 = 296 ppb at 20:45 on the 22.10.2001.) and could not be brought to operation before the evening after completing sampling at GW I sampling point. The registered value when the meter started operating again was 6.46 ppb. While working in the glove-box the O_2 value measured varied between 2.5 ppb and 17.8 ppb depending on the temperature and objects needed to be taken into the glove-box via the flushing chamber.

The usage of the centrifuge inside the box produced extra heat increasing the working temperature from the ambient ≈ 15°C up to ≈ 19–21°C, which may have an additional effect on formation of carbonates besides the release of dissolved CO_2. These condition changes especially in respect of calcite behaviour were evaluated by modelling calculations (EQ3/6, DATA0.com) using the analysis results (by Paavo Ristola Oy) of both sampling points. As both total Fe and Fe^{2+} were analysed the pair could be used in computing the corresponding Eh. Some of the modelling results are given in Table A5-1. At 15°C in GW I calcite is only saturated, whereas in GW II it is slightly oversaturated. Increasing the temperature up to 25°C has an effect on the saturation of calcite by increasing it and thus calcite also

Table A5-1. Results from EQ3 modelling.

		SA2273A	HA2780A
pH_{given}		7.7	7.9
Eh	V	0.062	0.055
Electrical imbalance	% of total charge	–1.5	0.5
I_{true}	M	0.128	0.489
pCO_2		–2.7	–4.1
pO_2		–51.0	–50.7
Calcite		Oversaturated	Saturated
at 15°C	SI = >	0.70	0.37
Calcite		Oversaturated	Oversaturated
at 25°C	SI = >	0.85	0.51

becomes supersaturated in GW I indicating possible precipitation. Thus calcite may be present as an artefact in the examined colloid samples. (Several other minerals also showed supersaturation but further modelling and evaluation was out of the scope of this work).

2.1 Setup and filtration

The cumulative fractionation of groundwater samples was performed inside the glove-box, which was installed in the tunnel close to the two sampling points in question. The tubing from the groundwater sampling point was connected via a quick coupling through the glove-box wall to enable the collection of groundwater directly inside the anoxic glove-box when needed.

Inside the glove-box a small centrifuge was operated with centrifugal ultrafiltration tubes. Three different cut-off sizes were used, 0.3 µm, 300 kD and 10 kD (6 tubes for each size). Groundwater without prefiltration collected in a plastic bottle inside the glove-box was pipetted (10 ml/tube/centrifugation round) in the six ultrafiltration tubes with the same cut-off size and spun for 10 to 30 minutes at 6,000 rpm in the six-place centrifuge rotor. This allowed 60 ml of groundwater to be handled per spinning round. The filtrates from the receiver tubes were combined and collected in a plastic bottle and a new 10 ml volume of groundwater/tube was added to the remaining concentrate in the tube and the spinning was repeated. When enough groundwater had been treated in this way, the concentrates (about 0.5–1.5 ml/tube) were rinsed with anoxic deionised water (10 ml of H_2O/tube) spinning once more in the centrifuge in order to remove salts. Again the filtrates were combined in one plastic bottle and the remaining concentrates were combined in another plastic bottle. Finally the filter tubes were rinsed with 1% HNO_3 (suprapure, 10 ml/tube) and the rinse solutions combined. The procedure is shown in Figure A5-1. Four different solution types were obtained for chemical analysis for each cut-off value; the filtrates, the concentrate rinse waters, the rinsed concentrates and acid rinses.

In addition to the solution samples filter membranes with two cut-off values, 0.4 µm and 0.05 µm, were prepared for SEM/EDS analysis. 60 ml of groundwater was filtered through the membranes using both sequential filtration and separate filtration without additional prefiltration. The membranes used in separate filtrations were washed with 10 ml of deionised anoxic water in order to remove salts. Thus eight filter membranes were obtained. The SEM micrographs and EDS spectra are presented in Appendix 1 and 2.

All samples prepared remained in the glove-box until brought back to Finland.

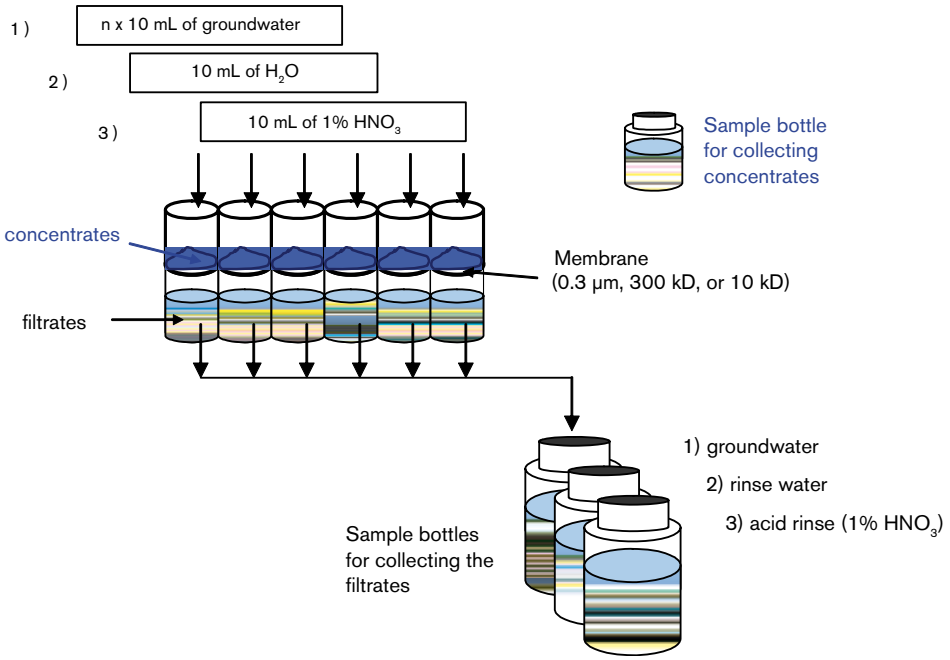

Figure A5-1. *The procedure in groundwater sampling.*

3 Analysis results

3.1 Solution analysis

Table A5-2 gives the analysis results for the solution samples collected in the ultrafiltration procedures. Small amounts of collected samples did not allow performance of anion analysis from other fractions than the filtrate; the amount of concentrate, in particular, was only a few millilitres resulting in rather high detection limits for Al and Si. The few Al results obtained are quite high compared to those obtained in the groundwater analysis (results from Paavo Ristola Oy) giving reason to suspect a possible contamination. The analysis results on filtrate and concentrate washing water clearly show that more salt is retained with the smaller cut-off sizes, more prominently with 10 kD ultrafilters.

Assuming that Na is in soluble form and represents the behaviour of salt retention, then calculating different element concentration ratios and comparing the results between the different solution samples, shows some indications that the soluble elements should follow the same ratios in the samples;

- The results for Si and Fe in both GW I and GW II samples are indicative of some retention occurring in all three cut-off sizes. Thus there are particles associated with these elements in all three fractions studied; particles > 0.3 µm, size ranges 300 kD−0.3 µm and 10−300 kD. However, the highest Fe retention was indicated for the 10 kD cut-off and thus the size range for the majority of Fe associated particles in both groundwater samples is 10−300 kD. Some Fe may have also become sorbed on the ultrafiltration devices. The majority of Si associated particles in GW I were also retained with the smallest cut-off indicating that the size range is 10−300 kD. In GW II no clear difference between the size ranges of Si associated particles could be seen.
- The results for acid rinse samples were subtly allusive of Mg retention, indicating Mg association mostly with particles > 0.3 µm for GW I and for GW II the association would involve all three fractions studied.
- Minor retention of Ca was seen in GW II samples in all three size ranges. This can partly be an artefact of calcite precipitation as modelling results indicated.

- Filtrate and washing water results for K indicated slight retention in both GW samples, somewhat more in the two bigger size ranges; > 0.3 µm and 300 kD−0.3 µm.
- If the suspect values for Al are considered only one (due to results < detection limit) indication of Al retention in GW I was seen for the smallest cut-off size.

Table A5-2. Analysis results for the various solution samples collected.

		SA2273A			HA2780A		
		GW I	GW I	GW I	GW II	GW II	GW II
		0.3 µm	300 kD	10 kD	0.3 µm	300 kD	10 kD
Concentration factors		62	57	18	129	80	46
Filtrates							
Na	mg/L	3,600	3,600	3,600	1,700	1,700	1,700
K	mg/L	14	14	14	15	14	15
Ca	mg/L	4,800	4,900	4,800	690	700	700
Mg	mg/L	37	37	36	111	112	113
Si	mg/L	2.4	2.4	2.4	3.3	3.3	3.3
Fe_{tot}	mg/L	0.050	0.054	0.058	0.623	0.653	0.609
Al	mg/L	1.9	2.8	1.6	1.3	1.2	1.1
Cl	mg/L	12,000	12,000	12,000	3,600	3,600	3,600
SO_4	mg/L	650	660	660	310	300	300
Br	mg/L	115	118	115	21	21	21
Rinsing water							
Na	mg/L	160	180	590	80	110	230
K	mg/L	0.67	0.75	2.26	0.79	1.02	2.02
Ca	mg/L	210	240	770	34	47	95
Mg	mg/L	1.6	1.8	5.8	5.6	7.1	14.3
Si	mg/L	0.16	0.18	0.47	0.21	0.26	0.50
Fe_{tot}	mg/L	0.003	0.008	0.013	0.029	0.043	0.040
Al	mg/L	< 0.2	< 0.2	1.50	< 0.2	< 0.2	< 0.2
Rinsed concentrate							
Amount of concentrate (ml)		1.95	2.11	6.60	2.10	4.1	7.18
Na	mg/L	180	160	480	82	87	160
K	mg/L	0.90	0.87	2.2	1.1	1.0	1.7
Ca	mg/L	240	220	640	34	36	66
Mg	mg/L	1.8	1.6	4.7	5.2	5.5	10.2
Si	mg/L	< 0.5	< 0.5	< 0.5	< 0.5	< 0.5	< 0.5
Fe_{tot}	mg/L	0.039	0.027	0.021	0.110	0.046	0.070
Al	mg/L	< 0.6	< 0.6	2.10	< 0.6	< 0.6	< 0.6
Acid rinse							
Na	mg/L	11.4	8.3	15.2	8.6	5.0	5.4
K	mg/L	< 0.2	< 0.2	< 0.2	< 0.2	< 0.2	< 0.2
Ca	mg/L	13.4	10.6	19.2	3.5	2.0	2.3
Mg	mg/L	0.11	0.08	0.16	0.50	0.29	0.31
Si	mg/L	< 0.1	< 0.1	< 0.1	< 0.1	< 0.1	< 0.1
Fe_{tot}	mg/L	0.027	0.035	0.013	0.120	0.084	0.426
Al	mg/L	< 0.2	< 0.2	< 0.2	< 0.2	< 0.2	< 0.2

< denotes below detection limit (given by the value).

3.2 SEM/EDS

The SEM micrographs and the EDS spectra obtained are presented in Appendix 1 and 2 for GW I and GW II groundwater samples respectively. In the EDS spectra the peaks of Au come from the gold coating of the specimen, and Cu and Zn peaks from the brassy specimen holder. In addition, Appendix 1 (Figure A5-10) includes micrographs of blank Nuclepore filters and the corresponding EDS spectrum. It has to be noted that the presented micrographs and the EDS spectra of single particles on a filter membrane specimen only cover a small selection of the specimen area, and thus other kinds of particles and elements involved may have remained undetected.

Figures A5-2 to A5-5 and A5-11 to A5-14 are of the GW I and GW II samples filtered sequentially and not washed with anoxic water, whereas Figures A5-6 to A5-9 and A5-15 to A5-18 are separately filtered GW I and GW II samples without prefiltration and washed with anoxic deionised water.

The high backgrounds in the EDS spectra suggest the presence of lighter elements, e.g. hydrogen, carbon, nitrogen and oxygen, which are not detected by EDS. These elements are major constituents in organic material and thus the high background can be considered as an implication of the presence of organic material, but also e.g. carbonates and hydroxides are possible. There is a distinct difference between the EDS spectra backgrounds of the two groundwater samples, compare e.g. Figures A5-2, A5-4, and A5-6, with Figures A5-11, A5-13, and A5-15.

Figures A5-3 and A5-12 micrographs of the 0.4 μm membranes show that both groundwater samples contain small particles (much smaller than the cut-off size of 0.4 μm) aggregated quite similarly but the amount is greater on the less saline GW II sample specimen. In addition to the aggregates of small particles also larger particles with different morphology are present. The EDS spectra give the presence of Fe, Ca, Si and Cl, of which Cl is an indication of possible salts remained on the specimen, most probably $CaCl_2$ (Figure A5-2) in the case of GW I by the ratio of the Ca and Cl peaks, and in the case of GW II both NaCl and $CaCl_2$ (Figure A5-11) may be possible. Fe is associated with the small particle aggregates.

When comparing Figures A5-5 and A5-14 of the 0.05 μm membrane specimen of the particle agglomerations the difference in the background level in the EDS spectra is more prominent for GW II again and only small peaks for Ca and Cl are seen. The high background may be due to organic material present. The morphology of the small particle aggregates is very similar to that seen on the 0.4 μm specimen (Figure A5-12). EDS spectra of the particle agglomerations show the presence of Fe, Ca, Cl and Si, but for the more saline GW I the peaks of Ca, Cl and Si are much more prominent and also peaks for S and Ti are detected indicating more inorganic nature of the aggregated particles. The ratio of Cl and Ca peaks support the presence of Ca also in other phases than $CaCl_2$.

Further characterisation of the small aggregated particles (e.g. Figures A5-3 and A5-12) is possible by making TEM specimens, however, such a study was not included here.

4 Discussion and conclusions

The results from SEM/EDS studies and the indicative results based on ultrafiltration samples are in good agreement with the characteristics of the particle phases present in the two groundwaters. However, the obtained results did not allow calculation of the actual concentration of the element association with the different particle phases.

Appendix 1

SEM micrographs and EDS spectra for groundwater sampled at Äspö Hard Rock Tunnel, sampling point HA2780A = GW I.

Figures A5-2 to A5-5 are of GW I sample filtered sequentially through the 0.4 µm and 0.05 µm Nuclepore filters. Figures A5-6 to A5-9 are of the separately filtered samples using the same pore sizes as in the sequential filtration.

Micrographs were taken of each filter with two different magnifications, 500- and 10,000-fold. For the 500-fold magnification the EDS spectrum is a general one over the filter, whereas in the case of larger magnifications (10,000-fold) the EDS spectra are of particles or an agglomeration, where the target area is about the size of circle with a diameter of 1 µm.

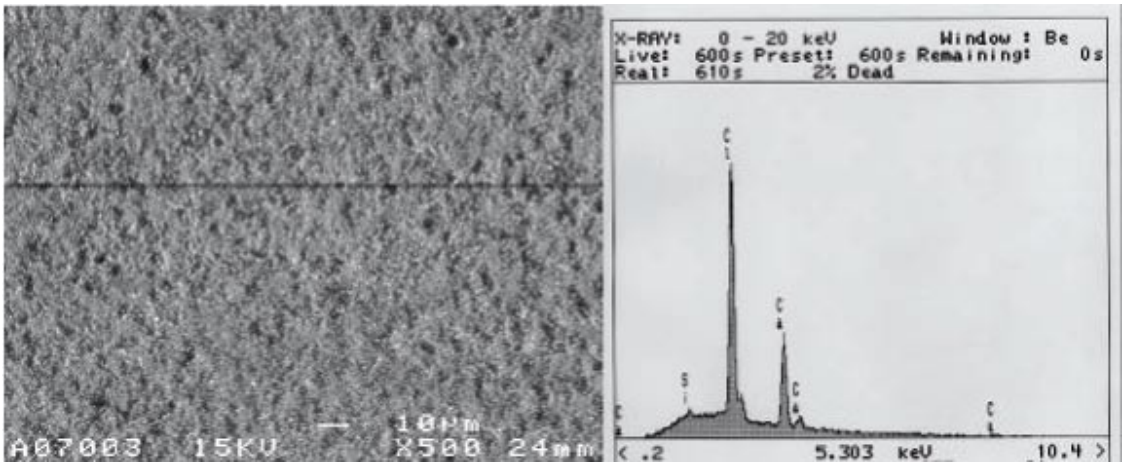

Figure A5-2. *SEM micrograph of the 0.4 µm filter membrane (magnification = ×500) on the left and on the right an EDS spectrum over the filter membrane.*

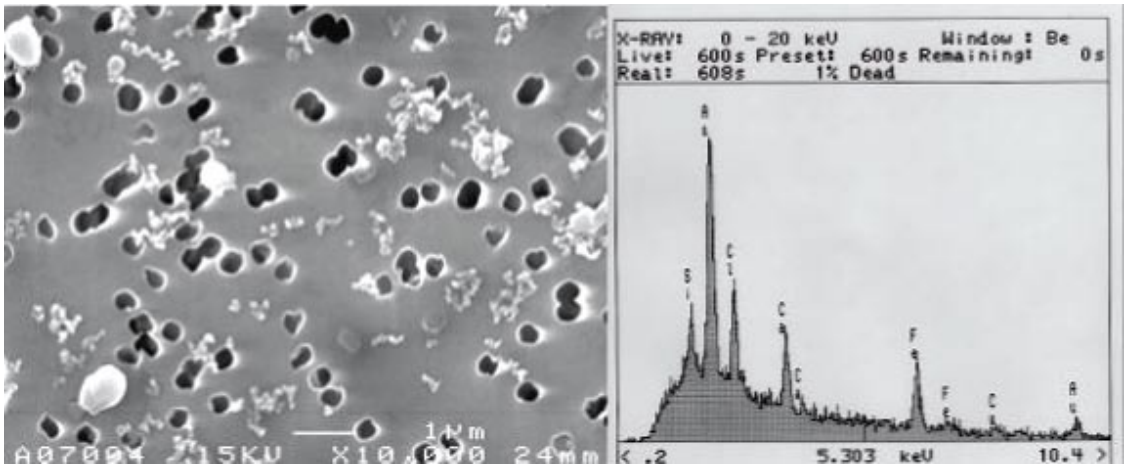

Figure A5-3. *SEM micrograph of the 0.4 µm filter membrane (magnification = ×10,000) on the left and on the right the EDS spectrum of a particle agglomeration.*

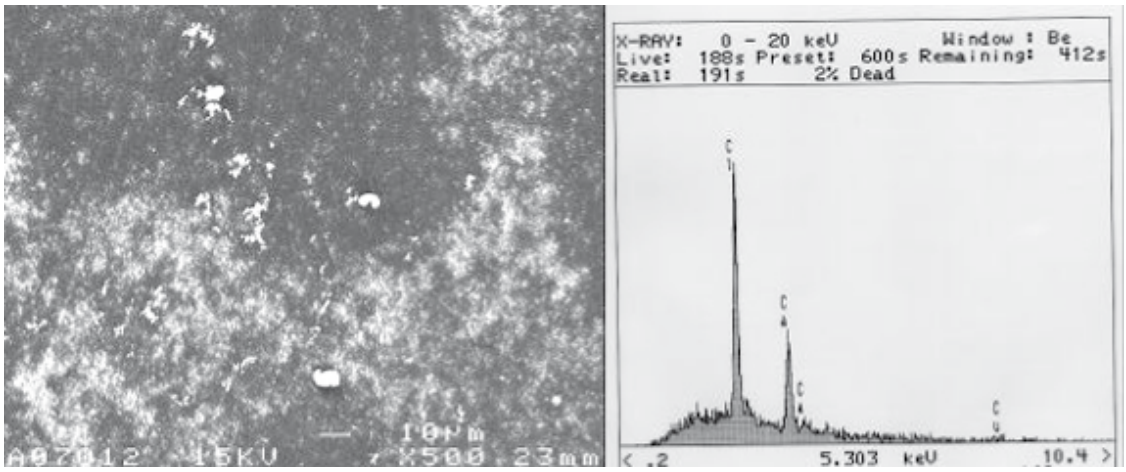

Figure A5-4. *SEM micrograph of the 0.05 µm filter membrane (magnification = ×500) on left and on the right an EDS spectrum over the filter membrane.*

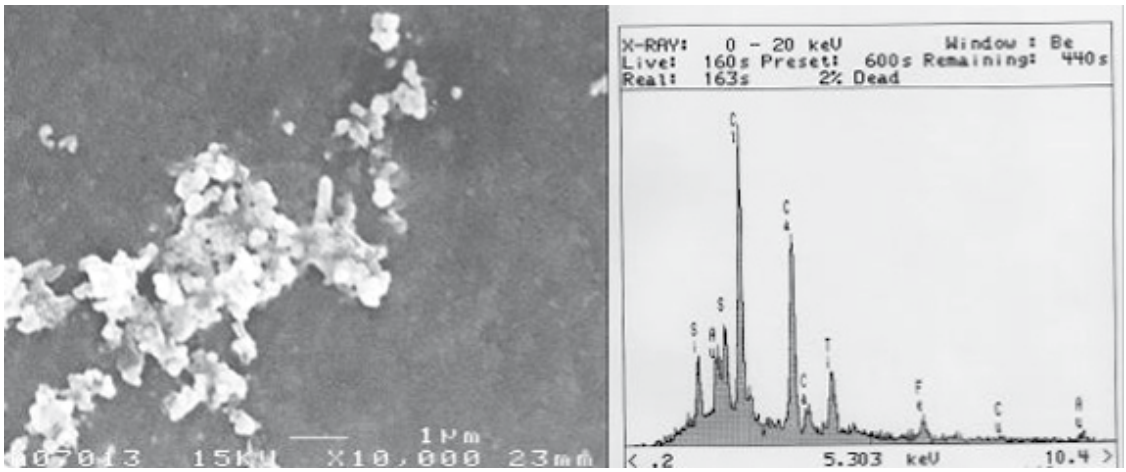

Figure A5-5. *SEM micrograph of the 0.05 µm filter membrane (magnification = ×10,000) on the left and on the right the EDS spectrum of a particle agglomeration.*

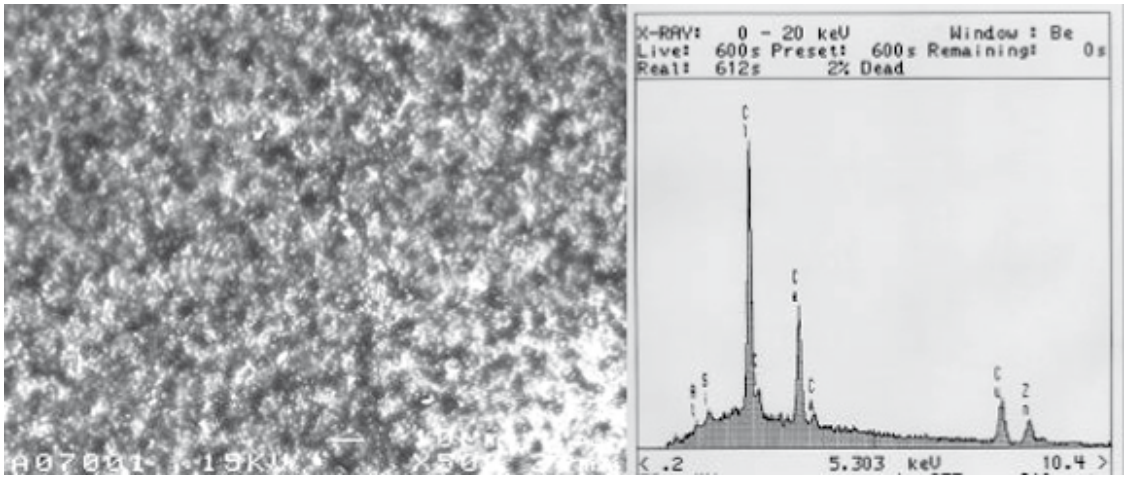

Figure A5-6. *SEM micrograph of the 0.4 µm filter membrane (magnification = ×500) on the left and on the right an EDS spectrum over the filter membrane.*

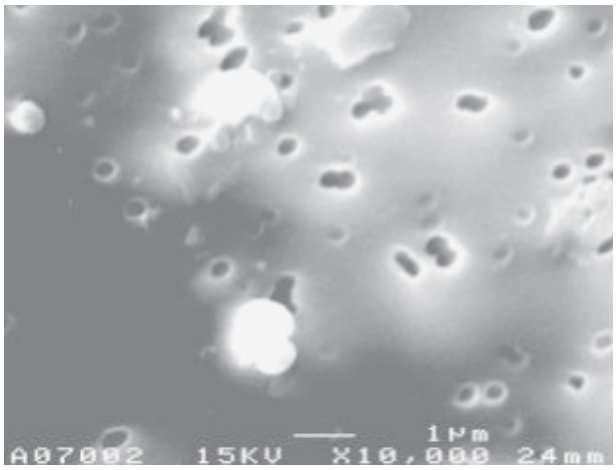

***Figure A5-7**. SEM micrograph of the 0.4 µm filter membrane (magnification = ×10,000) on the left. No EDS spectrum was obtained (not enough scattering due to small amount of material on the membrane).*

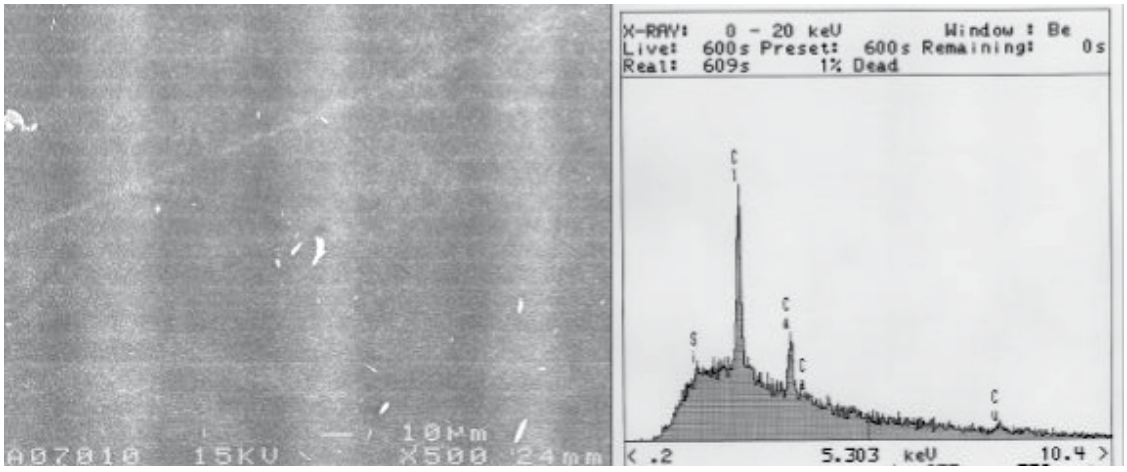

***Figure A5-8**. SEM micrograph of the 0.05 µm filter membrane (magnification = ×500) on the left and on the right an EDS spectrum over the filter membrane.*

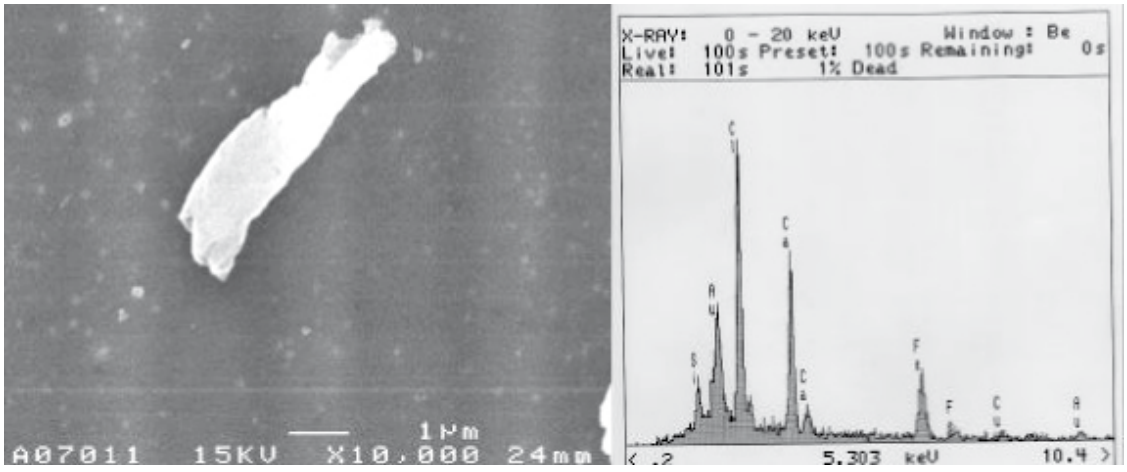

***Figure A5-9.** SEM micrograph of the 0.05 µm filter membrane (magnification = ×10,000) on the left and on the right the EDS spectrum of a particle.*

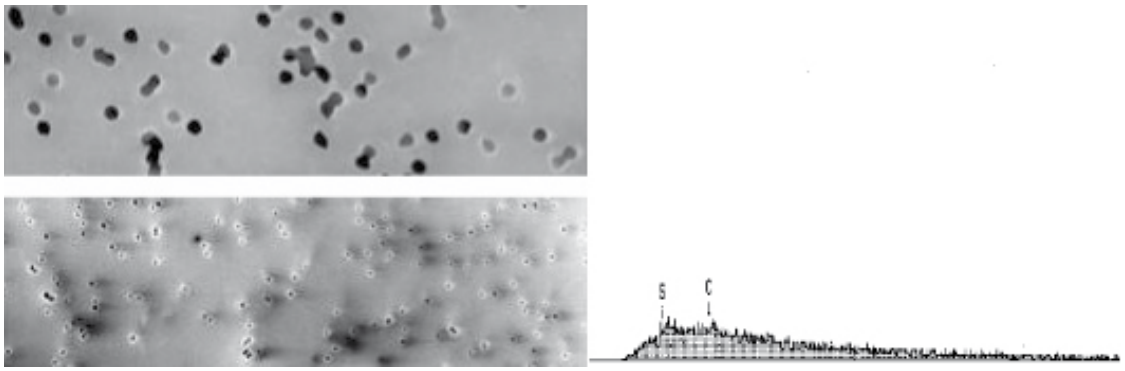

Figure A5-10. *On the left SEM micrograph of the blank 0.4 µm (upper) and 0.1 µm (lower) Nuclepore filter membranes (magnification = ×10,000) and on the right the EDS spectrum of a blank filter.*

Appendix 2

SEM micrographs and EDS spectra for groundwater sampled at Äspö Hard Rock Tunnel, sampling point SA2273A = GW II.

Figures A5-11 to A5-14 are of GW I sample filtered sequentially through the 0.4 µm and 0.05 µm Nuclepore filters. Figures A5-15 to A5-18 are of the separately filtered samples using the same pore sizes as in the sequential filtration.

Micrographs were taken of each filter with two different magnifications, 500-fold and 10,000- or 5,000-fold. For the 500-fold magnification the EDS spectrum is a general one over the filter, whereas in the case of larger magnifications (5,000- or 10,000-fold) the EDS spectra are of particles or an agglomeration, where the target area is about the size of circle with a diameter of 1 µm.

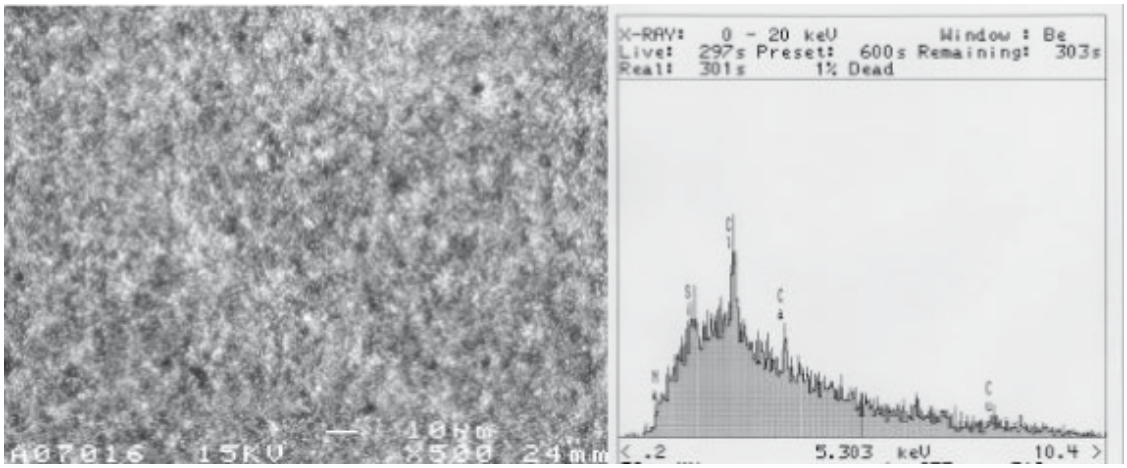

Figure A5-11*. SEM micrograph of the 0.4 µm filter membrane (magnification = ×500) on the left and on the right an EDS spectrum over the filter membrane.*

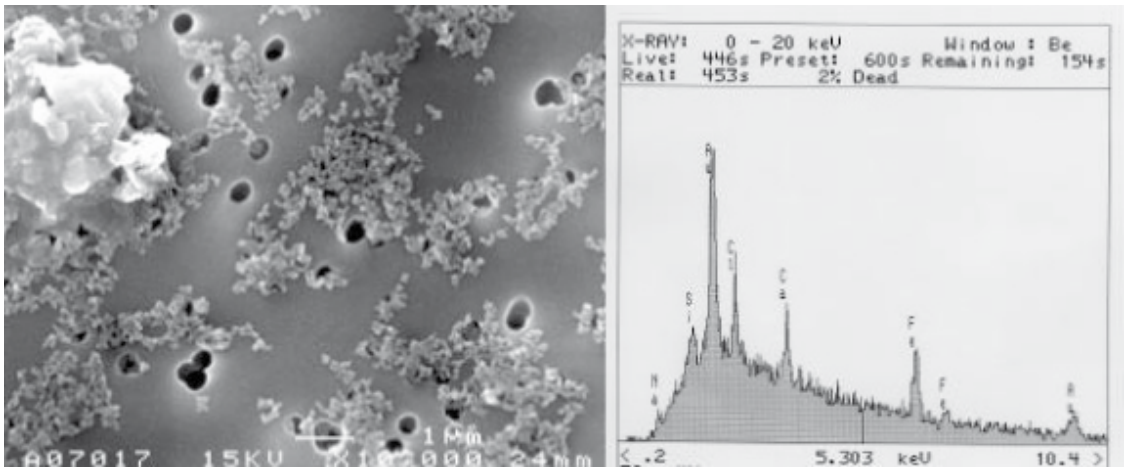

Figure A5-12. *SEM micrograph of the 0.4 µm filter membrane (magnification = ×10,000) on the left and on the right the EDS spectrum of a particle agglomeration.*

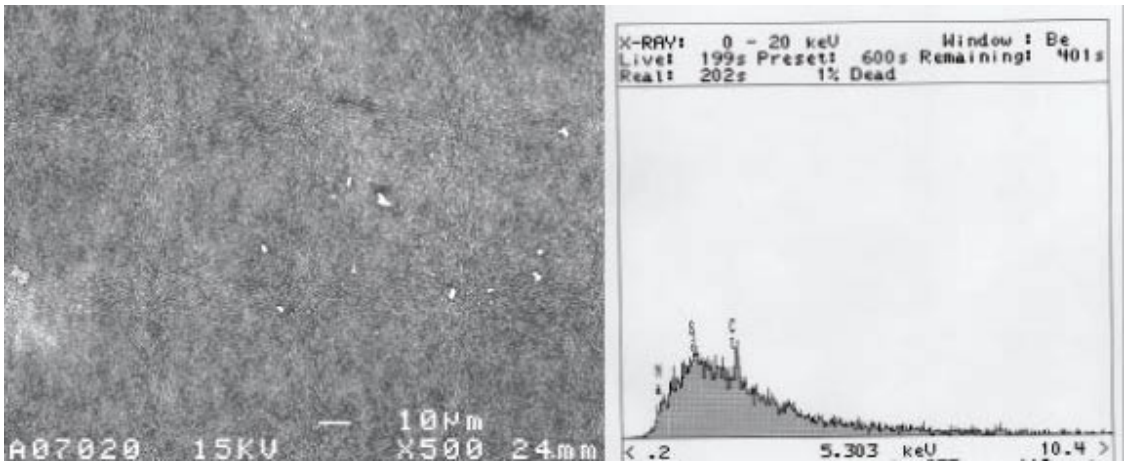

Figure A5-13. *SEM micrograph of the 0.05 µm filter membrane (magnification = ×500) on the left and on the right an EDS spectrum over the filter membrane.*

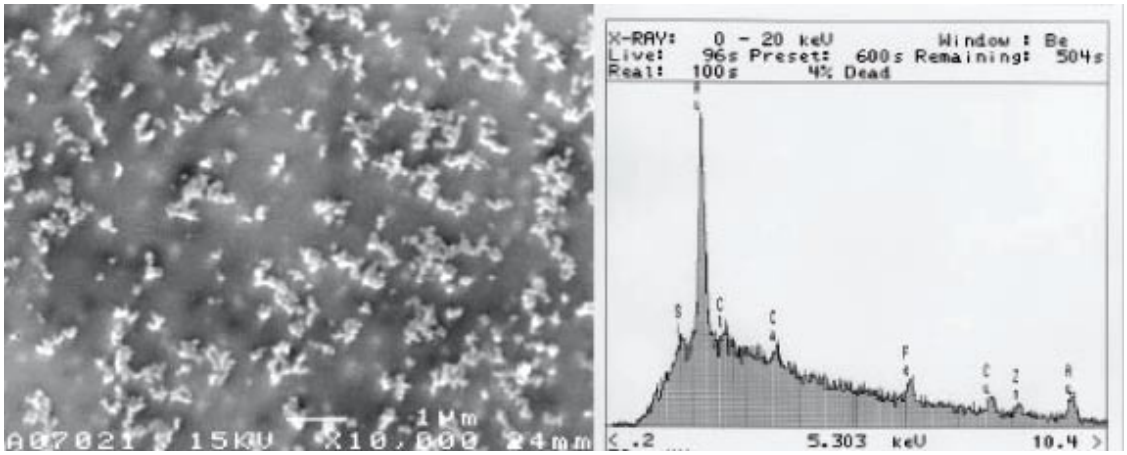

Figure A5-14. *SEM micrograph of the 0.05 µm filter membrane (magnification = ×10,000) on the left and on the right the EDS spectrum of a particle agglomeration.*

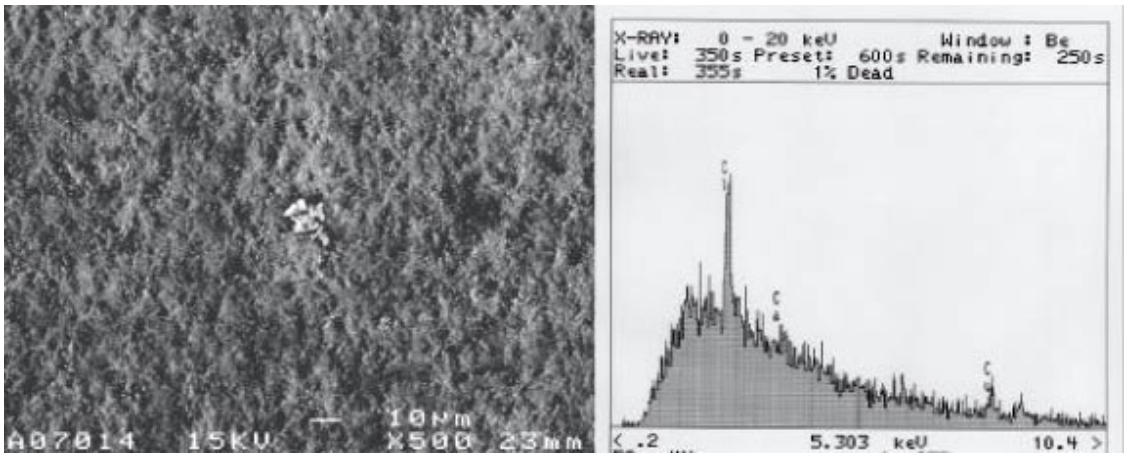

***Figure A5-15**. SEM micrograph of the 0.4 µm filter membrane (magnification = ×500) on the left and on the right an EDS spectrum over the filter membrane.*

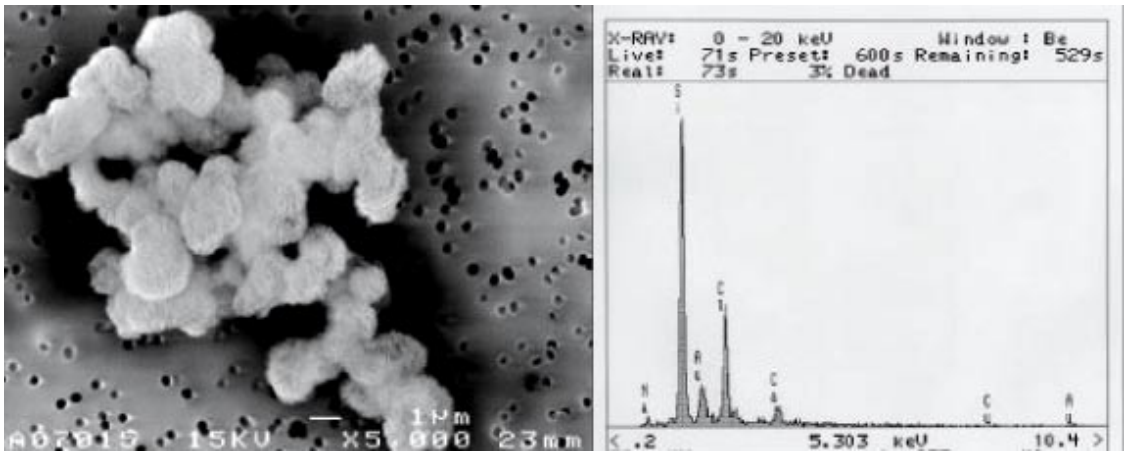

***Figure A5-16**. SEM micrograph of the 0.4 µm filter membrane (magnification = ×10,000) on the left and on the right an EDS spectrum of a particle agglomeration.*

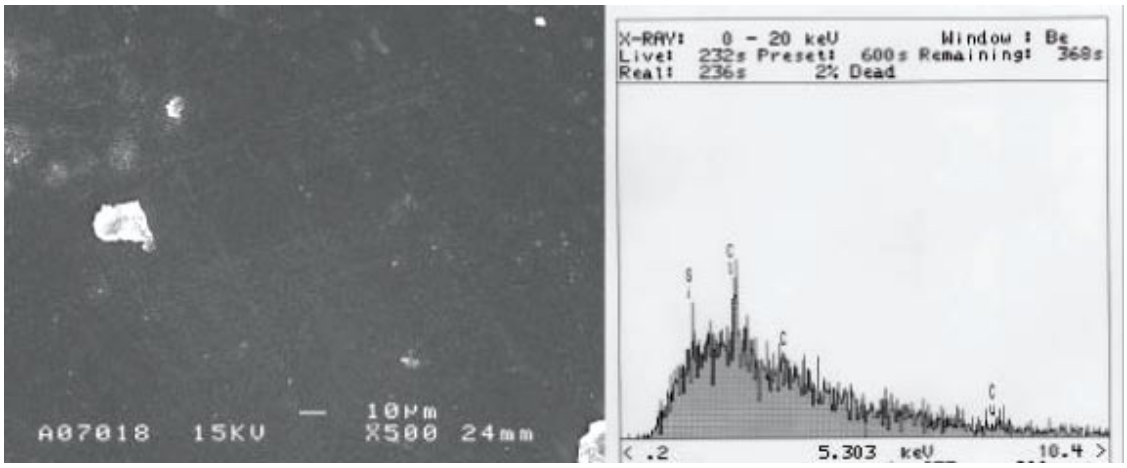

***Figure A5-17**. SEM micrograph of the 0.05 µm filter membrane (magnification = ×500) on left and on the right an EDS spectrum over the filter membrane.*

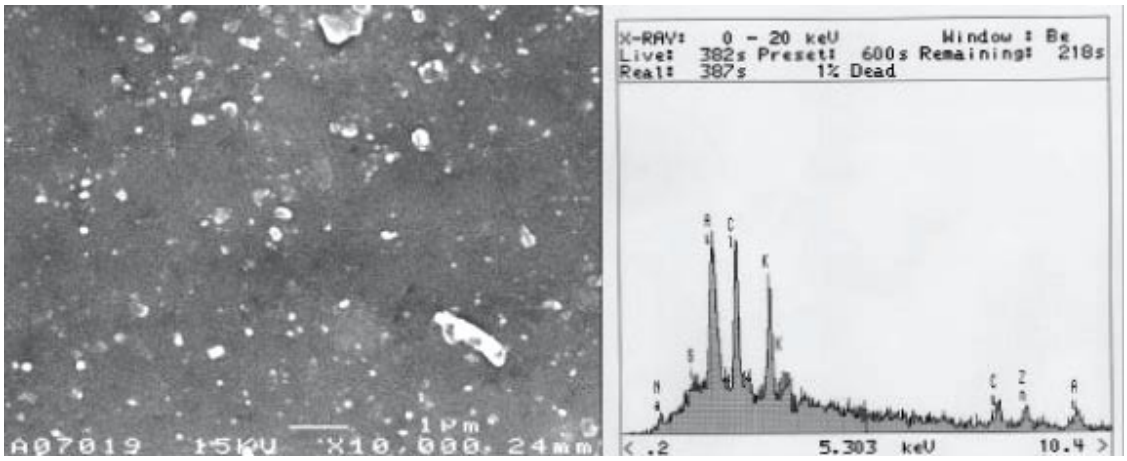

Figure A5-18. *SEM micrograph of the 0.05 µm filter membrane (magnification = ×10,000) on the left and on the right the EDS spectrum of the particles.*

Appendix 6

Groundwater sampling in the Äspö tunnel

Mia Rantanen, Consulting Engineers

Paavo Ristola, Industry and Power Plant Chemistry

2001-11-29

Contents

1 Background

The aim of the groundwater sampling for chemical analysis was to compare the sampling techniques and analysis between SKB and Posiva for QA-purposes and for Posiva to get experience in sampling groundwater from larger depths from underground facilities for the planning of ONKALO phase groundwater sampling.The boreholes sampled, represented different water types of different salinity ranges, since it is known that the colloid stability can change with the chemistry of the groundwater. The selected boreholes were used to measure the background concentration of colloids, humic substances and microbes. Experimental concepts for the colloid project were: laboratory experiments, background measurements, borehole specific experiments and possibly fracture specific experiments.

Three groundwater samples were collected by the Posiva team from the following sampling points HA2780A, SA2273A and KA1755A. The sampling in Äspö tunnel was carried out 22–26 October, 2001.

2 Experimental

The groundwater samples were collected according to Posiva field instructions /Ruotsalainen et al. 1998/. The same system and methods are used in all Posiva's groundwater samplings done in Finland since 1998. The on-line filtering and collecting systems were connected to the sampling line of the borehole. Most of the samples was filtered through Millipore 0.45 µm filter by an on-line filtering system (anions, cations, alkalinity, acidity, pH). Samples for the isotopes (^{3}H, ^{2}H, ^{18}O) were taken directly into dedicated containers. Parameters sensitive to atmospheric contamination or transport delay e.g. alkalinity, pH, Fe^{2+}, Fe_{tot}, S^{2-}_{tot}, anions, NH_4^+ were analyzed directly after sampling on-site in the field laboratory at Äspö. The other water samples for parameters to be analyzed in the laboratories in Finland were invariably preserved in accordance with the Posiva field instructions /Ruotsalainen et al. 1998/.

2.1 Experimental setup

The on-line collecting systems were set up in the SKB Hard Rock Laboratory. Each collecting system was equipped with a 0.45 µm filter and the system was rinsed and filled with nitrogen gas before put into operation in the field for groundwater sampling in the Äspö tunnel. The collecting system was connected with a teflon tube and a Swagelock fitting to the borehole. The teflon tube was rinsed with groundwater before the sampling was started.

Each collecting system was filled up with water. Water samples were then bottled in the field laboratory using nitrogen gas to the washed plastic and glass bottles. The samples were handled as shown in Table A6-1.

The samples were kept cold until delivery to Finland and transportation to other laboratories.

Table A6-1. Methods of sampling, bottling and preservation.

Parameters analysed in the field laboratory	Sample amount (L) and the type of the container	Filtered 0.45 µm	Other instructions
pH. alkalinity and acidity	1×0.5 Pyrex-glass bottle	x	titrations carried out in N_2-atmosphere
Conductivity	1×0.1 PE	–	
Fe_{tot}. Fe^{2+}	6×0.05 acid washed glass volumetric flask	x	4 ml ferrozine buffer solution
Cl	1×0.25 PE	x	
NH_4^+	2×0.1 PE	–	
S^{2-}	3×0.1 Winkler-bottle	Collected under N2-atmosphere. but not filtered	0.5 ml 1 M $Zn(Ac)_2$+ 0.5 ml 1 M NaOH
Parameters analysed in laboratory	**Sample amount (L) and the type of the container**		
pH. SiO_2	1×0.5 PE	x	
Conductivity	2×0.5 PE	–	
Anions	1×0.2 PE	x	
DIC/DOC	2×0.25 L glass bottle with glass stopper	x	
Metals. GFAAS, ICP-MS	1×0.2 PE. acid washed bottle	x	1 ml conc pa+. HNO_3
PO_4	1×0.5 PE	x	5 ml 4 M H_2SO_4
S_{tot}	1×0.1 PE	x	
^2H. ^{18}O	2×0.01 Venoject tube	–	
^3H	2×0.25 L dark. glass bottle	–	

2.2 Analysis

The analyses, which are marked in Table A6-2, were made in SKB's field laboratory immediately after each groundwater sampling. The analyses are based on the international standards and methods which are developed further for Posiva's purposes to analyze groundwater samples of high ionic strength.

The recovery tests have been made for ISE, anion and metal analyses. An acceptable level of the recovery is 80–120%. To check the quality of the results and methods a reference water /OL-SO, Vuorinen et al. 1997/ was analyzed both in field and in the laboratories in Finland. The accepted upper and lower limits for OL-SO water have been calculated from the analyzed results from several years. The commercial, certified reference waters were used for the metals, DIC and DOC-analyses in Consulting Engineers Paavo Ristola's Myyrmäki and Hollola laboratories.

3 Results and discussion

The results and analytical methods used are shown in Table A6-2.

The anion-cation ratio was calculated for all samples based on the total amount of anions and cations in meq/L in water samples. The ratio was for the samples HA2780A 0.992 and SA2273A 1.029 and KA1755A 1.023. The ratio should be about one for the accepted results.

Table A6-2. Results of the water analysis.

Analysis	Unit	HA2780A	SA2273A	KA1755A	Standard/Method
Conductivity 25°C[A]	mS/m	3,480	1,140	3,190	SFS-EN 27 888, conductivity electrode WTW Tetracon 325
Conductivity 25°C[B]	mS/m	3,440	1,120	3,220	SFS-EN 27 888, conductivity electrode Ingold, C 10.3
pH[A]		7.9	7.7	7.9	SFS 3021, pH-electrode Orion Ross 82-72BN
pH[B]		7.6	7.5	7.5	SFS 3021, pH-electrode Orion Ross 81-72 BN
Alkalinity, m-value[A]	meq/L	0.24	2.6	0.13	SFS-EN ISO 9963-1 and Gran-titration by extrapolation, Mettler-Toledo DL-50
Alkalinity, p-value[A]	meq/L	< 0.01	< 0.01	< 0.01	SFS-EN ISO 9963-1, Mettler-Toledo DL-50
Acidity, -p–value[A]	meq/L	0.06	0.24	0.05	SFS 3005, Mettler-Toledo DL-50
Bicarbonate, HCO_3[A]	mg/L	15	158	7.9	SFS 3005, calculated
Ammonium, NH_4^+[A]	mg/L	< 0.05	0.89	< 0.05	ASTM 1426, Orion 95-12 ISE
Sulfide, S^{2-}[A]	mg/L	< 0.01	< 0.01	< 0.01	SFS 3038, Philips PU 8670 UV-VIS spectrophotometer
Iron, (tot)[A]	mg/L	0.088	0.78	0.21	Central Electricity Research Laboratory by ferrozinethioglycol acid method, Philips PU 8670 UV-VIS spectrophotometer
Iron, Fe^{2+}[A]	mg/L	0.082	0.76	0.20	Central Electricity Research Laboratory by ferrozinethioglycol acid method, Philips PU 8670 UV-VIS spectrophotometer
Iron, (tot)[B]	mg/L	0.075	0.79	0.19	SFS 5074, Perkin-Elmer 4100 ZL HGA
Chloride, Cl[B]	mg/L	13,100	3,630	11,800	SFS 3006, Mettler-Toledo DL-50
Bromide, Br[B]	mg/L	97	17	89	Perkin-Elmer Elan 6000, ICP-MS
Nitrite, NO_2[B]	mg/L	< 0.05	< 0.05	< 0.05	SFS-EN ISO 10304-1, Shimadzu HPLC with UV-detector SPD6-A
Nitrate, NO_3[B]	mg/L	< 0.05	< 0.05	< 0.05	SFS-EN ISO 10304-1, Shimadzu HPLC with UV-detector SPD6-A
Phosphate, PO_4[B]	mg/L	< 0.006	< 0.006	< 0.006	SFS 3025, Shimadzu UV-VIS 120-02 spectrophotometer
Sulfate, SO_4[B]	mg/L	620	270	640	SFS-EN ISO 10304-1, Dionex DX-100
Silicate, SiO_2[B]	mg/L	8.9	12	8.5	Juoma- ja talousveden tutkimusmenetelmät, Shimadzu UV-VIS 120-02 spectrophotometer
Dissolved inorganic carbon, DIC[B]	mg/L	1.7	21	0.8	ASTM D4839, own developed analyzer with IR-detector
Dissolved inorganic carbon, DIC[C]	mg/L	2.4	32.3	1.2	SFS EN 1484, Shimadzu TOC-5000 analyzer
Dissolved organic carbon, DOC[B]	mg/L	0.9	3.6	0.5	ASTM D4839, own developed analyzer with IR-detector
Dissolved organic carbon, DOC[C]	mg C/L	1.0	4.8	0.7	SFS EN 1484, Shimadzu TOC analyzer
Sulfur, $S_{(tot)}$[B]	mg/L	210	100	210	Perkin-Elmer Elan 6000, ICP-MS

Analysis	Unit	HA2780A	SA2273A	KA1755A	Standard/Method
Aluminium, Al[B]	mg/L	< 0.025	0.028	0.007	Perkin-Elmer Elan 6000, ICP-MS
Potassium, K[B]	mg/L	14	15	10	Perkin-Elmer Elan 6000, ICP-MS
Calcium, Ca[B]	mg/L	4,600	670	4,000	Perkin-Elmer Elan 6000, ICP-MS
Magnesium, Mg[B]	mg/L	36	100	0.33	Perkin-Elmer Elan 6000, ICP-MS
Sodium, Na[B]	mg/L	3,500	1,500	3,100	Perkin-Elmer Elan 6000, ICP-MS
Manganese, Mn[B]	mg/L	0.27	0.85	37	Perkin-Elmer Elan 6000, ICP-MS
Lithium, Li[B]	mg/L	3.8	0.38	3.3	Perkin-Elmer Elan 6000, ICP-MS
Strontium, Sr[B]	mg/L	80	11	74	Perkin-Elmer Elan 6000, ICP-MS
Oxygen 18, ^{18}O[D]	‰ SMOW	–12.6	–9.0	–13.4	Finnigan Mat 251, MS
Deuterium, ^{2}H[D]	‰ SMOW	–84.5	–65.0	–91.7	Finnigan Mat 251, MS
Tritium, ^{3}H[E]	TU	1.0	8.8	0.6	
TDS	mg/L	22,100	6,400	19,800	Calculated

[A] analyzed in Äspö at SKB's field laboratory.
[B] analyzed in Consulting Engineers Paavo Ristola's laboratory at Myymäki or Hollola.
[C] analyzed in Teollisuuden Voima's Chemistry laboratory at Olkiluoto.
[D] analyzed in The Geological Survey of Finland (GTK).
[E] analyzed in The Central Isotope Research Laboratory of the Netherlands (CIO).

The reliability of the analysis can be investigated by calculating ion charge balance of the waters. For water, the ion charge balance is neutral. Ion charge balance (E) can be calculated using equation below:

$$E = \frac{[Cations] - [Anions]}{[Cations] + [Anions]} * 100 \quad (1)$$

All analyses were acceptable because the ion charge balance for the groundwater samples were between –1.4 ... 0.4%. The pH-values were normal for the groundwater samples (pH: 7.5–7.9; F and L). Sulphide was not found in any sample (S^{2-} determination level < 0.01 mg /L). The ratio of Fe^{2+}/Fe_{tot} was calculated for samples on the basis of field laboratory analysis (Fe_{tot}: 0.088–0.78 and Fe^{2+}: 0.082–0.76 mg/L; F). The ratio for Fe^{2+}/Fe_{tot} varied between 0.932–0.974.

Gran-titration was carried out for all samples to determined alkalinity values in field laboratory. The contents of bicarbonate (HCO_3, mg/L) were calculated from alkalinities and they were compared with the DIC-analyses made in the laboratory. The DIC-content was determined by two different analysers (in Table A6-2) in Teollisuuden Voima's and Paavo Ristolas's laboratories. The results were different. The difference between the two analyzers varied between 42–53%. Teollisuuden Voima's DIC-analyses fitted better with the alkalinity results (Figure A6-1) and they were used.

According to the classification by /Davis and DeWiest 1967/ a Ca-Na-Cl water type was found in boreholes HA2780A and KA1755A and a Na-Ca-Cl water type in borehole SA2273A.

TDS (Total Dissolved Solids) varied between 6,400 ... 22,100 mg/L. Waters can be classified as brackish (1,000 < TDS < 10,000 mg/L) and saline (TDS > 10,000 mg/L).

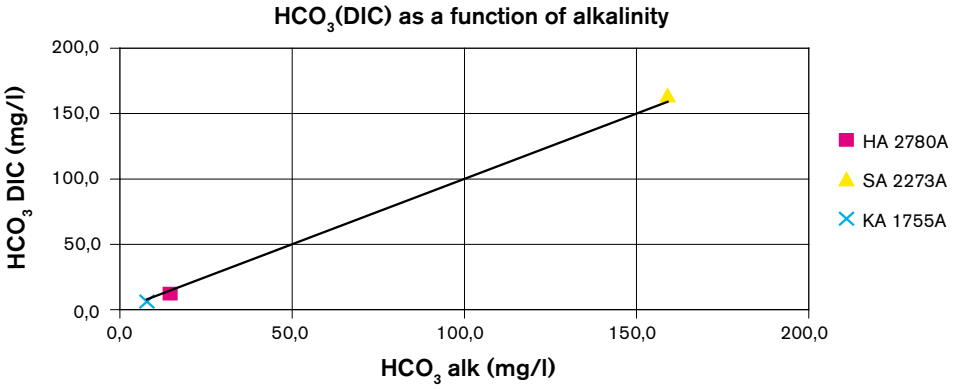

Figure A6-1. *HCO_3 (DIC) results as a function of alkalinity.*

4 References

Davis S N, DeWiest R J, 1967. Hydrology, 2. 3., Wiley, New York.

Ruotsalainen et al. 1998. Posivan vesinäytteenoton kenttätyöohje, rev.2, Posiva Työraportti 98-54.

Vuorinen et al. 1997. Groundwater chemistry of Olkiluoto – Saline and brackish groundwater – recipe for saline reference water, Posiva Working report 97-25.

Appendix 7

Äspö Hard Rock Laboratory

Compilation of groundwater chemistry data October 2001

Christina Mattsén, Svensk Kärnbränslehantering AB

February 2002

Contents

1 Methods and results

1.1 Methods

Water samples, class 4 and 5, have been collected and analysed according to SKB MD 431.011-01. In addition to the ordinary sampling (class 4) we have sampled and analysed carbon isotopes. Table A7-1 explains the different chemistry classes.

All sampling sections have been flushed such that five section volumes have been exchanged before sampling.

Water sampled for major components and DOC have been filtered on-line through Colly On-line High Capacity filters (0.45 um). Water for major cations has been filtered on-line through nucleopore filters (0.45 um). Unfiltered water was collected for all other isotopes.

Different parameters have been analysed at different laboratories (Table A7-2).

Table A7-1. SKB chemistry classes.

Class no	Description	Analyses	Optional
1	Simple sampling, basic control of water type	Electric conductivity pH Uranine*	
2	Simple sampling, control of water type	Electric conductivity pH, Cl, HCO_3 Uranine*	^2H, ^3H, ^{18}O Freeze stored back-up sample
3	Simple sampling, determination of non redox-sensitive major components	Electric conductivity pH, Cl, HCO_3, SO_4, Br Uranine* Major cations** (except for Fe, Mn), SO_4 as Sulphur by ICP-AES	^2H, ^3H, ^{18}O Freeze stored back-up sample
4	Extensive sampling, complete chemical characterisation	Electric conductivity pH, Cl, HCO_3, SO_4, Br, Fe (total, ferrous), Uranine*, DOC, major cations** SO_4 as Sulphur by ICP-AES ^2H, ^3H, ^{18}O Freeze stored back-up sample, preserved and non-preserved	HS^-, NH_4^+
5	Extensive sampling, complete chemical characterisation including special analyses	Electric conductivity pH, Cl, HCO_3, SO_4, Br, Fe (total, ferrous), Uranine*, DOC, major cations** SO_4 as Sulphur by ICP-AES ^2H, ^3H, ^{18}O Freeze stored back-up sample, preserved and non-preserved	HS^-, NH_4^+ F^-, I^- NO_2^-, NO_3^-, PO_4^{3-} TOC 14C-age, PMC, δ13C per mill PDB U, Th (elements and/or isotopes) Other trace elements (INAA and/or ICP-MS) 226Ra, 228Ra, 222Rn Or your decision

* Only measured when uranine was used in the drilling procedure and as long as no extra uranine has been added to the borehole e.g. in tracer tests.
** Major cations are Na, K, Ca, Mg, Si, Fe, Mn, Li, Sr.

Table A7-2. Laboratories used for analyses.

Laboratory	Parameter (method)
Äspö HRL, Sweden	pH, electric conductivity, Cl^-, HCO_3^-, SO_4^{2-}, Br^-, Fe (total and ferrous), NH_4–N, HS
SGAB Analytica, Sweden	Major cations (ICP-AES)
ALcontrol, Sweden	NH_4^+–N, NO_2^-, NO_3^-, PO_4^{3-},
Ångströmlaboratoriet, Sweden	Carbon-isotopes
University of Waterloo, Canada	Tritium
Fortum Power and Heat Oy, Finland	DOC
Institutt for Energiteknikk (IFE), Norway	Oxygen-18, Deuterium

1.2 Results

Sampled boreholes and sections are listed in Appendix 1 together with Äspö96 coordinates. The water compositions obtained from the analyses are shown in Appendix 2. Environmental isotope analyses are listed in Appendix 3 and Carbon-isotopes in Appendix 4.

The following SICADA queries were applied when extracting data:

gwchemistry/analyses/water/sampling_series, 01-10-15—01-10-16, GWCM

gwchemistry/analyses/water/water_composition, 01-10-15—01-10-16, GWCM

gwchemistry/analyses/water/h_o_isotope, 01-10-15—01-10-16, GWCM

gwchemistry/analyses/water/c_s_isotope, 01-10-15—01-10-16, GWCM

Appendix 1

Summary 2001, Activity history.

Idcode	Secup* (m)	Seclow* (m)	Sample no**	Sampling date	Class no**	Project	Northing Äspö96 (m)	Easting Äspö96 (m)	Elevation Äspö96 (m)
HA1330B	0.0	32.5	3465	2001-10-15	4	GWCM	6,975.80	2,123.31	–183.13
HA2780A	0.0	43.3	3467	2001-10-16	4	GWCM	7,451.30	2,159.26	–380.43
KA1755A	88.0	160.0	3469	2001-10-16	4	GWCM	7,499.20	2,020.44	–279.92
KA3110A	20.1	26.8	3464	2001-10-15	4	GWCM	7,299.63	2,332.45	–415.94
KR0012B	1.2	10.6	3466	2001-10-15	5	GWCM	6,165.91	2,167.10	–69.16
SA1229A	6.0	20.5	3471	2001-10-16	4	GWCM	6,885.16	2,105.46	–171.29
SA2074A	6.0	38.7	3468	2001-10-16	4	GWCM	7,290.03	2,348.26	–281.68
SA2273A	6.0	20.0	3470	2001-10-16	4	GWCM	7,149.70	2,221.64	–305.98

SICADA: Activity_history_sampling_series, 011015–011016.
* = Secup and Seclow is upper and lower limit of the samled section.
** = Class no shows SKB's chemistry class.

Appendix 2

Summary 2001, Water composition.

Idcode	Secup* (m)	Seclow* (m)	Sample no**	Sampling date	Na mg/l	K mg/l	Ca mg/l	Mg mg/l	HCO_3 mg/l	Cl mg/l	SO_4 mg/l	SO_4-S mg/l
Measurement uncertainty					5%	5%	5%	5%	5%	5%	10%	5%
HA1330B	0.0	32.5	3465	2001-10-15	1,570	17.1	337	118.0	201	2,960	312	121
HA2780A	0.0	43.3	3467	2001-10-16	3,320	15.1	4,450	35.6	19	12,800	654	223
KA1755A	88.0	160.0	3469	2001-10-16	3,050	11.6	4,200	36.6	9	11,720	646	225
KA3110A	20.1	26.8	3464	2001-10-15	1,430	35.1	257	128.0	196	2,730	269	102
KR0012B	1.2	10.6	3466	2001-10-15	172	2.6	40	7.8	329	168	37	14
SA1229A	6.0	20.5	3471	2001-10-16	1,520	26.2	277	124.0	264	2,850	224	94
SA2074A	6.0	38.7	3468	2001-10-16	1,240	9.6	394	80.4	174	2,520	237	91
SA2273A	6.0	20.0	3470	2001-10-16	1,570	14.9	675	100.0	158	3,640	253	102

Idcode	Secup* (m)	Seclow* (m)	Sample no**	Mn mg/l	Li mg/l	Sr mg/l	pH pH unit	El. Cond mS/m	Smpl-Flow l/min	Drill water mg/l	DOC mg/l	S_2 mg/l	NH4-N mg/l
Measurement uncertainty				0.05	0.05	0.1	0.1 unit%	0		10%	0.1 mg/l	0.10	0.20
HA1330B	0.0	32.5	3465	0.78	0.10	4.9	7.4	970	0.33	0.04	3.6	0.01	0.67
HA2780A	0.0	43.3	3467	0.26	3.36	75.2	7.6	3,250	5.00	0.03	1.4		0.10
KA1755A	88.0	160.0	3469	0.30	2.92	70.8	7.7	2,990	1.10	0.02	1.0		0.04
KA3110A	20.1	26.8	3464	0.69	0.08	3.7	7.7	910	2.00	0.05	5.0	0.09	0.79
KR0012B	1.2	10.6	3466	0.14	0.04	0.8	7.5	116	0.40	0.20	11.0	0.04	0.09
SA1229A	6.0	20.5	3471	0.66	0.09	4.6	7.3	950	1.50	0.06	4.8	0.01	1.58
SA2074A	6.0	38.7	3468	0.47	0.15	6.0	7.7	850	0.21	0.05	4.1	0.05	0.16
SA2273A	6.0	20.0	3470	0.78	0.35	10.7	7.5	1,150	2.40	0.04	3.2	0.02	0.48

SICADA: water_composition 011015–011016
* = Secup and Seclow is upper and lower limit of the samled section.
** = Class no shows SKB's chemistry class.

Appendix 3

Summary 2001, Environmental isotopes.

Idcode	Secup (m)	Seclow (m)	Sample	Sampling date	D (dev SMOW)	T (TU)	O_{18} (dev SMOW)
Measurement uncertainty					1 unit	1 unit	0.2 unit
HA1330B	0.00	32.5	3465	2001-10-15	–58.5	12.2	–7.2
HA2780A	0.00	43.3	3467	2001-10-16	–85.7	1.0	–11.9
KA1755A	88.00	160.0	3469	2001-10-16	–91.9	–0.8	–12.8
KA3110A	20.05	26.8	3464	2001-10-15	–58.9	12.2	–7.3
KR0012B	1.20	10.6	3466	2001-10-15	–73.9	13.1	–10.2
SA1229A	6.00	20.5	3471	2001-10-16	–57.3	12.0	–7.2
SA2074A	6.00	38.7	3468	2001-10-16	–64.0	10.2	–8.2
SA2273A	6.00	20.0	3470	2001-10-16	–65.0	8.9	–8.3

SICADA: h_o_isotopes, 011015-011016
* = Secup and Seclow is upper and lower limit of the samled section.
** = Class no shows SKB's chemistry class.

Appendix 4

Summary 2001, Carbon isotopes.

Idcode	Secup (m)	Seclow (m)	Sample	Percent modern Carbon pmc	C13 dev PDP	Age BP year	Age BP Corr year
Measurement uncertainty						100 years	
KR0012B	1.20	10.6	3466	86.9	–14.9	10	45

SICADA: c_s__isotopes, 011015-011016

Appendix 8

Background measurements of inorganic colloids in different Äspö waters

Susanna Wold, Trygve Eriksen
KTH

January 2003

Edited by: Susanna Wold, KTH, September 2005.

Contents

1 Background

Sorption of radionuclides on colloids can change radionuclide mobility in a deep bedrock repository of spent nuclear fuel, whereby colloids serving as a mobile carrier phase. Possible radionuclide carrying colloids in groundwater are clay and humic/fulvic colloids, as well as mineral oxides and silicates. It is important to study the effect of colloids on radionuclide mobility in the barriers of a repository for spent nuclear fuel. To be able to separate natural colloids in in-situ experiments, the background levels of colloids have to be determined. In this study the background concentration of inorganic colloids is measured in different types of groundwater, represented by waters from eight bore holes situated at different depths in the bedrock of the Äspö HRL tunnel. Two different techniques for concentration measurements are compared.

2 Sampling

A filter system, with 3,000, 450, 220 in serie and 220 and 50 nm pore sizes was connected in series to the outlet of the bore hole. The filters were initially flushed with argon since it is known that colloid formation can be initiated by oxygen exposure. Measured volumes of 50–1,000 ml water flowed through the filter system. The smaller volumes were chosen when filtering through the 220 and 50 nm series to avoid filter clogging. Since the expected colloid concentration is low, large volumes were chosen in the other filter series to allow collection of detectable amounts of colloids. The water flow through the filters was followed throughout the sampling to detect pressure drop caused by clogging, but was never detected. The filters were detached and immediately sealed in plastic cups in an exikator.

Water was collected in pressure vessels of steel. The vessels were flushed with water for about one minute before collecting 500 ml. The pressure vessels and the exikator were transported to KTH for analyses.

3 Experimental

3.1 ICP-MS and ICP-AES analysis

The filters were soaked in 0.5 ml 65% suprapure HNO_3 and 2.5 ml Millipore deionized, triple distilled water in acid washed vessels. After 1.5 hours the solutions were diluted to 20 ml with Millipore deionized triple distilled water. After 15 minutes the filters were removed and the diluted solutions were sent to SGAB commercial laboratory for ICP-MS, ICP-AES analysis. One extra filter for every bore hole was wetted with water and thereafter treated in the same way as the other filters and used as blanks.

3.2 PCS – Photon Correlation Spectroscopy

The signal in the PCS is roughly proportional to the concentration of colloid particles of different sizes. To enable measurements of particle concentration as well as particle size distributions, the PCS equipment was calibrated with solutions containing latex colloids with defined size distributions.

Water was filtered through 800, 200 and 100 nm syringe filters to plastic cuvettes. The PCS detects gas bubbles as well as dust as colloids, which is why it is important to minimise the impact from gas bubbles on the signal. The water was degassing in the cuvettes for a day before analysing with PCS. Degassing the samples is a compromise since oxygen exposure initiates colloid formation.

4 Results

4.1 PCS – Dynamic light scattering

All samples contained colloid concentrations lower than the PCS detection limit of 0.6 mg/L.

4.2 ICP-MS and ICP-AES analysis

The inorganic colloids in Äspö waters are mainly composed of iron hydroxides, silica and clay mineral. Fe, Si and Al are therefore assumed to represent the inorganic colloids in the analysed Äspö waters. The colloid content of the different Äspö waters can be seen in Table A8-1.

The colloid concentration in the Äspö waters is in the range of 1–149 ppb. Colloids in the size range > 50 < 220 nm are dominating in all the Äspö water samples except for the water sampled in bore hole SA2273 A. The colloid concentrations are very low and it is therefore questionable to define exact size distributions.

Filtering of water followed by ICP analysis of the leached colloids in solution seems to be a feasible method of measuring the colloid content in groundwater with low concentrations of colloids. The PCS technique is not sensitive enough to detect the low concentrations of colloids in the sampled groundwaters.

Table A8-1. Colloid content in the Äspö waters from different boreholes.

	Fe+Si+Al ppb	Total ppb
KA 3110 A	> 50 < 220 nm	18.4
	> 220 < 450 nm	1.1
	> 450 < 3,000 nm	1.5
	> 50 < 3,000 nm	21.0
HA 2780 A	> 50 < 220 nm	143.3
	> 220 < 450 nm	2.8
	> 450 < 3,000 nm	2.8
	> 50 < 3,000 nm	149.0
SA2273 A	> 50 < 220 nm	0.0
	> 220 < 450 nm	0.0
	> 450 < 3,000 nm	0.9
	> 50 < 3,000 nm	1.0
SA 2074 A	> 50 < 220 nm	56.9
	> 220 < 450 nm	11.9
	> 450 < 3,000 nm	18.7
	> 50 < 3,000 nm	87.0
KA 1755 A	> 50 < 220 nm	25.3
	> 220 < 450 nm	6.4
	> 450 < 3,000 nm	8.8
	> 50 < 3,000 nm	41.0
HA 1330 B	> 50 < 220 nm	3.6
	> 220 < 450 nm	0.6
	> 450 < 3,000 nm	0.7
	> 50 < 3,000 nm	5.0
SA 1229 A	> 50 < 220 nm	1.8
	> 220 < 450 nm	1.1
	> 450 < 3,000 nm	0.2
	> 50 < 3,000 nm	3.0
KR 0012 B	> 50 < 220 nm	23.8
	> 220 < 450 nm	0.6
	> 450 < 3,000 nm	7.4
	> 50 < 3,000 nm	32.0

Appendix 9

Total number of microorganisms in groundwater sampled during background colloid measurements along the Äspö HRL tunnel

Karsten Pedersen, Gothenburg University

Contents

1 Background

Colloids are defined as small particles in the size range 10^{-6} to 10^{-3} mm. Colloidal particles are of interest for the safety of spent nuclear fuel because of their potential to transport radionuclides from a faulty repository canister to the biosphere.

Microorganisms generally range in size between 2×10^{-4} to 10^{-2} mm, thereby overlapping colloid particles in size. Their organic character, with many different functional groups directed outwards from the cell surface, e.g. phosphates, amines, hydroxyl- and carboxyl-groups, makes them potent as radionuclide sorbents.

The natural background colloid concentrations from various boreholes along the Äspö HRL tunnel were studied. The boreholes represented different water types since it is well known that the colloid stability can change with the ion content of the groundwater. This is also true for microorganisms. Additionally, organic content and the chemical composition of the water influence microbe types and numbers. Eight selected boreholes were sampled to measure the background colloid content, humic substances and microorganisms. The results from microorganism enumerations are presented here.

2 Sampling

Eight different boreholes were sampled on 23 October 2001 as shown in Table A9-1. A test rack with 50 ml sterile plastic tubes with screw lids was supplied with 3 ml 30% formaldehyde. Triplicates of groundwater were collected from each borehole. The sampling was spread out over time, during which other sampling activities were performed. The samples were kept in cool storage until transport to and analysis in Gothenburg.

2.1 Experimental setup and filtration

Selected volumes were filtered on 13 mm diameter, black 0.22 Micron polycarbonate filters (Osmonic Inc), using a Millipore stainless steel filtration set-up, equipped with 13 mm funnels. In a first analysis 1 ml was filtered from all samples, using 1/3 atmosphere underpressure. The counting result guided on the filtered volume in the second analysis. The number of cells counted was aimed to be approximately 500 cells per filter. The filtration volumes are depicted in Table A9-1. The filter area was 70 mm^2.

Acridine orange was used for staining the cells. It was blended in a phosphate buffer. The buffer was prepared by dissolving 0.449 g KH_2PO_4 in 500 ml double distilled water, mixed with 0.588 g Na_2HPO_4 in 500 ml double distilled water and adjust pH to 6.7. Phosphate content was 6.6 mM. Ten mg acridine orange was added to 100 ml of buffer. After mixing and filtration through a 0.2 µm filter, sterilization was performed in an autoclave.

2.2 Microscopy analysis

Filters were mounted with immersion oil on microscope slides and observed under blue light in an inverted Nikon Diaphot 300 microscope at 1,000 times enlargement. A 100 times lens was used. Microbial cells show orange or green fluorescence in this light (See Figures A9-2 to A9-9). The counted frame size was 100×100 µm. 15 frames were counted on each filter.

Table A9-1. The boreholes were sampled on 23 of October 2001 at times indicated in the table. The sample volumes filtrated in two replicates analyses is also shown.

Borehole	First analysis time and volume (ml)			Second analysis time and volume (ml)		
	1A	2A	3A	1B	2B	3B
KR 0012 B	21:32	21:50	21:53	21:32	21:50	21:53
	1	1	1	1	1	1
SA 1229 A	16:32	16:38	16:47	16:32	16:38	16:47
	1	1	1	10	10	10
HA 1330 B	15:35	15:45	15:55	15:35	15:45	15:55
	1	1	1	5	5	5
KA 1755 A*	13:27	13:35	14:00	13:27	13:35	14:00
	3	3	3	10	10	10
SA 2074 A	10:25	10:43	10:52	10:25	10:43	10:52
	1	1	1	10	10	10
SA2273 A	14.22	14.33	14.58	14.22	14.33	14.58
	1	1	1	10	10	10
HA 2780 A	20:30	20:40	21:01	20:30	20:40	21:01
	1	1	1	10	10	10
KA 3110 A	09:03	09:25	09:43	09:03	09:25	09:43
	1	1	1	1	1	1

* KA1775 was filtered three times. The first filtration A, was considered possibly corrupt (contaminated). A third filtration, C was therefore performed.

3 Results and discussion

A total of 13,158 cells distributed over 24 samples, two (one sample – triplicate) replicate filtrations and 375 frames were registered. The results are shown in Table A9-2.

The numbers ranged more than two orders of magnitude, with the highest numbers in the shallowest and the deepest borehole investigated, KR0012B and KA3110A. A comparison of the obtained data with earlier data on total numbers of microorganisms in Fennoscandian Shield groundwater is shown in Figure A9-1. The obtained data lies within the range of all available data.

There was an obvious difference in size and appearance between the boreholes, from 0.2 μm up to several μm. Borehole HA1330B showed the largest cells (Figure A9-4); most other boreholes had small or very small cells – see Figures A9-2 to A9-9 for details. Thin flaks were observed in KR0012B.

Table A9-2. Results from two repeated filtrations. See Table A9-1 for sample volumes.

Borehole	First analysis cells $ml^{-1} \times 10^4$			Second analysis cells $ml^{-1} \times 10^4$			Overall mean cells ml^{-1} x10^4 (S.D.)
	1A	2A	3A	1B	2B	3B	
KR0012B	40	21	27	48	46	22	35 (12)
SA1229A	1.9	2.9	2.1	2.6	2.0	2.0	2.3 (0.4)
HA1330B	(0.13)	(0.14)	(0.14)	1.1	4.2	3.4	2.9 (1.3)
KA1775A	0.67	1.0	2.4	5.3	0.97	1.3	1.9 (1.6)
SA2074A	0.51	0.05	0.7	0.16	0.15	0.15	0.29 (0.2)
SA2273A	0.93	0.79	1.3	3.1	2.2	2.7	1.8 (0.9)
HA2780A	0.37	0.28	0.14	0.52	0.09	0.14	0.26 (15)
KA3110A	26	14	30	27	11	23	22 (7.0)

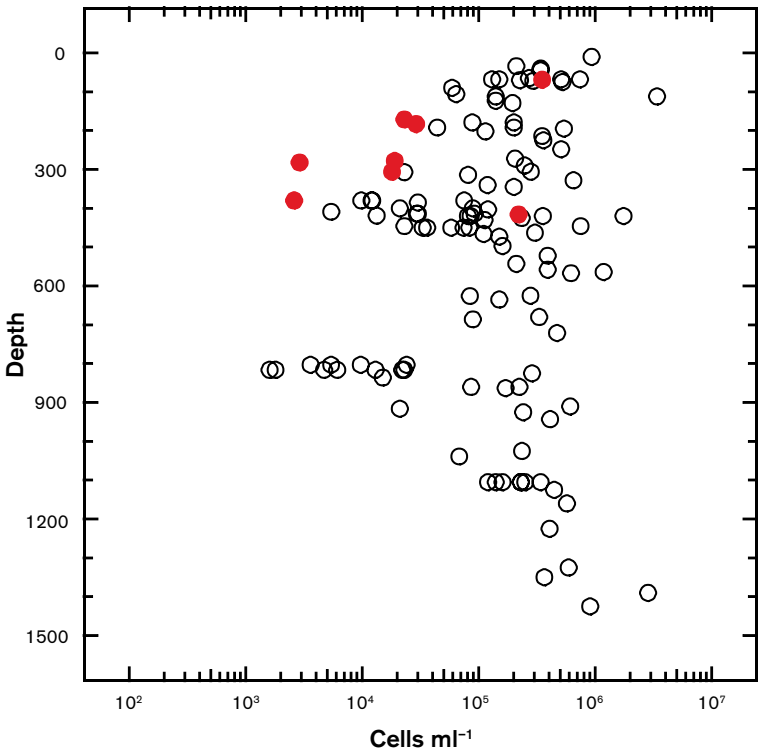

Figure A9-1. *The overall means from Table A9-2 plotted with the available data base on total numbers of microorganisms from Stripa research mine, Äspö HRL area, Laxemar boreholes KLX and investigation sites in Finland (Olkiluoto, Hästholmen, Kivetty, Romuvaara) and the natural uranium analogue in Palmottu.*

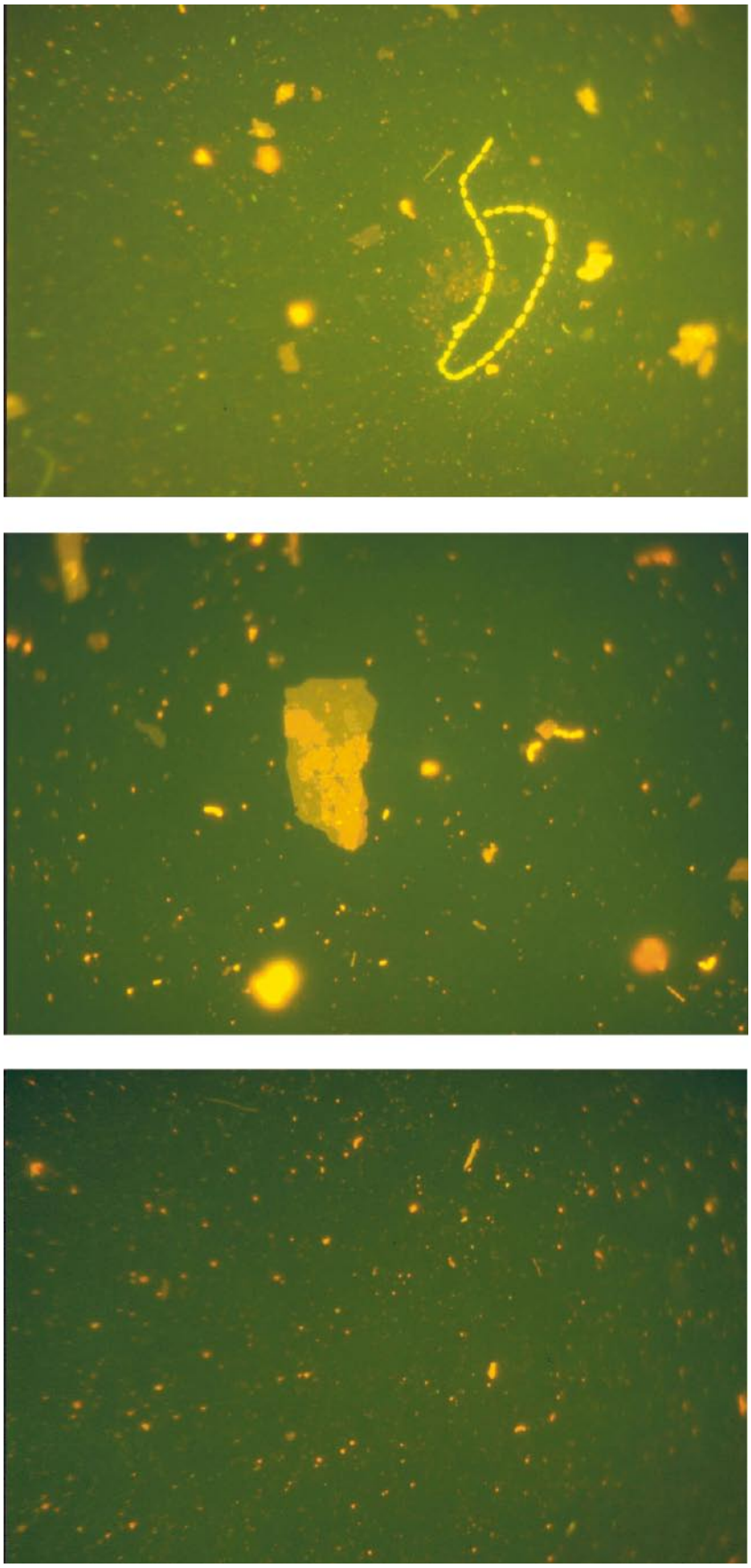

Figure A9-2. *KR0012B, filter 1B, 2B and 3B. Frame size is 130×85 µm.*

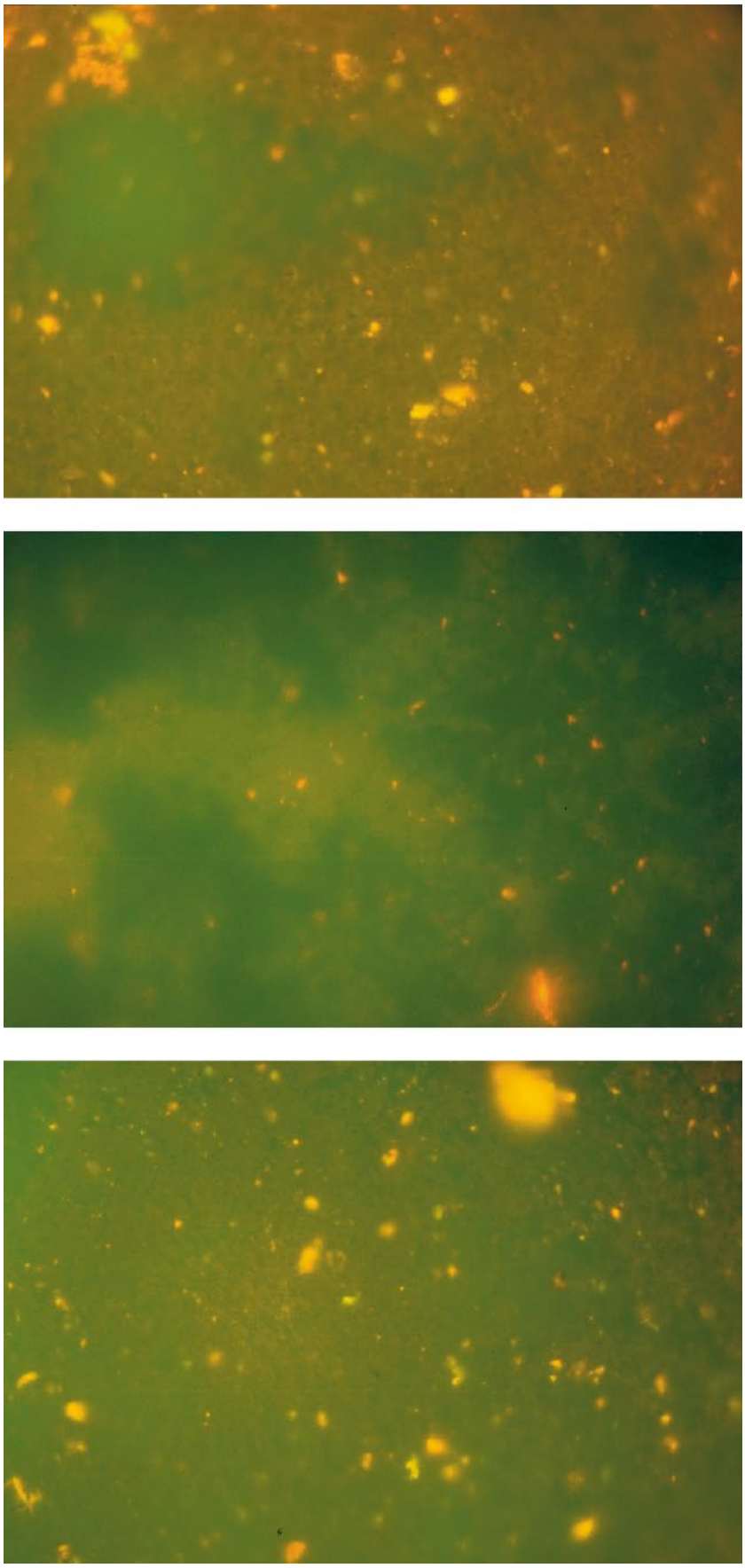

Figure A9-3. *SA1229A filter 1B, 2B and 3B. Frame size is 130×85 µm.*

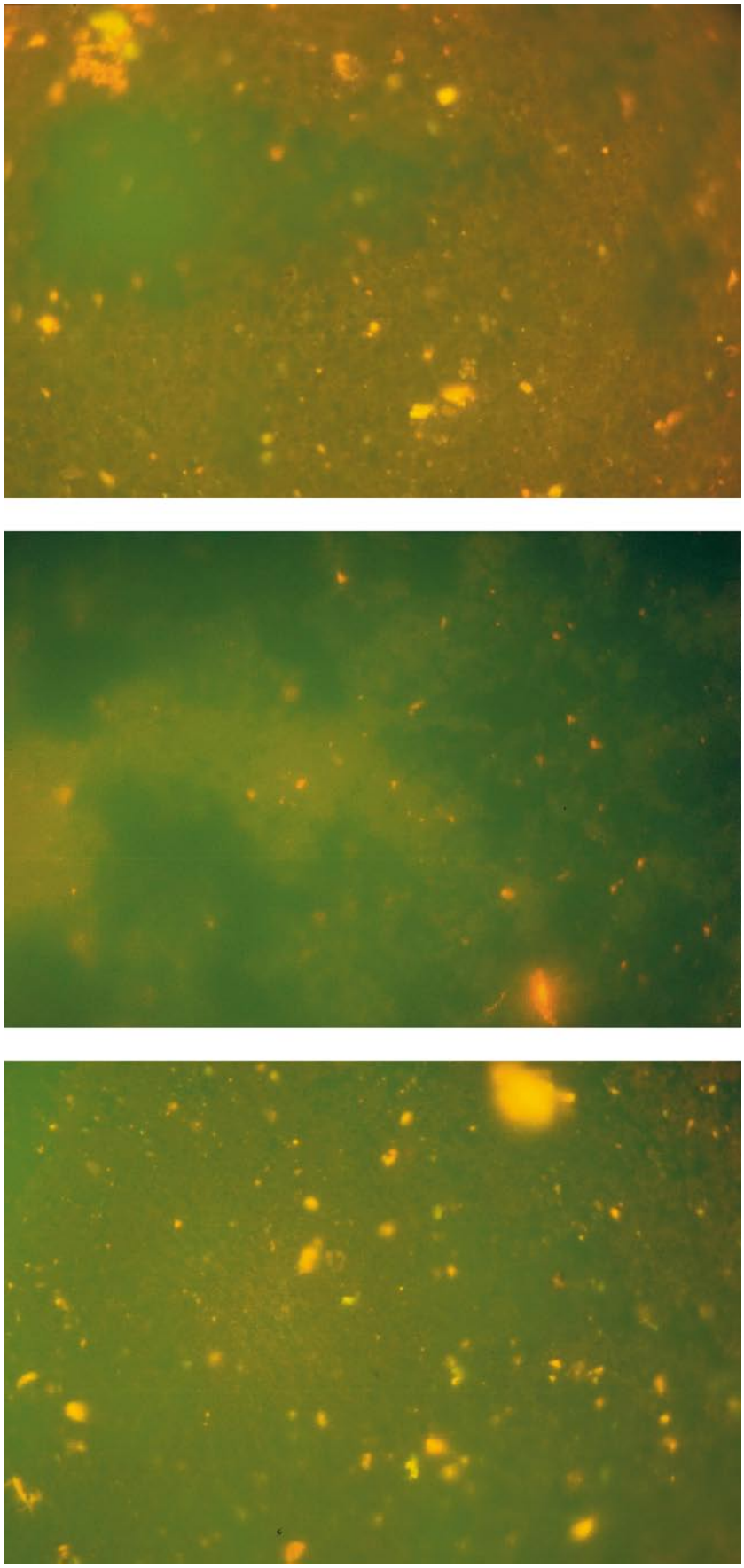

Figure A9-4. *HA1330B, filter 1B, 2B and 3B. Frame size is 130×85 µm.*

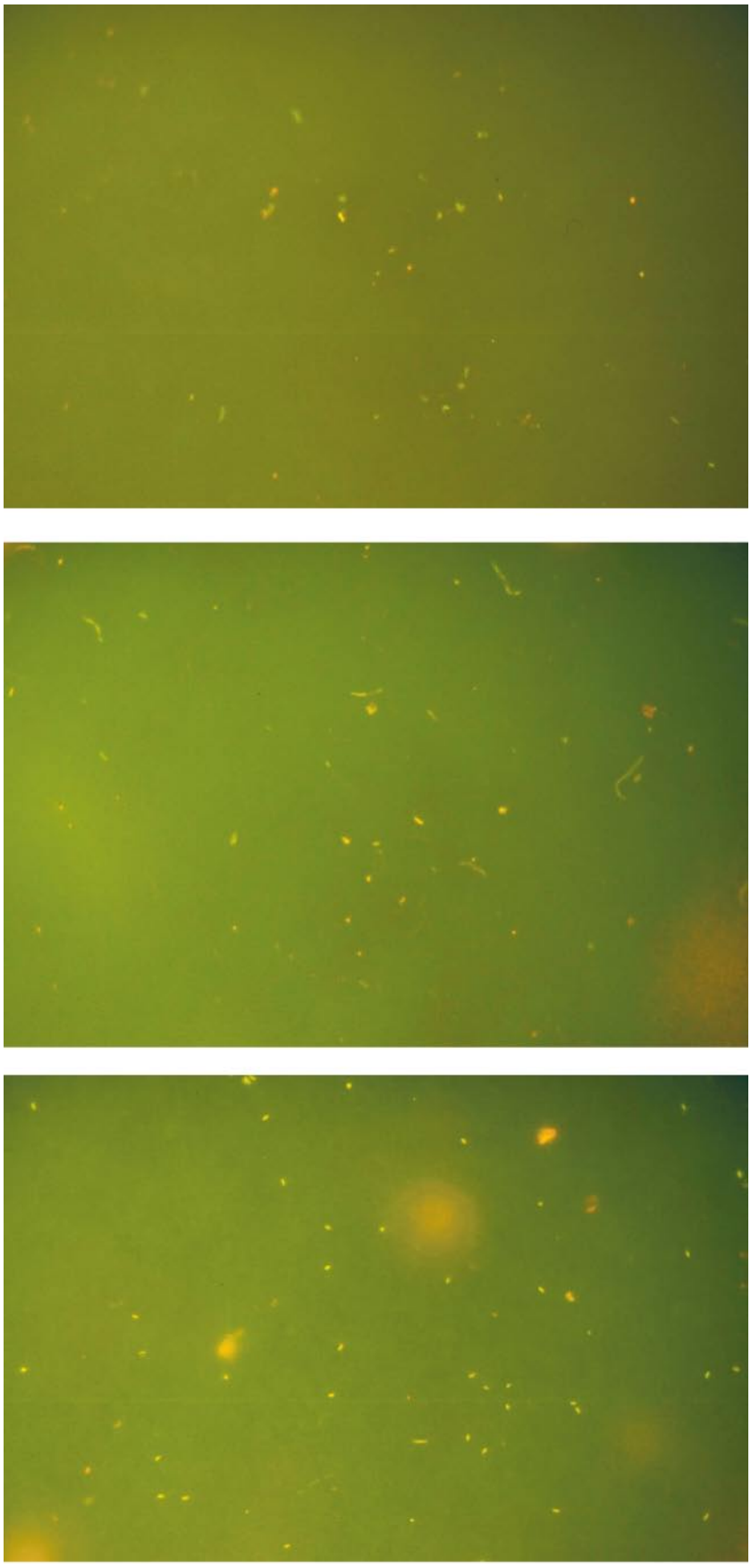

Figure A9-5. *KA1775A, filter 1B, 2B and 3B. Frame size is 130×85 µm.*

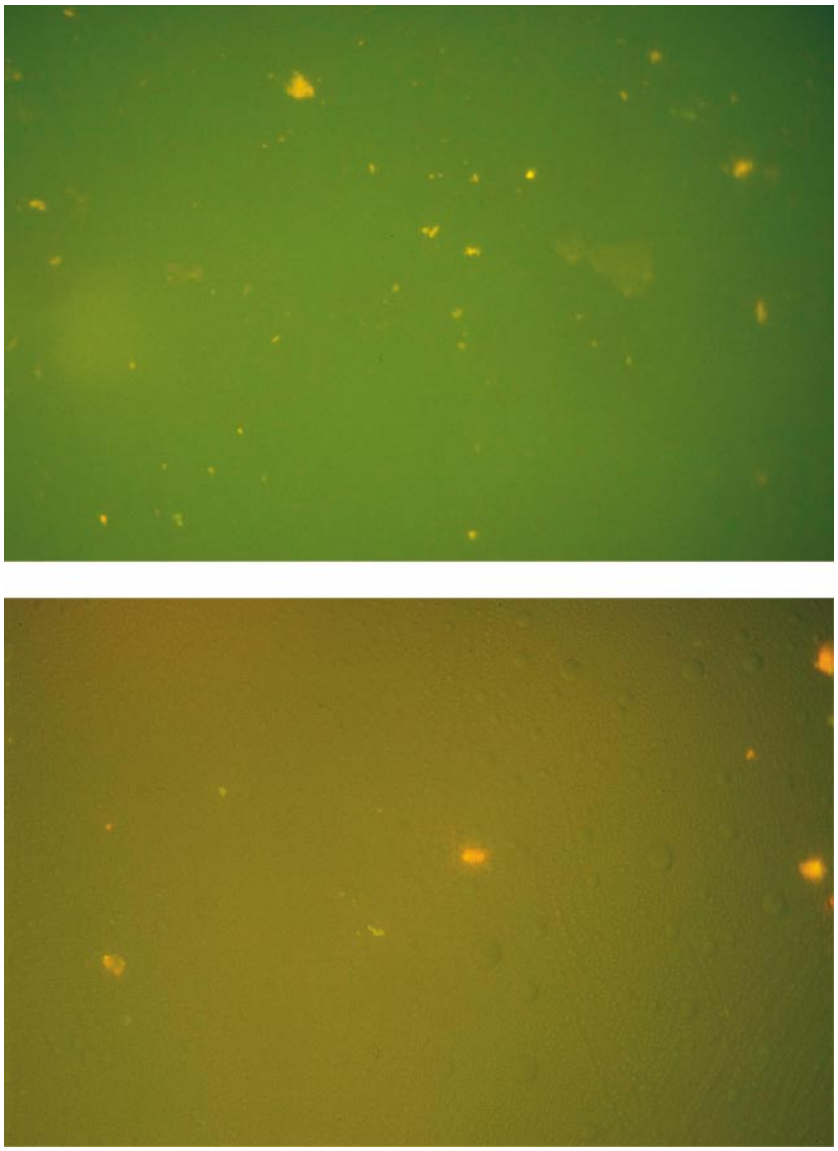

Figure A9-6. *SA2074A, filter 1B, 2B and 3B. Frame size is 130×85 µm.*

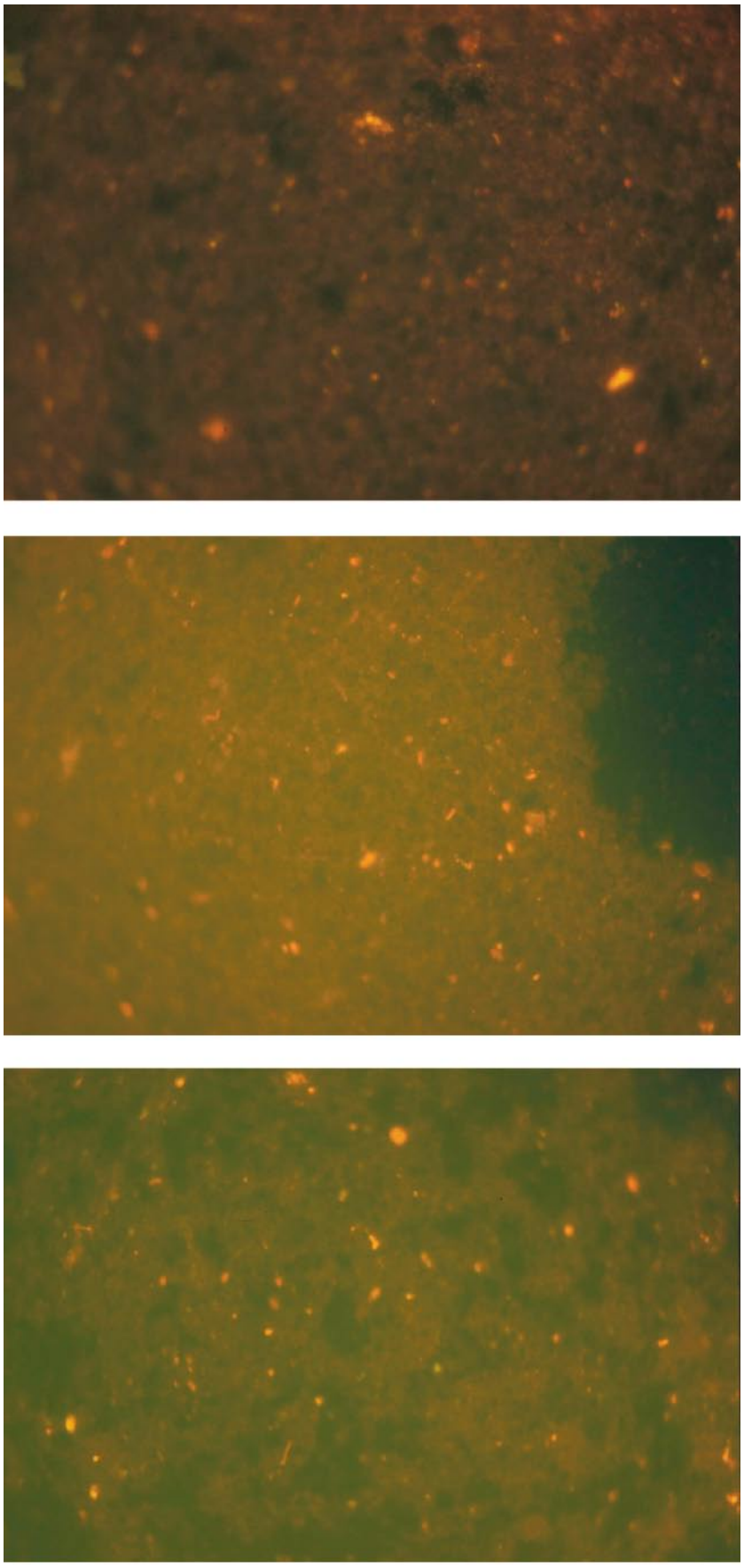

Figure A9-7. *SA2273A, filter 1B, 2B and 3B. Frame size is 130×85 µm.*

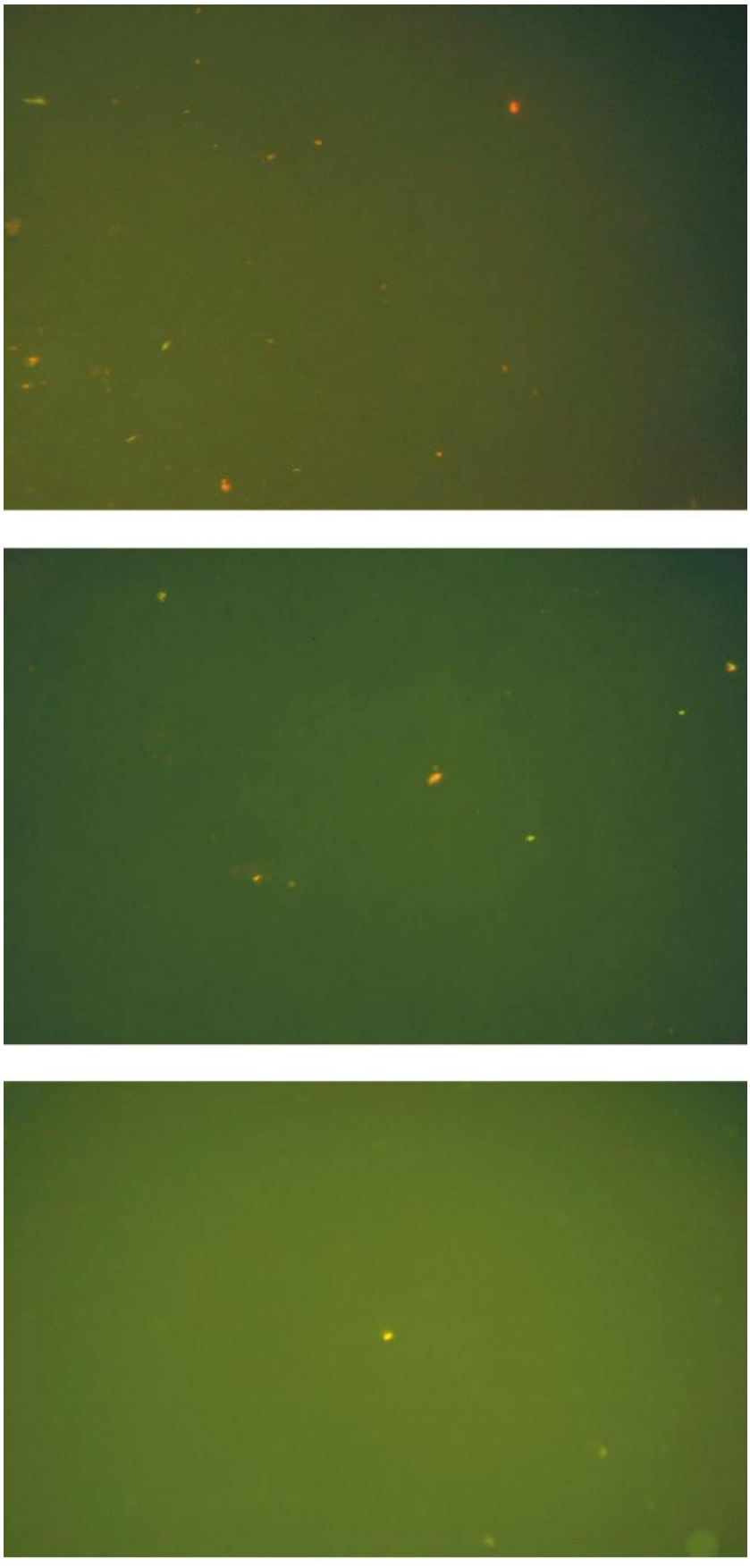

Figure A9-8. *HA2780, filter 1B, 2B and 3B. Frame size is 130×85 µm.*

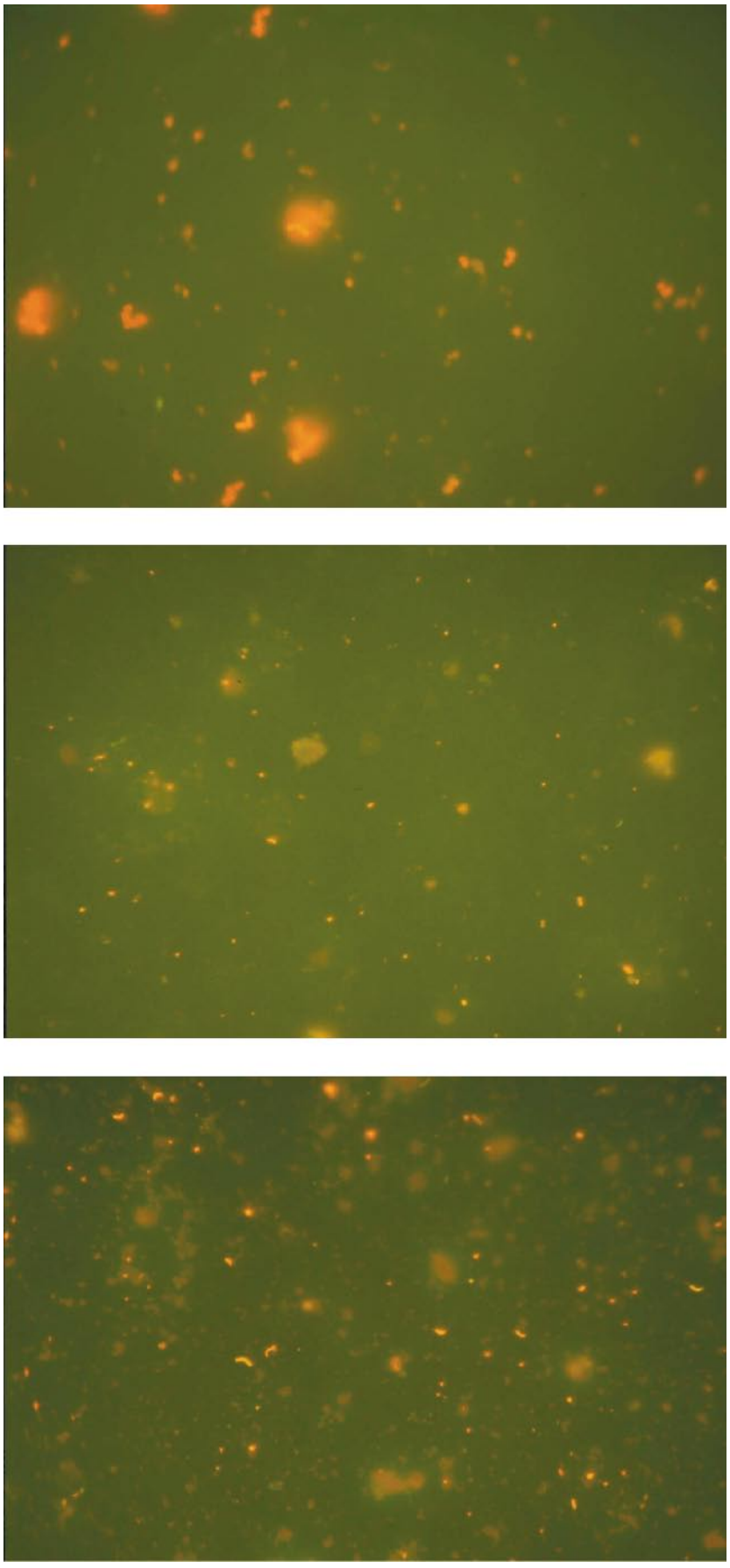

Figure A9-9. *KA3110A, filter 1B, 2B and 3B. Frame size is 130×85 µm.*

Appendix 10

Electric conductivity measurements along the Äspö tunnel

Ioana Gurban

Contents

1 Background and aim of sampling

The aim of the sampling is to measure the electrical conductivity of all the major water venues at the Äspö tunnel in order to measure the variability of the groundwater chemistry, which may affect the colloid stability. The electrical conductivity data collected along the tunnel was evaluated and then compared with the borehole data.

2 The sampling procedure

The water venues along the tunnel were sampled directly in plastic bottles of 100 ml capacity. From water venues high up on the tunnel walls or from the tunnel ceiling, the water was sampled using a funnel adapted to the sampling bottle. The bottles were brought to the Äspö laboratory for analysis, since a mobile electric conductivity-meter was not available.

3 Number of samples

All the water venues along the tunnel and in the accessible tunnel niches were sampled, taking one water sample from each water venue. For wide water venues representative samples were taken. For example, for a water venue of a width of 10 m, a sample was taken in the beginning, one in the middle and the third at the end of the water venue. When possible, water venues were collected from the left side, the right side and the ceiling of the tunnel in order to better capture the variability of the water chemistry. 195 samples were collected along the tunnel in total.

4 Sampling locations

The sampling locations were all the water venues along the tunnel, identified by A (left side on the tunnel), B (right side on the tunnel) and T (ceiling). The samples were labelled with an ID code according to SKB procedure.

5 Results and discussion

A total of 195 samples were taken and analyzed at Äspö laboratory, following the Class1 procedure. The preliminary results for electrical conductivity are shown in Table A10-1. The results will be compared with the electrical conductivity measurements from the tunnel boreholes. The modelling and comparison will be done using the visualization and interpolation tool Tecplot. Sections along the tunnel will be presented for interpretation and analysis of the variability of the groundwater chemistry along the tunnel.

Table A10-1. Results of the electrical conductivity measurements along the Äspö tunnel.

Sample nr	Start date	Idcode	Secup (m)	Seclow (m)	Sample no	Cond (mS/m)	Northing	Easting	Elevation	Coord system
1	10/23/01 3:00	TASA	502	502	3495	120	6366728	1551706	–69.48	RT38-RH00
2	10/23/01 3:00	TASA	170	170	3478	710	6366415	1551815	–23	RT38-RH00
3	10/23/01 3:00	TASA	128	128	3476	410	6366375	1551828	–17.8	RT38-RH00
4	10/23/01 3:00	TASA	282	282	3484	1,170	6366520	1551778	–38.68	RT38-RH00
5	10/23/01 3:00	TASA	293	293	3486	1,210	6366531	1551774	–40.22	RT38-RH00
6	10/23/01 3:00	TASA	150	150	3475	400	6366396	1551821	–20.20	RT38-RH00
7	10/23/01 3:00	TASA	821	821	3504	940	6367030	1551601	–112.62	RT38-RH00
8	10/23/01 3:00	TASA	293	293	3485	1,160	6366531	1551774	–40.22	RT38-RH00
9	10/23/01 3:00	TASA	769	769	3501	740	6366980	1551618	–105.36	RT38-RH00
10	10/23/01 3:00	TASA	220	220	3481	920	6366462	1551798	–30.00	RT38-RH00
11	10/23/01 3:00	TASA	842	842	3506	980	6367049	1551594	–115.56	RT38-RH00
12	10/23/01 3:00	TASA	267	267	3483	1,060	6366506	1551783	–36.58	RT38-RH00
13	10/23/01 3:00	TASA	492	492	3493	310	6366719	1551709	–68.08	RT38-RH00
14	10/23/01 3:00	TASA	320	320	3487	1,200	6366556	1551765	–44.00	RT38-RH00
15	10/23/01 3:00	TASA	949	949	3509	1,100	6367152	1551569	–130.54	RT38-RH00
16	10/23/01 3:00	TASA	860	860	3508	960	6367066	1551588	–118.08	RT38-RH00
17	10/23/01 3:00	TASA	839	839	3505	990	6367047	1551595	–115.14	RT38-RH00
18	10/23/01 3:00	TASA	202	202	3479	970	6366445	1551804	–27.48	RT38-RH00
19	10/23/01 3:00	TASA	853	853	3507	970	6367060	1551591	–117.10	RT38-RH00
20	10/23/01 3:00	TASA	687	687	3498	430	6366903	1551645	–95.38	RT38-RH00
21	10/23/01 3:00	TASA	555	555	3497	150	6366778	1551688	–76.90	RT38-RH00
22	10/23/01 3:00	TASA	209	209	3480	1,060	6366451	1551802	–28.46	RT38-RH00
23	10/23/01 3:00	TASA	437	437	3490	1,000	6366667	1551727	–60.38	RT38-RH00
24	10/23/01 3:00	TASA	83	83	3477	940	6366331	1551835	–13.30	RT38-RH00
25	10/23/01 3:00	TASA	788	788	3503	930	6366998	1551612	–108.00	RT38-RH00
26	10/23/01 3:00	TASA	470	470	3492	640	6366698	1551716	–65.00	RT38-RH00
27	10/23/01 3:00	TASA	788	788	3502	710	6366998	1551612	–108.00	RT38-RH00
28	10/23/01 3:00	TASA	555	555	3496	170	6366778	1551688	–76.90	RT38-RH00
29	10/23/01 3:00	TASA	232	232	3482	1,030	6366473	1551794	–31.68	RT38-RH00
30	10/23/01 3:00	TASA	448	448	3491	560	6366677	1551723	–61.92	RT38-RH00
31	10/23/01 3:00	TASA	415	415	3489	660	6366646	1551734	–57.30	RT38-RH00
32	10/23/01 3:00	TASA	410	410	3488	950	6366641	1551736	–56.60	RT38-RH00
33	10/23/01 3:00	TASA	500	500	3494	120	6366726	1551706	–69.20	RT38-RH00
34	10/23/01 3:00	TASA	764	764	3499	860	6366976	1551620	–104.86	RT38-RH00
35	10/23/01 3:00	TASA	765	765	3500	740	6366977	1551620	–104.96	RT38-RH00
36	10/23/01 13:30	NASA1049A	1,049	1,049	3,525	880				
37	10/23/01 13:30	NASA1265A	1,265	1,265	3,545	940				
38	10/23/01 13:30	NASA1272B	1,272	1,272	3,547	935				
39	10/23/01 13:30	NASA2156B	2,156	2,156	3,584	870				
40	10/23/01 13:30	NASA2198A	2,198	2,198	3,587	1,160				
41	10/23/01 13:30	NASA2198A	2,198	2,198	3,586	990				
42	10/23/01 13:30	TASA	2,542	2,542	3,598	940	6367761	1551326	–339.01	RT38-RH00
43	10/23/01 13:30	TASA	1,070	1,070	3,529	935	6367268	1551546	–147.48	RT38-RH00
44	10/23/01 13:30	TASA	2,340	2,340	3,594	1,110	6367685	1551486	–314.08	RT38-RH00

Sample nr	Start date	Idcode	Secup (m)	Seclow (m)	Sample no	Cond (mS/m)	Northing	Easting	Elevation	Coord system
45	10/23/01 13:30	TASA	2,289	2,289	3,590	1,170	6367709	1551531	–306.94	RT38-RH00
46	10/23/01 13:30	TASA	2,168	2,168	3,585	870	6367788	1551607	–291.8	RT38-RH00
47	10/23/01 13:30	TASA	1,050	1,050	3,524	900	6367249	1551552	–144.68	RT38-RH00
48	10/23/01 13:30	TASA	2,150	2,150	3,583	880	6367806	1551607	–289.28	RT38-RH00
49	10/23/01 13:30	TASA	2,122	2,122	3,581	855	6367834	1551608	–285.36	RT38-RH00
50	10/23/01 13:30	TASA	1,023	1,023	3,522	930	6367223	1551561	–140.90	RT38-RH00
51	10/23/01 13:30	TASA	2,030	2,030	3,578	840	6367914	1551586	–274.28	RT38-RH00
52	10/23/01 13:30	TASA	2,265	2,265	3,588	1,170	6367721	1551553	–303.58	RT38-RH00
53	10/23/01 13:30	TASA	1,065	1,065	3527	920	6367263	1551547	–146.78	RT38-RH00
54	10/23/01 13:30	TASA	2,310	2,310	3592	915	6367699	1551513	–309.88	RT38-RH00
55	10/23/01 13:30	TASA	2,348	2,348	3595	1,280	6367682	1551479	–315.20	RT38-RH00
56	10/23/01 13:30	TASA	2,435	2,435	3596	1,650	6367693	1551402	–325.59	RT38-RH00
57	10/23/01 13:30	TASA	1,122	1,122	3531	920	6367317	1551528	–154.76	RT38-RH00
58	10/23/01 13:30	TASA	2,580	2,580	3600	1,360	6367799	1551332	–342.80	RT38-RH00
59	10/23/01 13:30	TASA	2,020	2,020	3577	840	6367919	1551577	–272.88	RT38-RH00
60	10/23/01 13:30	TASA	2,015	2,015	3576	825	6367922	1551573	–272.18	RT38-RH00
61	10/23/01 13:30	TASA	991	991	3520	950	6367193	1551572	–136.42	RT38-RH00
62	10/23/01 13:30	TASA	2,001	2,001	3575	825	6367930	1551561	–270.22	RT38-RH00
63	10/23/01 13:30	TASA	2,000	2,000	3574	830	6367930	1551560	–270.08	RT38-RH00
64	10/23/01 13:30	TASA	978	978	3515	960	6367180	1551573	–134.60	RT38-RH00
65	10/23/01 13:30	TASA	1,980	1,980	3571	835	6367941	1551543	–267.28	RT38-RH00
66	10/23/01 13:30	TASA	978	978	3518	940	6367180	1551573	–134.6	RT38-RH00
67	10/23/01 13:30	TASA	1,870	1,870	3569	950	6367958	1551447	–253.68	RT38-RH00
68	10/23/01 13:30	TASA	978	978	3516	980	6367180	1551573	–134.6	RT38-RH00
69	10/23/01 13:30	TASA	1,765	1,765	3568	3,100	6367909	1551354	–239.72	RT38-RH00
70	10/23/01 13:30	TASA	1,749	1,749	3567	1,640	6367894	1551349	–238.12	RT38-RH00
71	10/23/01 13:30	TASA	1,735	1,735	3565	3,110	6367880	1551346	–236.46	RT38-RH00
72	10/23/01 13:30	TASA	969	969	3514	960	6367171	1551572	–133.34	RT38-RH00
73	10/23/01 13:30	TASA	1,691	1,691	3563	720	6367837	1551338	–230.30	RT38-RH00
74	10/23/01 13:30	TASA	1,686	1,686	3562	790	6367832	1551338	–229.60	RT38-RH00
75	10/23/01 13:30	TASA	1,435	1,435	3560	825	6367612	1551424	–198.58	RT38-RH00
76	10/23/01 13:30	TASA	1,430	1,430	3559	820	6367607	1551426	–197.88	RT38-RH00
77	10/23/01 13:30	TASA	1,400	1,400	3558	810	6367579	1551436	–193.68	RT38-RH00
78	10/23/01 13:30	TASA	1,387	1,387	3555	840	6367566	1551440	–191.86	RT38-RH00
79	10/23/01 13:30	TASA	952	952	3510	1,190	6367155	1551569	–130.96	RT38-RH00
80	10/23/01 13:30	TASA	1,318	1,318	3552	940	6367501	1551463	–182.20	RT38-RH00
81	10/23/01 13:30	TASA	1,315	1,315	3551	940	6367498	1551464	–181.78	RT38-RH00
82	10/23/01 13:30	TASA	952	952	3511	1,100	6367155	1551569	–130.96	RT38-RH00
83	10/23/01 13:30	TASA	1,306	1,306	3550	940	6367490	1551467	–180.52	RT38-RH00
84	10/23/01 13:30	TASA	1,305	1,305	3549	940	6367489	1551467	–180.38	RT38-RH00
85	10/23/01 13:30	TASA	1,272	1,272	3548	940	6367458	1551478	–175.76	RT38-RH00
86	10/23/01 13:30	TASA	1,340	1,340	3554	910	6367522	1551456	–185.28	RT38-RH00
87	10/23/01 13:30	TASA	1,265	1,265	3544	940	6367451	1551481	–174.78	RT38-RH00
88	10/23/01 13:30	TASA	1,728	1,728	3564	2,950	6367873	1551345	–235.48	RT38-RH00
89	10/23/01 13:30	TASA	978	978	3517	965	6367180	1551573	–134.6	RT38-RH00
90	10/23/01 13:30	TASA	1,265	1,265	3546	940	6367451	1551481	–174.78	RT38-RH00

Sample nr	Start date	Idcode	Secup (m)	Seclow (m)	Sample no	Cond (mS/m)	Northing	Easting	Elevation	Coord system
91	10/23/01 13:30	TASA	1,400	1,400	3557	810	6367579	1551436	–193.68	RT38-RH00
92	10/23/01 13:30	TASA	1,230	1,230	3543	950	6367418	1551492	–169.88	RT38-RH00
93	10/23/01 13:30	TASA	1,880	1,880	3570	540	6367963	1551456	–255.08	RT38-RH00
94	10/23/01 13:30	TASA	1,983	1,983	3572	830	6367939	1551546	–267.70	RT38-RH00
95	10/23/01 13:30	TASA	990	990	3519	950	6367192	1551572	–136.28	RT38-RH00
96	10/23/01 13:30	TASA	2,000	2,000	3573	830	6367930	1551560	–270.08	RT38-RH00
97	10/23/01 13:30	TASA	1,205	1,205	3542	1,020	6367395	1551501	–166.38	RT38-RH00
98	10/23/01 13:30	TASA	1,395	1,395	3556	820	6367574	1551437	–192.98	RT38-RH00
99	10/23/01 13:30	TASA	955	955	3513	1,060	6367157	1551570	–131.38	RT38-RH00
100	10/23/01 13:30	TASA	1,200	1,200	3539	900	6367390	1551502	–165.68	RT38-RH00
101	10/23/01 13:30	TASA	995	995	3521	930	6367197	1551571	–136.98	RT38-RH00
102	10/23/01 13:30	TASA	2,020	2,020	3579	840	6367919	1551577	–272.88	RT38-RH00
103	10/23/01 13:30	TASA	2,118	2,118	3580	835	6367838	1551609	–284.8	RT38-RH00
104	10/23/01 13:30	TASA	1,040	1,040	3523	940	6367239	1551556	–143.28	RT38-RH00
105	10/23/01 13:30	TASA	2,135	2,135	3582	870	6367821	1551608	–287.18	RT38-RH00
106	10/23/01 13:30	TASA	1,200	1,200	3540	900	6367390	1551502	–165.68	RT38-RH00
107	10/23/01 13:30	TASA	1,052	1,052	3526	900	6367251	1551552	–144.96	RT38-RH00
108	10/23/01 13:30	TASA	2,283	2,283	3589	1,220	6367712	1551537	–306.10	RT38-RH00
109	10/23/01 13:30	TASA	960	960	3512	1,100	6367162	1551571	–132.08	RT38-RH00
110	10/23/01 13:30	TASA	1,198	1,198	3541	900	6367388	1551503	–165.4	RT38-RH00
111	10/23/01 13:30	TASA	2,290	2,290	3591	1,300	6367709	1551530	–307.08	RT38-RH00
112	10/23/01 13:30	TASA	1,065	1,065	3528	900	6367263	1551547	–146.78	RT38-RH00
113	10/23/01 13:30	TASA	2,335	2,335	3593	1,120	6367688	1551491	–313.38	RT38-RH00
114	10/23/01 13:30	TASA	1,197	1,197	3538	900	6367387	1551503	–165.26	RT38-RH00
115	10/23/01 13:30	TASA	1,121	1,121	3530	950	6367316	1551529	–154.62	RT38-RH00
116	10/23/01 13:30	TASA	2,478	2,478	3597	1,060	6367715	1551366	–331.61	RT38-RH00
117	10/23/01 13:30	TASA	1,600	1,600	3561	835	6367749	1551338	–221.64	RT38-RH00
118	10/23/01 13:30	TASA	1,194	1,194	3537	910	6367384	1551504	–164.84	RT38-RH00
119	10/23/01 13:30	TASA	2,715	2,715	3610	2,560	6367932	1551355	–359.7	RT38-RH00
120	10/23/01 13:30	TASA	2,548	2,548	3599	970	6367767	1551326	–339.61	RT38-RH00
121	10/23/01 13:30	TASA	1,122	1,122	3532	970	6367317	1551528	–154.76	RT38-RH00
122	10/23/01 13:30	TASA	2,580	2,580	3601	1,370	6367799	1551332	–342.80	RT38-RH00
123	10/23/01 13:30	TASA	2,671	2,671	3608	2,040	6367888	1551348	–353.55	RT38-RH00
124	10/23/01 13:30	TASA	1,140	1,140	3535	1,140	6367333	1551522	–157.28	RT38-RH00
125	10/23/01 13:30	TASA	2,645	2,645	3606	1,710	6367863	1551343	–349.91	RT38-RH00
126	10/23/01 13:30	TASA	2,650	2,650	3607	1,640	6367868	1551344	–350.61	RT38-RH00
127	10/23/01 13:30	TASA	1,158	1,158	3536	910	6367350	1551516	–159.80	RT38-RH00
128	10/23/01 13:30	TASA	2,671	2,671	3609	1,720	6367888	1551348	–353.55	RT38-RH00
129	10/23/01 13:30	TASA	2,610	2,610	3605	2,010	6367828	1551337	–345.02	RT38-RH00
130	10/23/01 13:30	TASA	1,135	1,135	3534	940	6367329	1551524	–156.58	RT38-RH00
131	10/23/01 13:30	TASA	2,605	2,605	3603	1,810	6367823	1551336	–344.32	RT38-RH00
132	10/23/01 13:30	TASA	1,319	1,319	3553	940	6367502	1551463	–182.34	RT38-RH00
133	10/23/01 13:30	TASA	1,740	1,740	3566	3,110	6367885	1551347	–237.16	RT38-RH00
134	10/23/01 13:30	TASA	2,605	2,605	3604	2,300	6367823	1551336	–344.32	RT38-RH00
135	10/23/01 13:30	TASA	1,124	1,124	3533	920	6367318	1551528	–155.04	RT38-RH00
136	10/23/01 13:30	TASA	2,587	2,587	3602	1,410	6367806	1551333	–343.08	RT38-RH00

Sample nr	Start date	Idcode	Secup (m)	Seclow (m)	Sample no	Cond (mS/m)	Northing	Easting	Elevation	Coord system
137	10/24/01 3:00	TASA	3,520	3,520	3660	975	6367762	1551244	–448.78	RT38-RH00
138	10/24/01 3:00	TASA	3,495	3,495	3659	980	6367764	1551269	–449.27	RT38-RH00
139	10/24/01 3:00	TASA	3,455	3,455	3658	1,640	6367773	1551308	–449.23	RT38-RH00
140	10/24/01 3:00	TASA	3,437	3,437	3656	1,710	6367779	1551325	–449.81	RT38-RH00
141	10/24/01 3:00	TASA	3,437	3,437	3657	1,600	6367779	1551325	–449.81	RT38-RH00
142	10/24/01 3:00	TASA	3,426	3,426	3655	1,770	6367783	1551335	–449.99	RT38-RH00
143	10/24/01 3:00	TASA	3,365	3,365	3654	1,915	6367806	1551391	–444.78	RT38-RH00
144	10/24/01 3:00	TASA	3,314	3,314	3653	2,180	6367825	1551439	–437.39	RT38-RH00
145	10/24/01 3:00	TASA	3,314	3,314	3651	2,250	6367825	1551439	–437.39	RT38-RH00
146	10/24/01 3:00	TASA	3,312	3,312	3650	2,320	6367826	1551441	–437.1	RT38-RH00
147	10/24/01 3:00	TASA	3,280	3,280	3648	1,290	6367838	1551470	–432.46	RT38-RH00
148	10/24/01 3:00	TASA	3,277	3,277	3647	1,275	6367839	1551473	–432.02	RT38-RH00
149	10/24/01 3:00	TASA	3,275	3,275	3646	1,255	6367839	1551475	–431.73	RT38-RH00
150	10/24/01 3:00	TASA	3,270	3,270	3644	1,520	6367841	1551480	–431.01	RT38-RH00
151	10/24/01 3:00	TASA	3,248	3,248	3643	1,290	6367849	1551500	–427.82	RT38-RH00
152	10/24/01 3:00	TASA	3,248	3,248	3642	1,320	6367849	1551500	–427.82	RT38-RH00
153	10/24/01 3:00	TASA	3,233	3,233	3641	1,080	6367855	1551514	–425.64	RT38-RH00
154	10/24/01 3:00	TASA	3,190	3,190	3636	825	6367871	1551554	–419.41	RT38-RH00
155	10/24/01 3:00	TASA	3,160	3,160	3635	875	6367882	1551582	–418.22	RT38-RH00
156	10/24/01 3:00	TASA	3,135	3,135	3634	820	6367892	1551605	–417.69	RT38-RH00
157	10/24/01 3:00	TASA	3,135	3,135	3633	830	6367892	1551605	–417.69	RT38-RH00
158	10/24/01 3:00	TASA	3,122	3,122	3631	800	6367897	1551617	–416.66	RT38-RH00
159	10/24/01 3:00	TASA	3,122	3,122	3632	810	6367897	1551617	–416.66	RT38-RH00
160	10/24/01 3:00	TASA	3,110	3,110	3630	750	6367901	1551628	–415.00	RT38-RH00
161	10/24/01 3:00	TASA	3,275	3,275	3645	2,110	6367839	1551475	–431.73	RT38-RH00
162	10/24/01 3:00	TASA	3,090	3,090	3629	730	6367912	1551644	–412.20	RT38-RH00
163	10/24/01 3:00	TASA	3,090	3,090	3627	770	6367912	1551644	–412.20	RT38-RH00
164	10/24/01 3:00	TASA	3,088	3,088	3628	740	6367914	1551646	–411.92	RT38-RH00
165	10/24/01 3:00	TASA	2,929	2,929	3626	1,640	6367994	1551547	–389.66	RT38-RH00
166	10/24/01 3:00	TASA	3,290	3,290	3649	2,320	6367834	1551461	–433.91	RT38-RH00
167	10/24/01 3:00	TASA	3,314	3,314	3652	2,100	6367825	1551439	–437.39	RT38-RH00
168	10/24/01 3:00	TASA	2,929	2,929	3625	1,050	6367994	1551547	–389.66	RT38-RH00
169	10/24/01 3:00	TASA	2,920	2,920	3623	790	6367996	1551538	–388.4	RT38-RH00
170	10/24/01 3:00	TASA	2,920	2,920	3624	750	6367996	1551538	–388.40	RT38-RH00
171	10/24/01 3:00	TASA	2,917	2,917	3621	820	6367997	1551535	–387.98	RT38-RH00
172	10/24/01 3:00	TASA	2,916	2,916	3622	980	6367997	1551534	–387.84	RT38-RH00
173	10/24/01 3:00	TASA	2,916	2,916	3620	1,480	6367997	1551534	–387.84	RT38-RH00
174	10/24/01 3:00	TASA	2,915	2,915	3619	1,030	6367997	1551533	–387.70	RT38-RH00
175	10/24/01 3:00	TASA	2,900	2,900	3618	2,495	6368000	1551518	–385.60	RT38-RH00
176	10/24/01 3:00	TASA	3,540	3,540	3661	1,060	6367761	1551224	–448.34	RT38-RH00
177	10/24/01 3:00	TASA	2,800	2,800	3617	2,585	6367976	1551426	–371.60	RT38-RH00
178	10/24/01 3:00	TASA	2,770	2,770	3616	3,280	6367962	1551400	–367.40	RT38-RH00
179	10/24/01 3:00	TASA	2,768	2,768	3615	3,310	6367961	1551398	–367.12	RT38-RH00
180	10/24/01 3:00	TASA	2,760	2,760	3614	3,130	6367957	1551391	–366.00	RT38-RH00
181	10/24/01 3:00	TASA	2,750	2,750	3613	3,290	6367953	1551382	–364.60	RT38-RH00
182	10/24/01 3:00	TASA	2,740	2,740	3612	3,245	6367948	1551373	–363.20	RT38-RH00

Sample nr	Start date	Idcode	Secup (m)	Seclow (m)	Sample no	Cond (mS/m)	Northing	Easting	Elevation	Coord system
183	10/24/01 3:00	TASA	2,715	2,715	3611	3,570	6367932	1551355	–359.70	RT38-RH00
184	10/24/01 3:00	TASD	72	72	3640	1,020	6367812	1551599	–417.22	RT38-RH00
185	10/24/01 3:00	TASD	60	60	3639	940	6367823	1551594	–417.49	RT38-RH00
186	10/24/01 3:00	TASD	57	57	3638	1,130	6367826	1551593	–417.56	RT38-RH00
187	10/24/01 3:00	TASD	5	5	3637	1,530	6367874	1551574	–418.74	RT38-RH00
188	10/24/01 3:00	TASF	75	75	3666	2,215	6367812	1551327	–456.91	RT38-RH00
189	10/24/01 3:00	TASF	45	45	3665	1,795	6367804	1551298	–453.20	RT38-RH00
190	10/24/01 3:00	TASF	29	29	3664	1,775	6367800	1551283	–451.23	RT38-RH00
191	10/24/01 3:00	TASH	450	450	3667	1,780				
192	10/24/01 3:00	TASH	340	340	3669	1,330				
193	10/24/01 3:00	TASH	220	220	3668	1,090				
194	10/24/01 3:00	TASI	10	10	3663	960	6367753	1551258	–448.8	RT38-RH00
195	10/24/01 3:00	TASI	1	1	3662	960	6367762	1551257	–449.1	RT38-RH00

6 Visualization of the sampling points

The geometry of the tunnel volume was modelled with the TECPLOT code. The 195 sampling points were visualized. Figure A10-1 represents the electrical conductivity value of the sampling points along the tunnel walls. For comparison, the electrical conductivity available from the measurements in the tunnel boreholes during the last 2 years is presented.

The 2 data sets, electrical conductivity measured along the tunnel walls and measured in the tunnel boreholes are compared in Figure A10-2.

7 Conclusions

The aim of the project was to investigate the changes in groundwater composition along the tunnel wall and to compare the results with information from the drilled boreholes in the tunnel.

The results indicate that both data sets give the same basic information concerning groundwater composition (salinity) but greater detail variability is seen in the tunnel data. This indicates that tunnel data reflects local variability better than data from boreholes, but when sampling the tunnel wall close to the boreholes the groundwater salinity is the same in the borehole as in the water dripping from the wall.

These results support the colloid project, by showing that the groundwater composition obtained from the boreholes reflects well the major groundwater variability obtained in the whole tunnel.

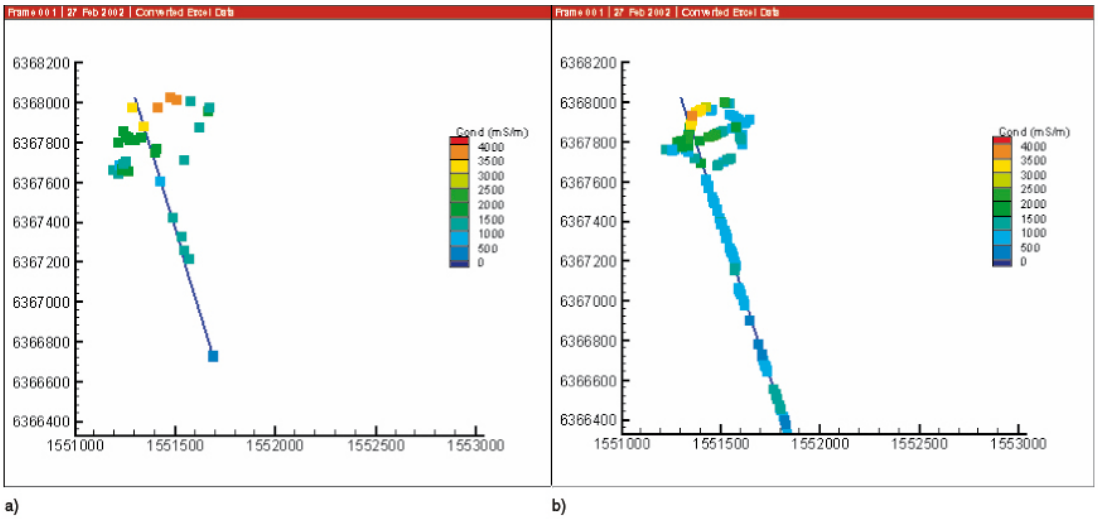

Figure A10-1. *a) Electric conductivity of the groundwater measured in tunnel boreholes; b) Electric conductivity of the groundwater measured along the tunnel wall.*

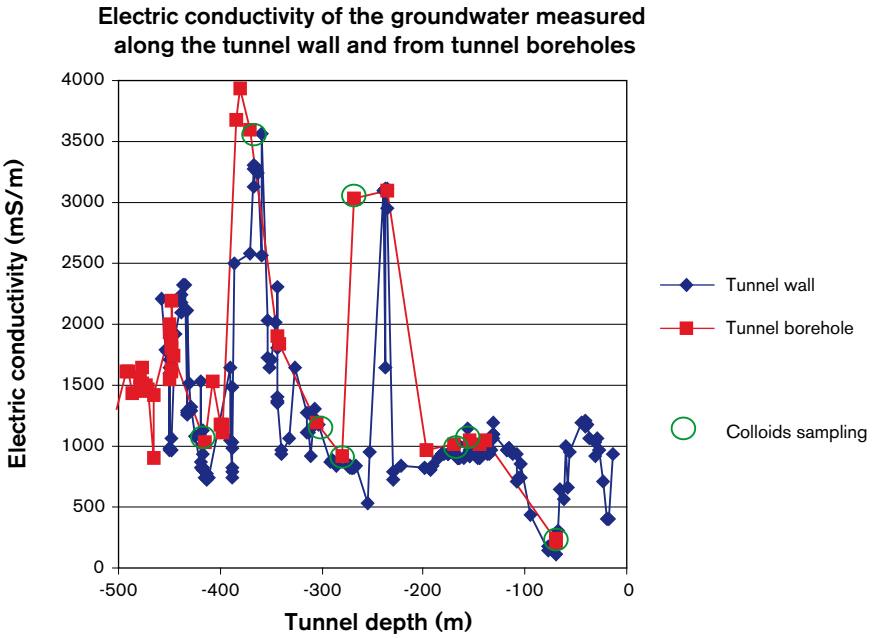

Figure A10-2. *Electrical conductivity data measured along the tunnel walls (blue) and electrical conductivity data measured in the tunnel boreholes (red) versus the tunnel depth. The green circles indicate the 8 boreholes used for colloid sampling.*

Appendix 11

Äspö Colloid Workshop

Review note by Claude Degueldre

Contents

1 Review of the presented work

The presentations from the groups were good with detailed tests and experimental results. The results presented concerned mainly groundwater data and data on colloids, bacteria and organics (humic/fulvic). Some specific remarks may be pointed out. A minimum of background on the rock and source terms (various water sources) is required in the general introduction. Some of the data reported during the talks have been given without an error bar (standard deviation or estimate) based on precision, without accuracy estimation and without detection limits. In some cases, the data presentation yields confusing figures or unrealistic values such as a negative activity. The present project takes a very useful approach on the role of inorganic/organic/bioorganic colloids in the Swedish nuclear waste management.

1.1 Tests in the laboratory

This is a must to understand and identify processes that are not directly observable in situ. Clay Technology AB (O. Karnland) follows systematically the sedimentation of bentonite colloids in batches, contacting bentonite (treated or not) with a range of neutral solutions changing the Na or Ca concentrations. Their pH ranges from 5.9 to 8.5 which is a bit larger than the Äspö groundwater pH (7.1–7.8) but which completes the picture. The ICP-AES tests of the solution/suspension were carried out systematically without filtration which in some cases yields ambiguous data. The work could be upgraded in these cases by comparing data from the filtered and not filtered phases. In addition, an attachment (sticking) coefficient should be extracted from these data.

The work is completed by PCS analysis (S. Wold). The PCS sensitivity could be somewhat increased selecting more adequate detection angles. Figures A11-1 to A11-4 are important. Figures A11-1 to A11-3 should be plotted on a log concentration scale. Connection between O. Karnland and S. Wold reports could be done by deriving an attachment (sticking) factor as a function of Na, Ca concentration and pH. The later result can be used by modellers. Data should also be compared from that reported in the literature.

2 Field work

2.1 Results from the German team

The use of LIBD with detection in photospectrometric mode and the development of the high pressure cell to work on line is welcomed (W. Hauser, B. Kienzler). The high pressure cell is an excellent tool for the in situ investigation. The presentation of the report is of high quality. For deriving a concentration the distribution is supposed to be gaussian which is not reflecting the reality, if a correction is possible for continuous distribution, it should be done, otherwise the assumption should be clearly stated. Both Figure A3-11 and A3-12 in Appendix 3, are interesting: they suggest that when the salt concentration decreases the colloid concentration increases and that (Figure A3-12) their average diameter increases also. If this is true, this implicates a transport reduction by filtration (size effect) and by sedimentation of the colloid in the low mineralised water (which is the opposite of what is suggested in the literature). However, Table A3-2 shows data ranging more than in Figure A3-11 and A3-12. Figure A3-14 is deduced from Table A3-5: calculated solid phases should not take into account quartz and pyrite, most of the waters are over-saturated with quartz, and instead of pyrite, troilite should be considered for the iron sulphide colloid phase. For these calculations the presence of organics e.g. fulvic may play an important role. So behind the excellent experimental work, some revisions of the data may be needed. Finally the very useful LIBD data (artefact-free, from redox Fe(II) oxidation and from

calcite precipitation) on the low colloid concentration in the highly saline water confirm what was reported earlier (SKB TR-95-24).

The fulvic study makes sense and the work suggested (G. Buckau) on the natural ^{14}C labelled fulvics was supported by the project leader and members. It is difficult to present 12 UV-Vis spectra in the same Figure, also normalized and without scale. What could be done for comparison? Change the order of UV spectra e.g. from DOC poor to DOC rich? It is sometimes interesting to present a derivative of the spectra to identify the components. Would it be the case here?

There may be a correlation between DIC and DOC as depicted by the reviewer below (Figure A11-1).

2.2 Results from the Finnish team

The introduction (M. Snellman) of the Finnish concept was welcomed.

The idea of using centrifugation-filtration is good and the efforts concerning the colloid work are substantial (U. Vuorinen). The work performed by SEM would, however, gain in usefulness if quantification of colloid concentrations was done i.e. provide colloid concentration and size distribution. This quantification performed in terms of specific size distributions should be done and compared with the results obtained by LIBD.

2.3 Results from the Swedish groups

The counting of bacteria is always a tremendous work (K. Pedersen). From the microbial entities: bacteria colonies, families, chains, or single entities, what is relevant to be counted for the transport or for the bio-activity? When routine bacteria counting is required, the use of a flow cytometer is suggested. The latter may be adapted for size distribution; however, counting at the microscope as realized so far allows morphological discrimination/ identification in some cases, which remains essential. Both manual counting and automatic on-line counting could provide useful information, for example during systematic studies. The bacteria analysis will also be upgraded with source identification (anthropologic, natural in situ bacteria), but as part of an extended study. The correlation bacteria density vs. DOC noted by Pedersen (and also by the reviewer) is depicted below (Figure A11-2).

If correlation also exists between DOC and DIC then the correlation bacteria density and DIC would confirm their occurrence by bio-activity (CO_2 source in waters originally depleted in bicarbonate) see Figure A11-3.

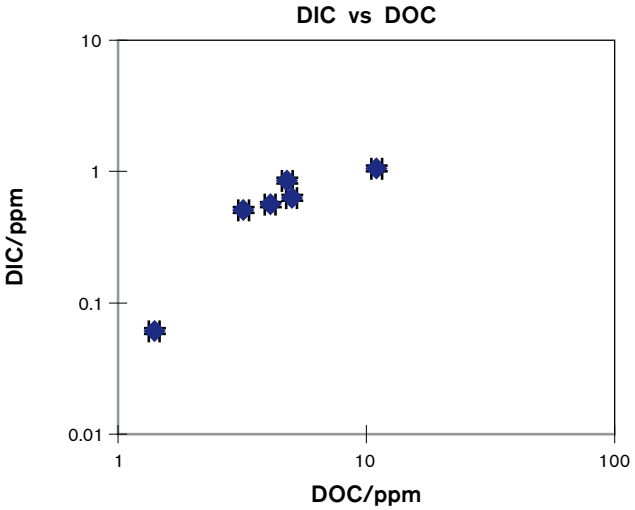

Figure A11-1. *Correlation between DIC and DOC (derived from SKB data, Table A4-1 in Buckau report).*

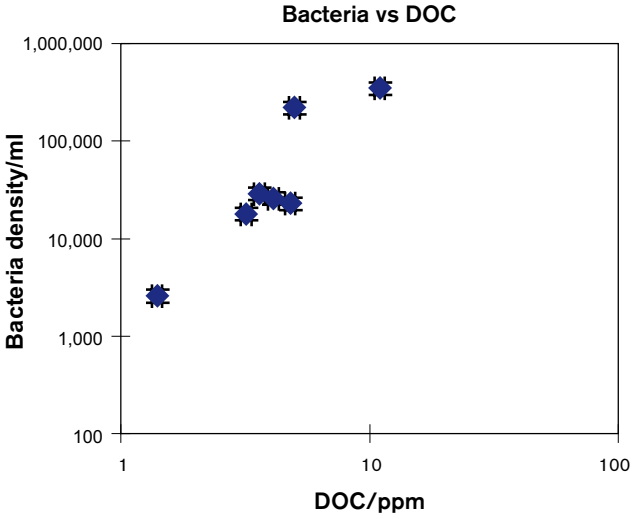

Figure A11-2. *Correlation between bacteria density and DOC (derived from SKB data, Table A4-1 in Buckau report, and from Table A9-2 in Pedersen report).*

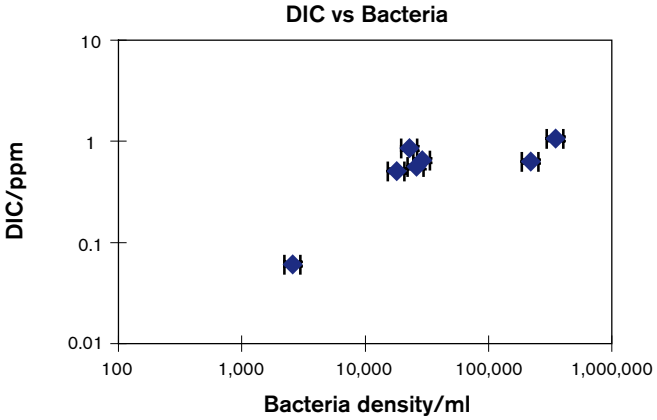

Figure A11-3. *Correlation between DIC and bacteria density (derived from SKB data, Table A4-1 in Buckau report and from Table A9-2 in Pedersen report).*

3 Review of the concept

To extract useful data from the Äspö colloid project and to supply data for a safety related study, it is important to focus on the 3 potential mobile phases:

1. Bacteria (natural and anthropogenic e.g. from activities during repository construction).
2. Colloids (natural and anthropogenic e.g. from the bentonite buffer).
3. Humic/fulvic (natural),
   and the interactions between these 3 phases together, as well as with host rock and the nuclides should be studied experimentally. These data should be utilized in models. However, priorities have to be made in the program. The model should take into account the various environments from the site to the biosphere.

In today's program, priority concerns the stability of the colloids with emphasis on the natural groundwater colloids and the bentonite colloids. Therefore tests on their coagulation (aggregation) and sedimentation are performed. These tests deliver kinetic information on colloid population stability which is necessary. However, colloid stability studies on a geological time scale e.g. considering potential secondary phase formation including groundwater or bentonite colloids should also be suggested. When reviewing the program, one has always to remember the goal: safety of a Scandinavian repository concept over a large distance and a large time scale.

Modelling will be carried out utilizing the data from the laboratory and field tests i.e. colloid generation, stability and transport. The first includes the tests which were presented and discussed by the program leader (bentonite erosion test), the second the application of the laboratory tests and the use of both approaches (as presented by the reviewer): following the colloid concentration for a given size in the batch as a function of time to calculate the attachment coefficient (e.g. Degueldre et al. 1996), or/and to follow the average size of the colloid population as a function of time during coagulation tests (e.g. Triay et al. 1996). Both approaches are complementary and could be applied using the PCS unit as presented by S. Wold. Colloid transport was also included in the review talk and concerned colloid partitioning with the host rock. Those concepts and data are important and will support the results obtained so far for the natural entities: bacteria, colloids and organics. Their size distributions summarized in Figure A11-4 shows the continuity of the entities size distribution studied in this project.

A conclusion on the effect of colloids in the frame of the migration of safety relevant nuclides will be required. The study will provide important data on the colloid source terms and properties: the generation rate as well as their stability and transport properties for the natural colloids, bacteria and organics, and, for the bentonite colloids: stability and transport potential with emphasis on the colloid facilitated mechanism. The work of the groups must focus on these goals. This is a key issue for the success of the Äspö colloid project.

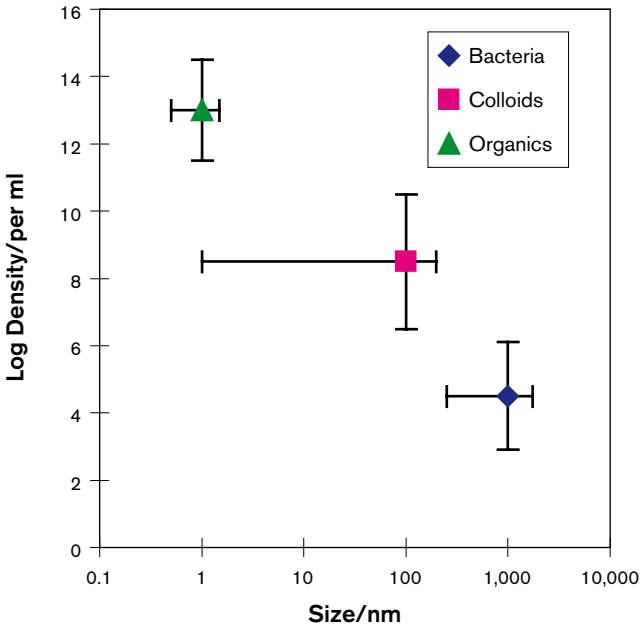

Figure A11-4. *Size distribution scheme of the studied mobile entities: bacteria, colloids and organics /derived from SKB data, Table A4-1 in Buckau report, Table A3-2 in Hauser report and Table A9-2 in Pedersen report).*

4 References

Degueldre C, Grauer R, Laube A, Oess A, Silby H, 1996. Colloid properties in granitic groundwater systems. II: Stability and transport study. Applied Geochemistry 11(5), 697–710.

Triay et al. 1996. Los Alamos National Laboratory report.

Appendix 12

Colloid reactor, laboratory testing and evaluation

– Deionized waters

Marcus Laaksoharju, Geopoint

January 2003

Edited by Susanna Wold, September 2005.

Contents

1 Background and aim

Colloids are small particles in the size range of a nanometer to a micrometer. The aim of the Colloid experiment at Äspö HRL and Olkiluoto was to test if the bentonite barrier in contact with groundwater could release stable colloids in measurable quantities. The plan was to install so called colloid reactors (bentonite enclosed by a filter tube consisting of 1 µm polypropylene filter textile) in 5 boreholes. Laboratory tests indicated that the no measurable colloid content was obtained when using a natural salinity range of Cl 1,000–13,000 mg/L /Wedholm and Holmqvist 2002/. The aim of the simplified test described here was to ensure that the results obtained by /Wedholm and Holmqvist 2002/ were not due to clogging of the filter tube used in the reactor. Non-saline water (drinking water) was used in contact with the colloid reactors since it is well known that bentonite colloids are stable in dilute waters /Wold and Eriksen 2001/.

2 Preparation and experimental setup

A simplified test was performed. The bentonite reactor was prepared by crushing MX-80 and sifting it through a 2 mm sieve. It was tightly packed into the one filter tube. The ends of the filter tubes were sealed with plastic plugs, which were fastened with steel casings under high pressure. For the experiment a standard Nuclepore vacuum pump, Millipore filter holder and Nuclepore 0.2 µm (∅ = 47 mm) PC membrane were used (see Figure A12-1).

Figure A12-1. *The setup for the experiment – the colloid reactor (in the fore front) the vacuum pump, filter holder, filters and a bucket.*

The experiment was conducted by filtering water for 5 minutes using a constant under pressure of 0.3 bars. The filtering was performed 3 times for each test setup. The 5 test setups consisted of 1.8 L water in contact with the colloid reactor in the bucket for 1 day to 1 week. The water was changed and the bucket was carefully cleaned between the tests. The analytical procedure consisted of comparing the filtered volume of water from the test setups with the blank sample consisting of drinking water (not in contact with the colloid reactor). It was assumed that the larger the difference of the filtered volumes between the samples from the test setups and the blank, the larger the colloid release from the reactor.

3 Results and conclusions

The analytical results from the tests are presented in Table A12-1. In Figure A12-2 the percent of colloids and particles in the water in contact with the colloid reactor as a function of time is shown.

The conclusion from the experiment is that the filter textile is not clogging with time and the textile is suitable for its purpose. Already after one day colloid contents of more than 49–62% can be obtained compared with the colloid content in drinking water. A prolonged waiting time of one week gives about 18% more colloids. The colloid formation is regulated by the chemistry of the water and not by the porosity of the filter. The obtained results are in good agreement with experiments conducted earlier at CLAYTECH where large amount of bentonite colloids were obtained by using a metal filter of 10 µm (30% porosity) in contact with deionised water. No stable colloids were observed when a solution of 0.1 mol/L NaCl was used (Ola Karnland, pers comm 2002).

Table A12-1. Results from the test with water in contact with the colloid reactor.

Date and time	Test no	Experimental time (h)	Conditions
2002-12-27:16.00	1	0	Blank sample (drinking water)
2002-12-28:15.00	2	23	250 ml in contact with colloid reactor
2002-12-29:14.00	3	23	250 ml in contact with colloid reactor
2003-01-05:19.00	4	173	250 ml in contact with colloid reactor
2003-01-06:17.00	5	22	250 ml in contact with colloid reactor
Test no	**Filter no 1: volume filtered (ml)**	**Filter no 2: volume filtered (ml)**	**Filter no 3: volume filtered (ml)**
1	330	362	362
2	128	137	133
3	199	176	163
4	92	89	82
5	154	134	147
Test no	**Average volume filtered (ml)**	**% of colloids and particles**	
1	351	0	
2	133	62	
3	179	49	
4	88	75	
5	145	59	

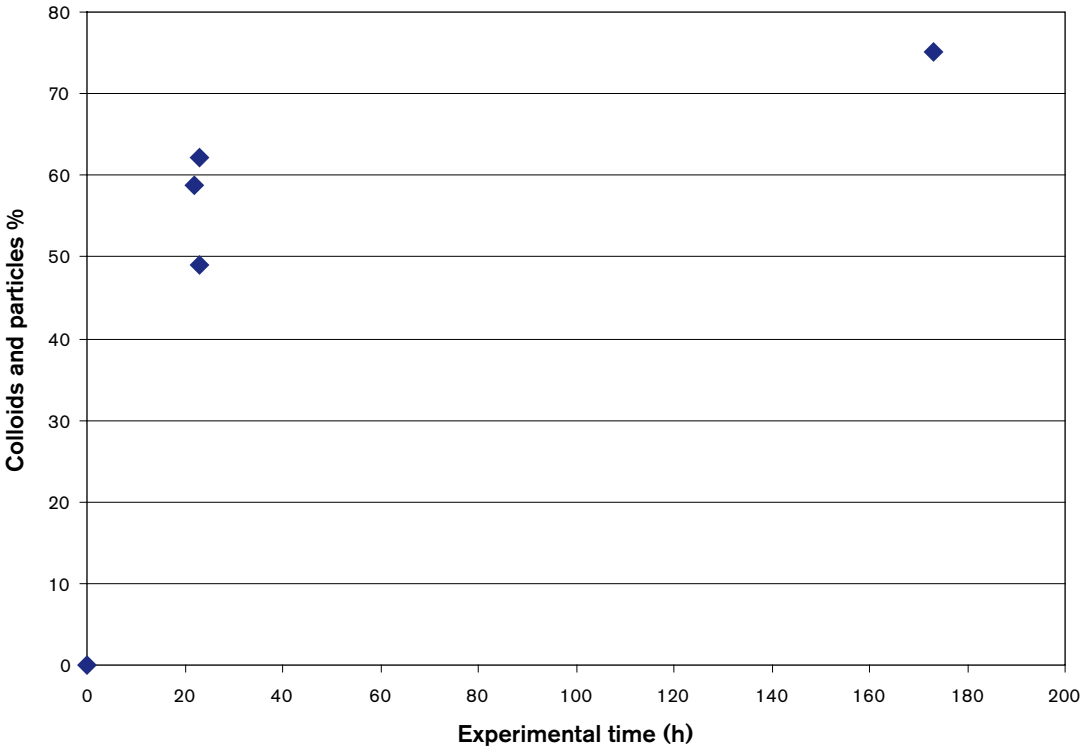

Figure A12-2. *The percent of colloids and particles in the water in contact with the colloid reactor as a function of time.*

4 References

Wedholm K, Holmqvist M, 2002. Colloid reactor, laboratory testing and evaluation. Second test round. SKB ITD in progress.

Wold S, Eriksen T, 2001. Formation of inorganic colloids in solutions of different ionic strength in contact with bentonite. SKB ITD-01-02.

Appendix 13

Colloid reactor laboratory testing and evaluation

– In 1,000 mg/L and 13,000 mg/L Cl^- solutions

Krister Wedholm, Geosigma AB

Magnus Holmqvist, Geosigma AB

December 2002

Edited by: Susanna Wold, KTH, September 2005.

Contents

1 Background

Colloids are small particles in the size range of one nanometer to one micrometer. Natural inorganic colloids in deep granitic groundwaters have been shown to consist of clay minerals (Al-silicates), silica and iron hydroxides. The ability of these small particles to travel far in bedrock makes them potential carriers of radionuclides from a defected nuclear waste repository to the biosphere. This part of the program was a preparation for the in situ bentonite reactor study.

2 Preparation

Two filter tubes were formed by folding and sewing together pieces of polypropylene filter textile. The seams of the tubes were covered by a strip of the same material glued to the inside with textile glue. This method proved effective in the introductory laboratory testing and evaluation.

Bentonite (MX-80) was crushed and sifted through a 2 mm sieve. It was then tightly packed into the two filter tubes. The ends of the filter tubes were sealed with plastic plugs, which were fastened with steel casings under high pressure.

Filter tube no 1 with a length between the casings of 39.7 cm, and outer diameter of 4 cm, contained 601.7 grams of bentonite.

Filter tube no 2 with a length between the casings of 39.8 cm, and outer diameter of 4 cm contained 586.2 grams of bentonite.

NaCl (Ultrapure) was added to deionized water giving the solution a Cl^- concentration of 1,000 or 13,000 mg/L, which corresponds to ionic strengths of 0.03 and 0.37 M. The Cl-concentrations were chosen to represent deep bedrock groundwaters with ionic strength in the low and high limits. Na-bentonite colloids are known to aggregate and sediment in the region of 0.01–0.1 M NaCl at pH 8–9 but the exact limit for the ionic strength is not known.

The reactor housing, made by transparent PVC, was mounted at a wall so that the water inlet end was at a slightly lower level than the outlet end, see Figure A13-1. Needle valves were placed on each side of the reactor to make possible adjustment of the flow.

For the first part of the tests filter tube no 1 was placed in the reactor housing. The 1,000 mg/L solution was allowed to pass through the reactor under 5 bar N_2 gas pressure of. By a needle valve the flow rate was adjusted to 10 ml/min.

Filter tube no 2 was placed in a pressure vessel containing a solution of 13,000 mg/L Cl^-. N_2 gas was allowed to bubble through the vessel.

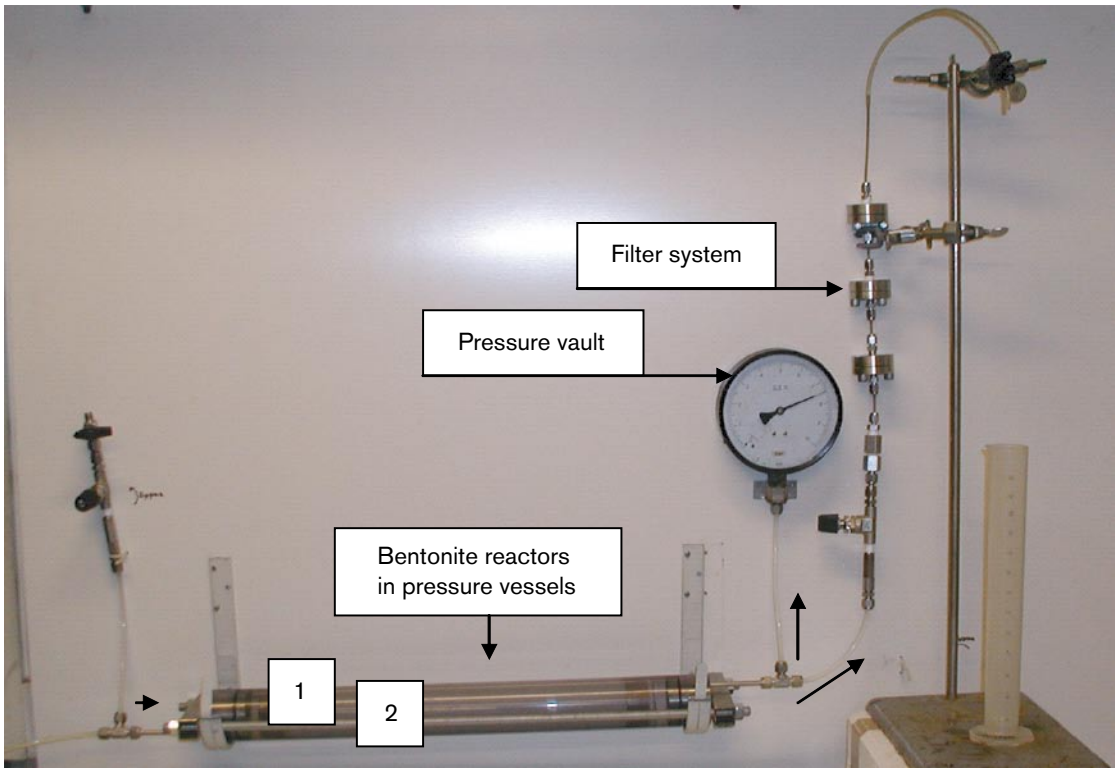

Figure A13-1. *The reactor setup.*

3 Sampling

After 10 days of continuous flow through the reactor sampling 1 started.

A series of filters (3, 2, 1) with a pore size of 0.45, 0.22 and 0.05 micrometers were used for the sampling of bentonite colloids from the solution before and after passing the reactor. When sampling the solution before the reactor the connection to the reactor was removed. The flow was adjusted by a ball valve. 200 ml water was passing the filter system.

The filters were put in acid washed vessels filled with 0.5 ml suprapure HNO_3 and 2.5 ml deionized water. After 1.5 hours the solution was diluted to 20 ml. After additional 15 minutes the filters were removed and the solution sent to Analytica AB (SGAB) for analysis with ICP-SFMS (Inductively Coupled Plasma – Sector Field Mass Spectrometry) and ICP-AES (Inductively Coupled Plasma – Atomic Emission Spectrometry).

The flow rate was decreased to 1 ml/min and the reactor was left for five days before sampling 2. The flow was adjusted by a needle valve. In this sampling 80 ml of water passed the filters.

After sampling number 2, the second part of the tests commenced. The pressure vessels were filled with 13,000 mg/L NaCl solution. Filter tube 1 was removed from the reactor tube and replaced by tube no 2. The change was made inside a plastic tent filled with N_2 to protect the filter tube from coming in contact with O_2. Tube no 1 had swollen from a diameter of 4.2 cm to 5.0. It was placed in 1,000 mg/L NaCl solution in a pressure vessel with a N_2 pressure of 7 bars. The flow in the reactor tube was adjusted to 10 ml/min and it was left for five days to reach stable conditions before sampling 3. The volume was the same as in sampling 1, 200 ml.

The flow was decreased to 1 ml/min and the reactor was left for three days before sampling 4. The volume was the same as in sampling 2 namely 80 ml. The results of this sampling have not yet been reported.

4 Results

The evaluation criteria stated in the Activity Plan were:

- Is the general function of the colloid reactor satisfactory?
- Is the bentonite colloid concentration significantly higher in the water after passing the reactor?
- Does the bentonite colloid concentration decrease with increasing Cl^- concentration?
- Does the bentonite colloid concentration increase with increasing flow rate?

At the first sampling the levels were not much lower than in the first test round. There may have been some kind of mistake at the sampling using the old poorly deionized water. In the other samplings the values are however much lower.

The differences between after and before passing the reactor were expected to be small, which is confirmed by the experimental results, see Table A13-1. The uncertainties in the ICP-analysis were reported from Analytica to be as follows in the recorded concentration ranges: Fe: 18%, Si: 10%, Al: 74%. There were errors in the sampling procedures as well. An estimate of 26% has been added to all the cations. No additional Fe, Si ore Al were found in the outlet samples, which means that bentonite colloids are not stable in the experimental conditions. In sampling 4 and 5 with 1,000 mg/L Cl^-, the results are not clear. It seems like there are more colloids in the solutions before the reactor, than after. This must somehow be an error in the sampling.

Table A13-1. Experimental conditions and results.

Sampling	Placing	Salinity mg/l Cl^-	Flow ml/min	Filter µm	Fe µg/l (ppb)	Si µg/l (ppb)	Al µg/l (ppb)
1	After	1,000	10	0.45	30 ± 13	38 ± 14	6 ± 6
2	After	1,000	10	0.22	1 ± 0.4	40 ± 14	5 ± 5
3	After	1,000	10	0.05	2 ± 0.9	37 ± 13	6 ± 6
1	Before	1,000	10	0.45	15 ± 7	55 ± 20	8 ± 8
2	Before	1,000	10	0.22	1 ± 0.4	42 ± 15	7 ± 7
3	Before	1,000	10	0.05	2 ± 0.89	38 ± 14	7 ± 7
4	After	1,000	1	0.45	9 ± 4	8 ± 3	4 ± 4
5	After	1,000	1	0.22	1 ± 0.4	6 ± 2	3 ± 3
6	After	1,000	1	0.05	1 ± 0.4	6 ± 2	2 ± 2
4	Before	1,000	1	0.45	57 ± 25	50 ± 18	76 ± 76
5	Before	1,000	1	0.22	2 ± 0.9	39 ± 14	5 ± 5
6	Before	1,000	1	0.05	3 ± 1	12 ± 4	5 ± 5
7	After	13,000	10	0.45	70 ± 31	2 ± 0.7	1 ± 1
8	After	13,000	10	0.22	2 ± 0.9	1 ± 0.4	1 ± 1
9	After	13,000	10	0.05	2 ± 0.9	2 ± 0.7	0 ± 1
7	Before	13,000	10	0.45	150 ± 66	5 ± 2	6 ± 6
8	Before	13,000	10	0.22	2 ± 0.9	3 ± 1	1 ± 1
9	Before	13,000	10	0.05	2 ± 0.9	2 ± 0.7	2 ± 2

Appendix 14

Colloid reactors, borehole installations and monitoring programme

Äspö Hard Rock Laboratory and Olkiluoto

Gert Nilsson, Pia Wacker
Geosigma AB

June 2003

Edited by: Susanna Wold, KTH, September 2005.

Contents

1 Introduction

1.1 Background

Colloids are small particles in the size range 1–1,000 nm. Natural inorganic colloids in deep granitic groundwaters generally consist of clay minerals (Al-Silicates), Si and Fe-hydroxides. The ability of these small particles to travel far in bedrock makes them potential carriers of radionuclides from a defected nuclear waste repository to the biosphere.

To investigate if the bentonite barrier can release stable colloids an in situ colloid reactor was developed. The reactor has been tested and evaluated in laboratory tests. Background values of colloid content, and electrical conductivity was measured in the activity in the Äspö HRL-tunnel.

The design of the reactor allows natural groundwater to pass and saturate the bentonite. Reactors were installed at Äspö HRL-tunnel (4 reactors) and at Olkiluoto (2 reactors). The purpose of choosing both Äspö and Olkilouto for installation was to get different groundwater conditions. An important difference is that the groundwaters in Äspö contain a lot of Ca^{2+} whereas in Olkilouto groundwaters the concentrations are not even measurable. Olkilouto groundwaters also contain measurable amounts of DOC, which might have a stabilizing effect on benonite colloids.

The groundwater was sampled both before and after bentonite passage. Several filter sizes were used to filtrate the sampled water, in order to study what sizes present colloid particles might have. Al, Si and Fe were choosen as markers for the bentonite colloids and water samples and filters were sent for laboratory analyses. The installation of the colloid reactors, maintenance and sampling procedures are further described in AP TD F91-03-003.

1.2 Hypotheses

The present study programme aims to investigate if bentonite can release stable colloids in contact with groundwater. Colloid stability depends on:

- flow rate,
- ion content of the groundwater,
- microbes,
- other chemical/physical properties of the groundwater (e.g. humic substances).

1.3 Objectives

The project aims to in situ study the role of the bentonite barrier as a colloid source in a deep bedrock repository for spent nuclear fuel.

2 Performance and evaluation procedure

2.1 Preparation

Six tubes were formed by folding and sewing together pieces of polypropylene filter textile. A strip of the same material glued to the inside with textile glue covered the seams of the tubes.

Bentonite (MX-80) was crushed and sifted through a 2 mm sieve. It was then tightly packed into the filter tubes. The ends of the filter tubes were sealed with plastic plugs, which were fastened with steel casings under high pressure. The filter tubes were weighted and measured before put in the reactor housing.

The reactor housing (Figure A14-1) was made of stainless steel and had a connected length of 1,000 mm. The maximum diameter of the reactor was 54 mm. The reactor has two sampling lines. One comes from the inside of the reactor and the other is lead through and allows sampling of water which has not had contact with reactor interior.

2.2 Instrumentation

At Äspö HRL tunnel the reactors were installed in four boreholes, while two reactors were installed at Olkiluoto (Table A14-1).

At each sampling site, a needle valve was used to obtain desired flows. In order to prevent clogging of the "after" needle by aggregated colloids, two parallel-coupled filters (pore sizes 0.45 µ.m) are mounted in between the borehole and the "after" outlet (Figure A14-2). The parallel coupling made it possible to replace or clean one of the filters without affecting the flow (the flow could be directed from one filter to the other by simultaneously turning two 3-way valves). Needle valves and filters were mounted on sampling boards, place outside the boreholes.

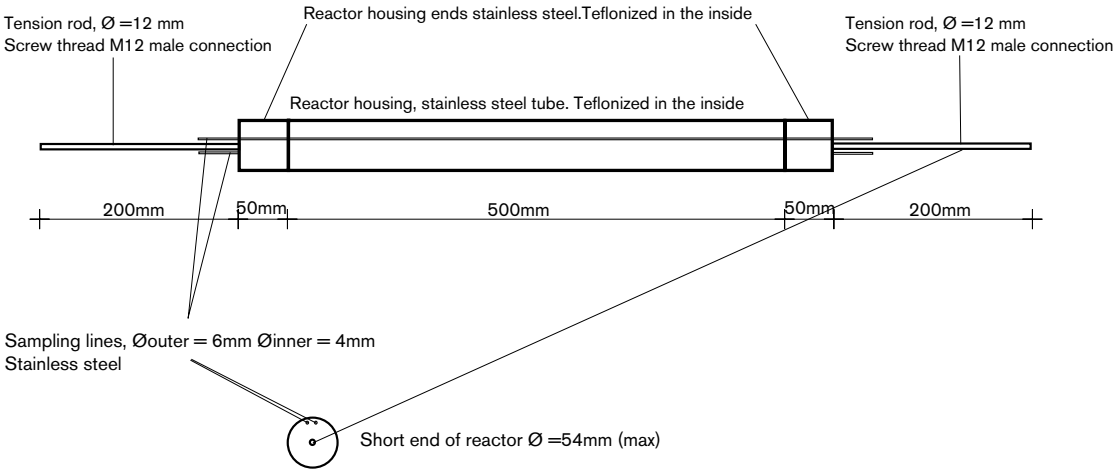

Figure A14-1. *Bentonite reactor.*

Table A14-1. Boreholes used for the colloid reactor tests.

Location	Borehole	Secup (m)	Seclow (m)	Borehole diameter (m)	Inclination	Salinity Cl^- (mg/l)	NaCl (M)
Äspö	KA1755A	88	160	0.056	–19.833°	11,720 (2001-10-16)	0.33
Äspö	SA2273A	1	20	0.057	–10.000°	2,850 (2001-10-16)	0.08
Äspö	SA2780A	6	20	0.057	–10.000°	2,860 (1998-04-15)	0.08
Äspö	KA3385A	32.05	34.18	0.057	–33.500°	12,800 (2001-10-16)	0.36
Olkiluoto	PVA1			0.056	–9.2°	940 (1996-11-14)	0.03
Olkiluoto	PVA3			0.056	–49.97	3,600 (1996-11-25)	0.10

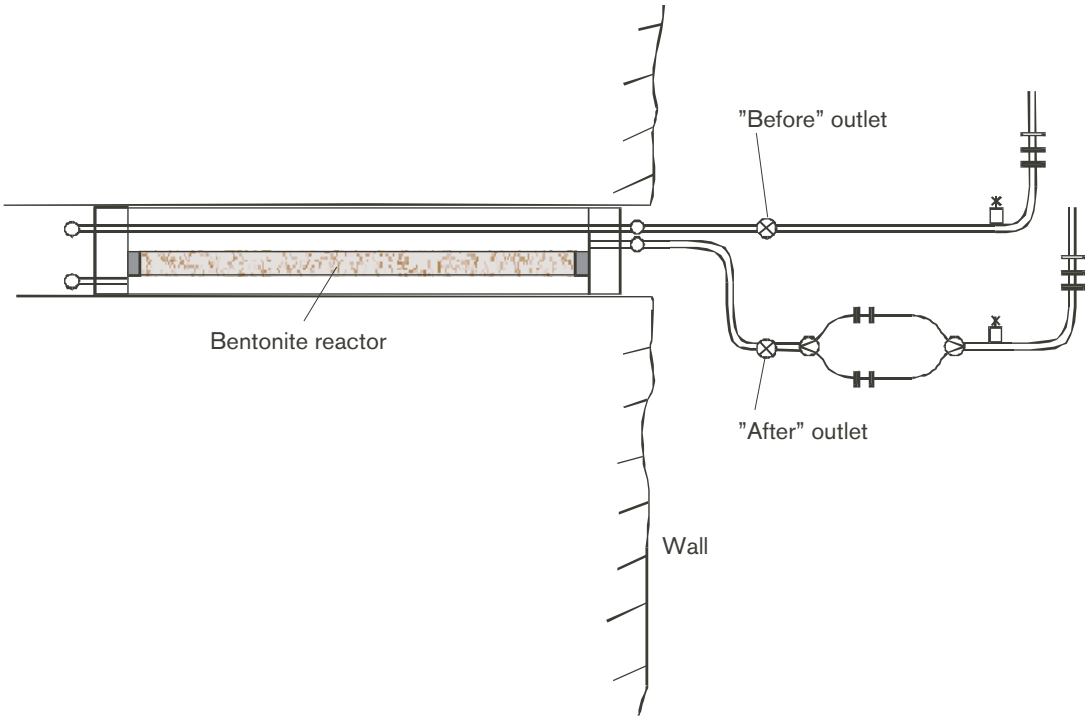

Figure A14-2*. Outside-borehole configuration. The filter holders at the very right of the figure are not permanently installed, but will be put in place during sampling.*

After installation the flow was set to roughly 20 ml/minute in the “before” outlet and 10 ml/minute in the “after” outlet. These flows were intended to circulate to entire sections in which the reactors were installed. After about 10 days of circulation adjustments were made on the valves to obtain a stable flow of 10 ml/minute (the flow first to be sampled).

2.3 Maintainance

The maintenance during the first week was done daily and subsequently on a weekly basis. At the inspections, the flow was measured whereupon, if necessary, adjustments were made to the valve, in order to obtain the desired flow. Furthermore, the filter was replaced or rinsed as necessary and the equipment was inspected in order to find any leakages.

3 Sampling of water and filters

The samplings were made at dates as given in Table A14-2. When the 10 ml/min sampling was finished, the flows were set to 5 ml/min, and subsequently, after completion of the 5 ml/min sampling, all flows were set to 1 ml/min.

Table A14-2. Activity date table.

Activity	PVA1 and PVA3 (Olkilouto)	1755, 2273, 2780 and 3385 (Äspö HRL Tunnel)
Installation	January 9–10 and 13–15	January 21
Sampling 10 ml/min	February 20–21	February 12–14 and 17–19
Sampling 5 ml/min	March 31–April 1	March 17–21
Sampling 1 ml/min	May 6–7	April 9–12

3.1 Chemical analysis of anions, cat ions, alkalinity, pH and conductivity

Water was sampled from each outlet ("before" and "after") and sent to laboratory for analysis with respect to chemical properties. Chemical analyses of anions, cat ions, alkalinity, pH and conductivity were done when the flow was 10 ml/min. Analyses of conductivity and pH were done when the flow was 5 and 1 ml/min.

3.2 Preliminary indications, "fast test"

In order to get preliminary indications upon whether colloids are present or not, water from the "before" and "after" outlet was led through a filter holder with filter size 0.05 µm. If filter clogging was noticed, the test was repeated in order to see if the clogging seemed repeatable. Each test had, if possible, a duration of at least 1 hour. The water volume that passed the filter and the time were noted.

3.3 Chemical analysis of filters

For the filter sampling, water from the "before" as well as the "after" outlet was led through series coupled filter holders (Millipore 25 mm High pressure holder 316 stainless XX4502500). Three filter holders for each outlet were used, loaded with filter sizes 0.05, 0.22 and 0.45 µm (Millipore MF™ Membrane Filters 25 mm, Filter TYPE: 0.45 µm HA, CAT NO HAW P02500; 0.22 µm White GSWP, CAT NO GSWP P02500; 0.05 µm White VMW, CAT NO VMW P02500). Since the presence of oxygen is known to affect the colloid content for redox sensitive elements, all filters, filter holders and tubes were filled with argon gas, Argon S 99.99%, for at least 30 seconds before the sampling started. The filter holders were rinsed cleaned with distilled water and, if necessary, 70–75% ethanol.

When possible the sampling was allowed to carry on until 1,000 ml of water had passed the filters. During the sampling sequence, no adjustments were made upon the valves, in order to avoid any disturbance of the flow rate. At the end of the sampling, the volume of water that had passed the filters was noted.

When the filter holders were dismantled, each filter was transferred into a Petri dish using plastic tweezers. The Petri dishes were carefully sealed and stored cool. As control samples two filters, size 0.05 and 0.45 µm were also sent for laboratory analysis. Blanks, just filters, were also sent for laboratory analysis. All filters were kept in Petri dishes and were sent to the laboratory.

The filters were soaked up in HNO_3 and H_2O_2 in covered Teflon beakers in a microwave oven. The solution was analyzed with ICP-AES or ICP-SMS.

4 Results

In all text, figures and tables below, "after" refers to the after reactor passage outlet, and "before" refers to the before reactor passage outlet.

4.1 Chemical analysis of anions, cat ions, alkalinity, pH and conductivity

The analysis results of alkalinity, pH and conductivity at 10, 5 and 1 ml/min are plotted in Figures A14-3 to A14-7. Extensions “A” and “B” stand for “after reactor” and “before reactor”, respectively.

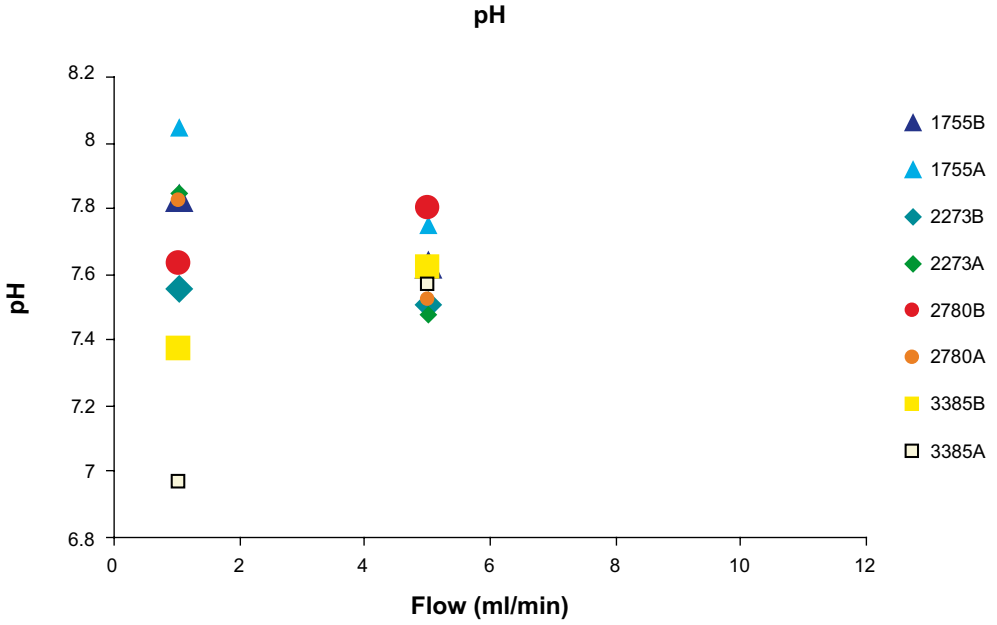

Figure A14-3. *pH, Äspö HRL Tunnel.*

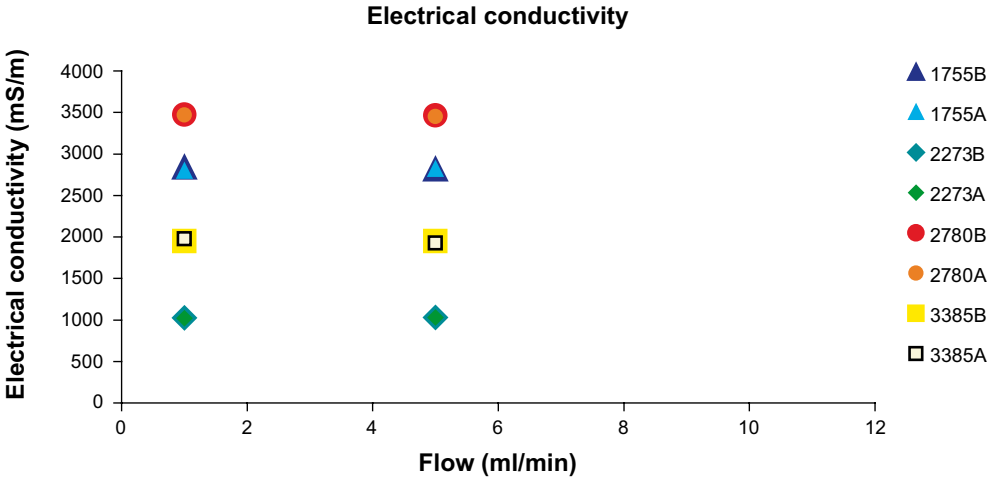

Figure A14-4*. Electrical conductivity, Äspö HRL Tunnel.*

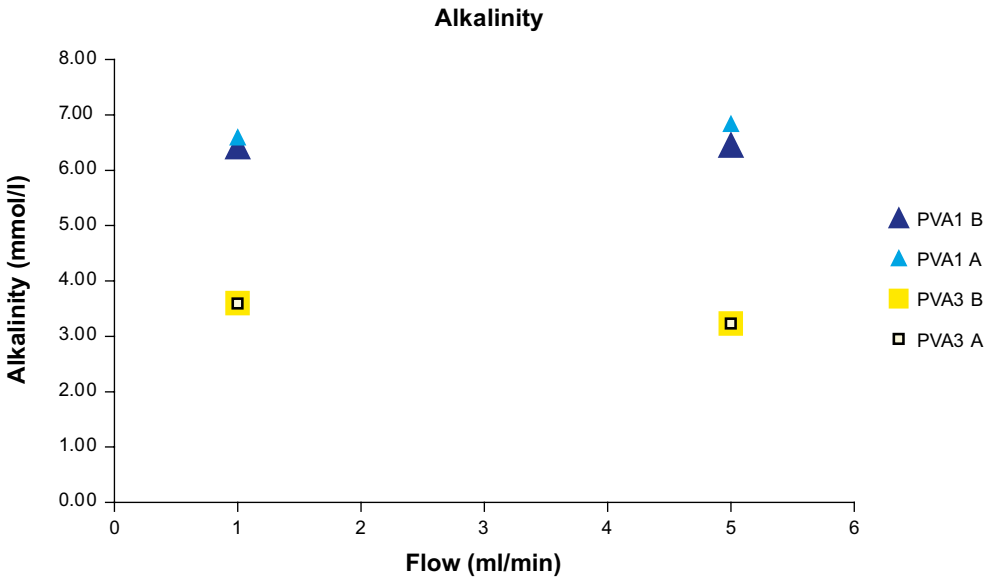

Figure A14-5. *Alkalinity, Olkiluoto.*

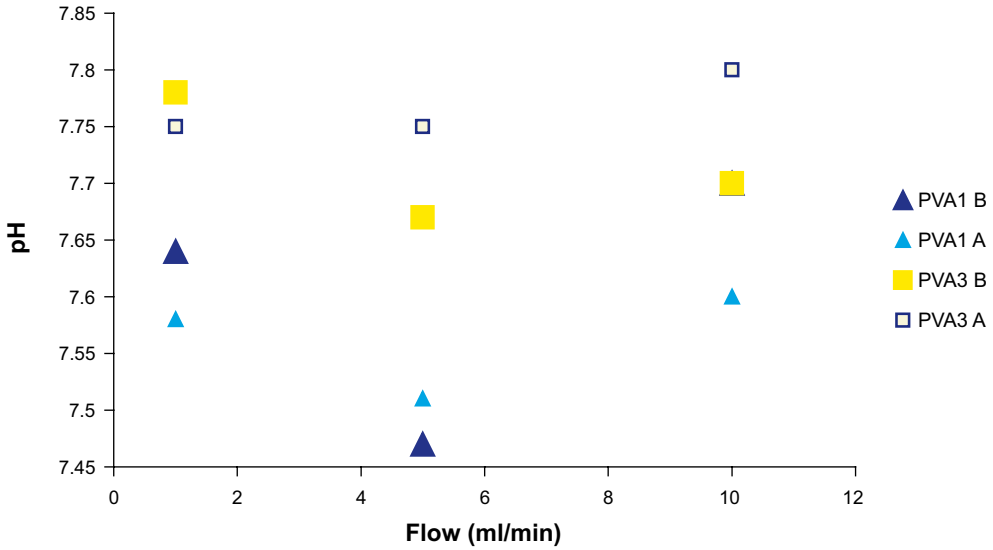

Figure A14-6. *pH, Olkiluoto.*

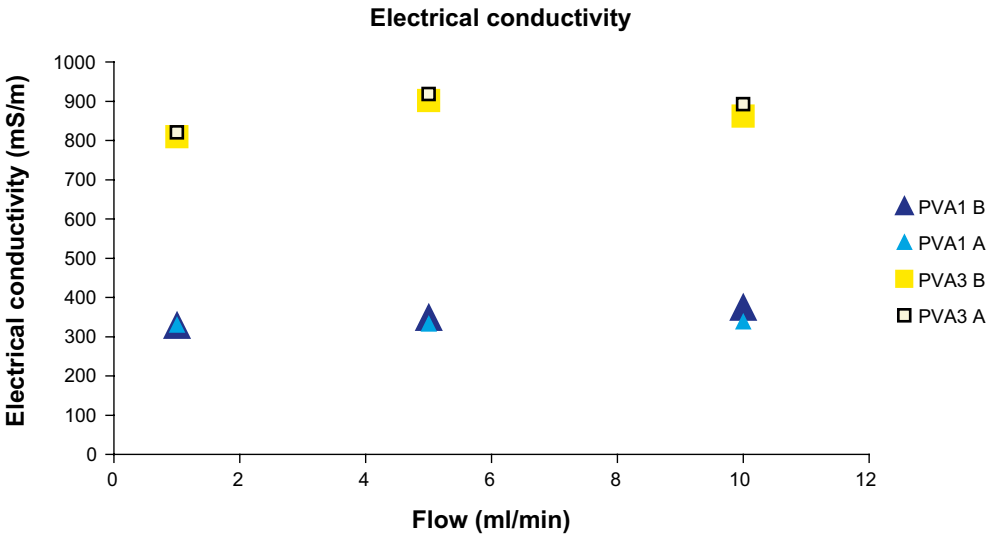

Figure A14-7. *Electrical conductivity, Olkiluoto.*

4.2 Preliminary indications, "fast test"

No clogging was observed during the time of the test. Because of the continuous flow only one "fast test" was conducted for each outlet. The "fast test" did not give any clear indication of clogged filters during the test time.

4.3 Chemical analysis of filters

All filters were analyzed with respect to the content of the following cat ions:
Na, K, Ca, Mg, Si, Fe, Mn, Li, Sr, S, Al, Cd, Co, Cr, Cu, Hg, Mo, Ni, P, Pb, V, Zn.

Several of these parameters displayed low concentrations throughout the data set (at or below detection limits), e.g. Mn, Li, Cu and P.

Laboratory analysis of blanks (dry, unused filters), resulted in masses of Al, Fe and Si that were below detection limits (Al < 0.02 ± 0.01 µg tot, Fe < 5 µg tot and Si < 5 µg tot).

As control samples, filters were dipped in water taken from the "before" outlet. The analysis displays low levels of Al, Si and Fe, except for all Si analyses at a flow rate 10 ml/minute, where the total mass of Si is at the same level as the mass obtained at the filters after sampling (after passage of about 1,000 ml water). Results from the analyses of the control samples are shown in Table A14-3.

Results of the laboratory analyses from the bentonite reactor filter tests are given in Table A14-4. Since the data given by the laboratory represented the total mass of each parameter, each cat ion content has been divided by the volume water sampled, in order to obtain the corresponding concentration. The Al-, Fe and Si-contents of the filter resulted in Si, Fe and Al-levels below detection limits. The uncertainty in the ICP-analysis in the concentration ranges analyzed, are set at Al 74%, Fe 18% and Si 10% by the commercial laboratory Analytica. The error attached to the sampling procedure is estimated at 26%.

Table A14-3. Analysis results of the filter control samples from Äspö HRL Tunnel and Olkiluoto.

Borehole	Flow (ml/min)	Filter size (µm)*	Si (µg tot)	Fe (µg tot)	Al (µg tot)	Si/Al
1755	10	0.05	18.5	< 5	0.05	370
1755	10	0.45	19.0	< 5	0.02	950
1755	5	0.05	< 5	< 5	0.07	
1755	5	0.45	< 5	< 5	0.05	
1755	1	0.05	< 5	< 5	0.31	
1755	1	0.45	< 5	< 5	0.0.2	
2273	10	0.05	18.4	< 5	0.38	48.421
2273	10	0.45	18.6	< 5	0.09	206.67
2273	5	0.05	< 5	< 5	0.52	
2273	5	0.45	< 5	< 5	0.09	
2273	1	0.05	< 5	< 5	0.04	
2273	1	0.45	< 5	< 5	0.02	
2780	10	0.05	10.5	< 5	0.07	150
2780	10	0.45	9.66	< 5	0.05	193.2
2780	5	0.05	< 5	< 5	< 0.02	
2780	5	0.45	< 5	< 5	< 0.02	
2780	1	0.05	< 5	< 5	0.0081	
2780	1	0.45	< 5	< 5	0.15	
3385	10	0.05	19.5	< 5	0.07	278.57
3385	10	0.45	20.3	< 5	0.01	2,030
3385	5	0.05	< 5	< 5	< 0.02	
3385	5	0.45	< 5	< 5	0.061	
3385	1	0.05	< 5	< 5	0.08	
3385	1	0.45	< 5	< 5	0.12	
PVA1	10	0.05	20.2	< 5	0.037	545.95
PVA1	10	0.45	19.9	< 5	0.106	187.74
PVA1	5	0.05	< 5	< 5	0.107	
PVA1	5	0.45	< 5	< 5	< 0.02	
PVA1	1	0.05	< 5	< 0.0001	< 0.02	
PVA1	1	0.45	< 5	0.24	0.03	
PVA3	10	0.05	19.6	< 5	0.09	217.78
PVA3	10	0.45	18.6	< 5	0.14	132.86
PVA3	5	0.05	< 5	< 5	< 0.02	
PVA3	5	0.45	< 5	< 5	0.4	
PVA3	1	0.05	< 5	0.01	< 0.02	
PVA3	1	0.45	< 5	0.06	0.3	

Table A14-4. Results from laboratory analysis, Si, Al and Fe. Äspö HRL Tunnel and Olkiluoto. (BD: below detection limit).

Borehole	Flow (ml/min) Outlet (before/after)	Bypass	Si (µg/L)	Fe (µg/L)	Al (µg/L)
1755	10-before	680	83.8	BD	1.1
1755	10-after	580	97.0	BD	0.7
2273	10-before	no flow	BD	BD	BD
2273	10-after	no flow	BD	BD	BD
2780	10-before	1,000	55.3	5.6	0.8
2780	10-after	400	141.5	BD	0.7
3385	10-before	1,050	44.3	BD	0.3
3385	10-after	1,050	26.6	BD	0.2
1755	5-before	1,160	BD	BD	1.0
1755	5-after	1,000	BD	BD	BD
2273	5-before	1,102	BD	BD	0.2
2273	5-after	1,171	BD	BD	0.2
2780	5-before	3,655	BD	BD	0.1
2780	5-after	2,838	BD	BD	0.1
3385	5-before	2,280	BD	BD	0.0
3385	5-after	4,870	BD	1.12	0.1
1755	1-before	1,000	BD	18.0	1.1
1755	1-after	850	BD	0.94	1.2
2273	1-before	1,746	BD	0.79	0.1
2273	1-after	1,032	BD	4.44	0.6
2780	1-before	532	BD	(32.7)*	0.4
2780	1-after	1,945	BD	13.6	0.1
3385	1-before	1,179	BD	2.7	0.4
3385	1-after	1,056	BD	4.2	0.8
PVA1	10-before	1,168	52.1	BD	0.3
PVA1	10-after	470	135.3	21.4	2.5
PVA3	10-before	905	62.9	8.2	0.2
PVA3	10-after	1,005	59.7	BD	0.5
PVA1	5-before	1,030	BD	BD	0.2
PVA1	5-after	790	BD	BD	0.3
PVA3	5-before	920	BD	12.6	0.2
PVA3	5-after	1,150	BD	BD	0.5
PVA1	1-before	800	BD	1.8	0.3
PVA1	1-after	1,007	BD	2.5	0.3
PVA3	1-before	1,180	BD	(28.6)*	0.4
PVA3	1-after	1,270	BD	7.9	0.2

* Probable errors.

5 Discussion

5.1 Different flow rate comparison

Samples taken at a flow rate 10 ml/min generally have a higher level of Al, Fe and Si and other cation content compared to samples taken at 5 or 1 ml/minute. This is most obvious for Si, which is present at levels above detection limit only at a flow rate of 10 ml/min (at Äspö HRL Tunnel as well as at Olkiluoto). In larger flow rates the suspension increases. This indicates that it is not colloids we see, rather filling material that is suspended by the pumping flow.

5.2 Inter borehole comparisons

Filter analyses with respect to Si Al and Fe indicate that no consistent differences can be found between the six boreholes used within the project.

5.3 "Before" and "After" outlet comparisons

The results from the laboratory analyses are unequivocal. No stable colloids are found in any borehole which is in accordance with theory that bentonite colloids are not stable in brackish or saline groundwaters (Figures A14-8 to A14-12).

Only flows and boreholes are included in which the result of both the "after" and the "before" analyses was above detection limit. Accordingly Si plots 5 and 1 ml/minute and Fe plots 10 and 5 ml/minute have not been plotted.

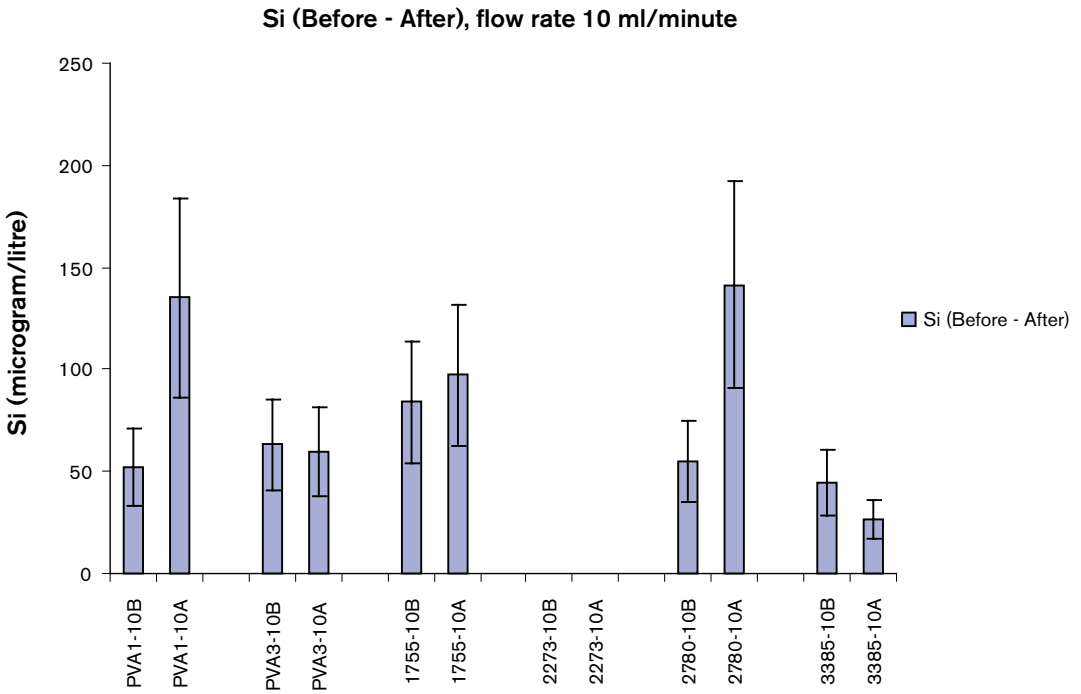

***Figure A14-8**. Silica – comparison of "before" and "after" outlet with the sum of all the filters used. Olkiluoto and Äspö HRL. Flow rate 10 ml/min.*

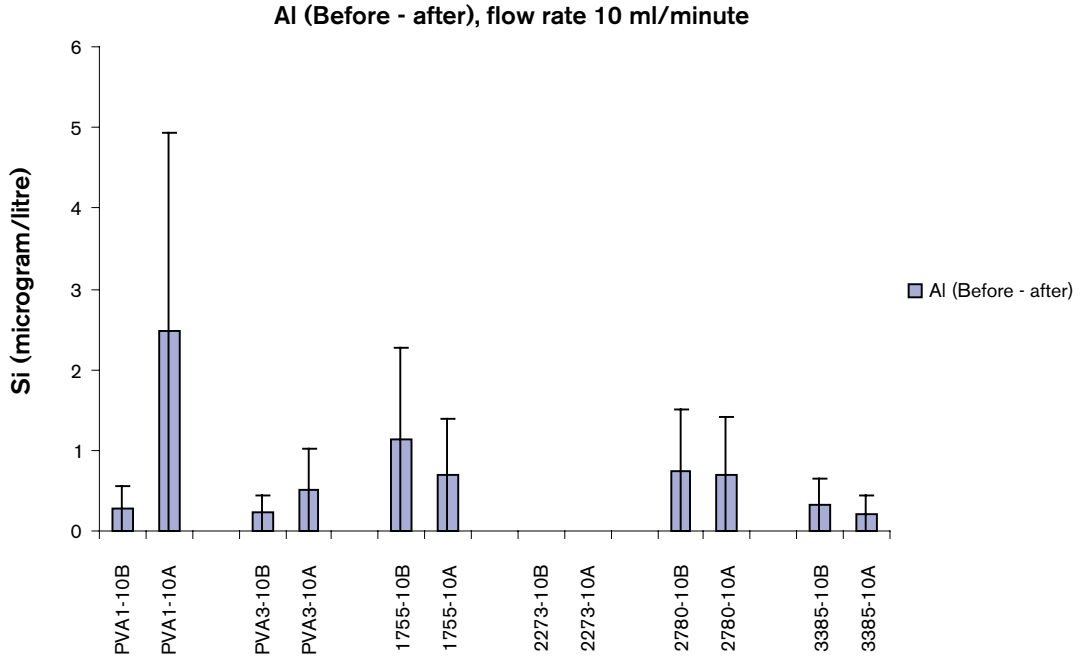

***Figure A14-9**. Aluminium – comparison of "before" and "after" outlet with the sum of all the filters used. Olkiluoto and Äspö HRL. Flow rate 10 ml/min.*

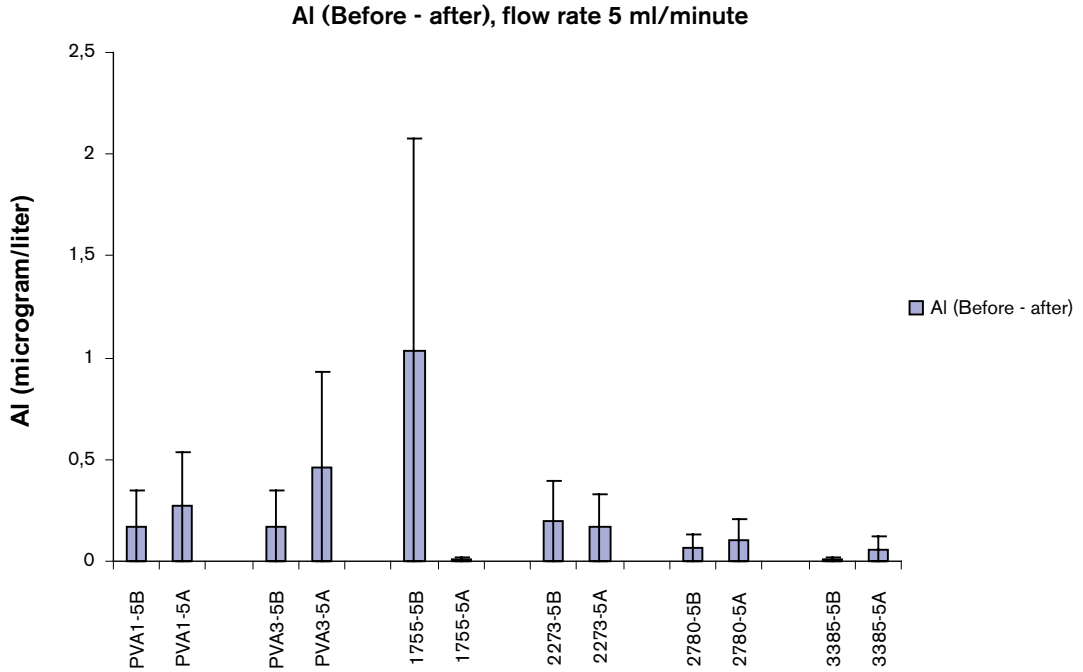

***Figure A14-10.** Aluminum – comparison of "before" and "after" outlet with the sum of all the filters used. Olkiluoto and Äspö HRL. Flow rate 5 ml/minute.*

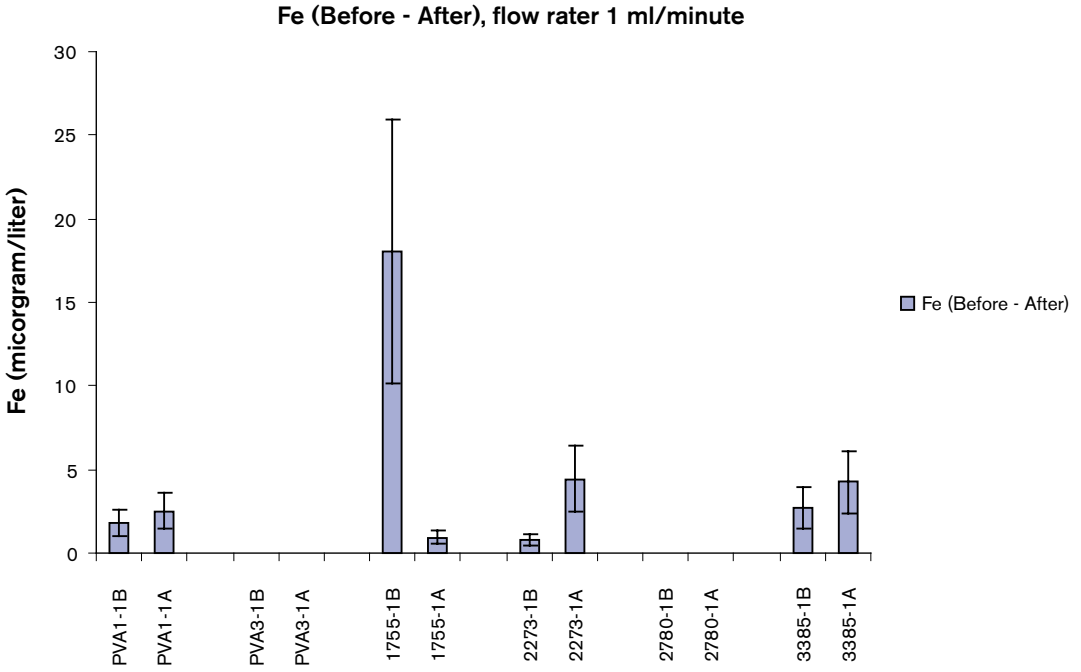

Figure A14-11. *Iron – comparison of "before" and "after" outlet with the sum of all the filters used. Olkiluoto and Äspö HRL. Flow rate 1 ml/min. Probable erroneous laboratory results from boreholes PVA3 and 2780 have been neglected.*

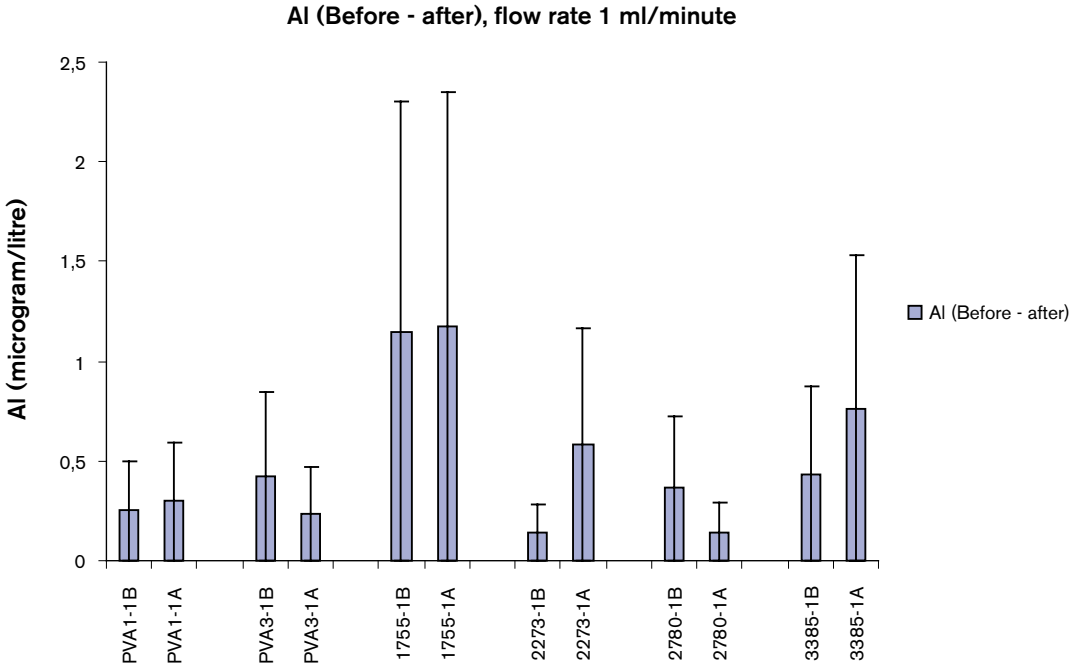

Figure A14-12. *Aluminum – comparison of"before" and "after" outlet with the sum of all the filters used. Olkiluoto and Äspö HRL. Flow rate 1 ml/minute.*

5.4 Comparison different filter sizes

Laboratory filter analyses do not indicate any consistent differences in the colloid size between the “before” and the “after” outlet, at any of the six boreholes used at this study.

Si is very homogeneously distributed between the three different filter sizes (Figure A14-14).

The predominant part of the Fe content is at the smallest filter size at Olkiluoto and Äspö borehole 1755, whereas laboratory results of samples taken from the remaining boreholes at Äspö HRL are inconclusive (Figure A14-14).

For Al, the content on the smallest filter size predominates at Äspö HRL, whereas the samples from Olkiluoto show no consistent distributions (Figure A14-16).

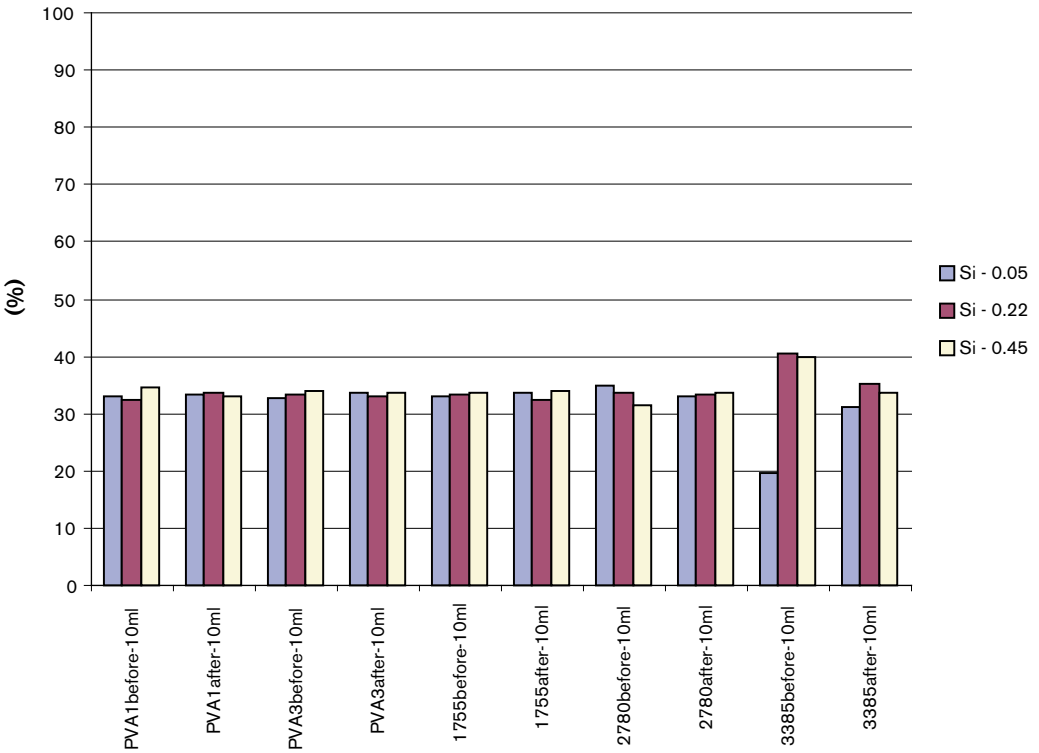

Figure A14-13. *Si – distribution of total mass through filter sizes. Olkiluoto and Äspö HRL Tunnel. All data refers to samples taken at a flow rate of 10 ml/min.*

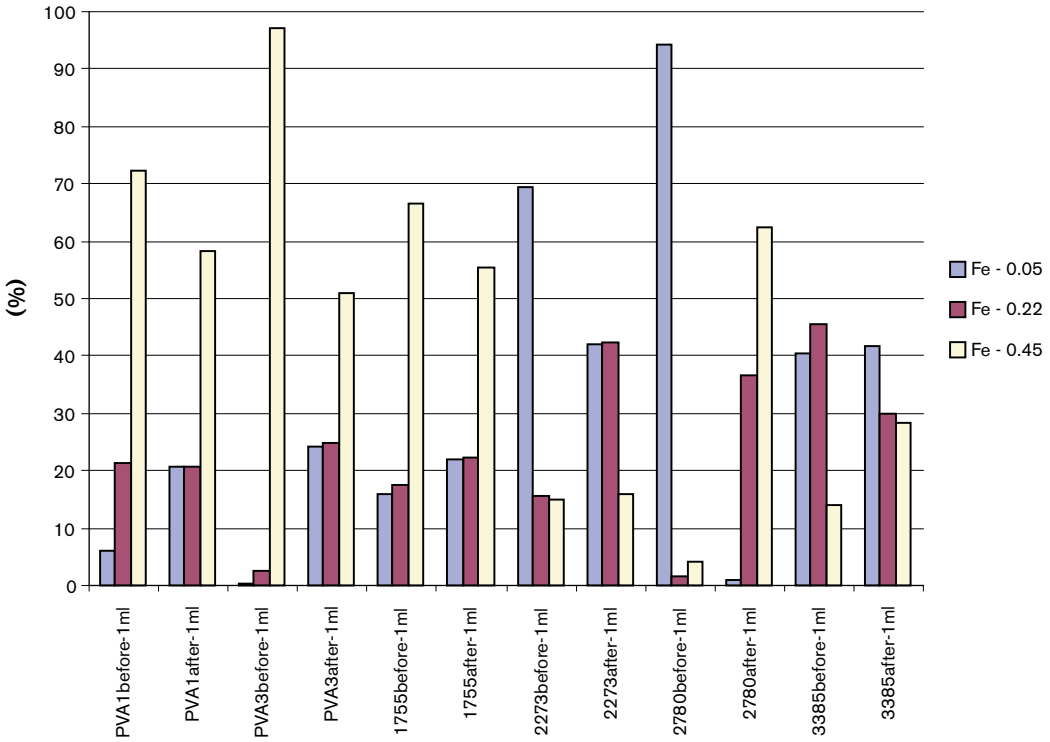

Figure A14-14. *Fe – "distribution" of total mass through filter sizes 0.05, 0.22 and 0.45 µm. Olkiluoto and Äspö HRL Tunnel. All data refers to samples taken at a flow rate of 1 ml/min.*

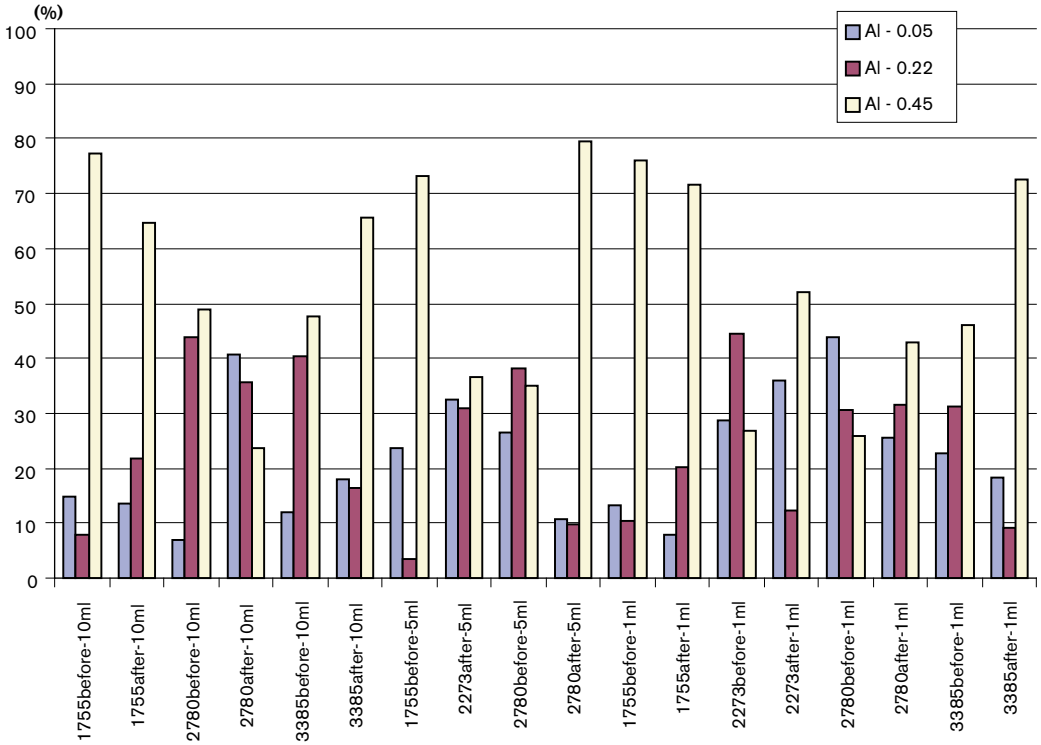

Figure A14-15a. *Al – distribution of total mass through filter sizes. Äspö HRL Tunnel – all flows. Please note that for some of the tests the "before" or "after" value might be below detection limits, and consequently not included in the graph.*

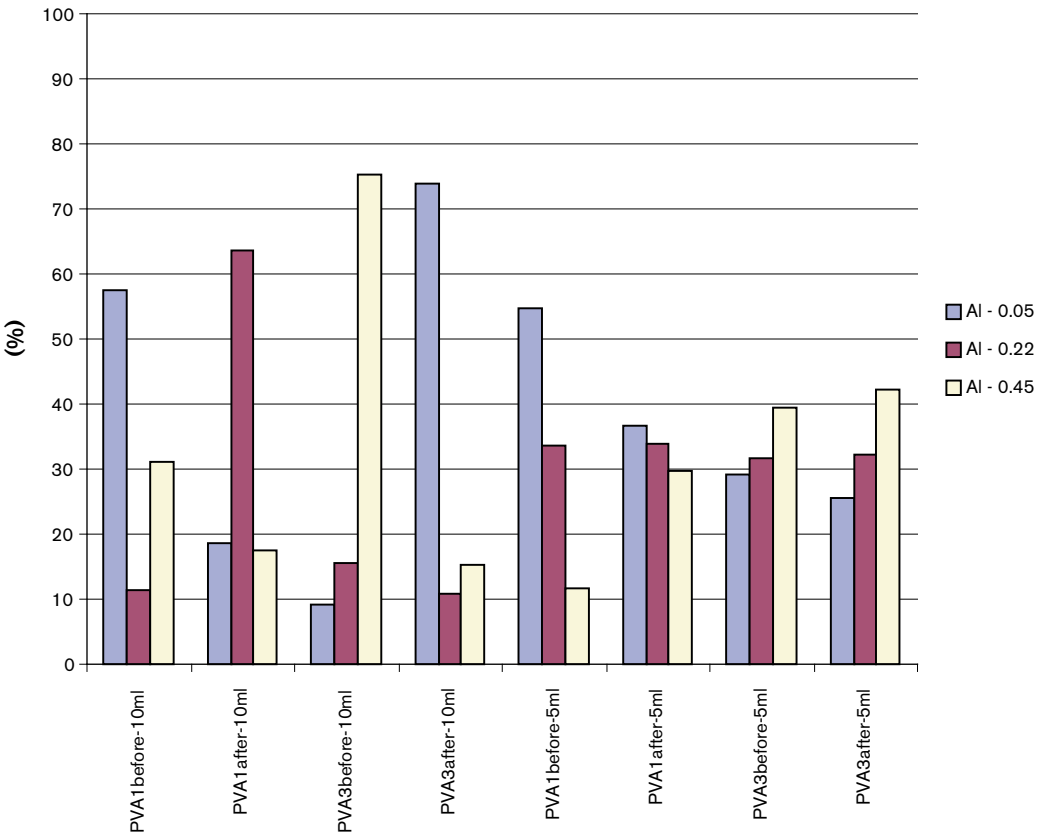

Figure A14-15b. *Al – distribution of total mass through filter sizes. Olkiluoto – flow 5 and 10 ml/min.*

5.5 Comparison between different sampling volumes

When comparing sampled volume from the "before" outlet with that from "after" reactor passage, it becomes clear that the cat ion content to some degree depends upon the volume of sampled water. The highest levels of colloids and cat ions are found on filters where the volume of sampled water was small. Low cation content on the other hand, is often associated with a large volume of sampled water. The colloid concentration is thus an artefact. When starting the flow in the boreholes loose mineral material was suspended to the solution. When larger water volumes passed the filters the solutions were diluted.

Figures A14-16 to A14-18 show plots for Si, Al and Fe, respectively. The concentration of each cat ion has been plotted against the corresponding volume used for that sampling period. Only analyses resulting in concentrations above detection limit for all three filter sizes are included in the plots.

The trend can clearly be seen in the Si plot, and is also indicated for Al. The plots use all available results, regardless of flow rate, borehole and outlet used.

These trends confirm that it is not colloids we see, rather suspended mineral from e.g. filling material.

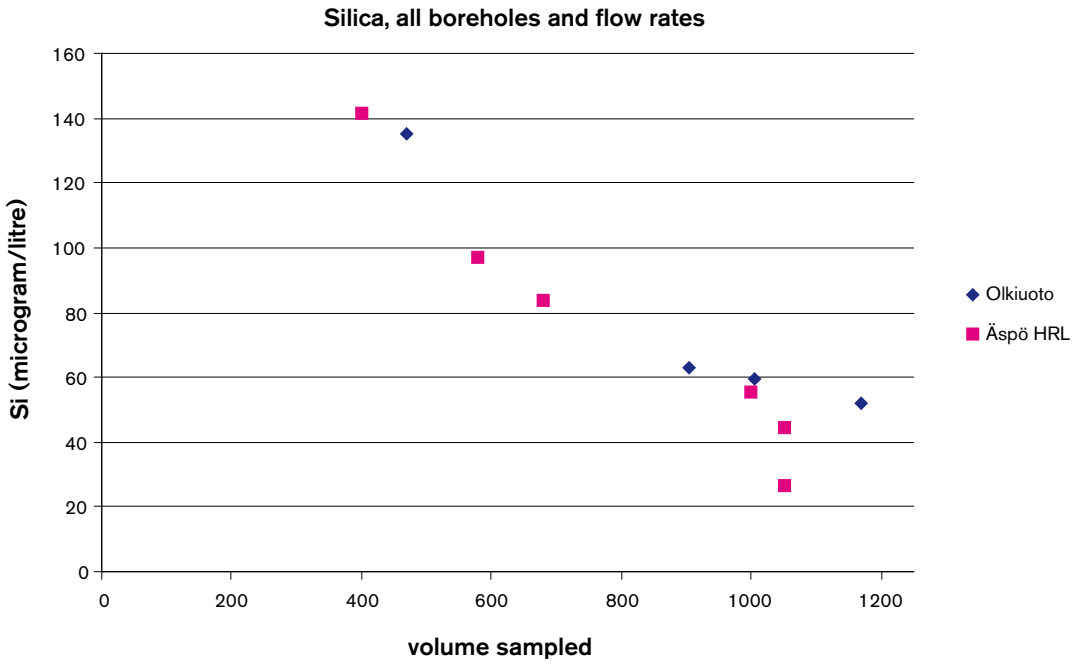

Figure A14-16. *Silica – sum of the filters used. Olkiluoto and Äspö HRL Tunnel. All data originate from samples taken at a flow rate of 10 ml/min.*

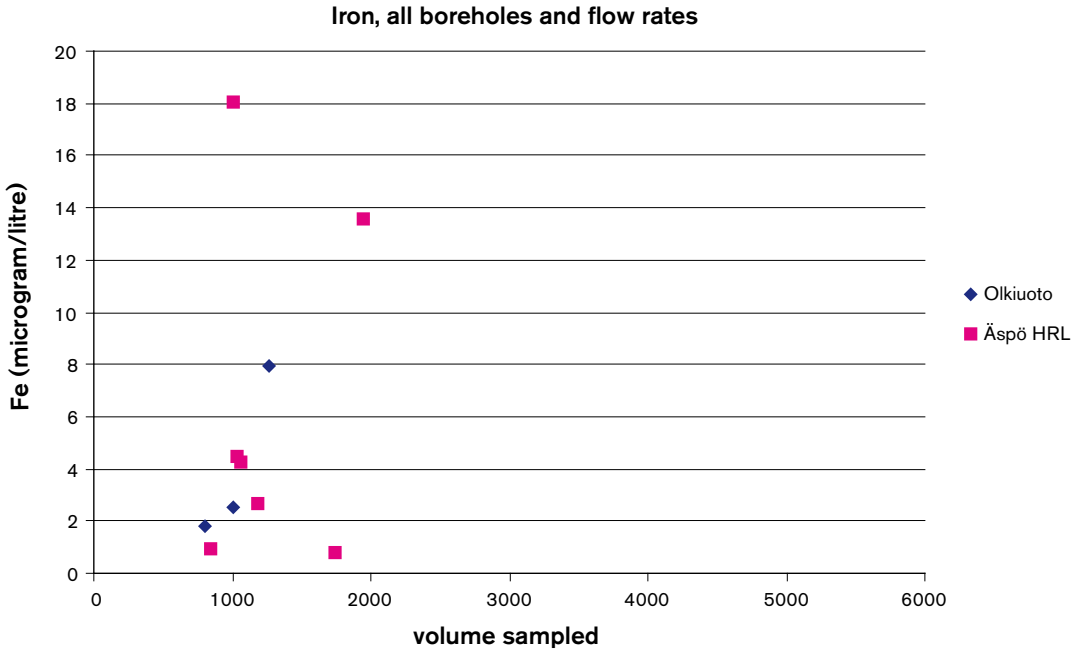

Figure A14-17. *Iron – sum of all filters used, all available data. Olkiluoto and Äspö HRL Tunnel.*

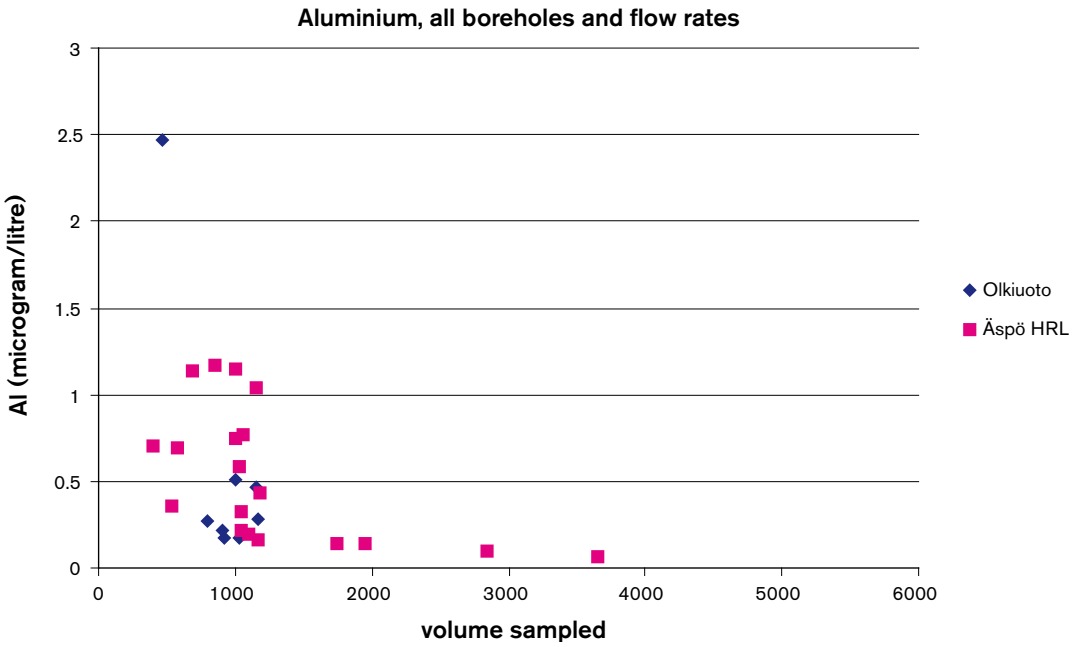

Figure A14-18. *Aluminum – sum of all filters used, all available data. Olkiluoto and Äspö HRL Tunnel.*

Appendix 15

Bentonite as a colloid source in groundwater conditions at Olkiluoto

Ulla Vuorinen, VTT Processes

Hannele Hirvonen, TVO Nuclear Services

October 2004

Contents

1 Introduction

In the safety of final disposal of spent nuclear fuel colloidal particles are one key issue, because they play a central role in regulating concentration and speciation of trace elements, and thus, may transport radionuclides released from a faulty fuel canister in the repository to the biosphere. Colloidal particles may not only be mobile, but may also move faster than average groundwater flow velocity in a fractured medium.

In general, colloids are defined as small particles in the size range of 1 nm to 1 µm. They can be either inorganic (e.g. oxides, minerals) or organic (humic and fulvic acids, bacteria) and are ubiquitous in natural aquatic environments. In this context, however, the size of colloids of interest is < 0.45 µm, because only colloids which do not sediment in a very slow groundwater flow can be potential carriers of radionuclides in disposal conditions.

According to the present concept of final disposal bentonite clay is a planned component in the disposal vault and Wyoming bentonite, MX-80, is one potential bentonite. Questions have arisen whether bentonite clay can be a potentially harmful source of colloids in the groundwater conditions at Olkiluoto. This study aims at estimating the amount of bentonite colloids emanating from bentonite sources assembled at two groundwater stations (PVA1 and PVA3) in the VLJ-tunnel at Olkiluoto. PVA1 is situated at the depth of 37.5 m /Pitkänen and Snellman 1990/ and PVA3 at 95.6 m /Rautio 1989/ in the tunnel. Before any estimations on the bentonite colloids can be given there has to be an assessment of the natural background of groundwater colloids. An evaluation of the size of montmorillonite particles (TEM, Transmission Electron Microscopy) emanating from effectively dispersed MX-80 has been given by /Pusch 1999/: over 90% were < 0.3 µm, unless the dispersed clay particles aggregate.

The clay content of MX-80 bentonite is dominated by montmorillonite ($(Na,Ca)(Al,Mg)_2(Si_4O_{10})(OH)_2 \cdot nH_2O$), the dioctahedral low charged clay mineral of the smectite group. For the principal smectite in MX-80 bentonite /Huertas et al. 2000/ gives the following composition: $[Na_{0.21}Ca_{0.08}K_{0.02}]Al_{1.51}Mg_{0.27}Fe_{0.17}Ti_{0.01}[Si_{3.98}Al_{0.02}O_{10}](OH)_2$.

Additionally, quartz (SiO_2), cristobalite (SiO_2), feldspar ($XAl_{(1\,2)}Si_{(3-2)}O_8$, X = Na,K,or Ca), chlorite ($(Fe,Mg,Al)_6(Si,Al)_4O_{10}(OH)_8$), pyrite (FeS_2), illite ($K_{0.7}(Si_{3.3}Al_{0.7})(Al_2)O_{10}(OH)_2$) kaolinite ($Al_2Si_2O_5(OH)_4$), carbonates and mica occur /Kaufhold et al. 2002/. Table A15-1a) shows one result of a mineralogical analysis of MX-80 /Müller-Vonmoos and Kahr 1983/ in which ~ 2 wt % of the material remained as “unidentified” /Bradbury and Baeyens 2002/. The montmorillonite content given in Table A15-1a) is according to recent data too low. It should be around 85% according to more recent mineralogical determinations /SKB 2004). The chemical composition of MX-80 bentonite is shown in Table A15-1b) provided by Volclay Ltd (1) /Keto 2003/ and another composition (2) by /Pusch et al. 1999/. /Bradbury and Baeyens 2002/ also give an inventory of the amorphous iron (hydr)oxide, chloride and sulphate in MX-80, Table A15-2.

According to the chemical compositions of MX-80 Si and Al are the major components, but lesser amounts of Fe, Mg, K, Na and Ca are present. The presence of these elements especially Si and Al in larger quantities in the colloid fraction may be an indication of clay colloids. However, the amount of clay colloids may also be so small that the possible increase in the concentrations of Si and Al in the samples falls within the uncertainty range of the analyses or the concentrations are below the detection limit of the analysis method. However, if there otherwise is evidence of the presence of colloids, but the evidence in concentrations is negligible it of course implies that the concentration of colloids is very small.

Table A15-1. a) Mineralogical composition of oven-dried MX-80 and b) chemical composition of MX-80 bentonite. The compositions are expressed in wt %.

a) Mineralogical composition		b) Chemical composition		
Mineral	**wt %**		**[1] wt %**	**[2] wt %**
Montmorillonite $(Na,Ca)(Al,Mg)_2(Si_4O_{10})(OH)_2 \cdot nH_2O$	75	SiO_2	63.0	61–95
Kaolinite ($Al_2Si_2O_5(OH)_4$)	< 1	Al_2O_3	21.2	22–25
Mica	< 1	Fe_3O_2	3.3	1–7
Quartz (SiO_2)	15.2	FeO	0.4	
Feldspar ($\boldsymbol{X}Al_{(1\,2)}\ Si_{(3\text{-}2)}\ O_8$, $\boldsymbol{X}$ = Na, K, or Ca)	5–8	Na_2O	2.6	0–1
Calcite ($CaCO_3$)	0.7	MgO	2.7	1–2
Siderite ($FeCO_3$)	0.7	CaO	0.7	0–0.6
Pyrite (FeS_2)	0.3	K_2O		0–3
Organic carbon	0.4	/[1] Keto 2003, [2] Pusch et al. 1999/		

Table A15-2. Iron (hydr)oxide content, and Cl^- and SO_4^{2-} inventories of MX-80.

Other constituents		(mmol kg-1)	References
Iron (hydr)oxide			
	amorphous	10.6 ± 0.4	/Bradbury and Baeyens 2002/
	total	25.9 ± 0.7	/Bradbury and Baeyens 2002/
NaCl		1.35 ± 0.1	/Bradbury and Baeyens 2002/
		1.04 ± 0.2	/Wanner et al. 1992/
$CaSO_4$		23.5 ± 0.9	/Bradbury and Baeyens 2002/
		26.6 ± 4.2	/Wanner et al. 1992/

Due to the ion-exchange nature of bentonite it readily exchanges Ca with Na, Mg and K, the result of which can be reflected in the changes observed in solutions contacting bentonite. Also dissolution of some readily dissolving minerals, like calcite and gypsum ($CaSO_4$), may increase the content of the corresponding ions in the contacting solution. Accordingly, this work includes analyses of groundwater from PVA1 and PVA3, both before and after interaction with the bentonite reactors.

For the estimation of the colloids in the groundwater before and after interaction with bentonite, ultrafiltrations were performed on the groundwater samples from the four groundwater sampling lines. The solution fractions obtained in ultrafiltration were analyzed. In addition to ultrafiltration, some filter membranes were produced for examinations with Scanning Electron Microscopy (SEM) and Energy Dispersive Spectroscopy (EDS).

2 Groundwater analysis

The assembly of the two bentonite reactors (= sources) at the two groundwater stations, (PVA1 and PVA3) was implemented so that by changing the sampling lines for groundwater samples could be collected either before or after interaction with the bentonite reactor. When starting the colloid sampling campaign groundwater was analysed at both groundwater stations from both sampling lines for elucidating the detectable changes brought about by the bentonite reactors. The samples were collected on three occasions first on February

10th of 2003, for a more complete analyzing for which the results are given in Table A15-3 (green columns). The additional analysis results in the table for PVA1 and PVA3 only, are from December 1999 (Fortum Power and Heat Oy), which also include results for Al and Sr.

A more complete table of the results (10th of February 2003) is found in Table A15-7 including the assigned relative standard deviations (RSD) calculated at least with three parallel samples, and tables for the two follow-up measurements on the 31st of March and 6th of May 2003 when only pH, alkalinity and conductivity were analyzed (Table A15-8 and A15-9).

The groundwater samples (in 2003) were collected on site and the analyses were carried out at TVO's laboratory in accordance with either SFS or other standards or generally approved and used methods (Table A15-15). A more detailed description of the groundwater analyses and results is presented in Chapter 7. The bottling and fixation of the samples was carried out according to established practices described in Tables A15-13 and A15-14.

Table A15-3. Analysis results of groundwater at the two groundwater stations (10.2.2003, green columns). B = after interaction with bentonite. The arrows in the table denote either increase or decrease in the measured value after interaction with bentonite. → = increase, → = decrease.

Analysis	Unit	PVA1	PVA1	PVA1 B	PVA3	PVA3	PVA3 B
Conductivity	mS/cm	3.20	3.38 →	3.20	8.40	8.43 →	8.60
pH		7.60	7.8 →	7.6	7.80	7.9	7.9
HCO_3^-	mg/L		375 →	400		210 →	200
Al	mg/L	0.008	< 0.05	< 0.05	0.005	< 0.013	< 0.013
Br-	mg/L	3.0	2.6 →	2.3	10	7.5 →	6.5
K	mg/L	13	14	14	13	14	14
Ca	mg/L	96	77	70	390	370	380
Cl^-	mg/L	780	805 →	760	2,570	2,520 →	2,580
S_{total}	mg/L	47	46 →	43	130	120 →	120
SO_4^{2-}	mg/L	145	140 →	130	370	360	380
S^{2-}	mg/L	0.06	0.03 →	0.02	0.03	< 0.01 →	<0.01
Mg	mg/L	29	31 →	29	108	100	110
Mn	mg/L	0.32	0.28 →	0.27	0.45	0.59 →	0.57
Na	mg/L	570	540 →	530	1,290	1,210 →	1,230
Fe_{tot}	mg/L	0.81	0.32 [1] →	0.14 [1]	0.03	0.031 [2] →	< 0.017 [2]
Si	mg/L	7.48	– →	–	5.1	– →	–
SiO_2	mg/L	16	15 [1]	15 [1]	11	10 [3]	10 [3]
DOC	mg/L	9.5	7.2	6.7	6.5	2.1	<1.8
DIC	mg/L	81	86 →	88	41	47 →	46
Sr	mg/L	0.87	–	–	4.0	– →	–

–) denotes not measured.
1) analysed by plasma emission spectrometry.
2) analysed by graphite oven atomic absorption spectrometry.
3) analysed by spectrophotometry.

Table A15-4. Electric conductivity (EC) and pH measured before, during and after colloid sampling. B = after interaction with bentonite. The arrows in the table denote either increase or decrease in the measured value after interaction with bentonite. → = increase, → = decrease.

Date	Analysis	Unit	PVA1	PVA1 B	PVA3	PVA3 B
10.02.2003	EC	mS/cm	3.38 →	3.20	8.43 →	8.60
	pH		7.79 →	7.62	7.87 →	7.91
27.02.2003	EC	mS/cm	–	–	8.62 →	8.92
	pH		–	–	7.68 →	7.76
05.03.2003	EC	mS/cm	3.53 →	3.38	9.12 →	9.04
	pH		7.40 →	7.53	7.67 →	7.72
31.03.2003	EC	mS/cm	3.48 →	3.33	9.01 →	9.18
	pH		7.47 →	7.51	7.67 →	7.75

–) denotes not measured.

In the tables and in the text the groundwater samples before interaction with bentonite are referred to as PVA1 and PVA3 (groundwater lines) whereas after the interaction PVA1B and PVA3B (colloid lines) are used. The analytical results of PVA1 and PVA3 showed that the compositions of the groundwaters differed quite significantly. Almost in every case the ionic concentrations were at least twofold in PVA3 groundwater compared to those in PVA1 groundwater (Tables A15-3 and A15-4), only the sulphide concentration was greater in PVA1 groundwater while the potassium concentrations were equal.

The trend of the effects of the bentonite reactor on the two groundwater compositions was quite the opposite. In the case of PVA1 calcium, chloride, sulphate, magnesium, sodium and conductivity showed a trend slightly decreasing after interaction with bentonite, (Table A15-13, see also Tables A15-8 and A15-9) while the trend in PVA3 was slightly increasing. The trends shown in alkalinity were opposite ones; alkalinity after interaction with bentonite increased in PVA1 groundwater but decreased in PVA3 groundwater.

The iron concentrations decreased most in the groundwater samples measured after the bentonite reactor, up to 55%. Also bromide and sulphide results indicated that the bentonite reactor decreased their amount over 10% from the original amount.

3 Groundwater sampling for colloid studies

Sampling of groundwater for the examination of colloids was started February 25, 2003 and completed March 5, 2003. Groundwater was continuously flowing at both sampling sites with a flow rate of about 9.5 ml/min through both sampling lines; the groundwater line and the colloid line with the bentonite reactor.

3.1 Preparations and set-up

All the samples collected were treated on site in a nitrogen (N_2 grade 6.0) flushed movable glove-box at ambient temperature. The tubing from the groundwater sampling station was connected via a quick coupling through the glove-box wall to enable the collection of groundwater directly inside the anoxic glove-box when needed. A particle filtering capsule, 0.45 µm (AquaPrep™600, PALL), was installed in the sampling line outside the glove-box. Sampling was started at the deeper level with the more saline groundwater PVA3 and then continued with PVA1.

Flushing of the movable glove-box with N_2 was already started in the laboratory and continued throughout the transportation and sampling procedures in the VLJ tunnel at Olkiluoto. The continuous flushing with nitrogen allowed maintaining a slight over pressure throughout the activities. Oxygen content inside the glove-box was continuously measured (Orbisphere) using a probe for dissolved oxygen.

Inside the movable glove-box a small centrifuge was operated with 15 ml centrifuge ultrafiltration tubes (Macrosep, PALL) for treating the groundwater samples. For SEM/EDS analyses sequential filtrations were performed with Nuclepore filter membranes in disk filtering devices. In order to avoid particle contamination from air the filters and centrifuge tubes were assembled in the laboratory under laminar flow, and to diminish oxygen contamination all equipment, membranes, tubes, sample bottles, pipettes etc were taken inside a laboratory glove-box (O_2 < 0.1 ppm) via a vacuum chamber. Inside the glove-box the assembled filters and ultracentrifugation tubes were closed inside plastic jars, and all the plastic bottles needed for collecting solution samples were tightly closed. In the glove-box all the items needed for the work to be performed in the movable glove-box were placed inside tightly closing steel vessels which were taken out from the glove-box and packed for transportation to the sampling sites at Olkiluoto. The items in the steel vessels were, prior to taking them inside the movable glove-box, additionally flushed with N_2. Despite of these meticulous considerations one can not avoid some O_2 entering the glove-box.

From previous work with the movable glove-box it was known that centrifugation inside the glove-box produces extra heat increasing the working temperature from the ambient temperature in the tunnel. In order to get an assessment of the effect of the temperature change (13–25°C) on the saturation index of calcite simple scoping calculations (EQ3/6, DATA0.com /Wolery 1992/) were performed. As input to the code the analytical data in Table A15-3 was used and a given value for O_2 fugacity (log f(O_2) = –65) for computing the redox. The results are presented in Table A15-5. Some saturation index results of Si and Fe minerals are included as well.

Calcite shows supersaturation in all other cases except in PVA1B groundwater at the two lower temperatures (13°C and 20°C). This implies that due to loss of CO_2, indicated by the log pCO_2 values > –3.5 (atmospheric), calcite may precipitate during sampling and appear as an artefact, but the temperature may have an effect only in the case of PVA1 B if higher than about 20°C.

Three Si-minerals, chalcedony, cristobalite and tridymite, were also included to see their saturation state in the groundwater samples at different temperatures. In the case of PVA3 and PVA3 B the computed values show only saturation and the same values for both samples. Whereas, in the case of PVA1 and PVA1B tridymite shows supersaturation at the lower temperatures, as well as, chalcedony in PVA1B. Comparing the saturation indices of the Si-phases (at 13°C) in PVA1 and PVA1B they are just slightly higher in PVA1B, which could imply an increase of silicate containing colloids possibly originating from the bentonite reactor. Prior to analyzing the groundwater samples were filtered with 0.45 µm filter and thus colloids (< 0.45 µm) were included in the analysis results.

No saturation indices for the iron minerals were computed in the case of PVA3B because the analysis result of iron was below the detection limit. The computed saturation indices show that goethite is supersaturated only in PVA1, while hematite is supersaturated in all the cases. However, the saturation indices of hematite in PVA1B are clearly smaller than in PVA1 indicating less supersaturation.

Table A15-5. Results from EQ3 modelling. PVA1 and PVA3 for the groundwaters and PVA1 B and PBA3 B for the groundwaters after interaction with bentonite. ss = supersaturated, s = saturated.

		PVA1	PVA1 B	PVA3	PVA3 B
pH		7.79	7.62	7.87	7.91
log fO_2 given	mV	–65	–65	–65	–65
Eh calculated at 13°C	mV	–134	–124	–138	–140
at 20°C		–168	–158	–175	–173
at 25°C		–193	–183	–198	–200
HS^-/SO_4^{2-} at 13°C	mV	–232	–220		
at 20°C		–241	–229		
at 25°C		–247	–235		
Electrical imbalance at 25°C	% of total charge	–2.62	–2.35	–1.57	–1.38
I_{true}	M	0.034	0.033	0.093	0.095
pCO_2 at 13°C		–2.35	–2.18	–2.75	–2.81
at 20°C		–2.31	–2.13	–2.71	–2.77
at 25°C		–2.28	–2.10	–2.68	–2.74
Calcite ($CaCO_3$) at 13°C	Saturation index (SI)	0.42 ss	0.22 s	0.75 ss	0.78 ss
at 20°C		0.52 ss	0.33 s	0.86 ss	0.88 ss
at 25°C		0.60 ss	0.40 ss	0.93 ss	0.95 ss
Chalcedony (SiO_2) at 13°C	SI	0.37 s	0.39 ss	0.20 s	0.20 s
at 20°C		0.21 s	0.23 s	0.04 s	0.04 s
at 25°C		0.11 s	0.13 s	–0.06 s	–0.06 s
Cristobalite(α) (SiO_2) at 13°C	SI	0.08 s	0.09 s	–0.10 s	–0.10 s
at 20°C		–0.07 s	–0.06 s	–0.25 s	–0.25 s
at 25°C		–0.17 s	–0.15 s	–0.34 s	–0.34 s
Tridymite (SiO_2) at 13°C	SI	0.47 ss	0.48 ss	0.30 s	0.30 s
at 20°C		0.31 s	0.33 ss	0.14 s	0.14 s
at 25°C		0.21 s	0.23 s	0.04 s	0.04 s
Goethite (FeOOH) at 13°C	SI	0.82 ss	0.15 s	0.06 s	
at 20°C		0.66 ss	–0.02 s	–0.11 s	
at 25°C		0.54 ss	–0.14 s	–0.22 s	
Hematite (Fe_2O_3) at 13°C	SI	2.58 ss	1.22 ss	1.05 ss	
at 20°C		2.26 ss	0.90 ss	0.74 ss	
at 25°C		2.04 ss	0.69 ss	0.52 ss	

3.2 Procedures

The cumulative centrifugation of groundwater samples was performed inside the glove-box, which was installed in the VLJ near by the two sampling points in question. The small centrifuge had a six-place fixed angle rotor for 15 ml test tubes. For concentration of groundwater ultrafiltration tubes (Macrosep, PALL) of three different cut-off sizes were used, 0.3 µm, 300 kD (≈ 60 nm) and 10 kD (≈ 2 nm). The prefiltered (0.45 µm) groundwater was collected (via the lead-in lines with quick coupling) inside the glove-box in a plastic (PE) bottle from which groundwater was pipetted (10 ml/tube/centrifugation round) into the six ultrafiltration tubes with the same cut-off size and spun for about 10 min to 60 min (depending on the cut-off value) at 3,783 RCF (Relative Centrifugal Force). This allowed 60 ml of groundwater to be handled per spinning round. The filtrates

from the receiver tubes were combined and collected in a plastic bottle and a new 10 ml volume of groundwater/tube was added to the remaining concentrate in the tube and the spinning was repeated. When enough groundwater had thus been treated, the concentrates (about 0.5–1.5 ml/tube) in the five tubes were rinsed with anoxic deionized water (10 ml of H_2O/tube) spinning once more in the centrifuge in order to remove a greater part of the salts. Again the filtrates were combined in one plastic bottle and the remaining concentrates were combined in a plastic test tube. Finally the filter tubes were rinsed with 1% HNO_3 (suprapure, 10 ml/tube) and the rinse solutions combined. A diagram of the procedure is shown in Figure A15-1. Altogether 6 different solution types were obtained for chemical analysis for each cut-off value; from the five centrifuge tubes the filtrates, the concentrate rinse waters, the rinsed concentrates and acid rinses, and from the sixth centrifuge tube two solutions, the not rinsed concentrates and the corresponding acid rinses.

In addition to the solution samples filter membranes with cut-off values of 0.4 µm, 0.2 µm, 0.1 µm, 0.05 µm, and 0.015 µm were prepared for SEM/EDS analysis. Groundwater was filtered through the membranes using sequential filtration with two membranes assembled consecutively with two disc devices (e.g. 0.4 µm/0.2 µm, 0.2 µm/0.1 µm) After filtration the membranes were washed with deionized anoxic water in order to remove salts. The SEM micrographs and EDS spectra are presented in Chapter 9.

All the samples collected were stored in the glove-box until taken to the laboratory at VTT Processes in Espoo, where the samples were acidified and kept in a refrigerator until analysis.

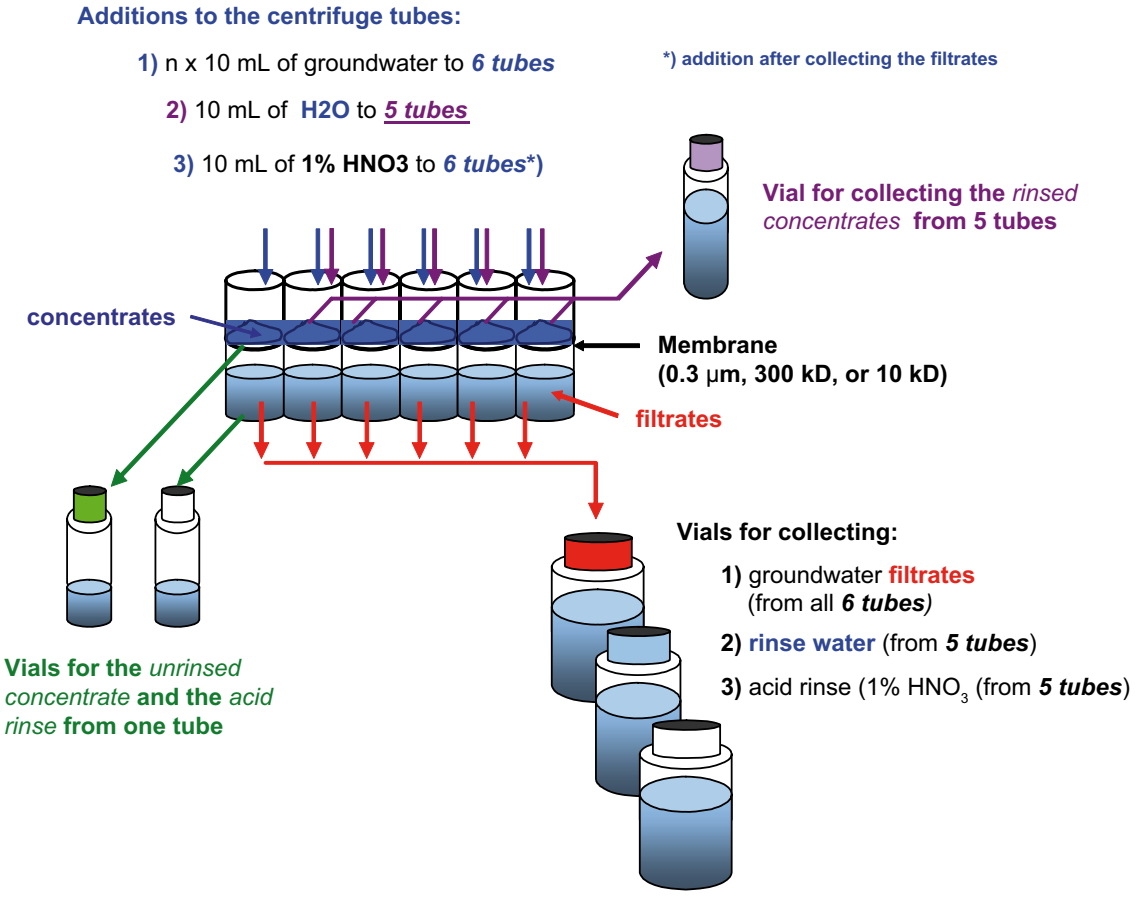

Figure A15-1. *Diagram of the procedure in groundwater sampling.*

4 Results

While working in the glove-box the O_2 value measured at PVA3 varied between 5.5 ppb and 17.0 ppb depending on the temperature and objects needed to be taken into or out from the glove-box via the flushing chamber. Using a centrifuge inside the glove-box produced extra heat increasing the working temperature at PVA3 from the ambient 10–11°C slowly up to 21°C during 9 hours of sample treatment. The corresponding variations at PVA1 were for O_2 5.6–18 ppb and for the temperature from the ambient 13–14°C up to 23°C.

4.1 Solution analysis

Table A15-16 gives the analysis results for the solution samples collected in the ultra-filtration procedures. IC (Ion Chromatography) was used to analyze Br, Cl and SO_4, ICP-AES (Inductively Coupled Plasma Emission Spectrometry) in Ca, Fe, Mg, Mn, Na, Si, and Sr analysis, except in the case of Fe in the unrinsed concentrate samples which were analyzed using GFAAS (Graphite oven Flame Atomic Absorption Spectrometry) excluding one sample with high Fe content (Fe = 4.7 mg/L). FAAS was used to determine K concentrations. Due to very small concentrations of Al it was analyzed with ICP-MS. However, Al is very susceptible to contamination from different sources and therefore the analysis results must be considered with some caution. Anions were not analyzed in the concentrate fractions, as the amounts collected were too small to allow complete analysis. Na and Cl in the samples can be considered to be in soluble form and represent the behaviour of salt retention. By calculating element concentration ratios in the samples and comparing the results between the different solution samples indications of colloidal association of an element can be made, because ratios of soluble elements in solutions are expected to remain unchanged.

Filtrate analyses:

The analysis results of Fe (Table A15-16, a)) gave clearly higher concentration in PVA1 and PVA3 filtrates (0.3 µm), about 0.8 mg/L and 0.08 mg/L, respectively, than obtained in the groundwater analysis performed before the colloid sampling, 0.3 mg/L and 0.03 mg/L, respectively. However, at least in PVA1 a higher concentration of Fe has been measured before 0.8 mg/L (Table A15-3) and thus the results may be due to natural variation. Also the measured Al concentrations in PVA3 filtrates (0.3 µm), 0.008 mg/L were higher than a previously measured one, 0.05 mg/L. All the other analyses results of the 0.3 µm filtrates were in line with the preceding groundwater results.

Similar trends as in the preceding groundwater analyses (Table A15-3) were also seen in the results of the filtrates when comparing the samples from groundwater lines and colloid lines (interaction with the bentonite reactors). In the case of PVA1 the concentrations of Na, Ca, Mg, Sr, Cl, Br, SO_4, and Fe showed a slight decreasing trend in PVA1B filtrates. The only exception was Fe in the filtrate of the smallest size ultrafilter (10 kD) indicating an opposite trend. Also Si showed a consistently slight increase in PVA1 B, implying increased release of non-colloidal Si (≈ 0.3 mg/L) possibly from bentonite. In the case of PVA3 subtly increasing trends were seen in PVA3 B for Ca, Sr, Mg, and SO_4. All the other analysis results before and after interaction with bentonite showed more or less the same values or showed no clear trend. However, it has to be born in mind that the changes mostly are within the error limits of the analysis methods.

When comparing the analysis results of the filtrates between the different cut-off samples the only elements indicating retention in the concentrate (= decreased concentration in the filtrate with decreasing cut-off) were Fe and Al, Fe even more clearly. Especially the

smallest cut-off devices retained more, indicating the presence of Fe- and Al-containing colloids smaller than 0.3 µm, but the size range is large, at least down to about 10 kD (≈ 2 nm) in the case of Fe. Based on the filtrate analysis Fe and Al are mostly colloidal. The estimated rough amounts of Fe and Al containing colloids in the sampled groundwaters are given in Table A15-6. Bentonite (the main component montmorillonite) mainly contains Si and Al, but Si content of the groundwater samples was too high to observe any retention of Si containing colloids, which together with Al containing colloids could imply to the presence of bentonite colloids.

Table A15-6. Rough estimates of the amounts of Fe and Al associated with colloids in the sampled groundwaters based on filtrate analysis.

	Fe (mg/L)		Al (mg/L)	
	300 kD–0.3 µm	10–300 kD	300 kD–0.3 µm	10–300 kD
PVA1	0.6	0.2	0.004	
PVA1B	0.4		0.001	
PVA3	0.03	0.04	0.001	
PVA3B	0.001	0.06	0.001	

Rinsing water analyses:

The content of elements in the different cut-off size samples within the same groundwater showed an increasing trend because more salt with more solution was retained by the smaller size ultrafilters. The calculated element ratios deviated enough only in the case of Fe in order to indicate other than soluble forms involved (Al was not analyzed in rinse water).

Concentrate analyses:

Two kinds of concentrates were analyzed, one that had been rinsed with anoxic deionized water (Table A15-16, d) and another, which had not been rinsed (Table A15-16, e). Rinsing was performed in order to remove most of the soluble salts in the concentrate leaving stable colloids in suspension.

In the analysis of the unrinsed concentrate doubtfully high values were seen for Si (40 mg/L), Fe (4.7 mg/L) and Al (0.71 mg/L) in the PVA1 0.3 µm sample, whether due to contamination or some kind of a burst could not be testified, but the element ratios for the different size filters (300 kD/0.3µm, 10 kD/300 kD) in PVA1 for Al (0.03, 0.86) and Fe (0.04, 0.82) suggested that Al and Fe were coupled, whereas Si (0.19, 1.04) had another source. However, contrary to Fe and Al the higher concentration of Si was not reflected in the filtrate analysis result. In the rinsed concentrate of PVA3B all Al concentrations showed slightly higher values than the corresponding ones in the unrinsed concentrate, an especially high questionable value (0.130 mg/L) was analyzed in the 0.3 µm sample. Otherwise the calculated element ratios in both concentrates indicated that Al and Fe could be associated with colloidal material when all the other elements followed, more or less, the ratios of soluble elements. It has to be borne in mind, however, that the concentrations of the elements other than Fe and Al are so much higher that detection of, for example, colloids associated Si is hampered by the presence of soluble Si.

Acid rinse analyses:

The ultrafiltration devices were last rinsed with acid in order to remove the material left on the filter membranes and vessel walls after removing the concentrates. The analysis results of acid rinses showed that the amount of elements generally decreased when preceded by rinsing with water (Table A15-16, c); exceptions were Al, Fe and Mn, the concentrations of which were about the same in both acid rinses (Table A15-16, c and d) indicating colloid related behaviour and/or mere sorption. The other element concentration ratios predominantly supported soluble material having remained in the devices, which is quite possible as the concentrations of the other elements in the concentrates were at least an order of magnitude, or even higher compared to those of Al, Fe and Mn. Therefore the amount of rinsing used may have been insufficient to completely wash off all remains.

4.2 Nuclepore filter membranes

Unfortunately several of the assembled sequential discs filtering devices were leaking allowing the solution to be filtered through to leak out of the device before passing through both membranes. Therefore only some membranes were good enough for SEM/EDS analysis. The SEM micrographs and the EDS spectra obtained are presented in Chapter 9. In the EDS spectra the peaks of gold (Au) originated from gold coating of the specimen and peaks of copper (Cu), and zinc (Zn) from the brassy specimen holder. Gold coating of the specimen was necessary for imaging, but unfortunately the Au peaks may have disguised the sulphur peaks, and S could not therefore always be detected. On some of the micrographs some rather exotic elements, rhodium (Rh), chromium (Cr) and titanium (Ti), were detected, the origin of which is unknown. One possible source could be equipment used in the bore-hole.

Generally, scanning of the filter membrane samples was first done with magnification of 10,000 and when typical particles in greater numbers were found on the membrane then the scanning was enlarged to 30,000. The EDS analysis was performed on the particles found on the membranes. The area on the membrane covered in the analysis consisted of a circle with a diameter of 1 µm, whereas the diameter of the active membrane area was about 2 cm. Thus the presented micrographs and the EDS spectra are of the typical particles, but cover only a small selection of the total specimen area, and thus other kinds of particles and elements may have remained undetected.

All the different cut-off sizes of the empty Nuclepore membranes used (0.4 µm, 0.2 µm, 0.1 µm, 0.05 µm and 0.015 µm) were first analyzed with SEM/EDS. The SEM micrographs of the empty membranes are shown in Figure A15-2 and the corresponding spectra in Figure A15-3. As these specimens were not gold coated and the material of the membranes was polycarbonate only carbon (C) and oxygen (O) were detected and due to the organic nature of the material a slight increase in the background was seen as well. In the following discussion about the elements present on the different membrane samples C and O are mostly left out of the discussion as they are present in any case and can not straightforwardly be referred to as due to e.g. organics or carbonates. However, in a few cases oxygen is regarded.

4.2.1 PVA1 filter membranes

The membranes in Figure A15-4 were sequentially assembled during filtration of 32 ml of PVA1 groundwater. A greater amount of particles remained on the 0.4 µm membrane (Figure A15-4a) than on the 0.2 µm membrane (Figure A15-4c), even if most of the particles were smaller in size than the holes in the membrane. The particles on the 0.4 µm

membrane formed small aggregates of different sizes. The elemental composition of the particles on the 0.4 µm membrane (Figure A15-5a) consisted mainly Fe, Ca, Cr, Si, Cl, but also traces of Na, Mg and Al. On the 0.2 µm membrane (Figure A15-5b) the major component of the small particle aggregates was Ca with little Cl and traces of Al, Si and Fe. Some precipitation of calcite is possible, but calcite is also a common fracture mineral at Olkiluoto. The presence of Al and Si implicates occurrence of mineral particles e.g. aluminosilicates. Rough evaluation of the particle size range on the 0.4 µm membrane is from 0.1 µm up to 0.4 µm (without large aggregates). On the 0.2 µm membrane the particle size was around 80 nm.

The smaller cut-off membranes in Figure A15-6 were also used sequentially; the 0.1 µm membrane (Figure A15-6a) with a 0.2 µm membrane (26 ml filtered) and the 0.05 µm membrane (Figure A15-6c) with a 0.1 µm membrane (23 ml filtered). The major element on the 0.1 µm membrane was Si with traces of Na, Al, Mg, Cl, Ca and Fe (Figure A15-7a). The increased oxygen peak insinuates to presence of silicate, SiO_2, which in amorphous form is amongst fracture minerals detected at Olkiluoto. Ti was dominant on the 0.05 µm membrane (Figure A15-7b) with additional traces of Si. The ratio of Na and Cl peaks indicates presence of salt while Si, Mg and Al infer to clay minerals and silicates. The size of the small particles forming the aggregate on the 0.1 µm membrane is roughly about 100 nm.

4.2.2 PVA1 B filter membranes

The filter membranes in Figure A15-6 were sequentially assembled for filtering of 18 ml groundwater from the PVA1 “colloid line”. The 0.4 µm membrane (Figure A15-8a) appeared to be quite empty indicating that groundwater particles passing the 0.45 µm prefilter (in the sampling line) also passed this filter. On the left side in the figure, just a few particles seem to have been caught in the filter holes. No EDS spectrum for this specimen is shown as it was similar to that of an empty membrane (Figure A15-3a).

Contrary to the 0.4 µm membrane the 0.2 µm membrane (Figure A15-8b) retained a lot of particles, which have formed large aggregates on the membrane, but also smaller particles that are able to pass the 0.2 µm filter were detected. The elements detected on the membrane were Si, Al, K, Fe, Cl, Na, Mg, S and Ca, as well, as an increase of the oxygen peak (Figure A15-9). The presence of Si, Al, Mg and K especially infer to the presence of clay minerals and the ratio of Al/Si (~ 0.43) implies that bentonite colloids are involved according to its composition (Table A15-1). The height of the oxygen peak gives further conformation of clay material. The presence of K may be an indication of K-feldspar as well. A rough estimate of the size range of the individual small particles on the membrane gives from 50 nm up to 0.2 µm.

Figure A15-10 shows micrographs of a 0.1 µm filter membrane (prefiltration with 0.2 µm), which appeared rather empty (micrographs a) and b)), but an area with more material on the membrane is shown in micrograph c) for which the EDS spectrum is shown in Figure A15-11, indicating the presence of Na, Cl, Si with a trace of Al, Ca, as well as Rh. Some salt (NaCl) is probably present with some silicates. The origin of Rh could perhaps relate to boring or some borehole equipment.

On the micrograph (Figure A15-12) of the smallest membrane 0.015 µm (prefiltered with 0.1 µm) only Si containing particles (Figure A15-13) were detected and traces of Cl and Fe. The roughly evaluated size range for the individual particles is from about 50 nm up to about 70 nm. The particles have formed larger aggregates and there is also a salt crystal (~ 0.4 µm white spot) in the middle of Figure A15-13a.

4.2.3 PVA3 filter membranes

Figure A15-14 shows the micrographs of two sequentially assembled filter membranes (16 ml filtered through); 0.4 µm and 0.2 µm. Very small and very few particles were detected on both membranes. The particles were smaller than the holes in the membranes but they were retained due to aggregation. The element ratio of Na and Cl on the 0.4 µm membrane (Figure A15-15a) indicated the presence of some NaCl, in addition the particles contained Si, Ca and Fe. On the 0.2 µm membrane (Figure A15-15) Ca dominated, which together with the increased height of the oxygen peak and ratio with it implicated the presence of calcite, which can be an artefact, but may also partly be colloidal calcite, which is a common fracture mineral at Olkiluoto. Traces of Fe were present as well. A rough estimate of the particle sizes seen on the micrographs is between 0.1 µm and 0.3 µm on the 0.4 µm membrane, and on the 0.2 µm membrane it is from about 30 nm up to about 60 nm.

The 0.05 µm membrane (Figure A15-16) (16 ml filtered through) was covered with a very fine material, which had dried and cracked like dry clay. The dominant element on this membrane was Ti (Figure A15-17). In addition to Ti Al, Si, Na and S were also present. The origin of Ti is unknown, but could perhaps be from the drilling equipment.

4.2.4 PVA3 B filter membranes

Figure A15-18 shows micrographs of two 0.4 µm filter membranes. The difference between the membranes was the amount of groundwater filtered from the "colloid line"; a) 42 ml b) 25 ml. The particles on the membranes appeared to be quite similar except that more salt crystals were seen in the case of a). The holes of both membranes were bigger than the particles retained on the membranes, but retention occurred due to aggregation. According to the EDS spectra, (Figure A15-19) in addition to Na and Cl (salt elements), only Si and Fe were detected.

Figure A15-20 shows micrographs of the two 0.2 µm membranes which were sequentially assembled during filtration with the 0.4 µm membranes in Figure A15-18. Very little material was found on the membranes, which appeared as aggregates of smaller particles. The EDS spectra (Figure A15-21) revealed the presence of Al, Si and K in addition to Na and Cl. Na, K and Cl were more distinguishable on the membrane through which more water was filtered (Figure A15-21a), whereas on the other membrane (Figure A15-21b) Al and Si were more distinct. The coexistence of Al, Si and K imply that clay minerals can be involved; however, the peaks in the spectra were so small that no ratio correlations could be examined. The smallest particles in the aggregates are about 50 nm.

Figure A15-22 shows micrographs of a 0.1 µm filter membrane through which 25 ml of groundwater was filtered (prefiltered with 0.2 µm). On the micrograph similar aggregates of small particles were seen to those on the other filter membranes. The main elements detected in the EDS spectrum (Figure A15-23) were Si and Fe in addition to Na and Cl.

The roughly evaluated range of the particles appearing on all these filters is between 30 nm up to about just over 100 nm excluding the salt crystals (Figure A15-18).

4.2.5 Filter membranes form delayed processing

Because in the field some filtrations were not successful a few new filtrations of the groundwaters from PVA1 and PVA3 were performed in the laboratory 2 days after collecting the groundwater (0.45 µm prefiltered) on the site. These membranes (Figures A15-24 and A15-26) showed larger precipitates/aggregates than those on the micrographs produced on the site. The EDS spectra of PVA1 membrane (0.1 µm,

Figure A15-25) and that of PVA3 (0.4 µm, Figure A15-27a) showed the presence of Ca which in relation to the O peak suggested calcite precipitation due to loss of CO_2 during storage, which is in good agreement with the modelling results of calcite supersaturation (Table A15-5). In the case of PVA1 Cl is the only other element detected on the membrane, whereas in the case of PVA3 traces of Mg, Al and Si were also present. The EDS spectrum of the 0.1 µm membrane showed Cl and Ca as major elements present, but some Na and Si was also detected. What is seen on these membranes are mainly artefacts which may disguise the colloids originally present.

5 Summary and conclusions

Prior to starting the colloid sampling campaign groundwater from both sampling lines, natural groundwater and "colloid", at both groundwater stations, PVA1 and PVA3, was analyzed. The groundwater analysis performed before and after contact with the assembled "bentonite reactors" indicated minor changes in the chemistry due to interaction with bentonite. A slight trend of opposite behaviour in some element analysis results (although mostly within the uncertainty range) was seen between the two groundwaters of different salinities. The observed differences may be due to several processes; to ion exchange with bentonite, dissolution of easily dissolving phases of bentonite, sorption as well as colloids emanating from bentonite. However, the groundwater chemistry could not give any indication of bentonite colloids released, but retention of Fe by the reactors seemed rather obvious.

For evaluating the amount of natural colloids and bentonite colloids released from the "bentonite reactors" centrifugal ultrafiltrations of the groundwater from the four sampling lines were performed as well as membrane filtrations. All the work was carried out inside a movable glove-box with N_2 atmosphere in order to avoid the disturbances brought about by the atmospheric gases (O_2 and CO_2). The sampling, even if performed by taking good care of various sources for artefacts, was not free of them completely; precipitation of calcite is difficult to avoid when CO_2 has a way to escape from groundwater and Fe is susceptible to precipitating if enough O_2 is available. Fast processing of samples on site helps to minimize artefacts, which was seen when some filter membranes produced later in the laboratory were examined with SEM/EDS.

The results from SEM/EDS studies and the indicative results based on ultrafiltration samples are in good agreement of the characteristics of the particle phases present in the two groundwaters. However, the obtained results did not allow calculation of the actual concentration of the element association with the different particle phases.

In the EDS spectra the peaks of Au, Cu, and Zn appear always, because they originate from sample preparation and the brassy specimen holder. Gold coating of the specimen was necessary for imaging, but unfortunately the Au peaks often disguise the sulphur peaks, and S can not therefore always be detected especially in the case of little material on a specimen. The results of SEM/EDS analysis show that after prefiltration in line (0.45 µm) only a few particles had collected on most membranes. Usually small particles, smaller than the cut-off of the membrane, formed larger aggregates on the membranes (0.4 µm, 0.2 µm, 0.1 µm and 0.05 µm). The most abundant elements detected with EDS were Ca, Fe, Si, Na, Cl, Al, Mg, and Na, but on a few membranes K and S were also present. More prominent peaks were detected on PVA1 membranes, especially for Fe and Ca. In addition to these common elements some rather peculiar elements, rhodium (Rh), chromium (Cr) and titanium (Ti)

were detected on a few membranes. Ti was detected in both groundwater samples before interaction with bentonite on the 0.05 µm membranes, whereas Cr was present only in PVA1 (before interaction with bentonite) on the 0.4 µm membrane and Rh was observed on the 0.1 µm membrane in PVA1 after interacting with bentonite. The origin of these "exotic" elements is not known but may possibly be from borehole and boring equipment. The common elements on the membranes refer to the possible presence of silicates, clay minerals, but also to the presence of some salt and calcite (artefacts). However, calcite may not entirely be present as an artefact because calcite is also a common fracture mineral at Olkiluoto like clay minerals, pyrite and amorphous Si.

The presence of bentonite colloids was indicated only on the 0.2 µm membrane from PVA1 groundwater after having interacted with bentonite. The elements present on the membrane included Si, Al, K, and Mg, implying clay colloids, and further, the ratio of Al to Si was representative of bentonite according to a given chemical composition of MX-80. In addition to the common clay mineral elements Fe, Na, Ca and Cl were also observed. The evaluated size range of the colloids aggregated on the membrane was from about 50 nm up to 0.2 µm.

The presence of clay colloids was also doubted on the 0.2 µm membranes of PVA3 groundwater (after bentonite reactor) because K, Al, Si, and traces of Mg were detected. Nevertheless, the amount of material on the membranes was too little to give distinguishable peaks in the EDS spectra to draw such a conclusion. The size of the smallest colloids in the aggregates was about 50 nm. If the colloids on the membranes are bentonite colloids their amount is much less than that observed in the case of PVA1, as even more groundwater was filtered through the PVA3 membrane.

The results from the solution analysis indicated that Fe and Al were associated with colloidal material and were present in all four groundwater lines. In the case of iron the content in PVA3 was less than in PVA1. However the concentration factors were not high enough to allow very exact evaluation of the amounts of Fe and Al associated colloidal material and no evaluation at all of Si, Mg or K associated colloids, which could have referred to the presence of bentonite. An increased concentration (≈ 0.3 mg/L) of soluble Si in all PVA1 groundwater (after bentonite reactor) filtrates was observed indicating origin from bentonite. Unfortunately, the analysis results of a couple of samples gave exceptionally high concentrations of Fe, Al and Si and were doubted for some kind of disturbance or contamination preventing further evaluation of the results.

Based on this study it can be concluded that:

In the groundwater at both groundwater stations, PVA1 and PVA3;

1) Before interaction with bentonite:
   - Fe and Al were found partly colloidal or were associated with colloidal material, which could be, e.g. amorphous SiO_2, clay minerals, but also calcite. The estimated size range was from about 50 nm up to about 400 nm (SEM) but in PVA3 up to about 300 nm. In PVA1 the estimated amount of colloids associated with Fe was about 0.2 mg/L in the size range from ≈ 2 to ≈ 60 nm and 0.6 mg/L in the size range from ≈ 60 nm to ≈ 300 nm , but for Al only 0.004 mg/L. The corresponding amounts in PVA3 were 0.04 mg/L and 0.03 mg/L for Fe and 0.001 mg/L for Al associated colloids. However, the Fe estimate may be too high in the larger particles range.

2) After bentonite interaction:
   – Bentonite colloids were detected (SEM/EDS) in the fresh groundwater (PVA1). The estimated size range was from about 50 nm up to about 200 nm, but the upper limit was difficult to evaluate due to large aggregates. In PVA3 no clear indication of the presence of bentonite colloids was obtained, but the element composition (EDS) insinuated the possibility, however, of only very small amounts. The estimated amount of Fe associated colloids in PVA1 in the size range from ≈ 60 to ≈ 300 nm was about 0.4 mg/L and for Al about 0.001 mg/L, whereas in the smaller size range from ≈ 2 to ≈ 60 nm no value could be extracted. The corresponding amounts in PVA3 were about 0.001 mg/L for both Fe and Al and about 0.06 mg/L for Fe in the smaller size range.

Fast processing of samples on the site decreases artefacts (shown by SEM/EDS of delayed processing), e.g. calcite precipitation, but on the other hand prefiltration with the 0.45 µm filter, even if it was a closed capsule, may have caused some oxidation of Fe resulting in additional formation of colloidal Fe. The capsule may have also retained particles smaller than the filter size.

As an overall conclusion it can be stated that Fe- and Al-colloids (< 0.45 µm) were found to be present in shallow, fresh and deeper saline groundwaters at Olkiluoto, however, they were a little less present in the saline groundwater. Interaction with bentonite causes no significant increase in the amount of colloids; on the contrary, a small decrease was observed. Only little evidence was gained of the presence of bentonite originating colloids in the fresh groundwater. The result is quite in line with studies on the decreasing effect of salinity on the stability of bentonite emanating colloids /Wold 2003/.

6 References

Bradbury M H, Baeyens B, 2002. Porewater chemistry in compacted re-saturated MX-80 bentonite: Physico-chemical characterisation and geochemical modelling. Paul Scherrer Institut, Würenlingen andVilligen, Switzerland. PSI Bericht Nr. 02-10, p 42.

Huertas F, Farias J, Griffault L, Leguey S, Cuevas J, Ramírez S, Vigil de la Villa R, Cobeña J, Andrade C, Alonso M C, Hidalgo A, Parneix J C, Rassineux F, Bouchet A, Meunier A, Decarreau A, Petit S, Viellard P, 2000. Effects of cement on clay barrier performance. ECOCLAY project. European Commission, Luxembourg. Nuclear science and technology series EUR 19609. 140 p.

Karttunen V, Mäntynen M, 2001. Pohjavesinäytteiden otto Eurajoen Olkiluodon kairanrei'istä KR12 ja KR6 vuonna 2001, Posiva Working report 2001-46, p (in Finnish).

Kaufhold S, Dohrman R, Ufer K, Meyer F M, 2002. Comparison of methods for the quantification of montmorillonite in bentonites. Applied Clay Science 22, pp 145–151.

Keto P, 2003. Natural Clays as Backfilling Materials in Different Backfilling Concepts. Posiva Oy, Olkiluoto, Finland. Posiva Working Report 2003-79, p 59.

Müller-Vonmoos M, Kahr G, 1983. Mineralogische Untersuchungen vonWyoming Bentonite MX-80 und Montigel. Nagra, Wettingen, Switzerland. NTB 83-13, p 15+13 app.

Paaso N (ed), Mäntynen M, Vepsäläinen A, Laakso T, 2003. Posivan vesinäytteenoton kenttätyöohje, rev. 3, Posiva Working Report 2003-02, p (in Finnish).

Pitkänen P, Snellman M, 1990. Olikiluosdon, Ulkopääm niemen geokemiallinen pohjavestiulkinta. (Geochemical interpretation of bedrock groundwater at Olkilouta, Ulkopää). Tellisuuden Voima Oy, Helsinki. TVO/VLJ-loppusijoitus Työraportti 90-12, p 49. (In Finnish.

Pusch R, 1999. Clay colloid formation and release from MX-80 buffer. Stockholm, Sweden: Swedish Nuclear Fuel Waste Management Co. SKB TR 99-31, 34 p.

Pusch R, Muurinen A, Lehikoinen J, Bors J, Eriksen T, 1999. Microstructural and chemical parameters of bentonite as determinants of waste isolation efficiency. European Communities, Luxembourg. EUR 18950 EN, p 121.

Rautio T, 1989. Ekstensiometrien asennusreikien kairus VLJ-luolassa. (Boring of assembly holes for extensometers in VLJ-tunnel). Teollosuuden Voima Oy, Helsinki, Finland. TVO/VLJ-lopposijoitus. Työraportti 89-12. (in Finnish).

SKB, 2004. Fud-program 2004 (In Swedish). Swedish Nuclear Fuel and Waste Management, Stockholm, Sweden. p 412.

Wanner H, Wersin P, Sierro N, 1992. Thermodynamic modelling of bentonite-groundwater interaction and implications for near field chemistry in a repository for spent fuel. Swedish Nuclear Fuel and Waste Management, Stockholm, Sweden. SKB Technical Report 92-37, p 28.

Wold S, 2003. On diffusion of organic colloids in compacted bentonite. Doctoral Thesis, Department of Chemistry, Royal Institute of Technology, Stockholm, Sweden. ISRN KTH/KKE-03/2-SE, p 53.

Wolery T J, 1992. EQ3/6, A Software Package for Geochemical Modeling of Aqueous Systems (Version 7.0). Livermore, CA, USA: Lawrence Livermore National Laboratory. UCRL-MA-110662 PT I-IV (PT I, September 14, 1992 66 p; PT II December 17, 1992 89 p; PT III, September 14, 1992 246 p; PT IV, October 9, 1992, 338 p)

7 Details on groundwater analyses and analytical data

7.1 Analytical results

Analyses results on the groundwater samples are presented in Tables A15-7, A15-8 and A15-9. All the analyses were performed in laboratory conditions by TVO Nuclear Services. The assigned relative standard deviations (RSD) were calculated from at least three parallel samples. Table A15-10 gives the analyses results on the simulated reference groundwater OL-SO.

Table A15-7. Analytical data of PVA1 and PVA3 groundwater samples before and after bentonite reactors at sampling on the 10th of February 2003. B = after interaction with bentonite.

Analysis	Unit	PVA1	RSD%	PVA1 B	RSD%	PVA3	RSD%	PVA3 B	RSD%
Conductivity	mS/cm	3.38		3.20		8.43		8.60	
pH		7.8		7.6		7.9		7.9	
p-figure, HCl uptake	mmol/L	< 0.05	0.00	< 0.05	0.00	< 0.05	0.00	< 0.05	0.00
p-figure, NaOH uptake	mmol/L	0.20	2.41	0.21	4.23	0.18	6.12	0.17	3.27
m-figure, HCl uptake	mmol/L	6.15	1.51	6.49	1.36	3.38	1.73	3.29	1.05
Hydrocarbonate	mg/L	375	0.00	400	0.00	210	0.00	200	0.00
Aluminium	mg/L	< 0.05	2.89	< 0.05	5.37	< 0.013	2.88	< 0.013	1.07
Bromide	mg/L	2.6	5.09	2.3	9.81	7.5	5.21	6.5	1.34
Potassium	mg/L	23	0.80	23	0.29				
Potassium	mg/L	14	6.82	14	3.79	14	5.35	14	0.69
Calcium	mg/L	77	0.51	70	0.62	370	1.45	380	1.68
Chloride	mg/L	805	0.74	760	0.56	2,520	0.14	2,580	0.44
$Sulphur_{total}$	mg/L	46	0.26	43	2.61	120	0.81	120	0.94
Sulphate	mg/L	140	0.67	130	0.26	360	1.15	380	0.74
Sulphide	mg/L	0.03	6.47	0.02	15.28	< 0.01	0.00	< 0.01	0.00
Magnesium	mg/L	31	0.47	29	0.40	100	2.28	110	0.92
Manganese	mg/L	0.28	1.04	0.27	2.63	0.59	0.69	0.57	7.06
Sodium	mg/L	540	1.03	530	0.46	1,210	1.00	1,230	0.93
Iron	mg/L	0.32[1]	2.21	0.14[1]	1.39	0.031[2]	2.72	< 0.017[2]	1.46
Silicate	mg/L	15[1]	0.20	15[1)]	0.07	10[3]	0.77	10[3]	0.86
Dissolved organic carbon (DOC)	mg/L	7.2	2.06	6.7	1.38	2.1	1.68	< 1.8	9.04
Dissolved inorganic carbon (DIC)	mg/L	86	0.38	88	0.40	47	0.99	46	0.17

[1] analyzed by plasma emission spectrometry.
[2] analyzed by graphite oven atomic absorption spectrometry.
[3] analyzed by spectrophotometry.

Table A15-8. Analytical data of PVA1 and PVA3 groundwater samples from sampling on the 31st of March 2003. B = after interaction with bentonite.

Analysis	Unit	PVA1	RSD%	PVA1 B	RSD%	PVA3	RSD%	PVA3 B	RSD%
Conductivity	mS/cm	3.48		3.33		9.01		9.18	
pH		7.47		7.51		7.67		7.75	
p-figure, HCl uptake	mmol/L	< 0.05	0.00	< 0.05	0.00	< 0.05	0.00	< 0.05	0.00
m-figure, HCl uptake	mmol/L	6.45	0.73	6.83	1.14	3.23	0.88	3.23	4.94

Table A15-9. Analytical data of PVA1 and PVA3 groundwater samples from sampling on the 6th of May 2003. B = after interaction with bentonite.

Analysis	Unit	PVA1	RSD%	PVA1 B	RSD%	PVA3	RSD%	PVA3 B	RSD%
Conductivity	mS/cm	3.28		3.29		8.09		8.20	
pH		7.64		7.58		7.78		7.75	
p-figure, HCl uptake	mmol/L	< 0.05	0.00	< 0.05	0.00	< 0.05	0.00	< 0.05	0.00
m-figure, HCl uptake	mmol/L	6.42	0.42	6.59	0.82	3.60	0.45	3.59	1.29

Table A15-10. Analytical data on the simulated reference groundwater OL-SO at PVA1 and PVA3 sampling dates. The last column gives the theoretical values for OL-SO water.

		Sampling date 10.2.2003	Sampling date 31.3.2003	Sampling date 6.5.2003	Theoretical value
pH		7.3	7.0	6.8	7.2
Conductivity	mS/m	3,740	3,830	3,880	
HCO_3	mg/L	10.40	–	–	10
F	mg/L	–	–	–	1.2
Cl	mg/L	14,500	–	–	14,000
Br	mg/L	102	–	–	105
SO_4	mg/L	4.3	–	–	4.2
SiO_2	mg/L	2.4	–	–	2.5
Ca	mg/L	4,000	–	–	4,000
K	mg/L	18	–	–	21
Na	mg/L	4,750	–	–	4,800
Mg	mg/L	55	–	–	55

7.2 Physico-chemical characteristics

The groundwater samples were weakly alkaline both before and after the bentonite reactor (pH 7.47–7.91). The lowest pH value was measured on the 31st of March in PVA1 groundwater. The bentonite reactor had either an increasing or decreasing effect on the pH value.

Conductivity in PVA1 changed only slightly on different measuring occasions (3.28–3.48 mS/cm) while in PVA3 it fluctuated between 8.09–9.01 mS/cm.

According to Davis and De Wiest's classification the water types at both PVA1 and PVA3 were Na-Cl type and according to the Davis's TDS-classification (Total Dissolved Solids) the waters are brackish (1,000 < TDS < 10,000). Total salinities of PVA1 and PVA3 groundwater before and after the bentonite reactor are presented in Table A15-11.

Table A15-11. Total salinities for PVA1 and PVA3 groundwaters. B = after interaction with bentonite.

Sampling point	Water type	TDS (mg/L)
PVA1	Na-Cl	2,000
PVA1 B	Na-Cl	1,950
PVA3	Na-Cl	4,800
PVA3 B	Na-Cl	4,910

7.3 Representativeness of analytical data

All analyses were performed in laboratory conditions.

7.3.1 Anions

Sulphate and bromide concentrations from all water samples were analyzed by ion chromatography, chloride by titration and sulphide by spectrophotometer. In pre- and post-reactor waters of PVA3 the sulphide concentrations were under the limit of detection (0.01 mg/L).

In five cases the RSD value exceeded the 5% limit of a competent result. The RSD values of bromide concentrations in pre- and post-reactor waters of PVA1 and in pre-reactor water of PVA3 were 5.09%, 9.81% and 5.21%, respectively. RSD values of sulphide concentrations in pre- and post-reactor waters of PVA1 were 6.49% and 15.28%. The bromide concentration in OL-SO reference water was 102 mg/L while the theoretical value is 105 mg/L.

7.3.2 Cations

Total iron concentrations were measured by plasma emission spectrometry (ICP) from PVA1 water samples and by graphite oven atomic absorption spectrometry (GFAAS) from PVA2 water samples with high-grade results (RSD < 3%). Result of iron concentration after the bentonite reactor in PVA1 was under the limit of detection (16.75 mg/L).

Aluminium, calcium, magnesium, manganese, sodium and potassium concentrations of groundwater sample from PVA1 were analyzed by ICP and flame atomic absorption spectrometry (FAAS) and of water sample from PVA3 by GFAAS and FAAS. Results of all aluminium concentrations were under the limit of detection (for ICP 0.05 mg/L and for GFAAS 12.5 mg/L). Analyses went well (RSD ≤ 5%) except in four cases. The RSD values, 6.82%, 5.35%, of potassium analyses in PVA1 and PVA2 groundwater and 5.37% and 7.06% values of aluminium and manganese analyses in PVA1 B and PVA2 B groundwater. Still the results can be considered moderate. The potassium and manganese concentrations in OL-SO reference water were 18 and 55 mg/L while the theoretical values were 21 and 55 mg/L.

7.3.3 Charge balance

The charge balance (CB) of the ions (Table A15-12) of the analyzed groundwater samples collected on the 10th of February 2003 at PVA1 and PVA3, before and after the bentonite reactors, was calculated according to the following formula

$$CB(\%) = \frac{\sum cations(mol/L) - \sum anions(mol/L)}{\sum cations(mol/L) + \sum anions(mol/L)} \times 100\%.$$

According to Hounslow's criteria the results for the water samples are within the acceptable limits (±5%).

Table A15-12. Charge balance in % of total charge in water samples of PVA1 and PVA3 collected on the 10th of February 2003. B = after interaction with bentonite.

Sample	CB (%)
PVA1	–2.48
PVA1 B	–2.28
PVA3	–1.45
PVA3 B	–1.31

7.4 Sample treatment and analytical methods

Table A15-13. Bottling and fixation of water samples at PVA1 sampling (PE = polyethylene).

Analysis	Sample volume (L) and receiver	Nitriding	Filtration 0.45 µm	Other arrangements
conductivity	1×0.25 PE	–	–	–
pH				
alkalinity	1×0.5 proper sampler	x	x	–
acidity				
S^{2-}	3×0.1 Winkler bottle	–	–	Sampling directly to Winkler bottle. Fixation: 0.5 ml $ZnAc_2$ and 0.5 ml 0.1 molar NaOH
Cl, Br, SO_4	1×0.5 PE	x	x	–
S_{tot},	1×0.25 PE	x	x	–
DIC/DOC	1×0.25 dark glass flask	x	x	
K, Na	1×0.25 PE, acid washed	x	x	Fixation: 1.25 ml conc HNO_3 /250 ml
Al, Ca, Mg, Mn, Fe, SiO_2	1×0.25 PE, acid washed	x	x	Fixation: 2.5 ml 4 molar H_2SO_4 /250 ml

Table A15-14. Bottling and fixation of water samples at PVA3 sampling (PE = polyethylene).

Analysis	Sample volume (L) and receiver	Nitriding	Filtration 0.45 µm	Other arrangements
conductivity	1×0.25 PE	–	–	–
pH				
alkalinity	1×0.5 proper sampler	x	x	–
acidity				
S^{2-}	3×0.1 Winkler bottle	–	–	Sampling directly to Winkler bottle.
				Fixation: 0.5 ml ZnAc and 0.5 ml 0.1 molar NaOH
Cl, Br, SO_4, S_{tot},	1×0.5 PE	x	x	–
SiO_2	1×0.25 PE	x	x	
DIC/DOC	1×0.25 dark glass flask	x	x	
Al, Fe, K, Ca, Mg, Na, Mn	1×0.25 PE, acid washed	x	x	Fixation: 1.25 ml conc HNO_3/250 ml

Table A15-15. Details about groundwater parameter measurements.

Parameters	Methods	Apparatus	Detection limits	Accuracy	Laboratory
pH	ISO-10532	Radiometer		0.05	TVO
		PHM 92			
Conductivity	SFS-EN-27888	Kemetron UPW Tetrametric 331		5%	TVO
Alkalinity	Titration /Paaso et al. 2003/	Mettler DL 50	0.05 mmol/L	2×RSD < 10% /Karttunen and Mäntynen 2001/	TVO
Acidity	Titration /Paaso et al. 2003/	Mettler DL 50	0.05 mmol/L	2×RSD < 20% /Karttunen and Mäntynen 2001/	TVO
DOC/DIC	SFS-EN 1484	Shimadzu TOC-5000	0.1 mg/L	2×RSD < 3%	TVO
Ca	FAAS	P-E 5100 PC	0.03 mg/L	2×RSD < 10%	TVO
	SFS 3018				
	ICP	ICP Meinhard	0.1 mg/L		
	SFS 3044				
Mg	FAAS	P-E 5100 PC	0.03 mg/L	2×RSD < 10%	TVO
	SFS 3018				
	ICP	ICP Meinhard	0.02 mg/L		
	SFS 3044				
Na	FAAS	P-E 5100 PC	0.01 mg/L	2×RSD < 10%	TVO
	SFS 3017				
	ICP		0.5 mg/L		
	SFS 3044				
K	FAAS	P-E 5100 PC	0.01 mg/L	2×RSD < 10%	TVO
	SFS 3017				
	ICP	ICP Meinhard	0.5 mg/L		
	SFS 3044				

Parameters	Methods	Apparatus	Detection limits	Accuracy	Laboratory
Al	GFAAS	P-E 5100 PC + HGA-600	0.009 mg/L	2×RSD < 10%	TVO
	SFS 5074 SFS 5502	ICP Meinhard			
	ICP		0.05 mg/L		
	SFS 3044				
Mn	GFAAS	P-E 5100 PC+ HGA-600	0.009 mg/L	2×RSD < 10%	TVO
	SFS 5074 SFS 5502	ICP Meinhard			
	ICP		0.002 mg/L		
	SFS 3044				
Fe (tot)	GFAAS	P-E 5100 PC + HGA-600	0.005 mg/L	2×RSD < 10%	TVO
	SFS 5074 SFS 5502	ICP Meinhard			
	ICP		0.002 mg/L		
	SFS 3044				
SiO_2	Spectrophotometer	Shimadzu 1601 UV-VIS	0.1 mg/L	2×RSD < 10%	TVO
	ICP	ICP Meinhard			
	SFS 3044		0.01 mg/L		
Cl	Titration /Paaso et al. 2003/	Mettler DL 50	5 mg/L	2×RSD < 5%	TVO
Br	IC	Dionex DX-100	0.5 mg/L	2×RSD < 8%	TVO
	SFS-EN ISO 10304-1				
S^{2-}	Spectrophotometer	Shimadzu 1601 UV-VIS	0.01 mg/L	2×RSD < 20%	TVO
	SFS 3038				
SO_4	IC SFS-EN ISO 10304-1	Dionex DX-100	0.2 mg/L	2×RSD < 6%	TVO
S(Tot)	H_2O_2 oxidation +IC	Dionex DX-100	0.2 mg/L	2×RSD < 6%	TVO

8 Solution analysis results from ultrafiltration

Table A15-16. Analysis results for the various solution samples collected in colloid sampling. The concentration factor was calculated based on the amounts of unrinsed concentrate and filtrates.

		PVA1 0.3 µm	PVA1 300 kD	PVA1 10 kD	PVA1 B 0.3 µm	PVA1 B 300 kD	PVA1 B 10 kD	PVA3 300 kD	PVA3 300 kD	PVA3 10 kD	PVA3 B 0.3 µm	PVA3 B 300 kD	PVA3 B 10 kD
Conc factor		145	65	44	116	74	55	58	84	44	74	82	53
a)	Filtrates (combined from all 6 centrifuge tubes)												
Na	mg/L	560	570	570	550	550	550	1,300	1,300	1,300	1,300	1,300	1,300
K	mg/L	14	13	16	13	14	13	16	14	17	14	16	15
Ca	mg/L	88	88	89	82	82	81	350	340	350	360	370	370
Mg	mg/L	32	33	33	30	30	30	100	100	100	110	110	110
Mn	mg/L	0.35	0.34	0.35	0.34	0.34	0.34	0.51	0.50	0.51	0.51	0.52	0.51
Sr	mg/L	0.93	0.94	0.95	0.88	0.88	0.88	3.8	3.8	3.9	4.1	4.1	4.1
Si	mg/L	7.0	7.0	7.0	7.3	7.3	7.3	4.8	4.8	4.9	4.8	4.9	4.8
Fe_{tot}	mg/L	0.80	0.19	0.042	0.54	0.11	0.11	0.089	0.056	0.012	0.085	0.084	0.025
Al	mg/L	0.0115	0.0079	0.0082	0.0090	0.0078	0.0080	0.0075	0.0064	0.0068	0.0096	0.0062	0.0079
Br	mg/L	2.3	2.1	2.2	2.1	2.1	1.9	6.4	6.2	6.0	5.9	6.3	6.3
Cl	mg/L	860	890	890	790	810	820	2,600	2,830	2,690	2,690	2,670	2,630
SO_4	mg/L	143	146	144	136	135	135	388	388	386	398	401	402

		PVA1 0.3 µm	PVA1 300 kD	PVA1 10 kD	PVA1 B 0.3 µm	PVA1 B 300 kD	PVA1 B 10 kD	PVA3 300 kD	PVA3 300 kD	PVA3 10 kD	PVA3 B 0.3 µm	PVA3 B 300 kD	PVA3 B 10 kD
b)	Rinsing water (combined from 5 centrifuge tubes)												
Na	mg/L	33	76	87	36	64	85	100	150	210	78	160	210
K	mg/L	0.8	1.8	2.0	0.8	1.5	2.0	1.2	1.7	2.3	0.9	1.8	2.3
Ca	mg/L	5.1	12	14	5.3	9.5	12	28	40	58	22	46	61
Mg	mg/L	1.9	4.3	5.0	1.9	3.5	4.6	8.3	12	17	6.6	13	18
Mn	mg/L	0.021	0.047	0.051	0.023	0.040	0.050	0.041	0.059	0.083	0.031	0.064	0.084
Sr	mg/L	0.06	0.13	0.14	0.06	0.10	0.13	0.31	0.45	0.64	0.25	0.51	0.67
Si	mg/L	0.39	0.90	1.0	0.46	0.82	1.1	0.37	0.53	0.76	0.28	0.58	0.75
Fe_{tot}	mg/L	0.032	0.012	< 0.005	0.033	0.011	< 0.005	0.006	0.005	0.009	0.005	0.008	< 0.005
Al	mg/L	n.a	n.a	n.a	n.a	n.a	n.a	n.a	n.a	n.a	n.a	n.a	n.a
Br	mg/L	< 5	< 5	< 5	< 5	< 5	< 5	< 5	< 5	< 5	< 5	< 5	< 5
Cl	mg/L	44	107	120	58	87	114	210	300	430	160	340	430
SO_4	mg/L	8	21	23	11	17	22	34	47	66	27	53	64
c)	Acid rinse (combined from 5 centrifuge tubes)												
Na	mg/L	0.8	2.3	3.1	1.3	1.9	2.9	3.2	4.6	5.1	3.5	3.9	5.0
K	mg/L	0.1	0.1	0.2	0.1	0.1	0.2	0.1	0.1	0.1	0.1	0.1	0.1
Ca	mg/L	0.47	0.69	1.20	0.49	0.62	1.10	1.10	1.50	1.90	1.20	1.30	1.80
Mg	mg/L	0.05	0.13	0.19	0.05	0.11	0.16	0.22	0.35	0.42	0.25	0.31	0.40
Mn	mg/L	0.020	0.022	0.034	0.027	0.028	0.045	0.038	0.038	0.040	0.027	0.039	0.043
Sr	mg/L	< 0.01	< 0.01	< 0.01	< 0.01	< 0.01	< 0.01	< 0.01	0.01	0.02	0.01	0.01	0.02
Si	mg/L	< 0.1	< 0.1	0.14	< 0.1	< 0.1	0.11	< 0.1	< 0.1	< 0.1	< 0.1	< 0.1	< 0.1
Fe_{tot}	mg/L	0.045	0.12	1.2	0.035	0.054	0.77	0.039	0.055	0.25	0.046	0.039	0.31
Al	mg/L	0.006	0.008	0.020	0.007	0.007	0.018	0.042	0.008	0.023	0.011	0.006	0.018
Br	mg/L	< 1	< 1	< 1	< 1	< 1	< 1	< 1	< 1	< 1	< 1	< 1	< 1
Cl	mg/L	8.4	9.4	11	8.6	9.4	11	12	14	15	12	13	15
SO_4	mg/L	0.8	1.0	1.2	0.9	1.1	1.1	1.1	1.8	1.8	1.4	1.6	1.8
d)	Rinsed concentrate (combined from 5 centrifuge tubes)												
Na	mg/L	34	50	90	41	50	67	81	130	170	75	130	180
Ca	mg/L	5.8	7.8	14	6.3	7.3	9.8	23	36	47	22	37	51
Mg	mg/L	2.0	2.8	5.0	2.2	2.6	3.5	6.5	10	13	6.2	10	15
Mn	mg/L	< 0.05	0.032	0.053	< 0.05	0.032	0.041	0.034	0.053	0.068	< 0.05	0.052	0.070
Sr	mg/L	< 0.1	0.08	0.15	< 0.1	0.08	0.1	0.24	0.39	0.51	0.24	0.40	0.55
Si	mg/L	0.53	0.62	1.1	0.57	0.68	0.88	0.31	0.49	0.64	0.33	0.48	0.66
Fe_{tot}	mg/L	0.130	0.071	0.190	0.074	0.049	0.200	0.069	0.270	0.100	0.035	0.046	0.073
Al	mg/L	0.230	0.039	0.017	0.090	0.032	0.013	0.033	0.038	0.018	0.130	0.047	0.018
e)	Concentrate, not rinsed (from the 6th centrifuge tube)												
Na	mg/L	610	600	620	600	620	590	1,400	1,500	1,300	1,500	1,400	1,400
Ca	mg/L	96	95	97	91	92	90	380	420	370	420	390	400
Mg	mg/L	38	34	35	32	32	32	110	120	110	120	110	120
Mn	mg/L	0.45	0.38	0.38	0.39	0.39	0.38	0.54	0.60	0.55	0.60	0.55	0.56
Sr	mg/L	1.1	1.0	1.0	0.95	0.98	0.96	4.1	4.5	4.1	4.7	4.3	4.4
Si	mg/L	40	7.4	7.7	8.0	8.1	8.0	5.2	5.8	5.1	5.7	5.1	5.1
Fe_{tot}	mg/L	4.7	0.17	0.14	0.6	0.17	0.3	0.083	0.18	0.21	0.090	0.093	0.072
Al	mg/L	0.0709	0.022	0.019	0.064	0.070	0.022	0.016	0.020	0.030	0.026	0.030	0.018

		PVA1 0.3 µm	PVA1 300 kD	PVA1 10 kD	PVA1 B 0.3 µm	PVA1 B 300 kD	PVA1 B 10 kD	PVA3 300 kD	PVA3 300 kD	PVA3 10 kD	PVA3 B 0.3 µm	PVA3 B 300 kD	PVA3 B 10 kD
f)	Acid rinse (from the 6th centrifuge tube)												
Na	mg/L	6.5	9.9	12	4.3	8.1	10	21	23	15	18	21	23
K	mg/L	0.2	0.3	0.3	0.1	0.2	0.3	0.3	0.3	0.3	0.3	0.3	0.4
Ca	mg/L	1.1	1.8	2.4	1.0	1.5	2.1	5.7	6.5	4.6	5.5	6.1	7.0
Mg	mg/L	0.36	0.56	0.67	0.21	0.44	0.55	1.6	1.8	1.2	1.5	1.7	1.9
Mn	mg/L	0.024	0.027	0.040	0.030	0.032	0.049	0.044	0.044	0.045	0.033	0.046	0.050
Sr	mg/L	< 0.05	< 0.05	< 0.05	< 0.05	< 0.05	< 0.05	0.06	0.07	0.05	0.06	0.07	0.08
Si	mg/L	< 0.5	< 0.5	< 0.5	< 0.5	< 0.5	< 0.5	< 0.5	< 0.5	< 0.5	< 0.5	< 0.5	< 0.5
Fe_{tot}	mg/L	0.082	0.18	1.2	0.042	0.047	0.93	0.03	0.059	0.29	0.062	0.047	0.33
Al	mg/L	0.018	0.020	0.022	0.013	0.010	0.018	0.013	0.011	0.022	0.014	0.010	0.018
Cl	mg/L	16	21	22	13	17	20	48	49	35	42	47	51

< denotes below detection limit (given by the value).

9 SEM micrographs and EDS spectra

9.2 Micrographs of empty Nuclepore membranes and their spectra

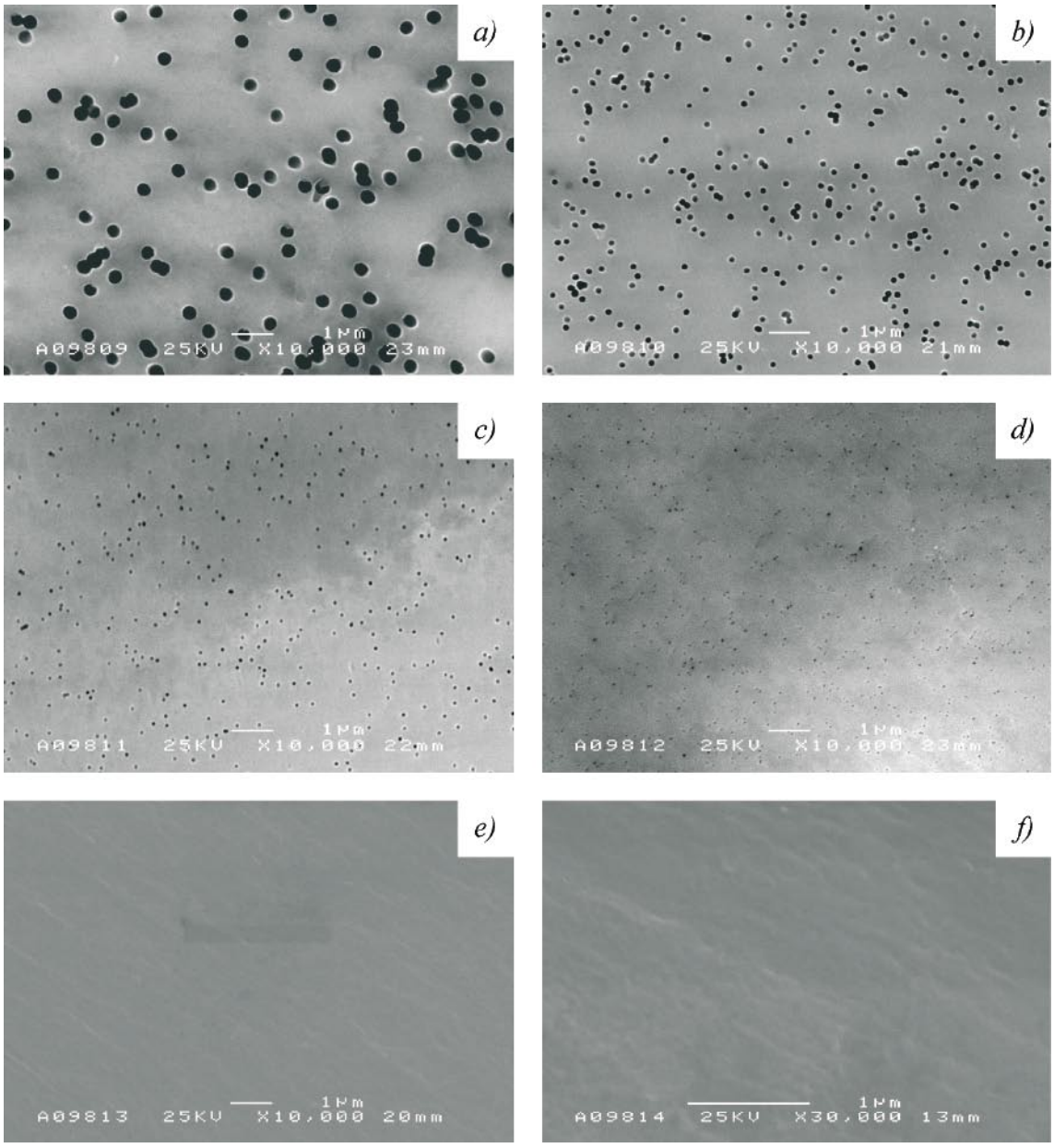

***Figure A15-2**. SEM micrographs of empty Nuclepore membranes with ×10,000 magnification* ***a)** 0.4 µm, b) 0.2 µm, c) 0.1 µm, d) 0.05 µm, e) 0.015 µm and f) with ×30,000 magnification for 0.015 µm.*

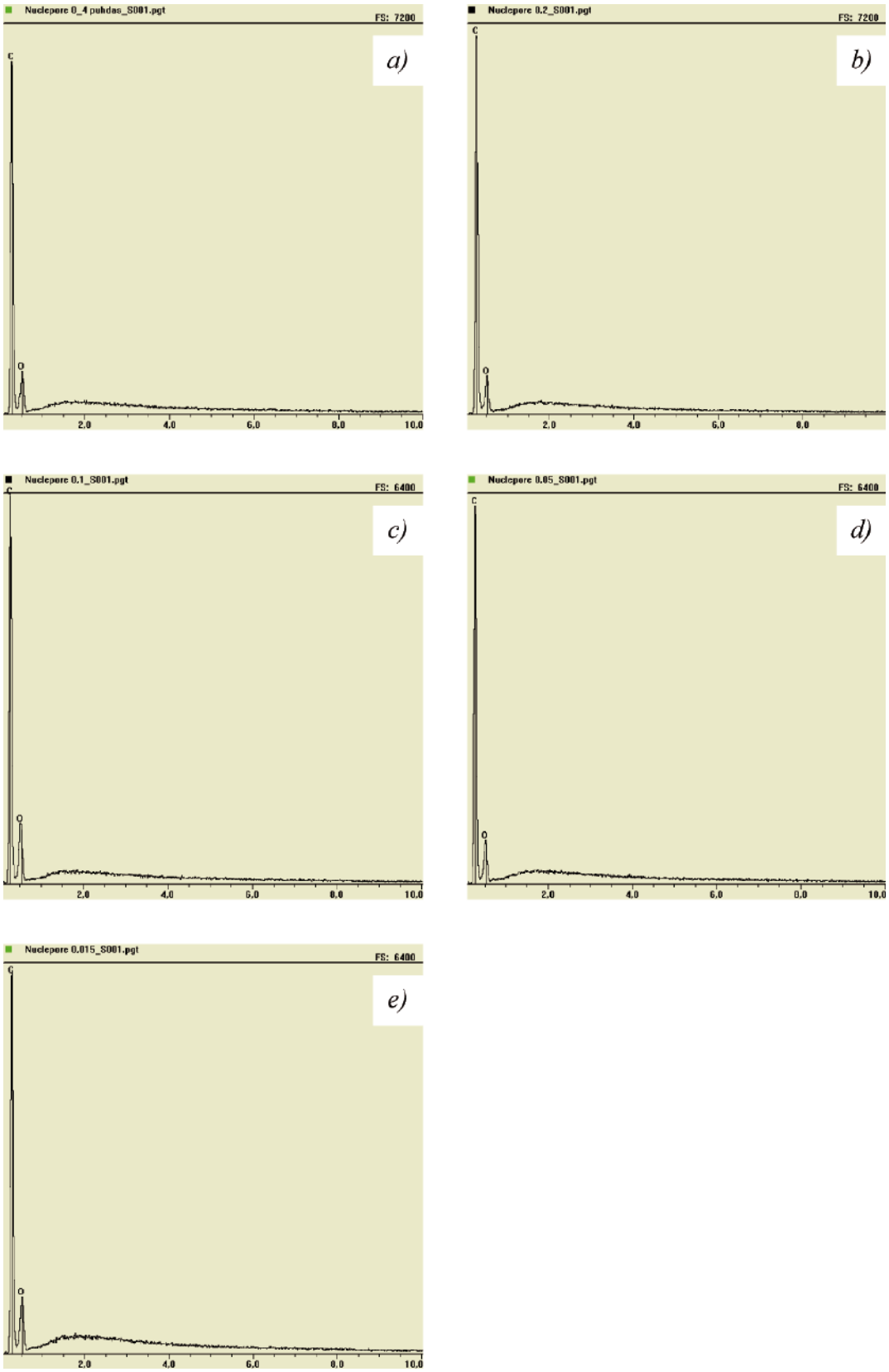

Figure A15-3. *EDS spectra for the empty Nuclepore filters in Figure A15-2a–e, respectively. The only elements detected are carbon (C) and oxygen (O).*

PVA1, groundwater sampled *before* the bentonite reactor

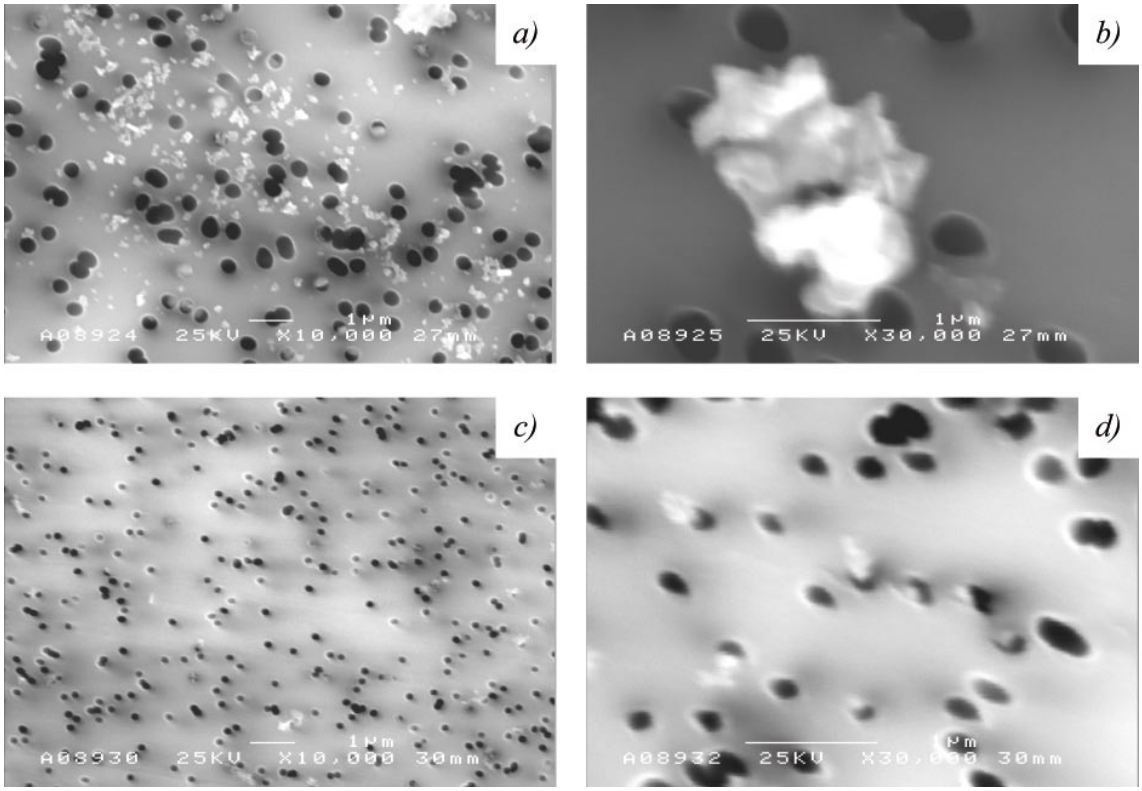

Figure A15-4. *PVA1 SEM micrographs of membranes:* ***a)*** *and* ***b)*** *of 0.4 µm membrane magnifications ×10,000 and ×30,000, respectively (prefiltration in sampling line with 0.45 µm);* ***c)*** *and* ***d)*** *of 0.2 µm membrane magnifications ×10,000 and ×30,000, respectively (prefiltration with the 0.4 µm membrane).*

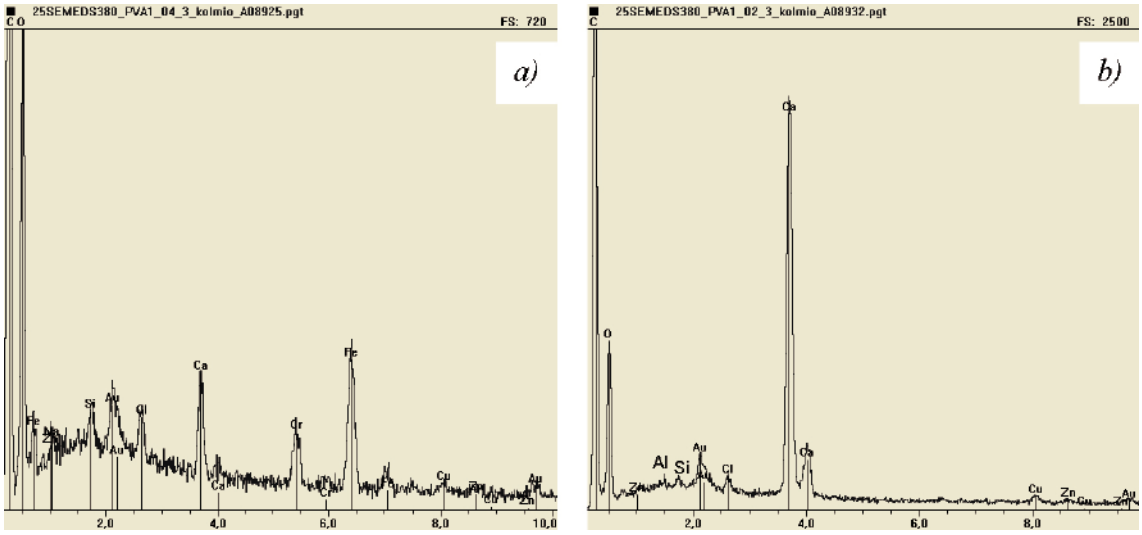

Figure A15-5. *EDS spectra of the* ***a)*** *0.4 µm membrane and* ***b)*** *0.2 µm membrane.*

PVA1, groundwater sampled *before* the bentonite reactor

Figure A15-6. *PVA1 SEM micrographs of membranes:* ***a)*** *and* ***b)*** *of 0.1 µm membrane magnifications ×10,000 and ×30,000, respectively (prefiltration with a 0.2 µm membrane);* ***c)*** *and* ***d)*** *of 0.05 µm membrane magnifications ×10,000 and ×30,000, respectively (prefiltration with a 0.1 µm membrane).*

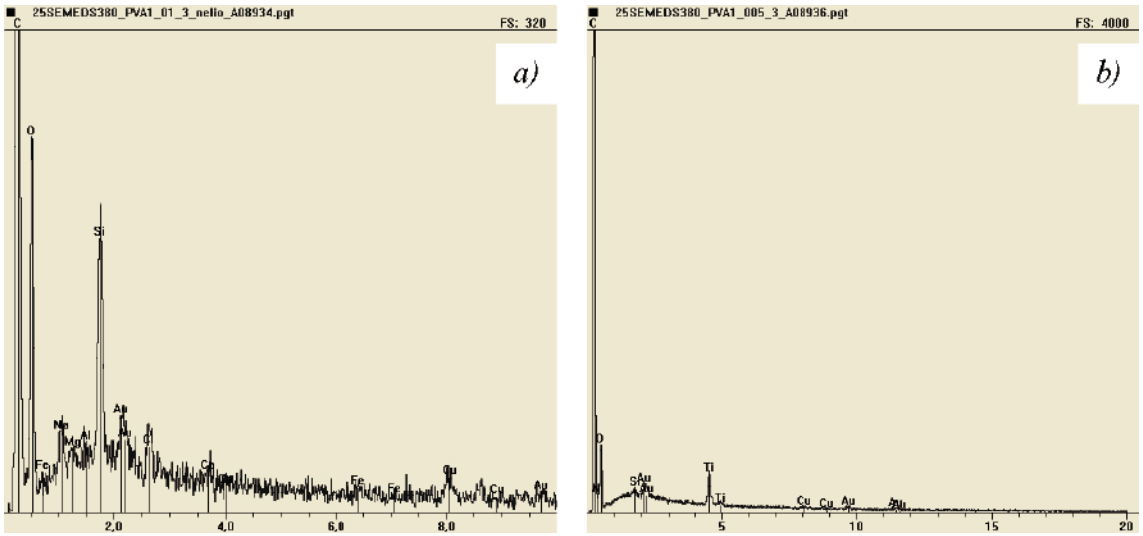

Figure A15-7. *EDS spectra of the* ***a)*** *0.1 µm membrane and* ***b)*** *0.05 µm membrane.*

PVA1 B, groundwater sampled *after* the bentonite reactor

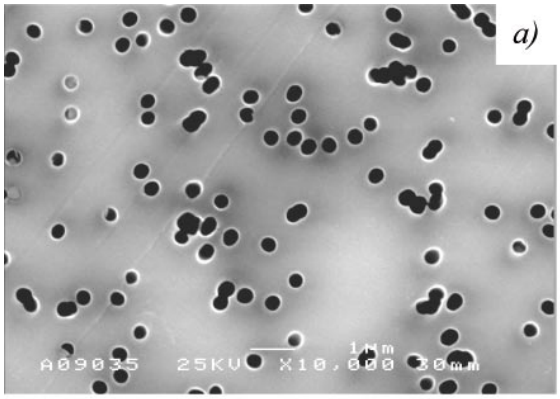

Note! No spectrum is presented for the 0.4µm membrane in A15-8a because there is too little of material on the membrane to give more information than the spectrum of an empty membrane in Figure A15-3a.

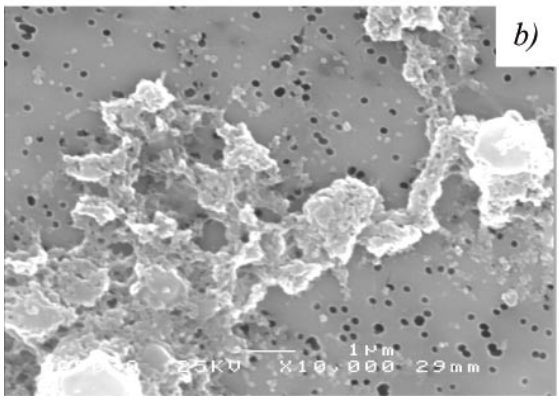

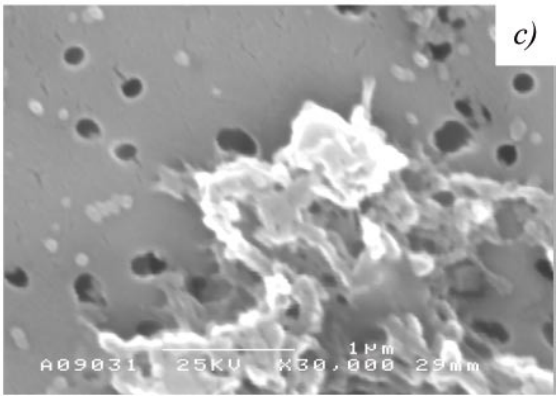

Figure A15-8. *PVA1 SEM micrographs of membranes:* ***a)*** *of 0.4 µm membrane magnification ×10,000 (prefiltration in sampling line with 0.45 µm);* ***b)*** *and* ***c)*** *of 0.2 µm membrane magnifications ×10,000 and ×30,000, respectively (prefiltration with the 0.4 µm membrane). 18 ml of groundwater was filtered.*

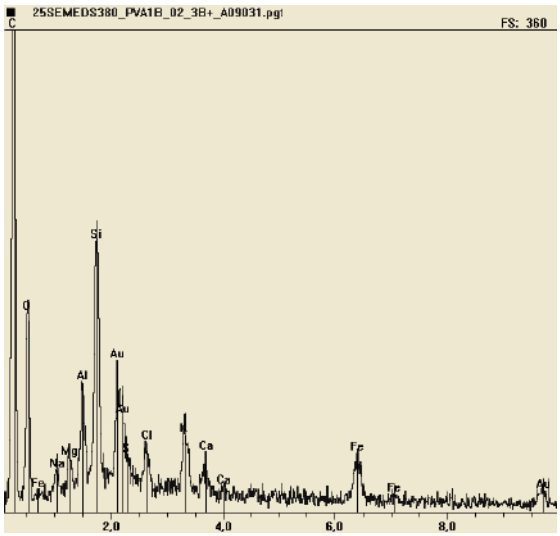

Figure A15-9. *EDS spectrum of the 0.2 µm membrane.*

PVA1 B, groundwater sampled *after* the bentonite reactor

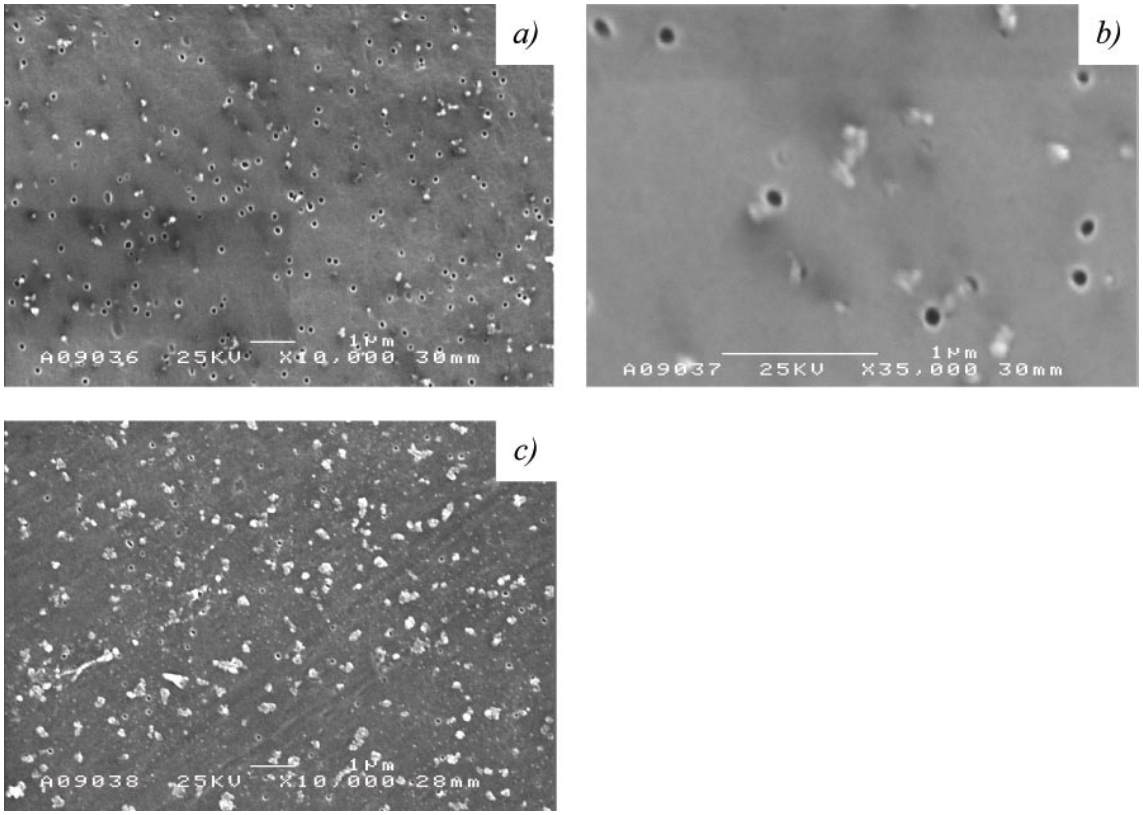

Figure A15-10. *PVA1 SEM micrographs of membranes:* ***a)*** *and* ***c)*** *of 0.1 µm membranes magnifications ×10,000 (prefiltration with a 0.2 µm membrane);* ***d)*** *of 0.1 µm membrane (in a) magnification ×35,000.*

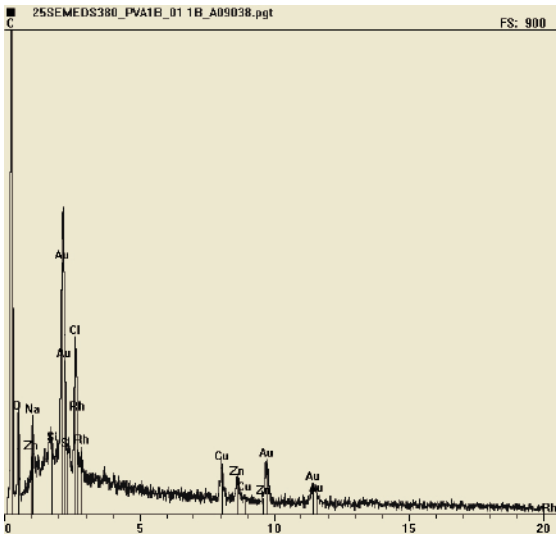

Figure A15-11. *EDS spectra of the above 0.1 µm membrane.*

PVA1 B, groundwater sampled *after* the bentonite reactor

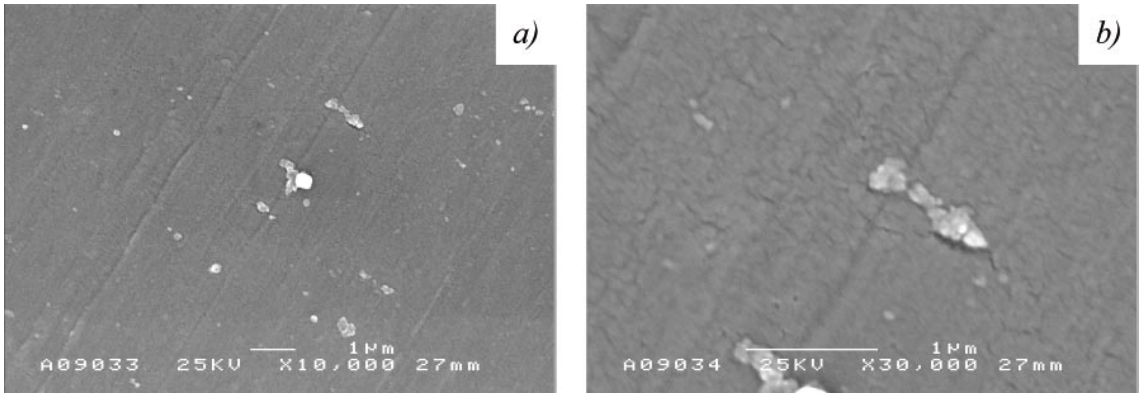

***Figure A15-12**. PVA1 SEM micrographs of a 0.015 µm membrane (prefiltration with a 0.1 µm membrane): **a)** membrane magnifications ×10,000, **b)** membrane magnification ×30,000.*

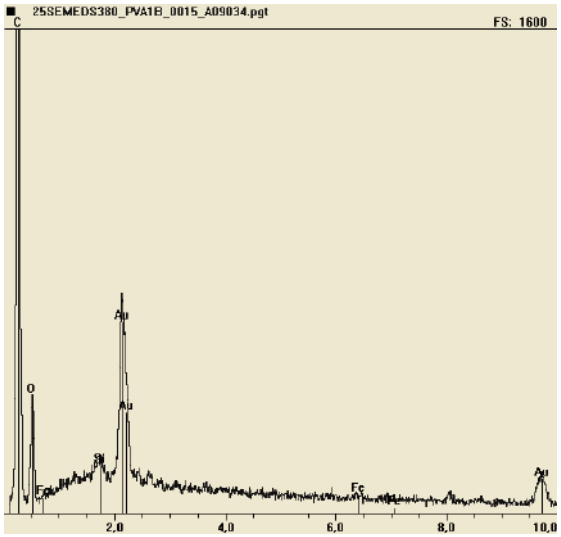

***Figure A15-13.** EDS spectra of the above 0.015 µm membrane.*

PVA3, groundwater sampled *before* the bentonite reactor

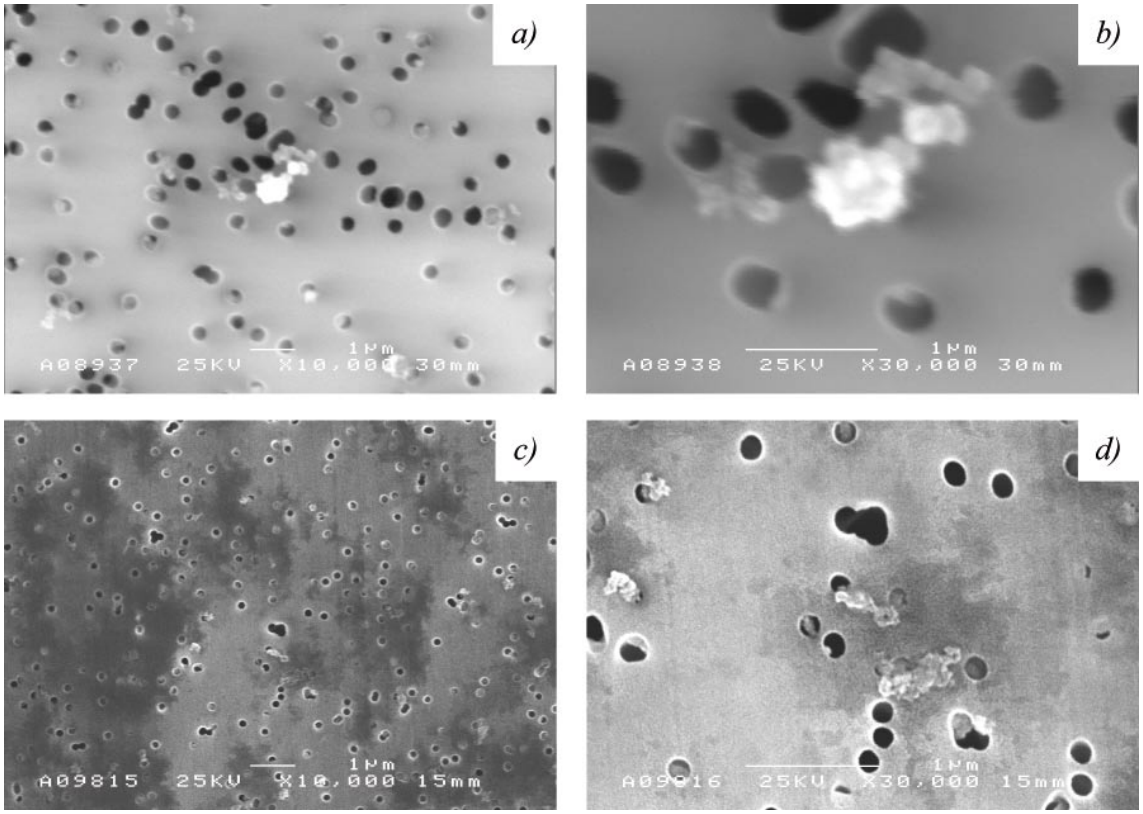

Figure A15-14. *PVA3 SEM micrographs of membranes:* ***a)*** *and* ***b)*** *of 0.4 µm membrane magnifications ×10,000 and ×30,000, respectively (prefiltration in sampling line with 0.45 µm);* ***c)*** *of 0.2 µm membrane magnifications ×10,000 (prefiltration with the 0.4 µm membrane).*

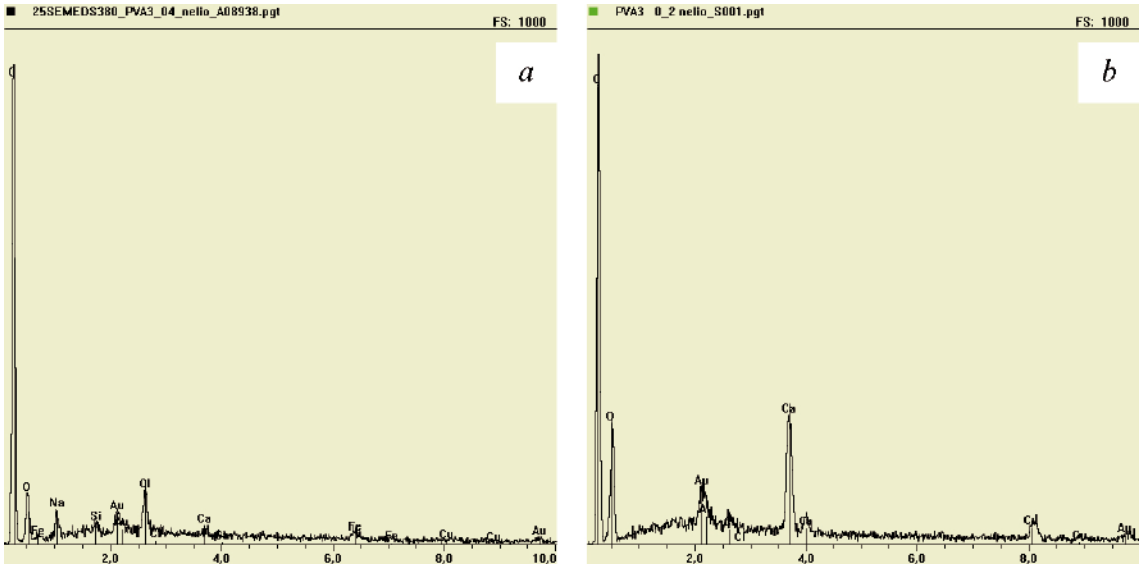

Figure A15-15. *EDS spectrum of the above 0.4 µm membranes a) = a and b) = c.*

PVA3 groundwater sampled *before* the bentonite reactor

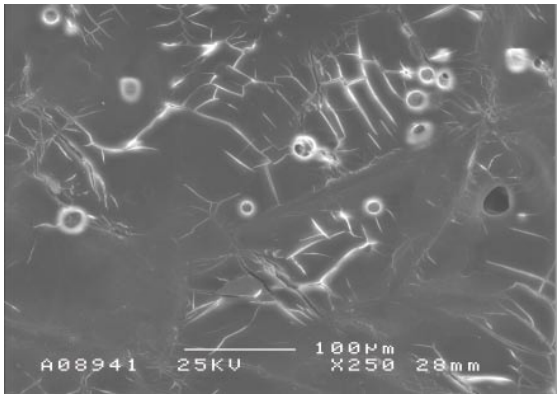

Figure A15-16. *PVA3 SEM micrograph of 0.05 µm membrane magnification ×250 (prefiltration with a 0.1 µm membrane). The membrane is covered with a very fine material, which has cracked like dry clay. The holes are presumably "canals" for water to go through.*

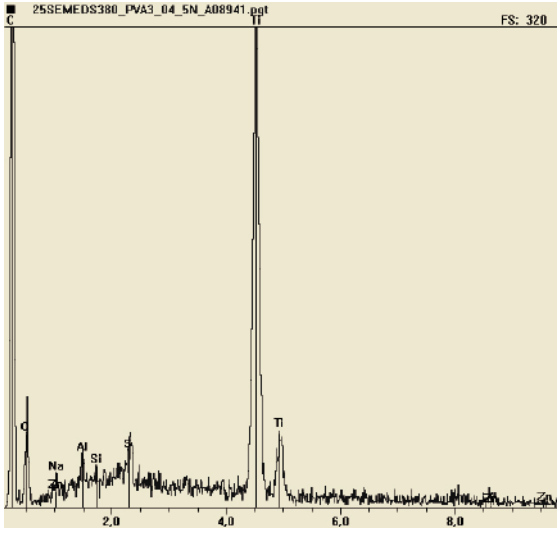

Figure A15-17. *EDS spectrum of the above 0.05 µm membrane. Titanium is the main element present, minor amounts of Na, Mg, Al, S and Cl.*

PVA3 B, groundwater sampled *after* the bentonite reactor

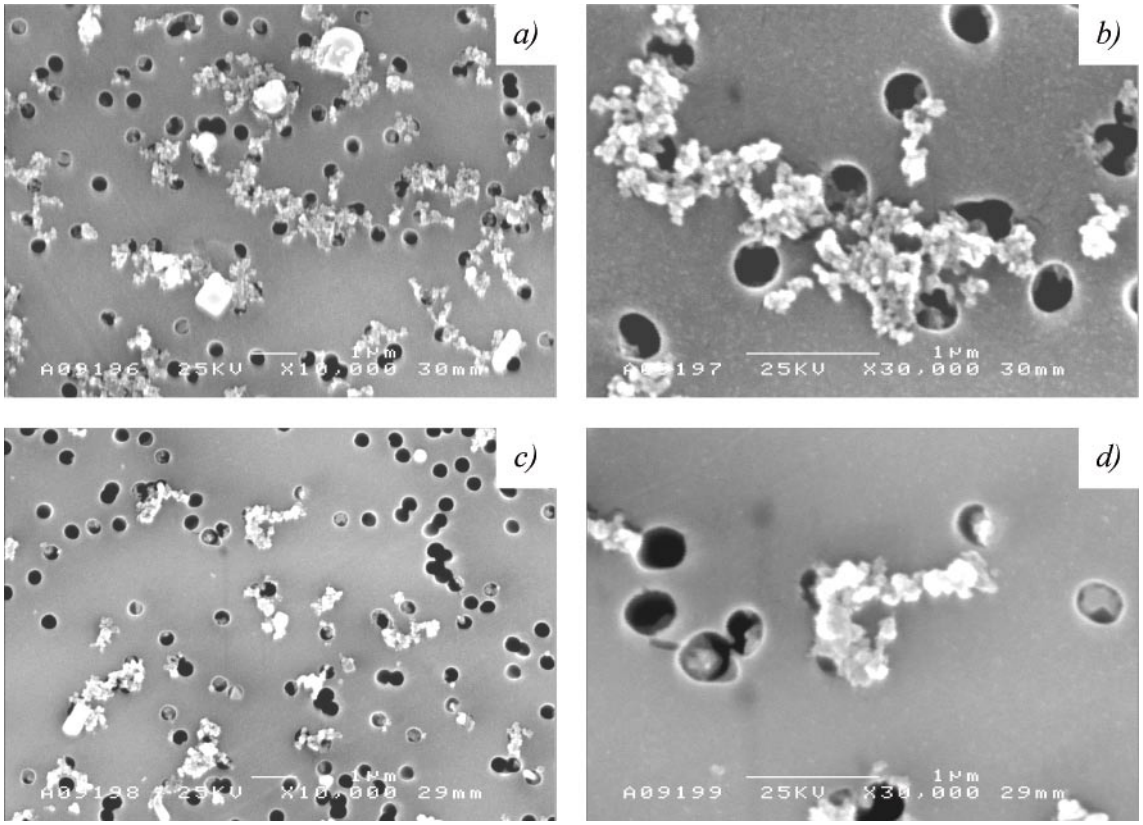

Figure A15-18. *PVA3 SEM micrographs of 0.4 µm membranes (prefiltration with 0.45 µm membrane):* ***a)*** *and* ***c)*** *magnifications ×10,000* ***c)*** *and* ***d)*** *magnifications ×30,000. The difference between the membranes is the amount of groundwater filtered; a) 42 ml and c) 25 ml.*

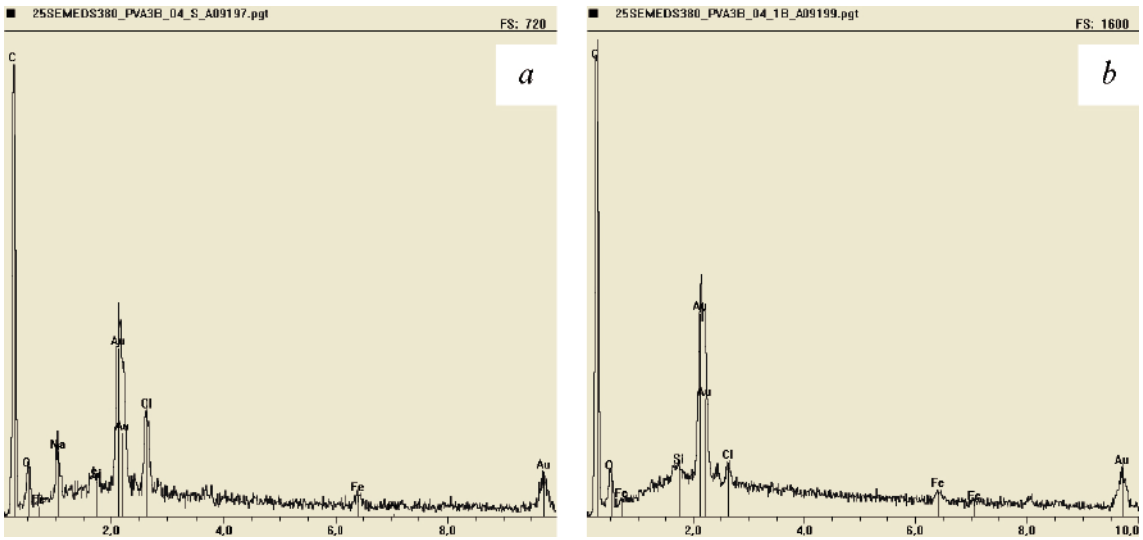

Figure A15-19. *EDS spectrum of the above 0.4 µm membranes* ***a)*** *for Figure A15-18b) and* ***b)*** *for Figure A15-18d).*

PVA3 B, groundwater sampled *after* the bentonite reactor

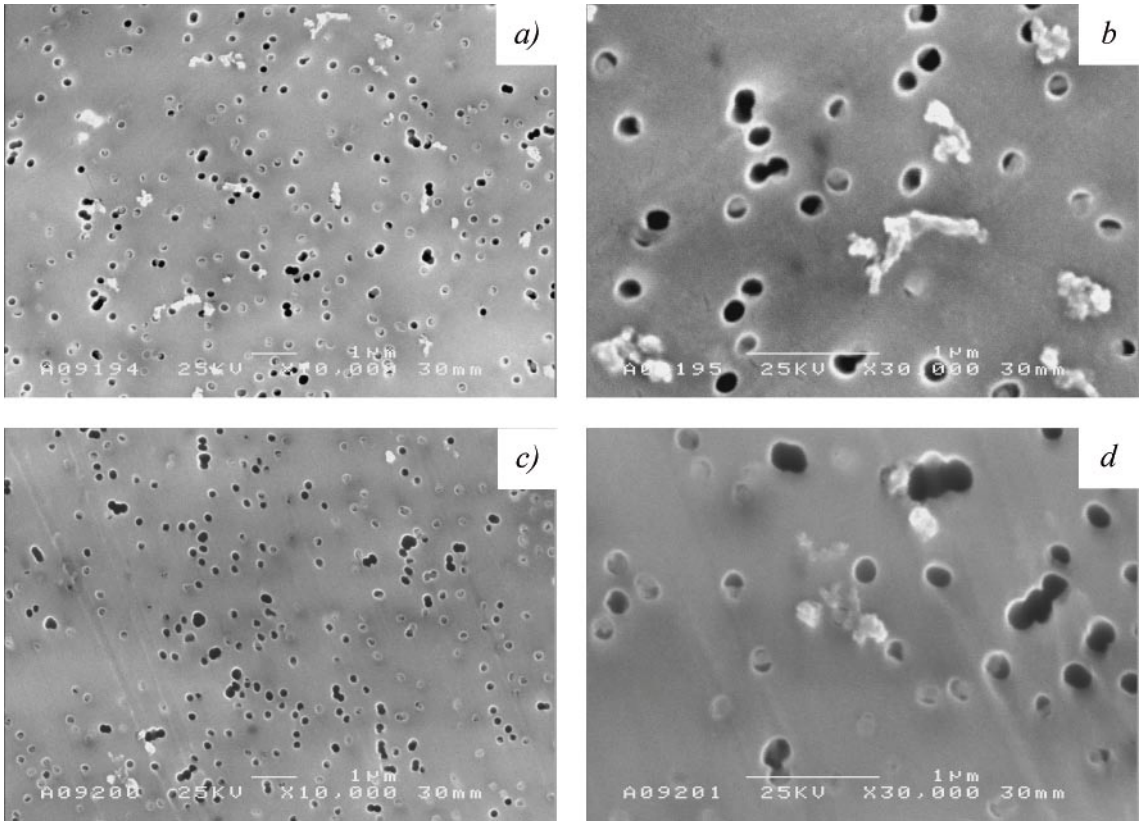

Figure A15-20. *PVA3 SEM micrographs of 0.2 µm membranes (prefiltration with 0.4 µm membranes in previous Figure A15-14):* ***a)*** *and* ***c)*** *magnifications ×10,000* ***c)*** *and* ***d)*** *magnifications ×30,000. The difference between the membranes is the amount of groundwater filtered; a) 42 ml and c) 25 ml.*

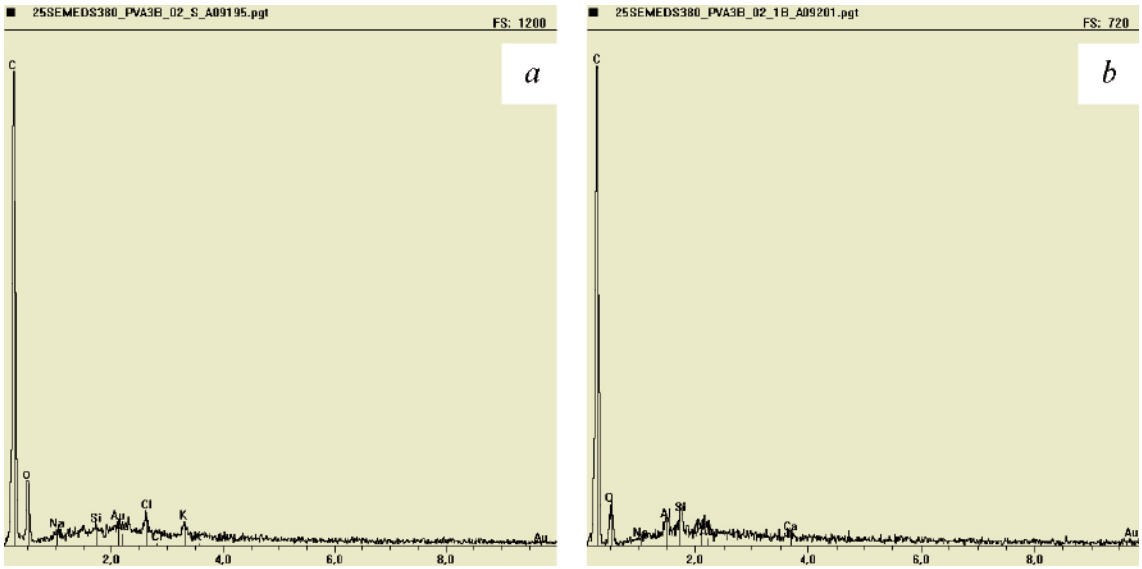

Figure A15-21. *EDS spectrum of the above 0.2 µm membranes* ***a)*** *= a and* ***b)*** *= c.*

PVA3 B, groundwater sampled *after* the bentonite reactor

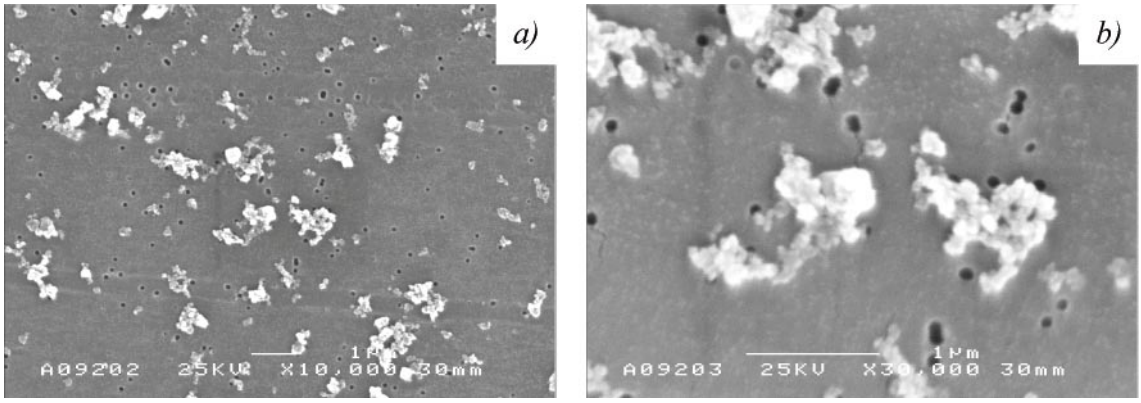

Figure A15-22. *PVA3 SEM micrographs of a 0.1 µm membrane (prefiltration with 0.2 µm membrane)* ***a)*** *magnifications ×10,000 and* ***b)*** *magnification ×30,000.*

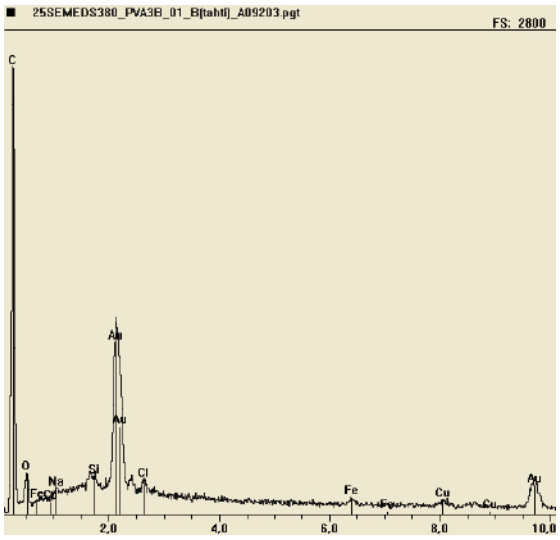

Figure A15-23. *EDS spectrum of 0.1 µm membrane in Figure A15-22b. The small peak between the marked Au and Cl peaks is also an Au peak.*

Micrographs and EDS spectra from a few delayed filtrations

A few filtrations with Nuclepore membranes were performed later in the laboratory glove-box after some days of collecting the groundwater samples. These micrographs show that Ca-containing larger particles (presumably calcite) were formed. The most obvious reason is calcite precipitation due to loss CO_2.

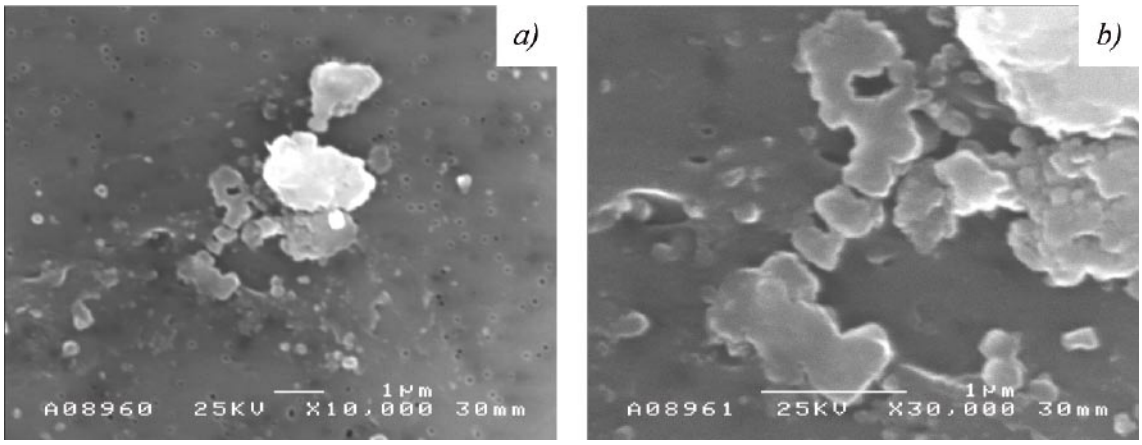

Figure A15-24. *PVA1 SEM micrographs of 0.1 µm membrane (prefiltration with 0.2 µm membrane):* ***a)*** *magnification ×10,000* ***b)*** *magnification ×30,000.*

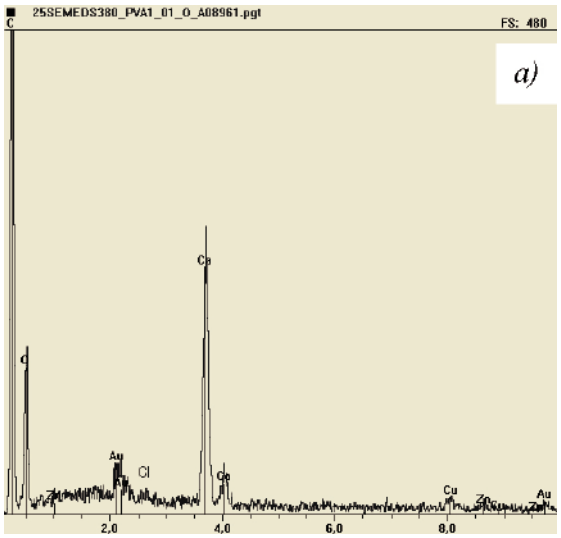

Figure A15-25. *EDS spectrum of the 0.1 µm membrane in Figure A15-24b.*

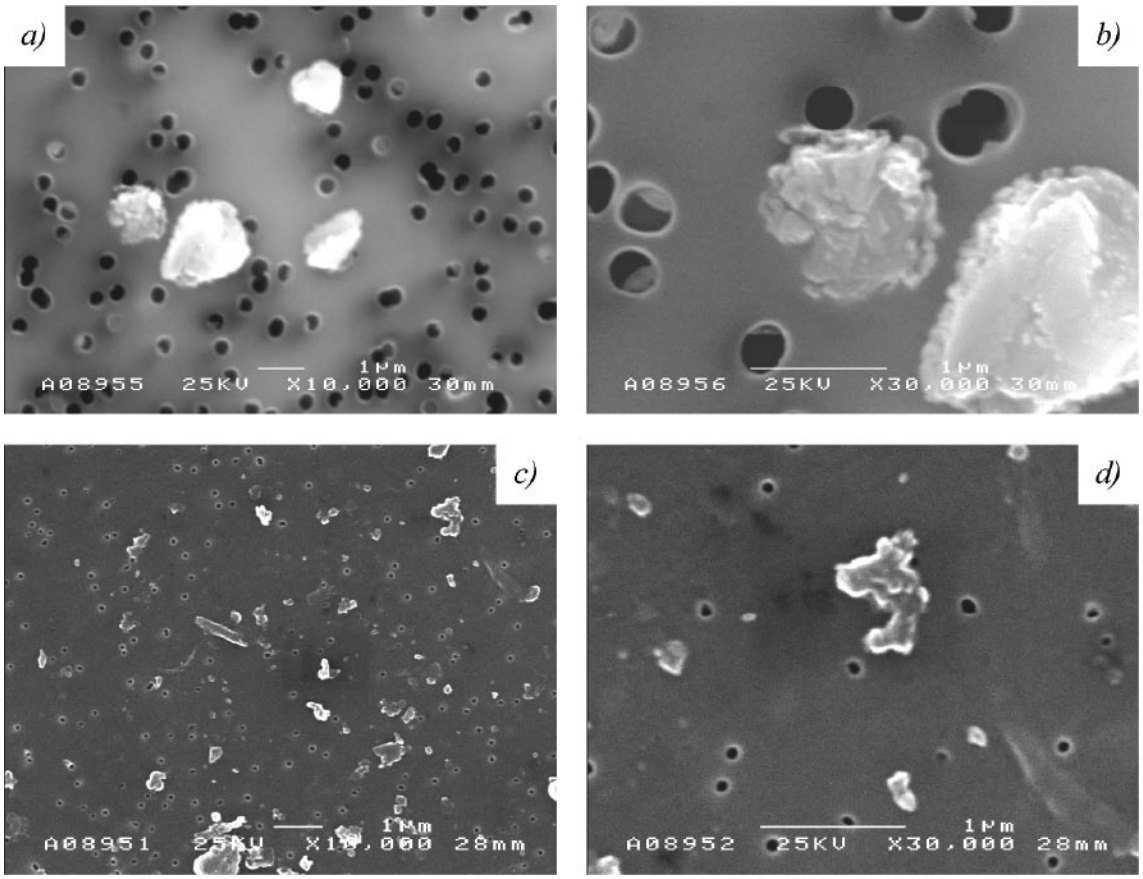

Figure A15-26. *PVA3 SEM micrographs of* ***a)*** *0.4 µm membrane magnification ×10,000 (prefiltration with 0.4 µm on site),* ***c)*** *0.1 µm membrane magnification ×10,000 (prefiltered with 0.2 µm membrane)* ***b)*** *and* ***d)*** *×30,000 magnifications of the membranes respectively.*

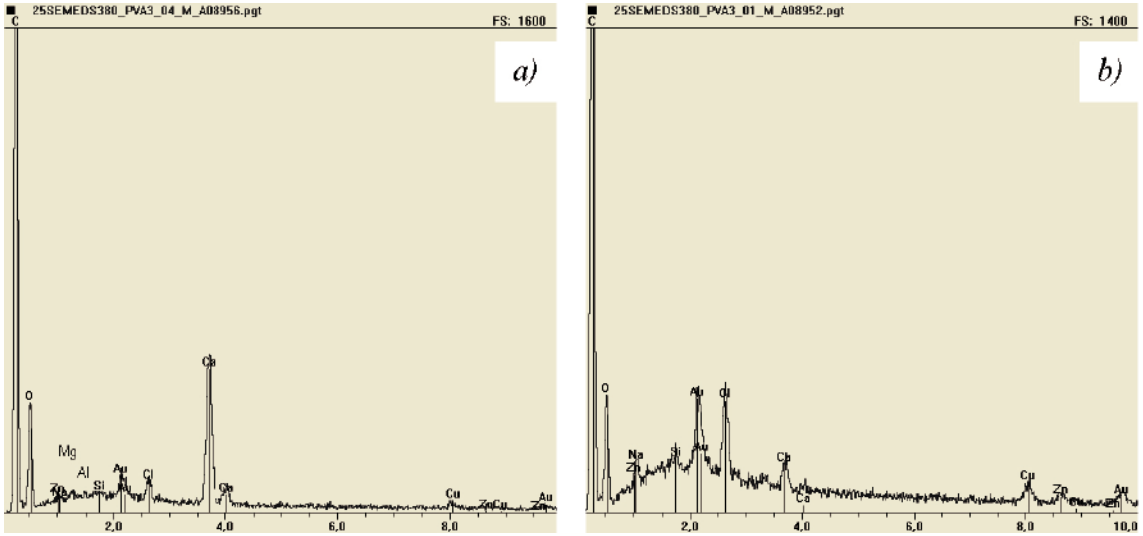

Figure A15-27. *EDS spectra;* ***a)*** *0.4 µm membrane and b****)*** *0.1 µm membrane.*

ISSN 1404-0344
CM Digitaltryck AB, Bromma, 2006